National Library
of Canada

Acquisitions and
Bibliographic Services Branch

395 Wellington Street
Ottawa, Ontario
K1A 0N4

Bibliothèque nationale
du Canada

Direction des acquisitions et
des services bibliographiques

395, rue Wellington
Ottawa (Ontario)
K1A 0N4

Your file Votre référence

Our file Notre référence

NOTICE

The quality of this microform is heavily dependent upon the quality of the original thesis submitted for microfilming. Every effort has been made to ensure the highest quality of reproduction possible.

If pages are missing, contact the university which granted the degree.

Some pages may have indistinct print especially if the original pages were typed with a poor typewriter ribbon or if the university sent us an inferior photocopy.

Reproduction in full or in part of this microform is governed by the Canadian Copyright Act, R.S.C. 1970, c. C-30, and subsequent amendments.

AVIS

La qualité de cette microforme dépend grandement de la qualité de la thèse soumise au microfilmage. Nous avons tout fait pour assurer une qualité supérieure de reproduction.

S'il manque des pages, veuillez communiquer avec l'université qui a conféré le grade.

La qualité d'impression de certaines pages peut laisser à désirer, surtout si les pages originales ont été dactylographiées à l'aide d'un ruban usé ou si l'université nous a fait parvenir une photocopie de qualité inférieure.

La reproduction, même partielle, de cette microforme est soumise à la Loi canadienne sur le droit d'auteur, SRC 1970, c. C-30, et ses amendements subséquents.

Canada

UNIVERSITY OF ALBERTA

Toppling Failure in Rock Slopes.

by

Radko Bucek ©

A THESIS
SUBMITTED TO THE FACULTY OF GRADUATE STUDIES AND RESEARCH
IN PARTIAL FULFILLMENT OF THE REQUIREMENTS FOR THE DEGREE OF

Doctor of Philosophy

IN

Mining Engineering

Department of Mining, Metallurgical and Petroleum Engineering

Edmonton, Alberta

Spring 1995

National Library
of Canada

Acquisitions and
Bibliographic Services Branch

395 Wellington Street
Ottawa, Ontario
K1A 0N4

Bibliothèque nationale
du Canada

Direction des acquisitions et
des services bibliographiques

395, rue Wellington
Ottawa (Ontario)
K1A 0N4

Your file Votre référence

Our file Notre référence

THE AUTHOR HAS GRANTED AN IRREVOCABLE NON-EXCLUSIVE LICENCE ALLOWING THE NATIONAL LIBRARY OF CANADA TO REPRODUCE, LOAN, DISTRIBUTE OR SELL COPIES OF HIS/HER THESIS BY ANY MEANS AND IN ANY FORM OR FORMAT, MAKING THIS THESIS AVAILABLE TO INTERESTED PERSONS.

L'AUTEUR A ACCORDE UNE LICENCE IRREVOCABLE ET NON EXCLUSIVE PERMETTANT A LA BIBLIOTHEQUE NATIONALE DU CANADA DE REPRODUIRE, PRETER, DISTRIBUER OU VENDRE DES COPIES DE SA THESE DE QUELQUE MANIERE ET SOUS QUELQUE FORME QUE CE SOIT POUR METTRE DES EXEMPLAIRES DE CETTE THESE A LA DISPOSITION DES PERSONNE INTERESSEES.

THE AUTHOR RETAINS OWNERSHIP OF THE COPYRIGHT IN HIS/HER THESIS. NEITHER THE THESIS NOR SUBSTANTIAL EXTRACTS FROM IT MAY BE PRINTED OR OTHERWISE REPRODUCED WITHOUT HIS/HER PERMISSION.

L'AUTEUR CONSERVE LA PROPRIETE DU DROIT D'AUTEUR QUI PROTEGE SA THESE. NI LA THESE NI DES EXTRAITS SUBSTANTIELS DE CELLE-CI NE DOIVENT ETRE IMPRIMES OU AUTREMENT REPRODUITS SANS SON AUTORISATION.

ISBN 0-612-01676-5

Canadä

UNIVERSITY OF ALBERTA

RELEASE FORM

NAME OF AUTHOR: Radko Bucek

TITLE OF THESIS: Toppling Failure in Rock Slopes

DEGREE FOR WHICH THESIS WAS SUBMITTED: Doctor of Philosophy

YEAR THIS DEGREE GRANTED: 1995

Permission is hereby granted to the UNIVERSITY OF ALBERTA LIBRARY to reproduce single copies of this thesis and to lend or sell such copies for private, scholarly or scientific research purposes only.

The author reserves all other publication right and other rights with the copyright in the thesis, and except as hereinbefore provided neither the thesis nor any substantial portion thereof may be printed or otherwise reproduced in any material form without the author's written permission.

(SIGNED) Bucek

PERMANENT ADDRESS:

c/o Department of Mining, Metallurgical and
Petroleum Engineering
University of Alberta
Edmonton, Alberta
Canada T6G 2G6

Date 27 Jan 1995

UNIVERSITY OF ALBERTA
FACULTY OF GRADUATE STUDIES AND RESEARCH

The undersigned certify that they have read, and recommend to the Faculty of Graduate Studies and Research, for acceptance, a thesis entitled Toppling Failure in Rock Slopes submitted by R. Bucek in partial fulfilment of the requirements for the degree of Doctor of Philosophy in Mining Engineering.

Professor K. Barron

Professor D.M. Cruden

Professor Z. Eisenstein

Professor I.R. Muirhead

Professor J.M. Whiting

for B Ladanyi

Professor B. Ladanyi

Date 27/1/95

Dedication

To my wife
for her continued encouragement and inspiration
especially for understanding at difficult times

and to my parents
for their persistent supports in my life and studies
and inspiring me to endeavor for the best

Abstract.

In rocks where the bedding steeply dips into the pit wall, the potential exists for toppling failures to occur in the highwall. The mechanisms of toppling failures are complex and are probably the least understood of all the modes of pit slope failure.

A theory defining the toppling mechanism and explaining the mechanisms of formation of the toppling failure plane in terms of the system of nonlinear equations, was formulated in this thesis. The derived equations are based on beam theory which is widely used in civil and mechanical engineering. The resultant system of equations is solved numerically using the Newton-Raphson method.

A computer model based on this theory was written to show the validity of the theory in practice, and a backanalysis of the failure of the 50-A-5 pit at the Luscar Mine, Cardinal River Coals Ltd. was done using this computer model.

During the course of the work new concepts concerning the toppling mechanism were formulated, and others were clarified.

An understanding was acquired that flexural toppling, block toppling and block flexural toppling are three distinct stages of one deformation process rather than three different toppling mechanisms.

It is possible to generalize at this stage, and to say that the failure in the flexural toppling mode will result in most cases in subsequent block or block flexural toppling.

Failure of the slopes by flexural toppling is governed by the shear forces generated by interacting blocks of bending rock columns. After the rock blocks start to split into smaller and smaller columns the resultant failure surface can be found as the plane of

highest tensile stresses.

Higher strength parameters define a stronger slope which would sustain more loading without a failure, but could finally fail in a more violent way than the slopes defined with lower strength parameters which tend to break partially at an earlier stage.

The progressive block flexural and block toppling above the basal surface created by flexural toppling will create additional zones of fractured rock which may connect to form a new failure plane with an unfavourable inclination and thus lead to triggering of an unexpected shear failure.

ACKNOWLEDGEMENTS

I would like to take this opportunity to thank the program supervisor, Dr. Ken Barron, Chairman of the Mining, Metallurgical and Petroleum Engineering Department, University of Alberta, for his supervision, guidance, encouragement and generosity shown throughout the whole program. Dr. Ken Barron keenly supported this work by ensuring funding and many other resources and by making available his time to discuss with me whenever it was required, and his solid and broad knowledge in mining engineering.

Sincere thanks also go to Keith Hebil, a senior engineer of Luscar Ltd., for numerous discussions and many valuable suggestions in development of this model. This program would not have been so successful, and fast to complete without his guidance.

I also wish to express my gratitude to my wife, Jana, and my father and mother for their support and encouragement.

The help of Mr. Doug Booth, whose assistance, especially in the computer technology and facilities, was indispensable for the completeness of the program, is also greatly appreciated.

Table of Contents

Chapter Page

1. INTRODUCTION 1

2. TOPPLING FAILURES - LITERATURE REVIEW 3
   - 2.1. Geological and structural description of the problem. 3
     - 2.1.1. Physical environment 3
     - 2.1.2. Modes of toppling 4
     - 2.1.3. Structural control of toppling 10
     - 2.1.4. Toppling on cataclinal slopes 12
     - 2.1.5. Toppling on anaclinal slopes 12
   - 2.2. Toppling models 13
     - 2.2.1 Limit equilibrium models 13
       - 2.2.1.1. Probabilistic stability analysis of block toppling failure. 19
       - 2.2.1.2. Probabilistic rock structure modelling 20
     - 2.2.2 Numerical models 22
     - 2.2.3. Physical models 25
     - 2.2.4. Discussion of the role of Limit equilibrium, Numerical and Physical models 29

3. THEORETICAL APPROACH 35
   - 3.2. Description of the problem 36
   - 3.3. Flexural toppling failure 37
   - 3.4. Block toppling failure 49
     - 3.4.1. Bending of columns of rocks with a crossjoint system 49
     - 3.4.2. Toppling and sliding of rock columns 58

4. SOLUTION OF THE SYSTEM OF EQUATIONS FOR FLEXURAL TOPPLING 66

5. TOPPLING MODEL 70
   - 5.1. Description of the model 70
   - 5.2. The computing routine 73

6. BACKANALYSIS OF THE FAILURE OF THE HIGHWALL AT THE 50-A-5 OPEN PIT COAL MINE AT THE LUSCAR MINE, CARDINAL RIVER COALS LTD 75
6.1 Introduction 75
6.2. Engineering geology of the 50-A-5 pit 76
6.3. Highwall design and development 78
6.4. Analysis of the failure 82
6.5. Influence of bedding dip 86
7. SUMMARY AND CONCLUSIONS 94
8. RECOMMENDATIONS 96
REFERENCES 98

Appendix A

Derivation of equations of the system of interacting cantilevers for block flexural toppling 102
A.1. The own weight of a single rock cantilever 103
A.2. Loading by the underlying cantilever 105
A.3. Loading by the overlying cantilever 108
A.4. Loading by the underlying water 110
A.5. Loading by the overlying water 112
A.6. Loading by seismic forces 114
A.7. Derivation of equations for combination of loads for n cantilevers 116

Appendix B

Derivation of equations of the system of interacting cantilevers for block toppling 122
B.1. Loading by the failed rock 123
B.2. Loading by the overlying cantilever 126
B.3. Derivation of equations for combination of loads for n cantilevers 132

Appendix C

Geometrical equations for a circle 139

Appendix D

Geometrical description of the toppling movement for interacting blocks on a stepped base 141
D.1. Two toppling blocks - case A 141
D.2. Two toppling blocks - case B 144
D.3. The lower block is sliding, the upper block is toppling - case C 146

Appendix E

Derivation of equations for the system of toppling blocks 148

Appendix F

Derivation of equations for the system of sliding blocks 154

Appendix G

Shear strength on the bedding planes 160

Appendix H

Solution of the system of nonlinear equations for toppling 163
H.1. Newton Raphson method 163
H.2. Bending equations for the Newton - Raphson method. (Flat base - continuous reaction) 164
H.3. Bending equations for the Newton - Raphson method. (Stepped base - point reaction) 172

Appendix I

Fortran source codes 178
I.1. Program Input 178
I.2. Program Fredy 192
I.3. Program Inshav 196
I.4. Program Flex 204
I.5. Subroutine Deflex 232
I.6. Subroutines Newton and Usrfun (nonlinear version) 237
I.7. List of subroutines 241

Appendix J

Location of the Luscar Mine, Cardinal River Coals Ltd and the 50-a-5 open pit coal mine 244

List of figures

Figure		page
2-1	Flexural toppling failure	7
2-2	Block toppling failure	8
2-3	Block flexural toppling failure	9
2-4	Stress distribution on the surface of a rock slope	10
2-5	Geometry of the slope with discontinuity	10
2-6	Geometry of the underdip slope with discontinuity	12
2-7	Geometry of the anaclinal slope with a discontinuity	13
2-8	Model for limiting equilibrium analysis of toppling on a stepped base	14
2-9	Forces acting on a toppling block	15
2-10	Forces acting on a sliding block	15
2-11	Relative displacement of toppling failure	27
3-1	System of two independent groups of three interacting cantilevers	37
3-2	System of interacting cantilevers	37
3-3	System of very long simple beams	37
3-4	System of beams lying on elastic foundations	38
3-5	Forces acting on one of the interacting cantilevers (flexural toppling)	38
3-6	Common radius of the system of concentric circles	43
3-7	Simplified geometrical relations for the system of cantilevers	45
3-8	Inline arrangement of two systems of perpendicular joints	49
3-9	Offset arrangement of two systems of perpendicular joints	50
3-10	Forces acting on one of the interacting cantilevers	52
3-11	System of interacting cantilevers on the stepped base	52
3-12	Geometry of the system of blocks on the stepped base kinematically free to topple or slide	58
3-13	System of forces acting on one (toppling) block from the system of interacting rock columns	60
3-14	Possible contacts between toppling blocks	61

3-15 System of forces acting on one (sliding) block from the system of interacting rock columns 63
3-16 Possible contacts for the sliding blocks 64
3-17 Excluded face-corner type of contact for the sliding and toppling blocks 65
5-1 A rock slope susceptible to toppling 70
5-2 Rock slope consisting of blocks of interacting cantilevers and blocks of non-interacting cantilevers 71
6-1 Cross-section through the highwall of the 50-A-5 pit 76
6-2 Slope surface just above the pit area 80
6-3 Slope surface just above the pit area 80
6-4 Hill surface around elevation 1890 m 81
6-5 A crack at the top of the hill 81
6-6 First bench - elevation 1852 m 83
6-7 Second bench - elevation 1840 m 83
6-8 Third bench - elevation 1828 m 84
6-9 Fourth bench - elevation 1816 m 84
6-10 Fifth bench - elevation 1804 m 84
6-11 Sixth bench - elevation 1792 m 85
6-12 Seventh bench - elevation 1768 m 85
6-13 Cross-section through the highwall - dip 50º........ 87
6-14 First bench 87
6-15 Second bench 88
6-16 Third bench 88
6-17 Fourth bench 88
6-18 Fifth bench 89
6-19 Sixth bench 89
6-20 Seventh bench 89
6-21 Cross-section through the highwall - dip 70º........ 90
6-22 First bench 90
6-23 Second bench 91

6-16 Third bench 91
6-17 Fourth bench 91
6-18 Fifth bench 92
6-19 Sixth bench 92
6-20 Seventh bench 92
A-1 Sketch of the loading of the single cantilever by it's own weight 103
A-2 Sketch of the loading of an n^{th} cantilever by reaction with the underlying cantilever 105
A-3 Sketch of the loading of an n^{th} cantilever by the reaction with the overlying cantilever 108
A-4 Sketch of the loading of the lower surface of a cantilever by hydrostatic forces 110
A-5 Sketch of the loading of the upper surface of a cantilever by hydrostatic forces 112
A-6 Sketch of loading of a cantilever by seismic forces 114
A-7 The geometry of the system of n interacting cantilevers 116
A-8 A sketch of combination of loads acting on one of the system of interacting cantilevers 117
B-1 Sketch of the loading of a single cantilever by the weight of already failed rock 123
B-2 Sketch of the loading of an n^{th} cantilever by the reaction with the overlying cantilever (block toppling) 126
B-3 The geometry of the system of n interacting cantilevers (block toppling).. 133
B-4 A sketch of combination of loads acting on one of the system of interacting cantilevers (block toppling) 133
C-1 Notation of the geometry of a circle 139
D-1 The geometry of two toppling blocks on the stepped base - case A 141
D-2 The geometry of two toppling blocks on the stepped base - case B 144
D-3 Geometry of the movement of one sliding and one toppling block on the stepped base 146

D-4 Critical position of the blocks after the critical contact corner-corner was established 147
E-1 System of forces acting on one from the system of interacting blocks . 148
E-2 Possible contacts between toppling blocks 149
E-3 Geometry of toppling blocks - block n being the higher one 149
E-4 Geometry of toppling blocks - block n being the lower one 150
F-1 System of forces acting on one block from the system of interacting blocks 154
F-2 Excluded face-corner kind of contact for the sliding and toppling blocks 155
F-3 Possible contacts for the sliding blocks 155
F-4 Geometry of the system of two sliding and one toppling blocks 156
I-1 The flowchart of the routine Flex 205
J-1 Plan of the 50-A-5 pit 244
J-2 Location of the 50-A-5 open pit mine 245

Nomenclature

α_n	angle between the side of a tilting block and the vertical
β	angle of the failure plane with the horizontal
Γ	$\alpha+\psi+\phi-90^0$
γ_w	unit weight of water
Δ_n	sliding distance of blocks at the foot of the slope in question, for one iteration step
ζ	angle of the slope below the crest
η	slope angle above the crest
$\theta(x)_n$	angle of tangent to the deflection curve with horizontal
λ_n	angle between the reaction P_n and the vertical
ξ_n	angle between sides of a toppling and a sliding block
$\sigma(x)_n$	normal stress
$\tau(x)_n$	shear stress
ϕ_n	angle of internal friction
ψ	angle of rock columns (cantilevers) with the horizontal
a1	height of the rock steps on the slope face below the crest
a2	height of the rock steps on the slope face above the crest
b	spacing of joints
$b^{\sim}$	thickness of cantilever
d_n	height of a cantilever
E_n	Young's modulus of rock
$e_{n,i}$	excentricity of acting force with respect to the contact point of a toppling block
F_n	loading force acting at the end of a cantilever
h	height of the rock slope under consideration
$h^{\wedge}_{v,n}$	height of the water column below the cantilever (stepped base)
$h_{v,n}$	height of the ground water column
I_n	moment of inertia

l_n	length of a cantilever
m	number of rock steps
M_n	bending moment
P_n	reaction force between toppling blocks
Q^{-}_{max}	moment of area above the neutral axis about the neutral axis
Q_n	seismic force
r_n	continuous reaction force between cantilevers [kN/m]
R_n	point reaction force between cantilevers (rock blocks) [kN]
$u< >$	singularity function
U_n	uplift water force
$V(x)$	shear force
V_n	water force acting on the side of a block
w_n	weight
W_n	weight of a block
$x_{(Q.,n)}$	length between the beginning and the point of action of the seismic force
$x_{r,n}$	length of the contact between two cantilevers
$x_{v,n}$	length of the submerged part of a cantilever
$y(x)_n$	deflection of a cantilever
y^{-}_{max}	distance of outer fibre from the neutral axis

1. INTRODUCTION

As stated by Richings (1981),"although the role of slope stability has not changed, there have been changes in the mining industry that have affected the geotechnician engaged in slope stability studies. The deposits currently being mined or evaluated are technically difficult, capital intensive, and economically marginal....As a rule, they are of a lower grade, more remotely located, and more technically difficult to develop. It should be noted at this point that not all of the difficulties encountered are inherent in the orebody. Some have been generated by the imposition of new mining regulations". In addition, the need for capital in the mining industry had outstripped most mining companies' ability to provide this financing internally. Mining companies have therefore been prime targets for oil companies anxious to diversify, or, alternatively, they have been required to turn to bank loans to finance projects. Some of these are business loans that are secured by assets and revenue from sources not associated with the project. The mining investor or decision maker is, therefore, often more sophisticated financially, but less sophisticated in mining terms. In this case, the viability of the project must be clearly shown before any financial commitment. The impact of these changes will be to force the geotechnician and mining engineer to attempt to quantify the risk and the financial implications of a slope design.

The mining engineer over the last few years has relinquished his responsibilities for making the judgment on pit slope angles and leaned heavily on the geotechnician to provide him with a single answer. There is, of course, no single answer. The mining engineer who is in a position to see all of the picture should make the decision on what slope design is feasible. To do this, he must be supplied with the probability of failure associated with the slope design angle and this should be expressed in some useful form. To assess the implications of the failure, the mining engineer must know whether the failure will be large or small, and whether it will be fast or slow. With that information, he may be able to say whether he can live with the slide, and he will at least be able to begin to quantify its economic implications. The answer may be very different for an interim in-pit slope and the one that contains a permanent haul road or defines a pit limit bordering on a metallurgical plant or major dump.

Furthermore, as stated by Aydan, Ichikawa, Shimizu and Murata (1991), the stability of rock slopes associated with the construction of power plants, highways and open pit mines is always of paramount importance during the lifetime of these structures. In comparison with slopes in soils, the failure modes in rocks are various and are generally governed by the structure of discontinuities rather than by the properties of the intact material. Therefore, any design scheme for rock slopes must consider all the kinematically possible modes of failure.

The design of stable open pit walls in the foothills and mountain surface coal mines of Alberta and British Columbia is essential to ensure safety of the operations. Simultaneously the economics of the operations demand that these pit slopes be cut at as steep an angle as possible to minimize the amount of waste rock it is necessary to excavate. Much engineering time and effort are therefore devoted to identifying the potential modes of slope failure, to analyzing the pit wall stability and to designing remedial measures in case of instability.

In many cases the pits are developed in steeply - dipping strata. Often it is desirable to excavate the footwall parallel to the strata to avoid undercutting the strata and initiating footwall failure. Much work has been done to address the stability of bedded footwall slopes and design guidelines for the support of bedded footwall slopes have been proposed. However, on the other side of the pit where the bedding dips in the opposite direction to the pit wall and, with steep bedding, the potential exists for toppling failures to occur in the highwall. The mechanisms of toppling failures are complex and are probably the least understood of all the modes of pit slope failure; as a result techniques for the analysis and assessment of the stability for the various potential modes of toppling failure are in their infancy and much work needs to be done to further develop practical design guidelines for this situation.

2. TOPPLING FAILURES - LITERATURE REVIEW

2.1. Geological and structural description of the problem.

2.1.1. Physical Environment.

The first classification of the toppling failure that was widely accepted by the geotechnical and geological society was the one published by Goodman and Bray in 1976. Following their paper, "Toppling is a mode of failure of slopes involving overturning of interacting columns. In rock, such columns are formed by regular bedding planes, cleavage, or joints which strike parallel to the slope crest and dip into the rock mass; this contrasts with the structure of slides in which the controlling discontinuities dip into the open space. Toppling mechanisms also operate in soft rocks and soils with vertical or backward inclined tension cracks. Since folding is well known as a deformational mechanism in layered rocks, and overturning is recognized as a fundamental failure mode for dams and retaining walls, it is surprising that folding and overturning were not until recently recognized widely in rock slopes. Such failures prove to be widespread in many different kinds of rock masses".

Cruden (1989), Cruden and Hu (1990) and Hu and Cruden (1992), formulated a thorough geological definition of the toppling failure, as well as the necessary terminology. They also showed, that toppling can occur over a much wider range of discontinuity orientations than stated by Goodman and Bray. Cruden and Hu used conveniently the fact, that rock slopes formed in the rock mass could be classified according to their orientation with respect to the orientation of the penetrative discontinuities, such as bedding planes or schistosity. Cruden and Hu (1990) summarised the terminology defined by Powell (1875) and Calloway (1879) in the following manner:

Cataclinal slopes are such slopes, in which the penetrative discontinuity dips in the same direction as the slope.

Anaclinal slopes are the slopes in which the penetrative discontinuity dips in the direction opposite to the slope.

Orthoclinal slopes are the slopes, in which the azimuth of the dip direction is perpendicular to the azimuth of the slope direction within the range of ±20 degrees.

Plagioclinal slopes are the remaining slopes which are oblique to the strike of the bedding or to another structure.

Cataclinal slopes may be further divided into *overdip slopes* that are steeper than the dip of the discontinuity and *underdip slopes* that slope less than the dip of the discontinuity. Slopes parallel with the dip of the discontinuity are called *dip slopes.*

Both cataclinal and anaclinal slopes containing steeply dipping penetrative discontinuities are potentially susceptible to toppling. It is possible to find favourable conditions for natural toppling everywhere. Of course, such conditions can be created in any steeply dipping layered rock strata by mining activity.

2.1.2. Modes of toppling

"The modes of failure that have long been recognized in slopes of jointed rock masses involve sliding on a surface within the mass, and falling or detachment from surfaces close to the edges of the mass; i.e. sliding failures by either translational or rotational movement, and rock-falls" (de Freitas and Watters, 1973). Certainly multiple modes of failure are common; however it is now evident that these modes, even when interacting, cannot explain all the failures that can be found in slopes of jointed rock. There are failures observed having a structure that cannot be explained by sliding. These can occur above surfaces whose dip would not allow sliding to develop with the present angles of friction and sometimes they occur above surfaces on which sliding has already taken place. As noted by Freitas and Watters a third mode of failure can occur in rock slopes in addition to sliding and rock falls. This third mode of failure is toppling.

There were few case histories dealing with toppling published before 1976. Some early descriptions of toppling failures were given for example by Zaruba and Mencl (1969), de Freitas and Waters (1973), Heslop (1974) and by Bukovansky, Rodriguez and Cedrun (1974). In none of these papers did the authors try to analyze the mechanism which triggered the failure.

In 1976, Goodman and Bray presented the first classification of toppling failures. Their classification has become broadly accepted, and included the following terminology:

> *Flexural toppling* (fig.2-1, page 7) can occur in rocks with one preferred discontinuity system oriented to form a rock slope composed of semicontinuous cantilever beams. These columns break in flexure as they bend forward. It is obvious that thinner layers of the same length tend to bend more and transfer the load to the thicker layers. Erosion or mining activity can trigger this mechanism. Failure then starts at the toe and progresses backwards, creating wide, deep tension cracks. The lower portion of the slope is covered with disoriented and disordered blocks. The bending and cracking continue until the line of the tension cracks intercepts the crest of the slope, provided that the geology did not change through the slope. The bending is gradual and there is no obvious base of this mechanism that could be discovered by drilling. "Water levels will vary greatly from one drill hole to another since there may be little or no hydraulic communication across the cantilevers. Flexural toppling occurs most notably in slates, phyllites, and schists" (Goodman and Bray 1976).
>
> *Block toppling* (fig. 2-2, page 8) can occur in the rocks with more than one system of joints, typically with one system of bedding planes and two systems of widely spaced joints. Longer, overturning columns at the crest of a slope are leaning on the shorter blocks at the toe creating a system of toppling and sliding blocks. "The base of this disturbed mass is better defined than in the case of the flexural toppling; it consists of a stairway which, generally, rises from one layer to the next" (Goodman and Bray, 1976). Because of the opened system of joints and interblock caves throughout the disturbed zone, the water pressure will not be

high. Block toppling occurs mostly in thick-bedded sedimentary rocks such as limestones and sandstones, as well as in columnar jointed volcanics.

Block flexure toppling (fig. 2-3, page 9) is characterized by pseudo-continuous flexure of the numerous blocks in highly jointed rock. Sliding is concentrated at the toe and there is a combination of sliding and toppling in the rest of the unstable slope. Sliding occurs either directly as a result of the thrust applied by the upper overturning block on the lower resisting block, or as a result of steepening of the joint angles of the toppling column, or as a combination of these two mechanisms. The character of the disturbed zone is again widely open but with fewer edge to face contacts than in the case of block toppling. Typical rocks susceptible to block flexural toppling are interbedded sandstone and shale, interbedded chert and shale, and thin bedded limestone.

Secondary toppling is a mode of behaviour "which may be excited by another, independent phenomenon where overturning would otherwise be unlikely to occur" (Goodman and Bray, 1976). In the paper Goodman and Bray described Slide head toppling, Slide base toppling, Creep toppling, Slide toe toppling and a Tension crack toppling.

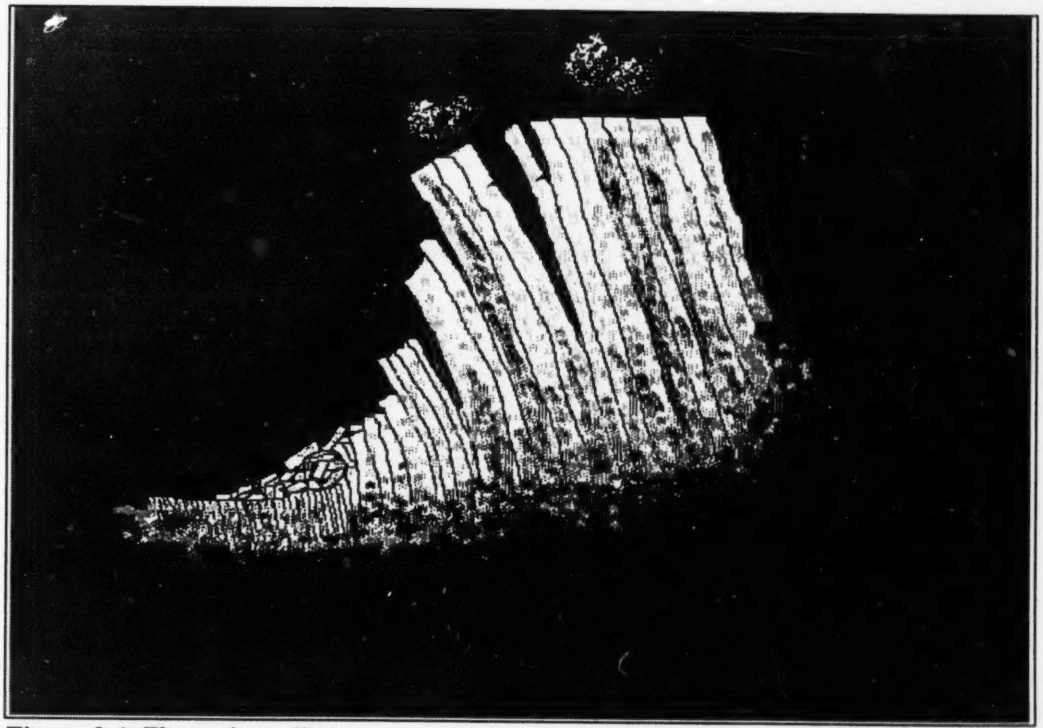

Figure 2-1 Flexural toppling.

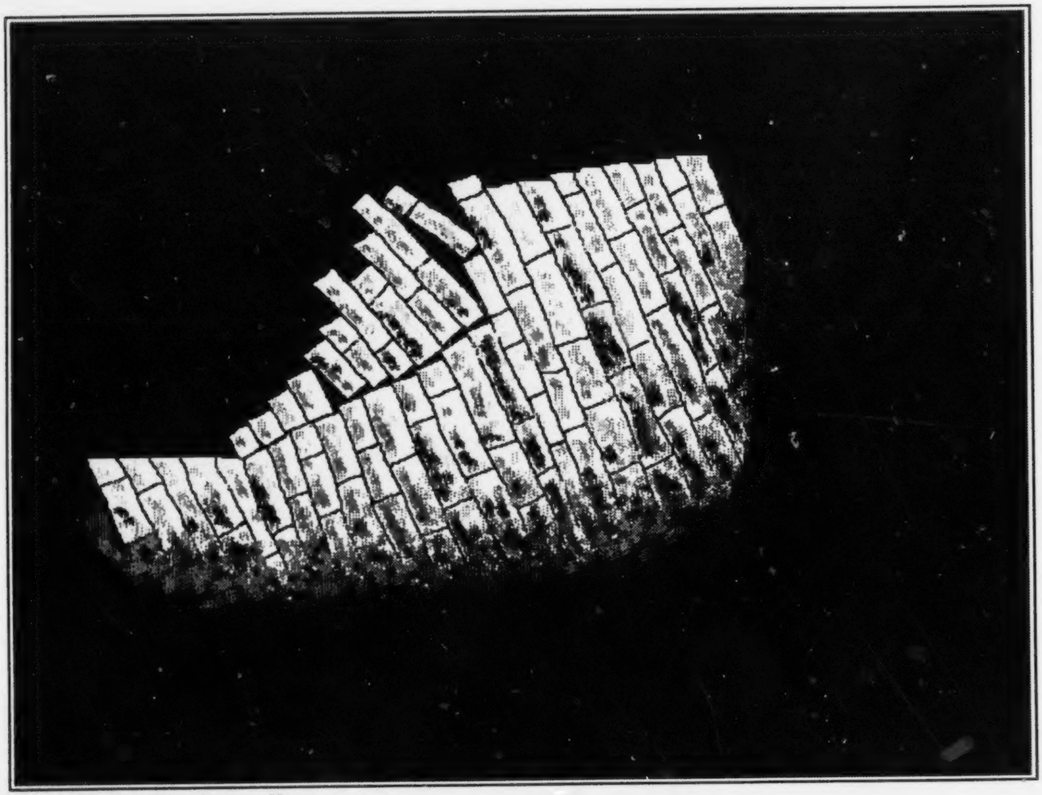

Figure 2-2 Block toppling.

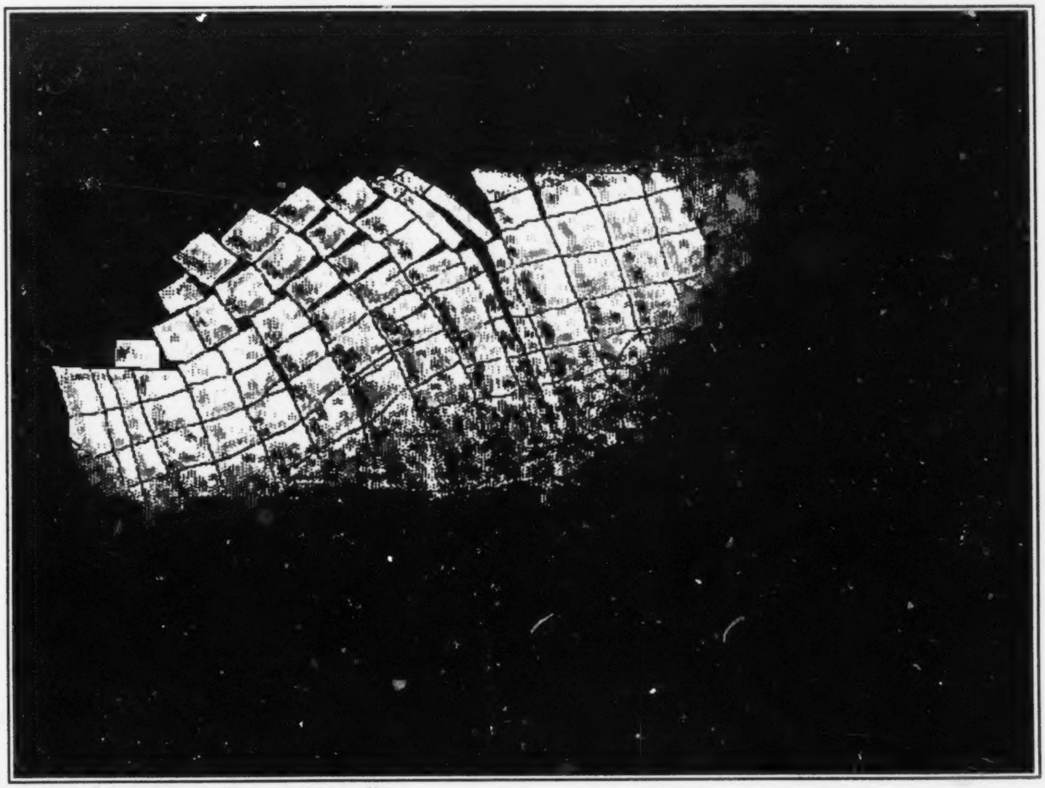

Figure 2-3 Block flexural toppling.

2.1.3. Structural control of toppling .

Cruden (1989) pointed out that toppling may occur on cataclinal slopes when

$$\beta + (90 - \psi) > \phi \qquad \textbf{(2-1)}$$

where β is the dip of a slope, ψ is the dip of a discontinuity, and ϕ is the angle of internal friction of the discontinuity. Equation 2-1 is valid for zero cohesion on the discontinuity, and for $\sigma_3 = 0$ (fig.2-4). These conditions are valid only at the surface of the slope where the maximum stress σ_1 is parallel to the slope. In both figures Θ is an angle between a normal to the discontinuity and the direction of σ_1. What this equation really says is, that under these conditions, sliding on the discontinuity is possible. That certainly does not mean that toppling is also possible. This equation can be taken as the broadest limit outside of which toppling is excluded. The geometry of such a slope is shown in fig. 2-5. According to Cruden (1989), it is likely that on the underdip cataclinal slopes *only Flexural toppling* can develop under gravity only by the gradual folding of the layers when the driving force in this case is the weight of the rock released on the surface by weathering processes. The driving force necessary for the triggering

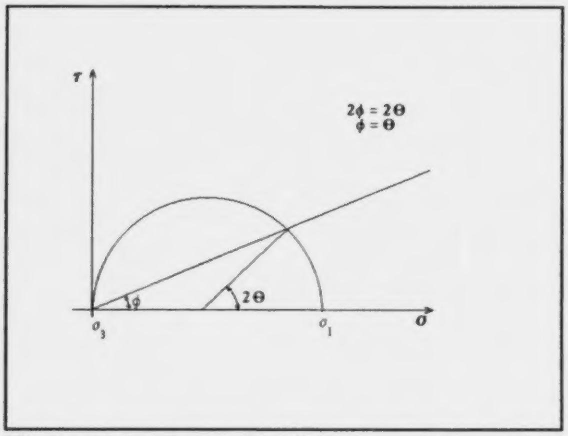

Figure 2-4 Stress distribution on the surface of a rock slope.

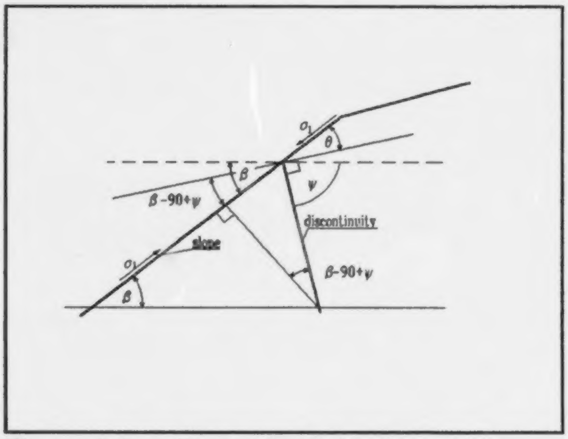

Figure 2-5 Geometry of the slope with discontinuity.

of any toppling process can be generally created by any activity which would sufficiently steepen the rock slope or change the loading of the rock, provided that the geometry of the rock-slope system is favourable for toppling (page 3).

According to Hu and Cruden (1992) *Block flexural topples* may also develop under gravity alone. This kind of topple occurs where the ratio of the spacing of strike joints to the bedding thickness is less than two. Toppling retrogresses gradually into the rock mass without creating any discontinuity at the base of the topple. In other words, no sliding surface is developed at the base of the failing rock mass. The movement is slow and finally the rotating rock layers again become stable without collapse of the rock slope. "Toppled bedding surfaces in *block flexural topples* appear smoothly folded in cross sections on scales much larger than the individual blocks, and bedding orientations gradually change along bedding layers" (Hu and Cruden, 1992). As the blocks move, little fine debris can enter the loosened rock structure .

Block toppling develops when the ratio of spacing of strike joints to the bedding thickness is larger than two and external forces may assist its initiation. The dip of bedding on the opposite side of the rupture surface can change by over 10°. Rupture surfaces are perpendicular to both bedding surfaces and the strike of joints; they generally extend less than 10 m and dip at around 35° downslope. Sliding on rupture surfaces either follows the strike joints or partly cuts through thin layers and partly follows the joints. When the rock mass is composed of layers of different thickness, sliding surfaces generally follow the weakest planes in the thicker units.

Block topples can be further divided to *Chevron topples* and *Multiple block topples*. *Chevron topples* are formed by only one layer of the blocks above a single rupture surface and they are characterized by steeper slopes (not less than 35°) When the toppled masses slide away, toppling progresses another few meters up the slope creating new sliding surface. *Multiple block topples* are formed by several "storeys" of toppled rock and they are characterized by the slopes gentler than 35°. In this thesis Hu and Cruden's classification, which is consistent with the original Goodman and Bray paper will be used.

2.1.4. Toppling on cataclinal slopes.

According to Cruden and Hu (1990) the common mode of failure on *overdip slopes* is sliding, governed by the geometry of a slope and discontinuities and by the strength parameters of the discontinuities. They did not observe toppling on these slopes.

The common mode of failure on the *dip slopes,* according to the same authors, is buckling. Sometimes buckling can be associated with toppling. Buckling generally can occur where the bedding layers are steep and the ratio of the thickness and the height is small.

Cruden (1989) pointed out that toppling may occur on *underdip slopes* when the geometry of a slope is as shown on fig. 2-6 and the basic condition given by equation 2-1 is fulfilled.

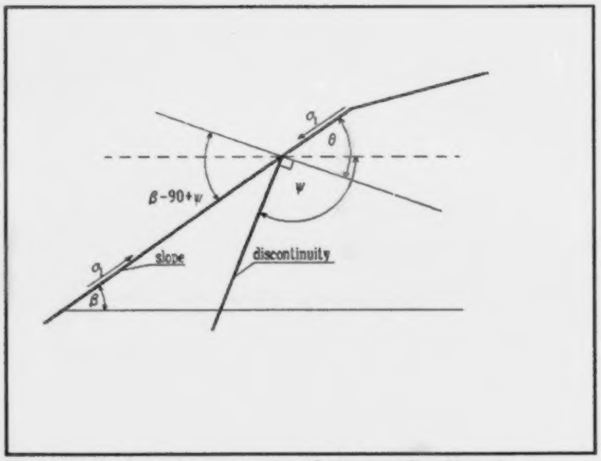

Figure 2-6 Geometry of the underdip slope with discontinuity.

2.1.5. Toppling on anaclinal slopes

The equation (2-1, p.10) is valid on anaclinal slopes including the comments. It is certainly true that as the rock mass topples, there must be some sliding between the toppled blocks. Wyllie (1980) documented such a movement in a Rocky Mountain surface coal mine. Commonly the failure mechanism is the combination of toppling on bedding and sliding on the cross joints. Common toppling was, according to Cruden and

Hu (1990), confined to cases where

$$\phi>(90-\psi) \lor \psi>2\phi \qquad \textbf{(2-2)}$$

assuming that the angle of friction on the joints is the same as that on the bedding planes.

Geometry of an anaclinal slope is shown in the fig. 2-7.

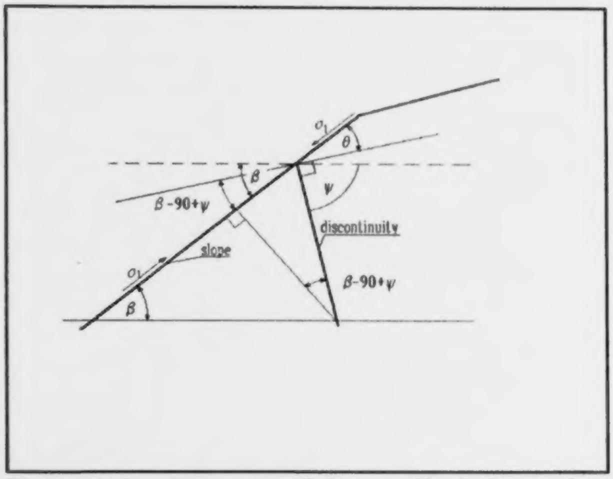

Figure 2-7 Geometry of the anaclinal slope with a discontinuity.

2.2. Toppling models.

The models used for analysis of the toppling failure can be divided into three categories:

a) Limit equilibrium models.
b) Numerical models.
c) Physical models.

2.2.1. Limit equilibrium models.

Limit equilibrium models are mathematical models usually exploiting the closed form solutions of the forces acting on the structure of interest. The equilibrium can also be expressed in the terms of stresses. There are some questions about the role of limit equilibrium analysis as well as about the role of the other methods. However, this problem will be discussed in section 2.2.4. of this chapter .

The first basic, and till now the only limit equilibrium model of toppling is that of Goodman and Bray (1976). They presented a simple analysis of *block toppling* on a positively stepped base. This model was later upgraded several times, (Scavia et al 1990, Piteau et al 1981) but the core of all the successive approaches remained unchanged. It was formed by the static equations formulated by Goodman and Bray (1976). Consider the regular system of blocks shown in the fig. 2-8. A slope at angle θ was excavated in a rock mass with layers dipping at 90-α. The toppling base is formed by a stepped surface with general inclination β. The constants a_1, a_2, and b shown in the figure are given by

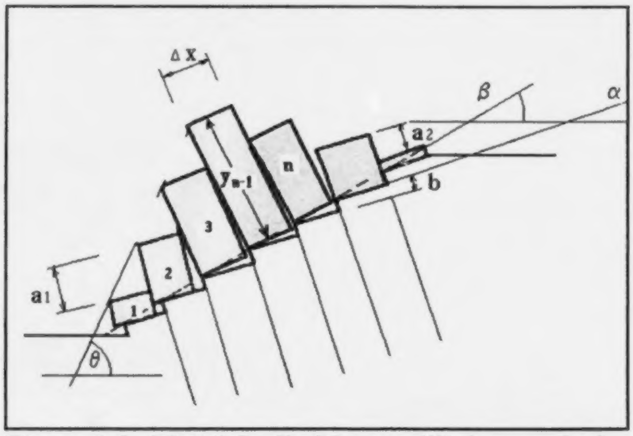

Figure 2-8 Model for limiting equilibrium analysis of toppling on a stepped base.

$$\begin{aligned} y_n &= n(a_1 - b) \\ y_n &= y_{n-1} - a_2 - b \end{aligned} \qquad \textbf{(2-3)}$$

The height difference between two blocks below and above the crest, and the height of the step n is

$$\begin{aligned} a_1 &= \Delta x \ \ \tan(\theta - \alpha) \\ a_2 &= \Delta x \ \ \tan\alpha \\ b &= \Delta x \ \ \tan(\beta - \alpha) \end{aligned} \qquad \textbf{(2-4)}$$

At the top of the slope, y_n / Δx < cot α and blocks are stable unless α > ϕ. This assumption is reasonable because the blocks close to the crest are short. Below the stable zone blocks tend to topple, the upper leaning on the lower ones. At the toe of the slope blocks are again shorter; $y_n / \Delta x < \cot \alpha$, and they will not topple under their own weight. However, the force transmitted from the unstable region can still cause these blocks to topple or slide. That is the reason why all the blocks,starting with the first toppling one, must be tested both for sliding and toppling. Forces acting on a toppling block are shown in the fig. 2-9 and forces acting on a sliding block are shown in the fig. 2-10.

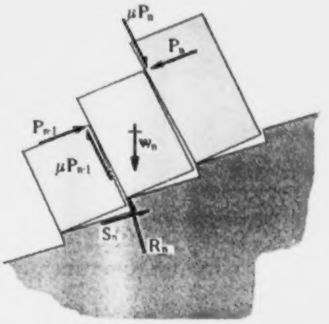

Figure 2-9 Forces acting on a toppling block.

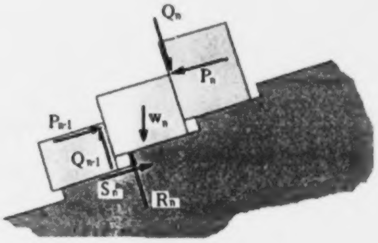

Figure 2-10 Forces acting on a sliding block

In a similar way to the geometry of the slope, the points of application of the acting forces can be calculated (eq.2-5).

$$\begin{array}{ll} \textit{Below the crest:} & M_n = y_n \\ & L_n = Y_n - a_1 \\ \textit{For the crest:} & M_n = y_n - a_2 \\ & L_n = y_n - a_1 \\ \textit{Above the crest:} & M_n = y_n - a_2 \\ & L_n = y_n \end{array} \qquad \textbf{(2-5)}$$

Finally, the force $P_{n,t}$ necessary to prevent toppling, and the force $P_{n,s}$ necessary to prevent sliding can be calculated (eq. 2-6).

$$P_{n-1,t} = \frac{P_n(M_n - \mu\Delta x) + (w_n/2)(y_n \sin\alpha - \Delta x \cos\alpha)}{L_n}$$

$$P_{n-1,s} = P_n - \frac{w_n(\mu\cos\alpha - \sin\alpha)}{1} - \mu^2 \qquad \textbf{(2-6)}$$

The factor of safety was defined by dividing the applied friction coefficient by the friction coefficient required for equilibrium with the given support force P_0. Unfortunately, for this kind of failure, the definition is not the happiest one as noted by Zanbak (1983).

Goodman and Bray's analysis deals only with the initial situation in the slope before any deformation occurs. However, once a column of rock starts to overturn, the acting forces start to change and the friction, necessary for equilibrium, changes as well. At the beginning, the magnitudes of overturning moments and subsequently the magnitudes of sliding forces increase, but later, when the blocks come again to the face to face contact, it drops sharply, and the calculated safety factor can rise above one, suggesting that the slope becomes stable again. Actually, according to Goodman and Bray (1976), this is exactly the case in many natural slopes.

An interesting case history of using of a variant of the method described above was presented in 1981 by Piteau, Stewart and Martin. They used this analysis formulated for *block flexural toppling* for analyzing a flexural toppling failure in a metal mine in Australia. They imbedded into the original solution various gravitational forces and water forces. However, there could be some doubts concerning the classification of the mode of toppling with respect to the original terminology of Goodman and Bray. The photographs presented as an example of the *flexural toppling* resemble more *block toppling* in one case and *block flexural toppling* in the other case. The biggest difference between Piteau's observation and the definition of the flexural toppling mode is the presence of a well developed basal discontinuity at the base of the topple classified by Piteau as a flexural one. The same discrepancy will be noted in the chapter concerning numerical methods.

This case history pertains to both bench design and overall slope design of a high wall in an open pit iron mine in Australia. Toppling in this case occurred along foliation joints developed along schistosity. As could be expected, the spacing of the foliation joints was found to be extremely important, and it varied from 30 cm to 150 cm. The authors of this analysis found that the best correlation between the model results and between the real slope behaviour was for an assumed spacing of the joints of 10 m. The big difference between the input and real field spacings was explained by a variation of the stresses along the joints. With increasing depth the stresses increase, and so does the shear strength along the joints. The other explanation was based on the assumption that it was not likely that there were many persistent foliation joints on the scale of the slope. On the other hand the spacing of the foliation in the benches was assumed to be 1.5 m.

It is not very surprising that with these assumptions the overall slope was found safe and the benches unsafe. What is interesting in this case history is that after adjusting the method according to field observations, it described the real situation with reasonable precision, and even reacted correctly to ground water level changes. It is even more interesting if it is realized that the method, according to the authors, was used for simulating the *flexural toppling* mechanism, which is not consistent with assumptions imbedded in the original Goodman and Bray analysis of the *block toppling* on a stepped base. However, the most important information to be learned from this paper is that the discontinuity sets important for the overall slope stability are not necessarily important for the bench stability and vice versa. As a result of this fact a mine slope can be stable, and the bench can fail, or the benches can be stable and still there might be an overall slope failure.

Another interesting example of using the "stepped base block toppling analysis" was given by Wyllie (1980). Three case histories of toppling failures of rock slopes were described in his paper. Two of them were simple block toppling failures suitable for the analysis used. The third case, failure of the high wall in an open pit coal mine on the eastern foothills of the Rocky Mountains, was an example of complex *block toppling* or *flexural toppling*. Features characterizing this failure, and the geological conditions of the site were identical to those observed at the locality studied in this thesis. The coal occured as an interbedded sequence between folded shales and sandstones. On the south limb of the asymmetrical syncline, layers with a spacing of about 2 m were overturned and dipped at about 70° into the pit. The beds formed tall, narrow slabs that underwent a toppling movement, which reduced support at the toe of the slope so that, eventually, the upper slope started to move. The first cracks were observed after seven months when the pit was 10 m deep. The pit was carefully monitored and it was mined to the designed depth of 150 m. About 18 months later the slope movement started to accelerate. Tension cracks developed at the top of the mountain approximately 300 m above the pit bottom, and about 600,000 m^3 of material failed along the pit crest. After that, all movements slowed down to the level of few mm a day or less. Wyllie believed that the decrease in the rate of movement was due to a drop of ground water pressure within the slope, as well as to an increase in the resistance, as deformation changed the edge-to-face contact between blocks to face-to-face contact again. From this note it was obvious that the author believed that it was the *block toppling* failure mode that governed the deformations. Unfortunately, Figure 5 in Wyllie's showing the bedding at the crest of the pit resembled more block *flexural toppling* than flexural toppling mode of failure. It was inferred that the continued movement of the toppling failure had removed support from the toe of the upper slope, and this had triggered the upper slide.

Analysis of the toppling failure was carried out using the Goodman and Bray model for *block toppling* with one slight modification that enabled the incorporation of different angles of internal friction for the sides and the base of slabs. Results showed that a friction angle of 25° on the sides and 42° on the base of the blocks was required for equilibrium. These are approximately correct values for shale and sandstone, respectively. After this minor improvement of the original method, the analysis provided reasonable answers. However, as mentioned by author, there is one important drawback of the procedure used. That is that the angle of a failure surface must be selected. The angle governs the height of the slabs that, in turn, has a significant affect on their tendency to topple. It is obvious from the character of the analysis that the calculated stability condition of the slope is highly dependent upon the angle selected for the failure surface.

Another case history using the model of toppling on a stepped base was published by Teme and West (1983), who studied the influence of allowing or not allowing drainage of the ground water on some secondary toppling failure mechanisms in discontinuous rock slopes.

Piteau and Martin (1981) and Zanbak (1983) presented design charts for rock slopes susceptible to toppling which were based on the calculations using the Goodman and Bray model.

The next important step forward among the limit equilibrium analysis of toppling was presented in 1990 by Scavia, Barla and Bernaudo .

2.2.1.1. Probabilistic stability analysis of block toppling failure.

The role of statistics in rock mechanics and in geotechnics has generally played an increasingly more important role in the recent years. This seems to be the logical direction of development. While the computational methods are dealing sometimes with minute details, the knowledge of a rock mass structure in particular cases is often very crude. Picking up one set of information from laboratory and field tests, and running them through some of the numerical models may be dangerous, and it can only be hoped that the result is not too far from reality. Statistics offers an opportunity to take into account all available data, and gives also an answer about the credibility of final results.

In 1990 Scavia, Barla and Bernaudo presented a 2-D limit equilibrium analysis of rock blocks resting on a stepped failure surface using a Monte Carlo simulation procedure and Markov Chains theory. Knowing the variability of the parameters describing the structure of a rock mass, a number of possible failure paths are generated using a Monte Carlo simulation. For each formed failure surface, the statistical distribution of the interaction forces is calculated, again using a Monte Carlo simulation. Then the probability of failure of one or more blocks is calculated using the Markov Chains theory. Thus the influence of variability of geometrical and strength parameters is incorporated into the original model to which the hydrostatic, seismic and externally applied forces were added.

2.2.1.2. Probabilistic rock structure modelling

According to Miller (1983), slope stabilities in discontinuous rock masses are primarily controlled by geologic structures because displacements occur along surfaces of weakness. Potential failure structures can be divided into two groups. Within the group of major structures are discontinuities such as faults, lithologic contacts, or other features with lengths comparable to the size of the study area. Within the group of minor structures are joints, foliation, and bedding planes. As noted earlier, stability of each slope should be evaluated in terms of structures important for stability of that particular slope. For example, stability of an overall slope and of a bench in the very same open pit could be governed by different structures. Discontinuity characteristics such as orientation, spacing, and length are random variables that can be modeled by statistical distributions estimated from mapping data. Mapped fracture orientations are plotted, for example, on Schmidt's lower-hemisphere projection, which allows contouring of pole densities that appear as clusters of points on the plot. Each cluster represents a fracture set. A histogram can be now constructed for each characteristic (dip, dip direction, spacing, length etc.) in a given design set, and the probability distribution that best describes the data is then determined. Once having the basic statistical information, a satisfactory simulation model should be selected.

The fracture set simulation procedures based on Monte Carlo techniques as used by Scavia, Barla and Bernaudo (1990) rely on random sampling of the probability distributions of fracture set properties, and they are not capable of incorporating known spatial correlations, and they often require excessive amounts of computer time.

Xing (1988) published the mathematical model of probabilistic analyses for a jointed rock slope in which a Monte-Carlo simulation technique, based on the random sampling of vectors with a jointly n-D normal distribution, was used, and the correlation between the failures was taken into account.

Kulatilake and Wathugala (1991) put down block development of eight 3D joint geometry modelling schemes that investigate statistical homogeneity, incorporate corrections for sampling biases and applications of stereographical principles. As they stated, a joint geometry pattern may vary from one statistically homogeneous region to another. Each statistically homogeneous region should be represented by a separate joint geometry model. This kind of assumption suggests that there could be some correlation among the structural features within some geological region, but this fact is still not incorporated into the model.

Unfortunately, the geological structures within some particular area are almost always spatially correlated, and in omitting this fact, an important piece of information is ignored. However, geostatistic methods can be employed to determine the nature and extent of the correlation (Miller, 1983). In classical statistics the samples collected to describe an unknown population are assumed to be spatially independent. In contrast, geostatistics is based on an assumption that in particular area samples are spatially correlated, and that this correlation can be statistically and analytically expressed as a function called the variogram function. Typically, weak second-order stationarity is assumed in such an analysis, and estimates of the variogram functions are computed along the main vector line of each design set. An example of a probabilistic analysis of bench stability for use in designing open pit mine slopes, utilizing the previously defined principles, was given in 1983 by Miller.

Another example of a local probability slope stability analysis introducing geostatistics was given in 1988 by Young and Hoerger. As they implied, procedures such as ordinary kriging, indicator kriging or mononodal kriging, are applicable to both scalar and vectorial random variables. In other words the joint orientation, for example, can be regionalised as scalar variable by separating dips from dip directions and assuming their mutual independency, or the directional data or vectorial variables can be directly regionalised to study joint orientation. It should be noted that geostatistics is general, and applicable to any characteristic parameters of physical properties for geotechnical materials such as strength values, elastic or plastic constants and flow parameters. Considering the dispersion of these parameters around their mean values as well as their spatial variations, the local probability analysis is a natural choice for solving various geotechnical problems. Unfortunately, the numerical procedures currently used in rock mechanics are based on deterministic methods and they are still waiting modification to a stochastic approach.

2.2.2. Numerical models

Numerical methods have been used with remarkable success in mechanical and aerospace engineering. As they were imported to rock mechanics, so was a design methodology that emphasized precise predictions of system behaviour. It has been suggested by Whyatt and Julien (1988) that there are four possible uses of the numerical model analysis: as an ultimate design tool, as a method of last resort, as an aid to judgement and as the calibrated model.

Using numerical methods as an ultimate design tool is, especially in geotechnics, a risky business. As recent numerical models are still of a deterministic nature, the system properties and mechanics of the studied rock mass must be defined as if they are exactly known. However, the difficulties and uncertainties inherent in defining of the rock mass properties are widely recognized, and it is acknowledged that as ultimate design tools numerical methods are inadequate. Unfortunately, for different reasons a similar conclusion can be drawn about each category of the design tools available.

As a method of last resort, numerical methods are sometimes used to establish some basis for design, when empirical or analytical methods are not available. They provide in this case, the only tool which can support an engineer's judgement in some untypical or new conditions.

As an aid to judgement, numerical models can be used for studies that identify the most threatening failure mechanisms as a guide to further site investigation, or assess the relative merits of alternate designs. Simply, the purpose of modelling data-limited problems is to gain understanding and to explore potential alternatives. In other words, numerical models are used to develop the intuition of the designer rather than providing design specifications.

Finally as a calibrated model, numerical methods are used as powerful design tool, and have often proved to be valuable in back-calculations of the cause of disastrous failures. The calibration process recognizes that rock mass behaviour often deviates significantly from that predicted by field and laboratory tests. However, it should be noted that the calibration process is not unique for numerical models and is widely used in almost all the modelling fields.

The most useful methods using numerical procedures are *finite elements, boundary elements, distinct elements and finite difference methods.* Models built up using these methods are now broadly used in geotechnics.

According to Brady and Brown (1985), the basis of the *finite element method* is a division of the defined domain surrounding the excavation into an assembly of discrete, interacting elements. The assumption made in the method is that transmission of internal forces between the edges of adjacent elements can be represented by interactions at the nodes of the elements. The procedure, as originally created, seeks to analyze the continuum problem. As noted by Cundall, Voegele and Fairhurst (1975), attempts are being made to overcome this restriction by incorporating joint elements to model discontinuities, (Goodman,1976; Shi, Goodman and Tinucci, 1985; Shi and Goodman, 1988), but even with this kind of element the displacements must necessarily remain small. This is important point, because often in general, and almost always in the case of toppling, the behaviour of a structure after failure is a matter of interest. The advantage of generally all differential methods, including finite elements, is their ability to deal with non-linear behaviour.

In the *boundary elements methods* the problem is specified and solved in terms of surface values of the field variables of traction and displacement. As only the boundary of a problem is defined, the method provides a unit reduction in the dimensional order of a system, resulting in significant advantage in computational efficiency, compared with the differential methods. However, these methods are best suited to modelling linear behaviour.

In the situation where the rock mass behaviour is dominated by discontinuities, (when their stiffness is much lower than that of the intact rock), the elasticity of the blocks can be neglected, and they may be ascribed rigid behaviour (Brady and Brown, 1985). Cundall (1987) was the first to treat a discontinuous rock mass as an assembly of quasi-rigid blocks interacting through deformable joints of definable stiffness. In his *distinct element method* the algorithm is based on a force-displacement law specifying the interaction between the quasi-rigid rock units, and a law of motion which determines displacements induced in the blocks by out-of-balance forces. According to Cundall (1987), the distinct element method was originally developed to model the progressive failure of rock slopes, and is normally used to determine if a rock mass will fail under a given set of applied loads (including gravity), or to calculate the displacements that are accumulated if the system finally stabilizes. The method uses Newton's law of motion to obtain velocities and displacements from unbalanced forces, and a dumping mechanism to remove elastic strain energy as the blocks displace to an equilibrium position.

The finite difference method, in general, involves division of the body into a number of two dimensional elements interconnected at their gridpoints (ITASCA,1987). At each gridpoint, the equations of the motion are solved with respect to time. The resulting equations from the finite difference and finite element methods are identical for particular examples.

There are some other methods available dealing with a discontinuous rock mass, which have been developed in recent years. In 1988 Shi and Goodman presented a new method for computing stress, strain, sliding and opening of rigid rock blocks. In the same year (1988) Cañizal and Sagaseta developed a numerical model for the analysis of discontinuous systems formed by parallelepiped blocks. Chen and Xiong (1991) published an elastic-viscoplastic block theory for rock masses established by introducing the deformations of discontinuities. This method does not necessarily demand employment of a numerical technique. Unfortunately, information about these methods is not sufficient to make a judgement about their versatility, and so it was accepted by the author of this thesis that they are suitable exclusively for the purposes listed by their creators. There are not many examples in the literature of using some of the numerical methods for modelling the toppling failure. In 1991 Orr and Swindels used the finite difference numerical code FLAC (Itasca, 1989) to model the flexural toppling failures identified in the field studies of Western Australian open pit gold mines. Failures occur there in a variety of highly to completely weathered rocks containing well developed, closely spaced foliation planes. An absence of penetrative discontinuities that may yield a basal release surface is a characteristic for the geology of the region. A number of flexural toppling failures of hanging walls were apparently progressive in nature, occurring over time spans of several minutes to weeks, and giving rise to a final, broadly-circular shape, both in plan and section. Analysis mirrored well this circular shape in the displacements vectors. Unfortunately, it is obvious that the location of the failure plane was not found and neither was the answer about post failure deformations and potential stabilisation, which is so characteristic for the toppling failure. The conclusion must be drawn, that even this commercially available routine is too general to model such a specific and complex failure mode as toppling.

2.2.3. Physical models.

Physical models are sometimes used when the numerical or analytical procedures are incapable of describing the structure under investigation, when the structure is of great importance, or whenever the results from mathematical modelling are too unusual or peculiar. They are usually costly and time consuming. On the other hand, they are sometimes able to provide better descriptive and clearer answers that any other methods. They were successfully used all over the world in many engineering fields such as bridge construction, tunnelling or geotechnics, as well as in geology where they were, for example, employed to model continental drift. Even if they have been gradually replaced by computer models in recent years, there have been some interesting studies carried out on behaviour of discontinuous rocks around the world.

As noted by Goodman (1976), in the physical model study, the real situation under consideration is replaced by a prototype, which will be duplicated at a convenient scale with a minimum of distortion with respect to the more important properties. The word prototype refers to an idealization of the field problem in which only those factors considered essential and relevant for the purpose of the study have been retained.

In 1985 Niyom and Sakurai published results from a study of potential toppling failures of varying dip of discontinuities and with different joint patterns by physical modelling, using two-dimensional aluminum block models. "At first, aluminum bars were stacked on the platform or base arm hinged to the main framework of the model. Then, by rotating the rotating arm which was initially set in the vertical direction, detailed study of the movement or displacement of the block model could be performed by using tracing paper attached to the platform for recording minute movements of the whole block model in a grid system". The most important target of this study was to find an empirical equation that could explain the failure behaviour in toppling. It was observed that for any joint (frame) inclination producing block movements, there was a base line that separates the displaced portion of the blocks from the unmoved portion. The angles from this base line to the platform were in the range of 5 to 10° for any joint inclinations and for $y/x = 1$ to 2 (Figure 2-11). Knowing the degree of initial movement and the base angle, and taking into account the consideration of the behaviour of toppling failure observed from block models, a relationship of displacement of two different points was expressed by equation 2-7. In the equation δ_0 and δ_1 are displacements, (x_0, y_0) and (x_1, y_1) are coordinates at two points A and B, and Θ is an angle in degrees between platform and base line (Fig. 2-11). The study comparing all displacements measured from block models, and displacements obtained by using the empirical equation (2-7) showed good agreement between two sets of data. It was also observed that stability of toppling mode of failure is lowest for a small degree of joint inclination and becomes higher when joint inclination increases. The authors also suggested that displacements of toppling could be determined by an empirical equation providing the sufficient monitoring of the slope is carried on.

$$\frac{\delta_1}{\delta_0} = \frac{y_1 - x_1 \tan\Theta}{y_0 - x_0 \tan\Theta} \qquad \textbf{(2-7)}$$

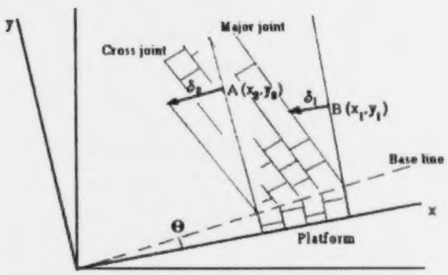

Figure 2-11 Relative displacement of toppling failure.

Barton (1974) simulated rock slope performance by a physical joint models. The models were two dimensional, discontinuous sets of approximately 40 000 discrete blocks divided by three groups of joints with angles of dip of 0°, 66° and 90°. The models were consolidated and stressed by rotating the model plane from a horizontal to vertical position, and then slopes were excavated in attempt to simulate the excavation of real slopes in jointed rock, while under realistic distributions of stress. Two models which were identically jointed, but which differed in the level of horizontal stresses, were compared.

According to numerical studies it was expected that failure should initiate at the zones of high stress gradients around the toe of the slope. Also it seemed to be reasonable to expect that the "high-stress" slope models would fail at smaller slope angles and/or excavation depths than the "low-stress" models. To the contrary, this anticipated behaviour proved wrong. Failure did not initiate at the toe, and by measuring the deformations, which were very small or zero in this zone, it was proved that it was not a region of the high stress gradient. Furthermore, the "high-stress" models proved to be much more stable than the "low-stress" ones. As a result the conclusion was drawn that only the vertical self weight induced stresses need to be considered in design of high slopes.

Several back analyses employing a simple equilibrium method of slices were performed. They were based on the assumption that the shear and normal stresses acting on the surfaces of shear failure were due only to self weight, and the horizontal stresses were ignored. There was relatively close agreement found between theory and model performance. It was eventually perceived that the normal and shear stresses acting on a steeply inclined joint set before excavation, reversed in magnitude when slopes were excavated above the same joints. This phenomenon could be understood as a kind of "overconsolidation" due to the fact that the slopes were originally consolidated under much higher normal stresses than the ones acting later during the failure. The effect of this preconsolidation was increasing the degree of interlocking of the rough surfaces of the tension joints, and thereby also increasing their shear strength. The effect was tested and proved correct in the subsequent laboratory tests on the rough rock joints.

In 1990 Warburton published the results of a study which tested, by means of the physical model, results from his mathematical block model. An assembly of medium density fibre board divided into blocks by 13 discontinuity planes was used as a prototype of a discontinuous rock system. The most important observation made in this study was that blocks which started to slide sometimes became stable again after undergoing some tilting or toppling movement. This behaviour has been observed many times in practice in the failures where toppling was involved.

As stated by Müller and Hofmann (1970): "The excavation of high rock slopes is an infringement on nature which makes considerable changes on the conditions of equilibrium." To study the influence of time effect, different strength parameters and different size and shape of the rock mass block structure, the authors decided to use a physical model built as two-dimensional body of equivalent materials which was subjected only to its own weight, and was regularly and continuously subdivided by two systems of joints. A slope was formed by excavation in horizontal layers at constant time intervals. It was demonstrated how differently a slope failure may develop over the course of time, and how different the picture at a particular moment of the development may be, depending on the geological conditions along an obviously pre-defined slip surface. Cases of block toppling failure or block flexural toppling followed by sliding or even by wedge failure were illustrated. (The case of toppling at the Havelock mine in Swaziland followed by a wedge failure was described by Heslop in 1974). The study showed clearly that the degree of separation along the two sets of joints makes a great difference to the deformation process. Depending on whether the separation along the joints is high or low and whether it is equal or different, shear displacements and toppling of the strata will occur along the set that consists of more persistent joints. It is therefore important to assess the continuity or discontinuity of the jointing, i.e. the degree of separation.

To close this section it should be noted that no mathematical or computer model can replace a good physical model as an aid to comprehend rock failure mechanisms which are not well understood. This is certainly the case with toppling, and a good physical model study would be a great help for further computer modelling.

2.2.4. Discussion of the role of Limit equilibrium, Numerical and Physical models.

There are neverending discussions in papers, as well as on the grounds of universities, about the role of the numerical, analytical or physical approaches in solving variety of engineering problems. Usually, as is common to human nature, everybody, or almost everybody advocates the method he or she is using. It is logical, and there is nothing wrong with that. Everybody is most familiar with the method they are using, and it probably serves well for the intended purposes. Unfortunately, as with each human product, no method or model is perfect; each has its advantages and its drawbacks. To obtain the best results for the questions asked, the purpose of a study must be clearly defined, and then the model picked which best suits the study purpose. An important issue, in using some method or approach, could be, for example, such an abstract thing as the experience in using that particular method.

The characteristics and advantages of three main groups from the family of modelling tools were given in the previous section. The variety of methods discussed was restricted by the narrow field of engineering, and by author's personal selection.

In the rest of this chapter the main limitations of the methods will be covered, and an attempt will be made to suggest the kind of problems, or purposes for which each method is the best when neglecting a personal experience factor. What is meant by the personal experience factor is expressed clearly by the fact that even the best method can fail when used by an inexperienced person, as well as by the fact that sometimes remarkable results are achieved by an experienced engineer with relatively simple tools.

The most important drawback of the limit equilibrium analysis of stability, as implied by Manfredini and Martinetti (1975), is the incapability of evaluating the progressive failure phenomenon. Generally, the joints show a brittle behaviour which is characterized by both a peak and a residual strength. The maximum available strength, or simply the strength, depends essentially on the mechanical properties of the particular soil or rock mass and on the distribution of the normal stresses along the potential failure surface. The exact evaluation of the distribution of the normal stresses generally requires consideration of the deformation characteristics of the soil but for majority of cases it could be approximated by some averages, as in the case of most of the methods of slices with sufficient precision. The real problem lies in the fact that the limit equilibrium method applied to a slope in near-failure conditions implies that the maximum strength is reached simultaneously by all the points on the failure surface; this does not actually occur. This could mean serious difficulties in the design and evaluation of the stability of a slope in a strain softening materials. Unfortunately, one of the important structures with distinctive strength softening behaviour is joints in rocks, which govern the behaviour of the rock mass.

Limit equilibrium methods are generally not used, and were never intended to be used, for calculating the rock deformations.

It will probably not be far from the truth to say, that conceptually limit equilibrium methods are close to the end of their development. That does not mean that they cannot be made more sophisticated and better aimed than they are now. They are also much easier to use; they consume much less input data time, computer time and computer space than numerical methods. There are almost no grounds for comparison of limit equilibrium models with physical models, because the purpose of using them is usually very different.

Limit equilibrium methods in the geotechnical field are still the basic tool predominantly used for design purposes, and in majority of the cases they provide adequate answers in reasonable time and cost ranges. They are simple to operate and simple to understand, and so it is much easier to avoid some fatal mistakes when using limit equilibrium methods than when using, for example, finite elements.

Numerical methods are in all aspects more complicated than the limit equilibrium methods. They are still under extensive development, and so all the comments are going to be made with respect to the present state of development.

Numerical methods are in general still restricted to relatively small deformations. This is not a big problem in case of deformations prior to failure. It could be a more important problem in case of deformations induced by yielding, which could be for some materials quite large and can involve developing of local cracks or other discontinuities. It is certainly a serious problem in case of toppling, when deformations can be measured in dozens of metres without knowing if the failure is going to be stabilised again at some later stage of overturning of the toppling blocks.

Another important drawback of numerical methods is their incapability of dealing effectively with discontinuities. Even if it is accepted as a fact that the elements developed for modelling discontinuities in the case of finite elements are working satisfactorily, they are again restricted to small deformations. In the case of distinct elements the ability of modelling the block behaviour is better (there are not sufficient tests of the method done yet), but the method as developed by Cundell (1987) is unable to take in account the failure through the solid rock which could be in progress at the same time as the deformations along the joints. This could be unfortunately the case with toppling.

Even if theoretically possible, there is still not a numerical method model capable of producing a clear definition of the failure surface. For example, a commercially successful finite difference program such as FLAC was not still ready in 1989 to deal with this important problem (Orr and Swindells 1991).

Another important disadvantage of modern numerical models, and especially of finite elements, is their need for excessive computer space and computing time. For example, if such an attempt is made, and the uncertainty of the knowledge of the elastic parameters and the exact values and directions of stresses in the real rock or soil were expressed in form of some probability distribution function at each node, then even when using simple Monte Carlo simulation the capacity and speed of current personal computers would be insufficient. But as shown for a much simpler model (Scavia, Barla and Bernaudo, 1990), the difference between the stochastic and deterministic approach could be the difference between a stable and an unstable slope as a result of the calculation.

Finally, the complex, and the time consuming data input process for numerical models is an important reason why this kind of model is still not being accepted by geotechnical engineers working at the actual structures, but they remain in the domain of the research projects, specially when dealing with geotechnical back analysis.

The last category of models discussed in this review is the group of physical models. One obvious disadvantage is the time necessary for their construction, and the expenses connected with this time consumption and sometimes with the laboratory equipment. The second disadvantage of physical models is their incapability of dealing with a combination of several parameters influencing the behaviour of actual geotechnical structures. Physical models are restricted to choosing a few, generally one or two, parameters and to scaling the model with respect to these parameters, restricting the affect of the rest of them to a minimum.

However, when choosing the most suitable type of the model for the intended purpose knowing the disadvantages of that particular method, it is possible to minimize their effect, and obtain the best possible results.

For example when using numerical models for studying some particular mechanism in some theoretical structure, there are no problems with uncertainties involving either the structure or the forces acting in this structure, as they are determined a priori as unique input parameters. A researcher can gradually change different parameters, obtaining exact answers about the reaction of each particular structure to changes of the parameters. That can help in understanding of behaviour of that structure in real situations. A similar case is back analysis, when the practical outcome is known, and model parameters can be changed to obtain that particular outcome. Again, this helps to understand the mechanisms taking place in some problematic geotechnical situation. Time is not an important factor for this kind of study, and the person carrying on the research is usually so familiar with the model that the complicated input is not a problem. There is certainly a great potential in the field of numerical models, but the time when these models are able to fully replace limit equilibrium and physical models is still far ahead.

Physical models are generally used for the purpose of research and in some special cases for the design purposes, as noted earlier in this chapter. Therefore the time necessary for carrying them out and their cost are not usually an important issue. The fact that a study is focused on a few parameters could even be an advantage for study purposes, because it is obvious which parameters affected behaviour of that particular model. This is not always the case in numerical models studies.

Finally, as believed by the author of this thesis, there is a single feature which is the most important one for any kind of model used in design of structures in the ground. There must be good correspondence or harmony among all the parts of the model. There is no point in using the most sophisticated procedures when calculating one relevant parameter, while neglecting, or using some very approximate procedure when calculating another important parameter. For example, when using an exact numerical method for calculating stability of a slope, neglecting the fact that the knowledge of geology, lithology, the geological structures as discontinuities, strength parameters, material parameters and the form of functions relating material deformations to acting forces is only very approximate, the result is an exact number, but without any knowledge as to the chance that it is correct. In the very same answer, there is no information about the position of this result within the spectrum of all possible answers. For example, the results of the numerical model study may indicate the failure of the structure. What is the chance that the result, and the parameters used for calculating deformations within this structure are correct? Is there some other combination of interpretation of the geological and engineering exploration results with much higher probability of occurrence? The answer is, likely, yes. There is certainly an outcome with higher probability of occurrence than the one based on randomly picked input parameters even when using judgement based on previous experience.

3. Theoretical approach.

3.1. Introduction.

Goodman and Bray (1976) described three basic modes of toppling, and classified them as Block, Block-flexural, and Flexural toppling. In the same paper they presented a simple analysis of Block toppling failure which, however, did not allow a search for the critical failure plane. Since then only a few attempts have been made to polish the original idea, and a number of case histories (Scaiva et al 1990, Piteau et al 1981) were presented where authors tried to use this theoretical analysis to deal with slopes where the geology did not satisfy almost any of the Goodman and Bray boundary conditions. Simply nothing better was available.

At the same time several mining companies throughout the world (Australia, (Orr et al 1991), Western Europe, (Scaiva et al 1990), Western Canada, (Hebil, 1993)) encountered geological conditions where toppling was the main failure mechanism, and their open pits experienced some major failures. That was the reason why in the year 1992, Luscar Ltd contacted the Mining, Metallurgical & Petroleum Engineering Department of University of Alberta, and asked for the research that would provide them with a procedure which would enable them to design stable pit slopes in geological conditions favourable for toppling.

3.2. Description of the problem.

The logical approach for dealing with this kind of problem would be to use some numerical routine such as finite elements or finite differences. Unfortunately, available programs use equations based on elastic theory, and a basic assumption of theory of elasticity is the one of continuity in the studied media. In other words, in classical linear elasticity theory it is assumed that displacements and displacement gradients are sufficiently small that no distinction need to be made between the Lagrangian and Eulerian descriptions. Several elements have been created for modelling discontinuities, but these elements are also restricted to small deformations. On the other hand, deformations taking place during toppling could be of magnitude of dozens of metres. They could be, and often are combined with sliding on the developed failure plane, and after undergoing this movement the toppling failure may stabilize without the overall collapse of the slope. Deformations taking place during block toppling, and flexural block toppling failures are obviously governed by discontinuities rather than by elastic properties of rock, and even in the case of flexural toppling, discontinuities are still as much of importance as the rock properties . For all these reasons, it would be necessary to develop a new model based on a combination of finite elements and distinct elements, but development of such a model would not only be difficult and time consuming, it also would be unlikely to be practical for mining design purposes. After discussion of the possible approach with officials of the Luscar company it was decided that the model used for the problem would be a a gridless routine capable of calculating stresses and deformations. .

3.3. Flexural toppling failure.

The model finally proposed for this failure mode was a system of interacting and noninteracting cantilevers (Fig. 3-1). This model is of course not a perfect approximation of reality, but assuming that rock behaves in a brittle manner, and that deformations within the solid rock before failure in tension are small, (in contrast the relative deformation between rock columns can be large), then all the practical models have one important common feature, and that is that the maximum bending moment occurs just above the support.

Examples of some possible static models of the system of interacting rock columns together with their characteristic moment diagrams are shown in Fig. 3-2, 3-3, and 3-4.

The maximum bending moments of the arrangements in Fig. 3-2 and Fig. 3-3 are the same, but the deflection curves of the cantilevers are obviously very different. The arrangement in Fig. 3-2 is the more realistic one of the two. The static model in Fig. 3-4 (next page) is probably the closest approximation to

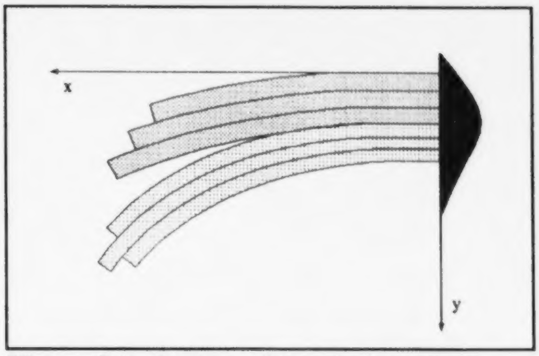

Figure 3-1 System of two independent groups of three interacting cantilevers.

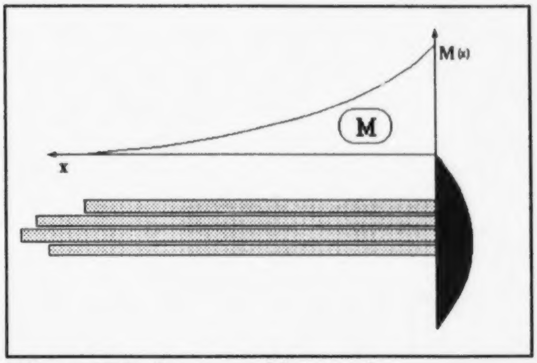

Figure 3-2 System of interacting cantilevers.

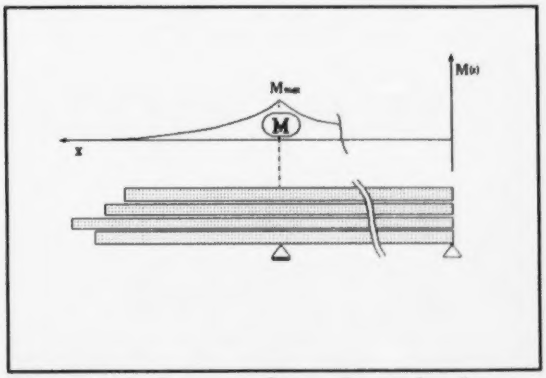

Figure 3-3 System of very long simple beams.

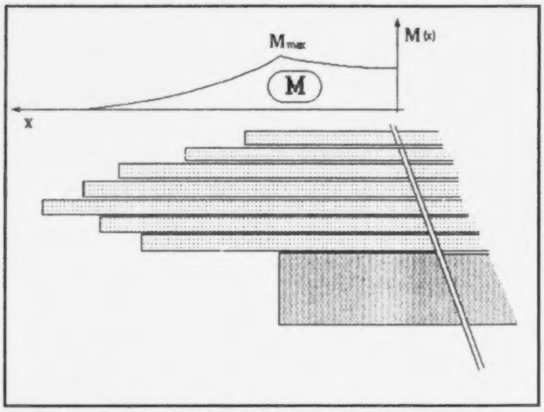

Figure 3-4 System of beams lying on an elastic foundation.

reality. On the other hand, solution of this problem would be possible only by using a numerical model, such as finite elements, but it is questionable if such a model would be able to handle deformations of cantilevers of length of dozens of meters. It is very likely that the basic assumption about small deformations would not be fulfilled. Furthermore the benefit of such a high precision model with respect to the information usually available about strength properties, for example in mining, would be questionable.

For the reasons mentioned before, the solution for the system of cantilevers in Fig. 3-2 was derived on the basis of the beam theory (appendix A). The system of forces

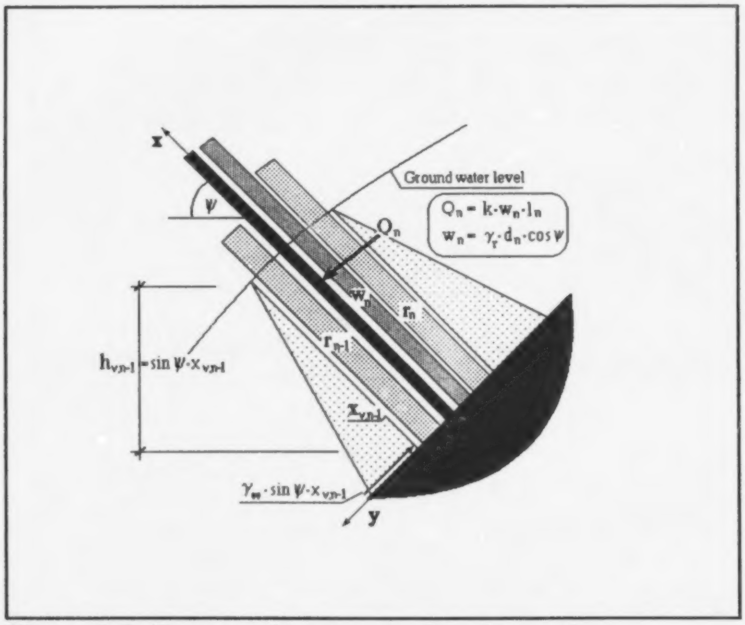
x
ψ
Ground water level
Q_n = k·w_n·l_n
w_n = γ_r·d_n·cos ψ
Q_n
w_n
r_n
r_n-1
h_v,n-1 = sin ψ·x_v,n-1
x_v,n-1
γ_w·sin ψ·x_v,n-1
y

Figure 3-5 Forces acting on one of the interacting cantilevers (flexural toppling).

acting on the one of the interacting cantilevers is shown in Fig. 3-5. They are reactions between cantilevers, the weight of the cantilever, water forces and seismic forces.

In the figure:

r_n .... reaction with the overlying cantilever

r_{n-1} .... reaction with the underlying cantilever

w_n .... weight of the cantilever

$h_{v,n-1}$ .... height of the water column below the cantilever

γ_w .... unit weight of water

Q_n .... seismic force

The equations for the model in Fig. 3-2, (system of interacting cantilevers), were derived according to the beam theory with following assumptions and boundary conditions.

Bending stresses:

1) Transverse cross sections perpendicular to the centroidal line of the beams before bending remain plane and perpendicular to the centroidal line in their deformed configuration.
2) Beams bend without twisting.
3) Beams consist of homogeneous and isotropic material which obeys Hooke's law.
4) Beams are straight with a rectangular cross-section.
5) The angle of internal friction, and the cohesion on bedding planes between the beams are zero.
6) The shape of the loading of the cantilever in question by reactions with overlying and underlying cantilevers is assumed to be a constant distributed load.

Shearing stresses:

7) Plain sections warp, but the shearing strain has little affect on the normal strain and, thus on the normal stresses.
8) Consequently, it is assumed that sections that are plane before deformation remain plane after deformation.

Equations describing the shear force $V(x)_n$ (3-1), bending moment $M(x)_n$ (3-2), angle between the tangent with the beam and horizontal $\theta(x)_n$ (3-3) and the deflection $y(x)_n$ (3-4) are derived and presented in the Appendix A as equations (A-39), (A-40), (A-41) and (A-42).

In these equations:

r_n .... reaction with the overlying cantilever

r_{n-1} .... reaction with the underlying cantilever

w_n .... weight of the cantilever

γ_w .... unit weight of water

Q_n .... seismic force

Geometrical parameters are shown in the figures A-1, ... A-8 in the appendix A.

In these equations the reaction with the overlying cantilever, the reaction with the underlying cantilever, shear force, bending moment, the angle between the tangent to the deflection curve with horizontal and the deflection itself are unknowns. There are actually five unknowns introduced and only four equations available. Unfortunately it is impossible to formulate any helpful boundary condition in terms of moments or shear forces; this is the main reason why the equation for deflection is introduced. The boundary condition in terms of deflections will be formulated later, together with the corresponding system of equations.

The shear force within the beam is given as

$$\begin{aligned}V(x)_n &= w_n(l_n-x) - r_{n-1}(x_{r,n-1}-x)\,u\langle x_{r,n-1}-x\rangle + r_n(x_{r,n}-x)\,u\langle x_{r,n}-x\rangle - \\ &\quad - \frac{\gamma_w \sin\psi}{2}(x_{v,n-1}-x)^2\,u\langle x_{v,n-1}-x\rangle + \\ &\quad + \frac{\gamma_w \sin\psi}{2}(x_{v,n}-x)^2\,u\langle x_{v,n}-x\rangle + \\ &\quad + Q\,u\langle x_{Q,n}-x\rangle\end{aligned} \tag{3-1}$$

Bending moment

$$\begin{aligned} M(x)_n = {} & w_n \frac{(l_n - x)^2}{2} - \frac{r_{n-1}}{2}(x_{r,n-1} - x)^2\, u{<}x_{r,n-1} - x{>} + \frac{r_n}{2}(x_{r,n} - x)^2\, u{<}x_{r,n} - x{>} - \\ & - \frac{\gamma_w \sin\psi}{6}(x_{v,n-1} - x)^3\, u{<}x_{v,n-1} - x{>} + \frac{\gamma_w \sin\psi}{6}(x_{v,n} - x)^3\, u{<}x_{v,n} - x{>} + \\ & + Q(x_{Q,n} - x)\, u{<}x_{Q,n} - x{>} \end{aligned} \tag{3-2}$$

The angle of tangent to the deflection curve with the horizontal

$$\begin{aligned} EI\theta(x)_n = {} & \frac{w_n}{6}[(l_n - x)^3 - l_n^3] - \frac{r_{n-1}}{6}[(x_{r,n-1} - x)^3\, u{<}x_{r,n-1} - x{>} - x_{r,n-1}^3] + \\ & + \frac{r_n}{6}[(x_{r,n} - x)^3\, u{<}x_{r,n} - x{>} - x_{r,n}^3] + \\ & - \frac{\gamma_w \sin\psi}{24}[(x_{v,n-1} - x)^4\, u{<}x_{v,n-1} - x{>} - x_{v,n-1}^4] + \\ & + \frac{\gamma_w \sin\psi}{24}[(x_{v,n} - x)^4\, u{<}x_{v,n} - x{>} - x_{v,n}^4] + \\ & + \frac{Q_n}{2}[(x_{Q,n} - x)^2 u{<}x_{Q,n} - x{>} - (x_{Q,n})^2] \end{aligned} \tag{3-3}$$

And finally the deflection

$$
\begin{aligned}
EIy(x)_n = {} & \frac{w_n}{24}[(l_n - x)^4 - l_n^3(l - 4x)] - \\
& - \frac{r_{n-1}}{24}[(x_{r,n-1} - x)^4 u\langle x_{r,n-1} - x\rangle - x_{r,n-1}^3(x_{r,n-1} - 4x)] + \\
& + \frac{r_n}{24}[(x_{r,n} - x)^4 u\langle x_{r,n} - x\rangle - x_{r,n}^3(x_{r,n} - 4x)] + \\
& + \frac{Q_n}{6}[(x_{Q,n} - x)^3 u\langle x_{Q,n} - x\rangle - x_{Q,n}^2(x_{Q,n} - 3x)] + \\
& + \frac{\gamma_w \sin\psi}{120}[(x_{v,n} - x)^5 u\langle x_{v,n} - x\rangle - 5x_{v,n}^4(x_{v,n} - x) + x_{v,n}^5(5 - u\langle x_{v,n} - x\rangle)] - \\
& - \frac{\gamma_w \sin\psi}{120}[(x_{v,n-1} - x)^5 u\langle x_{v,n-1} - x\rangle - 5x_{v,n-1}^4(x_{v,n-1} - x) + \\
& + x_{v,n-1}^5(5 - u\langle x_{v,n-1} - x\rangle)]
\end{aligned}
\tag{3-4}
$$

In the presented system of equations there are:

unknown	No. of unknowns	No. of available equations	Equation No
V(x)	n	n	3-1
M(x)	n	n	3-2
θ(x)	n	n	3-3
y(x)	n	n	3-4
r	n-1	0	

So it is obvious, that another n-1 equations are needed to solve the system.

To be able to formulate the missing equations, some other assumptions must be made:

9) During bending, all cantilevers remain in contact, and on the contact they follow the same deflection curve.

10) The shape of the deflection curve can be replaced at any arbitrary point of the curve by a circle of some particular radius.

Now it is possible to formulate another system of equations.

$$y(x_n)_n = y(x_{n+1})_{n+1} \tag{3-5}$$

When taking into account assumption 10), about the shape of the deflection curve, this equation expresses the fact that across the system of n cantilevers it is possible to define n-1 points with the same deflection, lying on the line which intersects the centre of concentric circles, defined by this centre and by the n-1 points with the equal deflection (Fig. 3-6). Introduction of equation 3-5 was important for another reason, and that was the necessity to ensure the compatibility of deformations within the system of interacting cantilevers. Unfortunately by introducing equation 3-5, an additional n-1 unknowns (distances x_n where the deflections are equal) were introduced. But from the equation of circle there can be defined additional geometrical conditions. This equation was derived in Appendix B as equation B-7. Using the general form for n cantilevers equation B-7 yields:

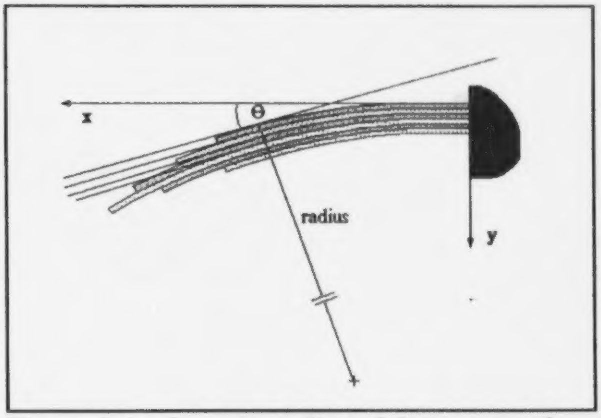

Figure 3-6 Common radius of the system of concentric circles.

$$y_n = x_n\left(\frac{1-\cos\theta}{1+\cos\theta}\right)^{\frac{1}{2}} \tag{3-6}$$

Notice that in the system of Equations 3-6 there is only one θ, because at the points x_n, as they are defined, the angle θ is constant.

Now it is possible to define the new system of equations which includes Equations 3-4, 3-5 and 3-6. In this system, where x_1 is an input, there are :

unknown	No. of unknowns	No. of available equations	Equation No
y	n	n	3-6
x_n	n-1	n-1	3-4
r	n-1	n-1	3-5
θ	1	1	3-4

So finally this system is determinate, and can be solved.

There are not many available methods for solving the system of nonlinear equations, in this particular case the system of 3n-1 equations. Certainly all of them are based on numerical procedures. The most common method which would be applicable for solving this problem is the Newton-Raphson method for a nonlinear system of equations (Press, Flannery, Teukolsky and Vetterling, 1989).

There is, in fact, another geometrical relation that can be used.

$$y_n = y_1 - \cos\theta \sum_{j=1}^{n-1} d_j \tag{3-7}$$

and

$$x_n = x_1 + \sin\theta \sum_{j=1}^{n-1} d_j \tag{3-8}$$

or rearranging Equation 3-8

$$\theta = \arcsin \frac{x_n - x_1}{\sum_{j=1}^{n-1} d_j} \tag{3-9}$$

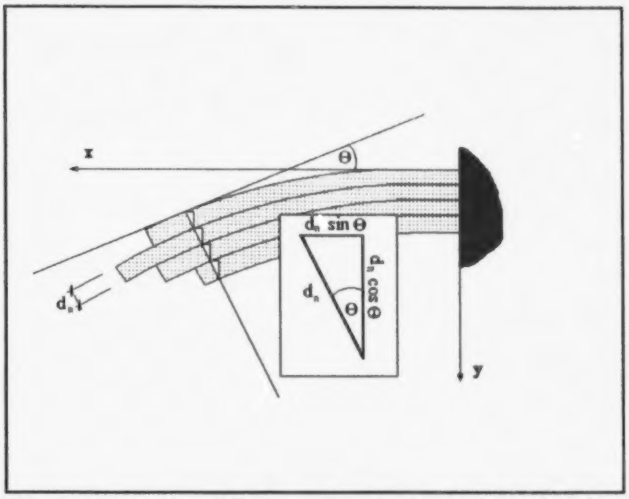

Figure 3-7 Simplified geometrical relations for the system of cantilevers.

The meaning of these equations is obvious from Fig. 3-7.

Introduction of Equation 3-9, simplifies the solution considerably. Equations 3-7, 3-8 and 3-9 express geometrically the compatibility of deformations of the system of interacting cantilevers, and then using equation 3-3 the system for n-1 unknown reactions can be solved. Substituting, for example, Equation 3-8 for $x(\theta)_n$ into the equation 3-3 there are:

unknown	No. of unknowns	No. of available equations	Equation No
θ	1	1	3-8
r	n-1	n-1	3-3

This system is obviously determinate, and can be solved for the unknown reactions between cantilevers. Solution will be again made using a numerical procedure, specifically the Newton-Raphson method. Subsequently, the inner forces acting within each of the n cantilevers can be calculated from the equations 3-1 and 3-2. At the same time the shape of the deflection curve can be determined from equation 3-4.

Unfortunately, for the reasons explained in Chapter 4 and in Appendix H, the approximation of the contact force by the uniformly distributed load r_n would not always work during solving the system of nonlinear equations. For such a case another system of equations is presented as equations 3-10, 3-11, and 3-12. The new system is identical to the previous one with the exception of the reaction between cantilevers which is approximated by a force R_n acting at the end of the shorter cantilever. The condition about continuity of deflections throughout the system of cantilevers was droppped out; instead the continuity is assumed to exist only at the end of the shorter cantilever. Derivation is presented in the Appendix A (equations A-43, A-44, A-45).

Now the bending moment is

$$
\begin{aligned}
M(x)_n = {} & \frac{w_n}{2}(l_n - x)^2 - R_{n-1}(x_{r,n-1} - x)\, u<x_{r,n-1} - x> + \\
& + R_n(x_{r,n} - x)\, u<x_{r,n} - x> - \\
& - \frac{\gamma_w \sin\psi}{6}(x_{v,n-1} - x)^3\, u<x_{v,n-1} - x> + \\
& + \frac{\gamma_w \sin\psi}{6}(x_{v,n} - x)^3\, u<x_{v,n} - x> + \\
& + Q_n(x_{Q,n} - x)\, u<x_{Q,n} - x>
\end{aligned}
\tag{3-10}
$$

the angle of tangent to the deflection curve with horizontal

$$\begin{aligned} EI\theta(x)_n = {} & \frac{w_n}{6}[(l_n - x)^3 - l_n^3] - \frac{R_{n-1}}{2}[(x_{r,n-1} - x)^2\, u\langle x_{r,n-1} - x\rangle - x_{r,n-1}^2] + \\ & + \frac{R_n}{2}[(x_{r,n} - x)^2\, u\langle x_{r,n} - x\rangle - x_{r,n}^2] - \\ & - \frac{\gamma_w \sin\psi}{24}[(x_{v,n-1} - x)^4\, u\langle x_{v,n-1} - x\rangle - x_{v,n-1}^4] + \\ & + \frac{\gamma_w \sin\psi}{24}[(x_{v,n} - x)^4\, u\langle x_{v,n} - x\rangle - x_{v,n}^4] + \\ & + \frac{Q_n}{2}[(x_{Q,n} - x)^2 u\langle x_{Q,n} - x\rangle - x_{Q,n}^2] \end{aligned} \tag{3-11}$$

and finally the deflection

$$\begin{aligned} EIy(x)_n = {} & \frac{w_n}{24}[(l_n - x)^4 - l_n^3(l - 4x)] - \\ & - \frac{R_{n-1}}{6}[(x_{r,n-1} - x)^3\, u\langle x_{r,n-1} - x\rangle - x_{r,n-1}^2(x_{r,n-1} - 3x)] + \\ & + \frac{R_n}{6}[(x_{r,n} - x)^3\, u\langle x_{r,n} - x\rangle - x_{r,n}^2(x_{r,n} - 3x)] + \\ & + \frac{Q_n}{6}[(x_{Q,n} - x)^3 u\langle x_{Q,n} - x\rangle - x_{Q,n}^2(x_{Q,n} - 3x)] - \\ & + \frac{\gamma_w \sin\psi}{120}[(x_{v,n} - x)^5 u\langle x_{v,n} - x\rangle - 5x_{v,n}^4(x_{v,n} - x) + x_{v,n}^5(5 - u\langle x_{v,n} - x\rangle)] - \\ & - \frac{\gamma_w \sin\psi}{120}[(x_{v,n-1} - x)^5\, u\langle x_{v,n-1} - x\rangle - 5x_{v,n-1}^4(x_{v,n-1} - x) + \\ & + x_{v,n-1}^5(5 - u\langle x_{v,n-1} - x\rangle)] \end{aligned} \tag{3-12}$$

The last step of the stability procedure is straightforward. Accepting the assumption that the cantilever in question failed when the acting tensile stress surpassed the strength in tension, or the acting shear stress surpassed the shear strength, then the following well known equations can be used to calculate:

$$\tau(x)_{\max} = \frac{V(x)\,\tilde{Q}_{\max}}{I\tilde{b}} \tag{3-13}$$

and

$$\sigma(x)_{\max} = \frac{M(x)\,\tilde{y}_{\max}}{I} \tag{3-14}$$

for rectangular crossection

$$\tilde{Q}_{\max} = \frac{\tilde{b}}{2}\,\frac{h^2}{4} \tag{3-15}$$

and finally

$$\tilde{y}_{\max} = \frac{d}{2} \tag{3-16}$$

3.4. Block toppling failure.

Block toppling failure cannot be described by only one set of equations. Assuming that there is some cohesion along joints, the blocks have to overcome this cohesion first before the toppling can take place. That is the reason why, in the case of this failure mode, first the strength of the rock columns will be tested for acting bending moments and shear forces, and if the strength of the rock with joints is overcome then the separated blocks would be tested for toppling.

3.4.1. Bending of columns of rock with a crossjoint system.

The model accepted for this failure mode follows in the beginning a similar path to the model for the flexural toppling failure. There are going to be introduced two changes which will not alter dramatically the form of equations already presented in the part 3.3., but first, the failure plane searching routine is going to be very different, and second, the new load F_n (page 51) is going to be introduced into the system of equations 3-1, 3-2, 3-3 and 3-4.

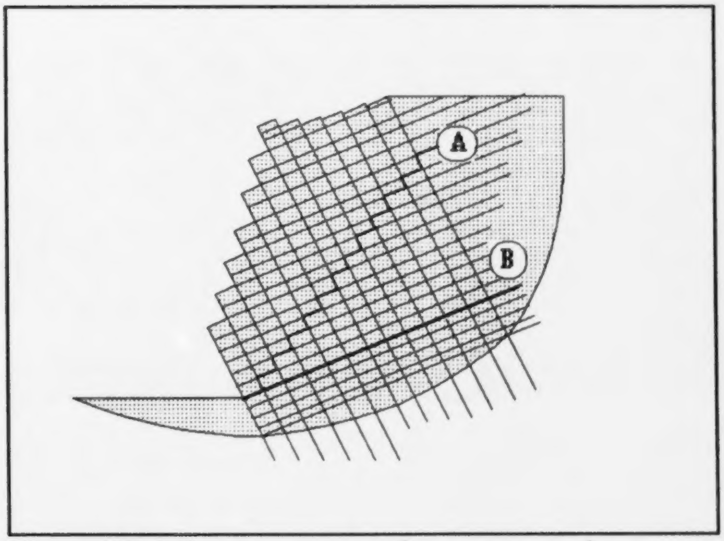

Figure 3-8 Inline arrangement of two systems of perpendicular joints.

In section 3.3., for the flexural mode of failure, it was assumed that cantilevers would break at the place of maximum moment. This does not necessarily have to be true in the case of block toppling failure. Because of the presence of cross joints, the failure plane can follow some path, defined by bedding planes and cross joints, which lies above the plane of maximum moments.

The arrangement of discontinuities in Fig. 3-8 (Inline arrangement of two systems of perpendicular joints) was used, for example, by Scavia, Bernaudo and Barla (1990). They were dealing with a system of joints and bedding planes persistent in both vertical and horizontal directions. In this case, it is obvious from the Figure 3-8, and it was confirmed by simple program based on Goodman and Bray equations, that the rock is going to fail along the failure plane B. Path A or any other path is in this case out of question, and is against the physical law which says that the movement, in this case a deformation, will always follow the path of minimum work.

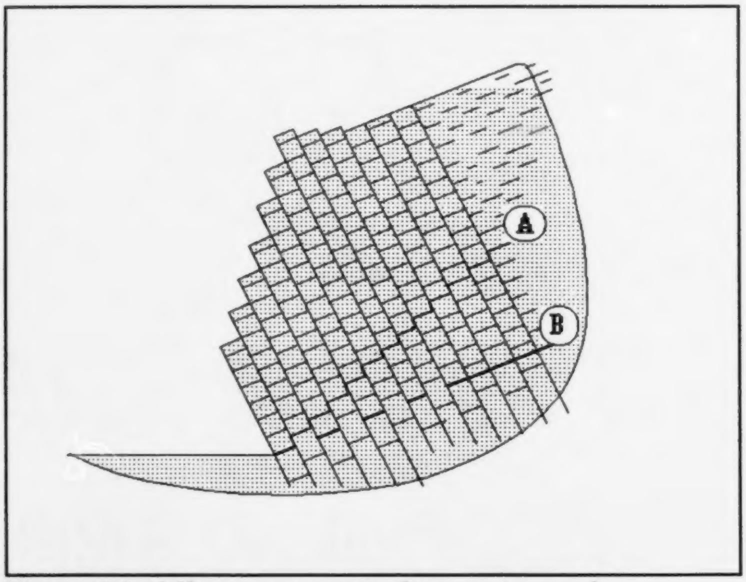

Figure 3-9 Offset arrangement of two systems of perpendicular joints.

The situation in Fig. 3-9 (Offset arrangement of two systems of perpendicular joints) is different. Blocks on any path below the path A have to overcome moments acting against the sense of rotation, and have to break through the solid rock. It is very likely, and it will be tested by the model, that the final failure plane will be quite close to the path A.

There is, theoretically, a possibility that the failure plane could be developed even below the path B (Fig. 3-8, Fig. 3-9). Such a deformation would demand that the lower block revolves around the corner of the stepped base of an upper block, shifting at the same time all blocks behind up the hill without breaking through some of the joints. In the authors opinion such a situation is extremely unlikely and has not been observed in any available case history or physical model. On the other hand, the assumption about the planar character of the failure plane, as well as the assumption about the position of the failure plane corresponds well with results of the physical modelling presented by Müller and Hofmann in 1970. Equations describing the inner forces acting within columns of toppling blocks defined by the stepped failure surface, as well as the equations for their deformations are developed in the Appendix B.

In open pit mining, the pit is created in a series of steps, bench after bench, and during each step a new failure plane can develop, loading underlying rock columns by the weight of the failed mass. The magnitude of this force, F, is a function of the state of the deformation of the failing rock, which determines the shape of the rock mass block above the failure plane. It was noted in the first chapter, that the whole toppling process is highly time dependent. This additional force is a typical example of such a dependency. The whole overturning process can last from several hours to days or months, changing the magnitude of the force acting at the top of the next, resisting layer. Unfortunately, it is beyond the scope of this thesis to deal with dynamics of the process.

The force F was not included in the flexural toppling equations for two reasons. First, as cited in Chapter 2, flexural toppling does not usually develop a failure plane. However, there are not enough observations available to be sure, and what is more, those which are available were made by Cruden (1989), Cruden and Hu (1990) and Hu and Cruden (1992) on natural slopes. Within the mining conditions, it is therefore theoretically possible that a failure plane might develop. It is however assumed that for the flexural toppling mode only one, if any, failure plane would develop in a highwall. This assumption will be tested by the model, and if necessary, the flexural toppling equations can be easily extended to include the force F.

Forces acting on one of the interacting cantilevers in case of block toppling are shown in Fig. 3-10. The notation of variables in the figure is exactly the same as for flexural toppling (Fig. 3-5). There is however introduced the new force F. The meaning of this force was explained in the previous paragraph. Also the length of the continuous

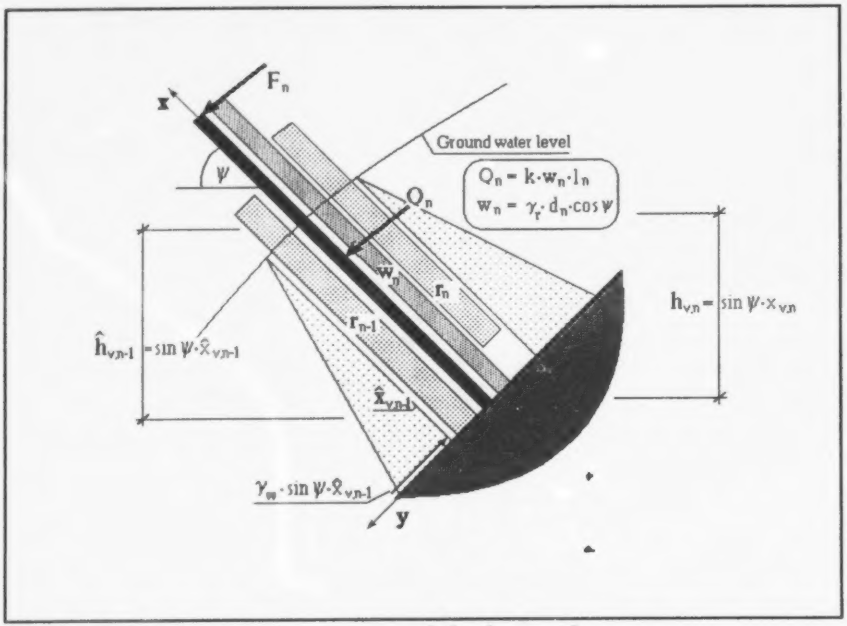
F_n
x
ψ
Ground water level
$Q_n = k \cdot w_n \cdot l_n$
$w_n = \gamma_r \cdot d_n \cdot \cos\psi$
Q_n
w_n
r_n
r_{n-1}
$h_{v,n} = \sin\psi \cdot x_{v,n}$
$\hat{h}_{v,n-1} = \sin\psi \cdot \hat{x}_{v,n-1}$
$\hat{x}_{v,n-1}$
$\gamma_w \cdot \sin\psi \cdot \hat{x}_{v,n-1}$
y

Figure 3-10 Forces acting on one of the interacting cantilevers (block toppling).

load describing the reaction with the overlying cantilever is different. The reason for this change is the possible stepped character of the basal failure plane as shown in Fig. 3-11.

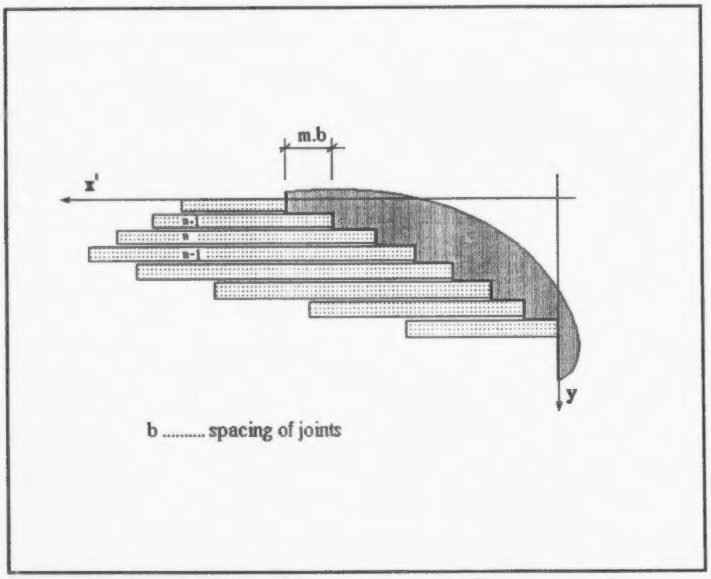
m.b
x'
n-
n
n-
y
b .... spacing of joints

Figure 3-11 System of interacting cantilevers on the stepped base (block toppling).

Equations for the model in Fig. 3-11 (System of interacting cantilevers on a stepped base), were derived according to the beam theory under the identical assumptions as the equations for flexural toppling.

Equations describing the shear force $V(x)_n$ (3-14), bending moment $M(x)_n$(3-15), angle between the tangent to the beam and the horizontal $\theta(x)_n$(3-16) and the deflection $y(x)_n$(3-17) are derived and presented in the Appendix B as equations B-26, B-27, B-28 and B-29.

Shear force within the beam is given as

$$\begin{aligned} V(x)_n = {} & w_n(l_n - x) + r_n\,(x_{r,n} - x)\,u\langle x_{r,n} - x\rangle - r_n\,(mb - x)\,u\langle mb - x\rangle - \\ & - r_{n-1}\,(x_{r,n-1} - x)\,u\langle x_{r,n-1} - x\rangle + \\ & + Q_n u\langle x_{Q,n} - x\rangle + F_n - \\ & - \frac{\gamma_w \sin\psi}{2}(\hat{x}_{v,n-1} - x)^2\,u\langle \hat{x}_{v,n-1} - x\rangle + \frac{\gamma_w \sin\psi}{2}(x_{v,n} - x)^2\,u\langle x_{v,n} - x\rangle \end{aligned} \tag{3-17}$$

Bending moment

$$\begin{aligned} M(x)_n = {} & w_n \frac{(l_n - x)^2}{2} + \\ & + \frac{r_n}{2}(x_{r,n} - x)^2\,u\langle x_{r,n} - x\rangle - \frac{r_n}{2}(mb - x)^2\,u\langle mb - x\rangle - \\ & - \frac{r_{n-1}}{2}(x_{r,n-1} - x)^2\,u\langle x_{r,n-1} - x\rangle - \\ & - \frac{\gamma_w \sin\psi}{6}(\hat{x}_{v,n-1} - x)^3\,u\langle \hat{x}_{v,n-1} - x\rangle + \frac{\gamma_w \sin\psi}{6}(x_{v,n} - x)^3\,u\langle x_{v,n} - x\rangle + \\ & + Q_n(x_{Q,n} - x)\,u\langle x_{Q,n} - x\rangle + F_n(l_n - x) \end{aligned} \tag{3-18}$$

The angle between the tangent to the deflection curve and the horizontal

$$
\begin{aligned}
EI\theta(x)_n = {} & \frac{w_n}{6}[(l_n-x)^3-l_n^3] + \\
& + \frac{r_n}{6}[(x_{r,n}-x)^3\, u{<}x_{r,n}-x{>} - x_{r,n}^3] - \frac{r_n}{6}[(mb-x)^3\, u{<}mb-x{>} - (mb)^3] - \\
& - \frac{r_{n-1}}{6}[(x_{r,n-1}-x)^3\, u{<}x_{r,n-1}-x{>} - x_{r,n-1}^3] - \\
& - \frac{\gamma_w \sin\psi}{24}[(\hat{x}_{v,n-1}-x)^4\, u{<}\hat{x}_{v,n-1}-x{>} - \hat{x}_{v,n-1}^4] + \\
& + \frac{\gamma_w \sin\psi}{24}[(x_{v,n}-x)^4\, u{<}x_{v,n}-x{>} - x_{v,n}^4] + \\
& + \frac{Q_n}{2}[(x_{Q,n}-x)^2 u{<}x_{Q,n}-x{>} - (x_{Q,n})^2] + \frac{F_n}{2}[(l_n-x)^2 - (l_n)^2]
\end{aligned}
\tag{3-19}
$$

And finally the deflection:

$$\begin{aligned}
EIy(x)_n = {} & \frac{w_n}{24}[(l_n - x)^4 - l_n^3(l - 4x)] + \\
& + \frac{r_n}{24}[(x_{r,n} - x)^4\, u<x_{r,n} - x> - x_{r,n}^3(x_{r,n} - 4x)] - \\
& - \frac{r_n}{24}[(mb - x)^4\, u<mb - x> - (mb)^3(mb - 4x)] - \\
& - \frac{r_{n-1}}{24}[(x_{r,n-1} - x)^4\, u<x_{r,n-1} - x> - x_{r,n-1}^3(x_{r,n-1} - 4x)] + \\
& + \frac{Q_n}{6}[(x_{Q,n} - x)^3 u<x_{Q,n} - x> - x_{Q,n}^2(x_{Q,n} - 3x)] + \\
& + \frac{F_n}{6}[(l_n - x)^3 - l_n^2(l_n - 3x)] + \\
& + \frac{\gamma_w \sin\psi}{120}[(x_{v,n} - x)^5 u<x_{v,n} - x> - 5x_{v,n}^4(x_{v,n} - x) + x_{v,n}^5(5 - u<x_{v,n} - x>)] - \\
& - \frac{\gamma_w \sin\psi}{120}[(\hat{x}_{v,n-1} - x)^5\, u<\hat{x}_{v,n-1} - x> - 5\hat{x}_{v,n-1}^4(\hat{x}_{v,n-1} - x) + \\
& + \hat{x}_{v,n-1}^5(5 - u<\hat{x}_{v,n-1} - x>)]
\end{aligned} \tag{3-20}$$

Solution of this system of equations is basically the same as for flexural toppling. The only difference is caused by the stepped character of a base. To formulate the geometrical equations describing the continuity of deformations, it will be necessary to shift the point x_n, (the point of constant angle θ) several times, to follow the stepped base. From the mathematical point of view this means only a little inconvenience. At the point of shifting the new θ is always going to be introduced, but an additional system of equations can be easily added to the original one by repeating the equation (3-16) k times for k different cross sections through the system of cantilevers in question. Unfortunately, while this solution would be ideal if the exact shape of the reaction force along the cantilever was known, it breaks down if the shape is not known (Chapter 5). It would be very difficult if not impossible to express the shape of the real reaction in form of a mathematical function and so, as for flexural toppling, another system of equations involving the point reaction force R is introduced:

In this system the bending moment is

$$\begin{aligned} M(x)_n = {} & \frac{w_n}{2}(l_n - x)^2 + \\ & + R_n\,(x_{r,n} - x)\,u{<}x_{r,n} - x{>} - R_{n-1}\,(x_{r,n-1} - x)\,u{<}x_{r,n-1} - x{>} - \\ & - \frac{\gamma_w \sin\psi}{6}(\hat{x}_{v,n-1} - x)^3\,u{<}\hat{x}_{v,n-1} - x{>} + \frac{\gamma_w \sin\psi}{6}(x_{v,n} - x)^3\,u{<}x_{v,n} - x{>} + \\ & + Q_n(x_{Q,n} - x)\,u{<}x_{Q,n} - x{>} + F_n(l_n - x) \end{aligned} \tag{3-21}$$

the tangent to the deflection curve with horizontal

$$\begin{aligned} EI\theta(x)_n = {} & \frac{w_n}{6}[(l_n - x)^3 - l_n^3] + \\ & + \frac{R_n}{2}[(x_{r,n} - x)^2\,u{<}x_{r,n} - x{>} - x_{r,n}^2] - \\ & - \frac{R_{n-1}}{2}[(x_{r,n-1} - x)^2\,u{<}x_{r,n-1} - x{>} - x_{r,n-1}^2] - \\ & - \frac{\gamma_w \sin\psi}{24}[(\hat{x}_{v,n-1} - x)^4\,u{<}\hat{x}_{v,n-1} - x{>} - \hat{x}_{v,n-1}^4] + \\ & + \frac{\gamma_w \sin\psi}{24}[(x_{v,n} - x)^4\,u{<}x_{v,n} - x{>} - x_{v,n}^4] + \\ & + \frac{Q_n}{2}[(x_{Q,n} - x)^2 u{<}x_{Q,n} - x{>} - (x_{Q,n})^2] + \frac{F_n}{2}[(l_n - x)^2 - (l_n)^2] \end{aligned} \tag{3-22}$$

and the deflection

$$
\begin{aligned}
EIy(x)_n = {} & \frac{w_n}{24}[(l_n - x)^4 - l_n^3(l - 4x)] + \\
& + \frac{R_n}{6}[(x_{r,n} - x)^3\, u{<}x_{r,n} - x{>} - x_{r,n}^2(x_{r,n} - 3x)] - \\
& - \frac{R_{n-1}}{6}[(x_{r,n-1} - x)^3\, u{<}x_{r,n-1} - x{>} - x_{r,n-1}^2(x_{r,n-1} - 3x)] + \\
& + \frac{Q_n}{6}[(x_{Q,n} - x)^3\, u{<}x_{Q,n} - x{>} - x_{Q,n}^2(x_{Q,n} - 3x)] + \\
& + \frac{F_n}{6}[(l_n - x)^3 - l_n^2(l_n - 3x)] + \\
& + \frac{\gamma_w \sin\psi}{120}[(x_{v,n} - x)^5\, u{<}x_{v,n} - x{>} - 5x_{v,n}^4(x_{v,n} - x) + x_{v,n}^5(5 - u{<}x_{v,n} - x{>})] - \\
& - \frac{\gamma_w \sin\psi}{120}[(\hat{x}_{v,n-1} - x)^5\, u{<}\hat{x}_{v,n-1} - x{>} - 5\hat{x}_{v,n-1}^4(\hat{x}_{v,n-1} - x) + \\
& + \hat{x}_{v,n-1}^5(5 - u{<}\hat{x}_{v,n-1} - x{>})]
\end{aligned}
\tag{3-23}
$$

Equations 3-21,3-22 and 3-23 were introduced in Appendix B as equations B-31, B-32 and B-33.

Finally the last step can be done, and the acting normal and shear stresses can be calculated from equations 3-10 and 3-11, and the safety factor expressing the ability of rock columns to resist the breaking through the joints can be calculated as the fraction of the available strength of the last, n^th^ cantilever to the strength required for equilibrium.

3.4.2. Toppling and sliding of rock columns.

The failure plane searching routine is exactly the same for bending, as well as for the toppling states of block toppling failure, and it was described in the previous section. Simply, if there is a cohesion acting on the crossjoints, first the rock columns must be tested for the strength (3.4.1.), and if this strength is overcome, then they will be tested for toppling. In the case of zero cohesion the whole procedure shrinks into the test of the system for toppling. The position of the failure plane is given by the geometry of the discontinuities, and it is independent of the cohesion acting on the crossjoints.

In the sketch of the system of blocks on the stepped base (Fig. 3-12),

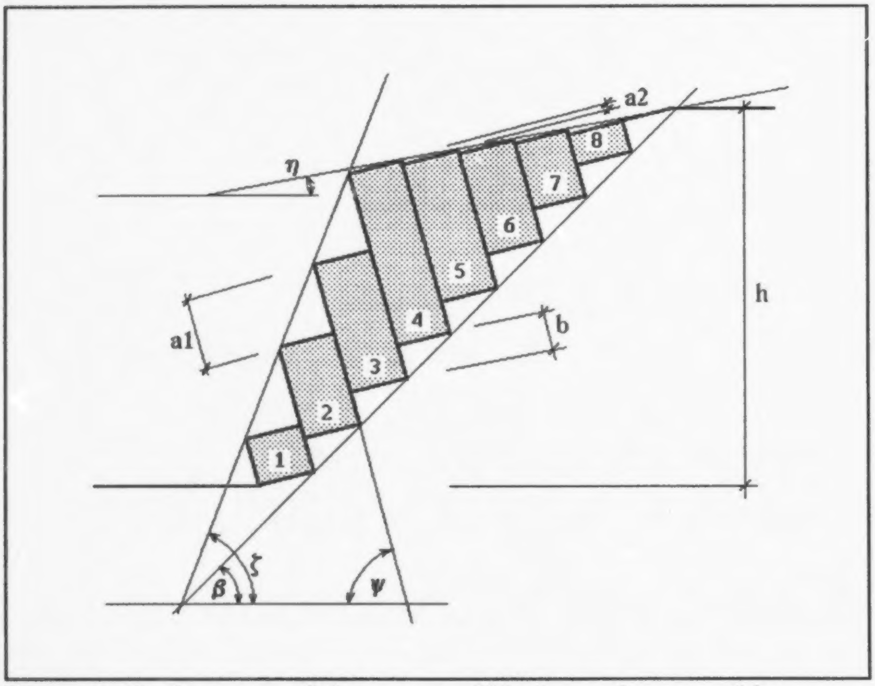

Figure 3-12 Geometry of the system of blocks on the stepped base kinematically free to topple or slide.

a slope at angle ζ is excavated in a rock mass with layers dipping at ψ. The angle of overall inclination of the stepped failure plane is β. Input parameters for defining the geometry of this slope are the width of blocks (constant in the figure 3-12), the spacing of joints, the angle ζ of the slope in question, the angle η of the original slope and the height of the hill, h, or alternatively the distance of the top of the hill from the toe of the slope.

Now, if the angle, ζ, of excavated slope, and the dip of crossjoints, $90-\psi$, are both greater than the angle of internal friction, ϕ, all blocks will tend to slide, and the only force which can possibly stop the movement is the resistance of the rock mass debris gradually accumulating at the toe of the slope.

If the dip of crossjoints, $90-\psi$, is smaller than the angle of internal friction ,ϕ, all blocks in the interacting system are kinematically free to either slide or topple, depending on their geometry, inclination and the forces caused by reaction with adjacent blocks. In order to formulate the problem, the following assumptions are made:

1) The moving blocks are either toppling or sliding, they never slide and topple at the same time.

The original Goodman and Bray toppling model (1976) is based on this assumption, and without it, the whole problem would be geometrically indeterminate.

2) Blocks do not change their mode of movement. That means that the toppling blocks will only topple, and the sliding blocks will only slide at any stage of the deformation.

This assumption, at some stage of the progressing deformation, ceases to be true. When this happens, the modelling has to be interrupted, and the last available information will be from the step preceding the critical state. It will be obvious later, from the text, that both assumptions are much better grounded than they might seem to be as formulated now, without explanation.

From assumption 1) it follows that the solution of the problem depicted in Fig. 3-12 can be divided into two categories. For each block within the system it is possible to define both sliding and toppling forces, and then to calculate the force necessary for equilibrium in sliding, and in toppling. It is assumed, that the larger of these two forces determines the mode of movement for each block. That is, if the force necessary for equilibrium of a block in toppling is positive and larger than the force necessary for equilibrium in sliding then the block will topple. From assumption 2) it follows that the block will never slide, but it can become stable again. In this way all the blocks in the system can be divided into the groups of either sliding, toppling or stable blocks.

Forces acting on one toppling block of the system of interacting, separated rock columns is shown in the Fig. 3-13.

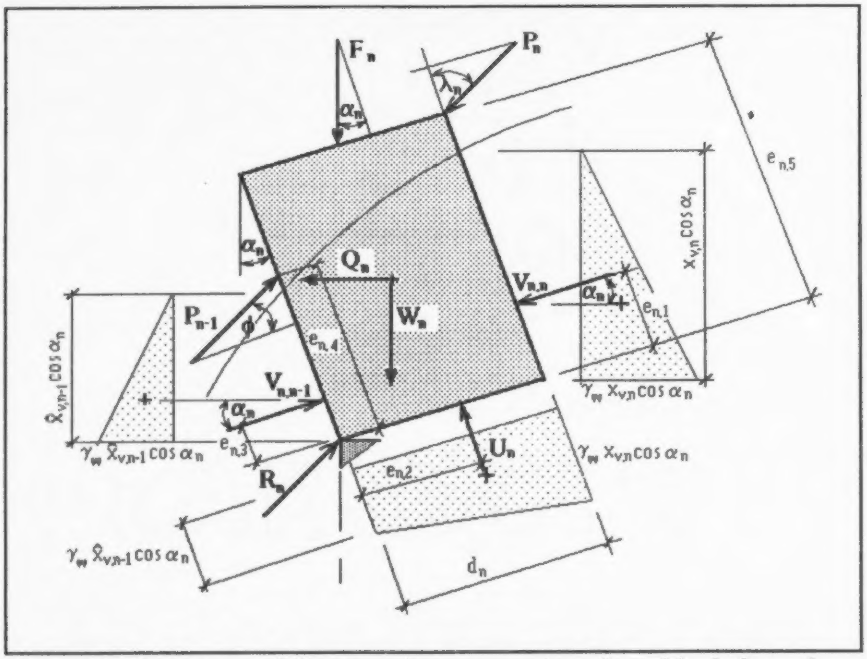
F_n
P_n
α_n
λ_n
$e_{n,5}$
Q_n
W_n
$V_{n,n}$
α_n
$e_{n,1}$
$x_{v,n} \cos \alpha_n$
$\gamma_w x_{v,n} \cos \alpha_n$
α_n
P_{n-1}
ϕ
$e_{n,4}$
$V_{n,n-1}$
$x_{v,n-1} \cos \alpha_n$
$\gamma_w x_{v,n-1} \cos \alpha_n$
α_n
$e_{n,3}$
R_n
U_n
$e_{n,2}$
$\gamma_w x_{v,n} \cos \alpha_n$
$\gamma_w x_{v,n-1} \cos \alpha_n$
d_n

Figure 3-13 System of forces acting on one (toppling) block from the system of interacting rock columns.

In Fig. 3-13 :

P_n	....	reaction with the upper block
P_{n-1}	....	reaction with the lower block
R_n	....	reaction with the stepped base
U_n	....	uplift water force

The nomenclature for the rest of the forces is the same as that for flexural toppling.

In Fig. 3-13 there are six different directions in which forces are defined to act.

In reality, the situation is more complicated. Gravitational forces act in the vertical direction, water forces can be defined in the direction perpendicular to the block, the seismic force is assumed to act in the horizontal direction, but all three reactions are free to act in some unknown direction. Now there are three equilibrium equations available, two for each of two perpendicular directions and one for moments, and four unknowns (P_{n-1}, R_n, and both directions). Notice that only one of the reactions P_n and P_{n-1} is actually unknown, because the other one was determined from the analysis of an adjacent block. To solve the problem, another assumption has to be accommodated:

3) At the corner - face contact of two blocks the direction of the reaction force is inclined from the normal to the face by the angle of internal friction ϕ.

Now the direction of reactions P_n and P_{n-1} is known, as shown in Fig. 3-13. If the block in question is in contact with the corner of the adjacent block, it is at the angle of internal friction ϕ, and if the block in question is in contact with the side of the adjacent block it is at the angle λ. The angle λ is function of the angle of internal friction ϕ and of the difference in the inclinations of adjacent blocks, and is defined in Appendix D. In the case of face to face contact, the reaction is inclined from the normal to the faces by the angle of internal friction ϕ.

The contacts that occur within a system of toppling blocks are shown in Fig. 3-14. It is obvious from this figure that three different moment equilibrium equations have to be defined for three different cases of contact combinations to calculate all possible magnitudes of reaction P_{n-1}. These equations are defined in Appendix E as equations E-8, E-9 and E-10 for the cases a), b) and c) in Fig. 3-14.

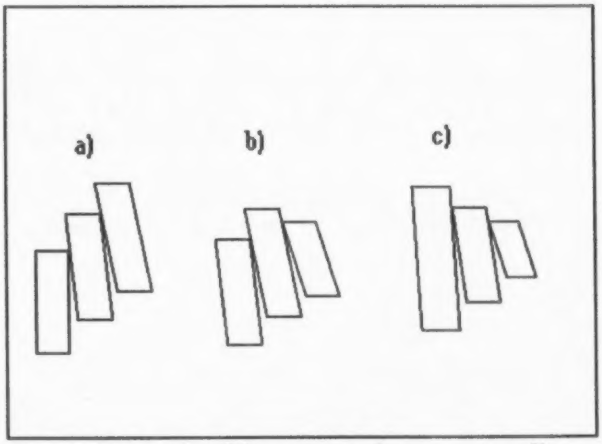

Figure 3-14 Possible contacts between toppling blocks.

Case a)

$$P_{n-1} = \frac{P_n(\sin\lambda_n l_n - \cos\lambda_n d_n)}{\cos\phi e_{n,4}} + \frac{1}{\cos\phi e_{n,4}}[C] \qquad \textbf{(3-24)}$$

Case b)

$$P_{n-1} = \frac{P_n(\cos\phi e_{n,5} - \sin\phi d_n)}{\cos\phi e_{n,4}} + \frac{1}{\cos\phi e_{n,4}}[C] \qquad \textbf{(3-25)}$$

and finally Case c)

$$P_{n-1} = \frac{P_n(\cos\phi e_{n,5} - \sin\phi d_n)}{\sin\lambda_n l_n} + \frac{1}{\sin\lambda_n l_n}[C] \qquad \textbf{(3-26)}$$

As mentioned before, for the face to face contact both reactions P_n and P_{n-1} are parallel and they are inclined from the normal to the face by the angle of internal friction ϕ (Appendix E). This situation is defined by equation 3-25, Case b.

The direction and magnitude of the reaction R is not of interest just now, but knowing P_n and P_{n-1} , it can be easily calculated from either parallel or vertical equilibrium equations.

For sliding, the situation is slightly different. All sliding blocks are parallel, and the unknowns are not only reactions P_{n-1}, R_n and their directions, but also the position of both forces. Clearly another assumption is needed. This assumption can be obtained by generalising the assumption 3 by defining the direction of the reaction between the block and the stepped base.

4) The direction of the reaction force between the stepped base and the base of the sliding block is inclined from the normal to base by the angle of internal friction ϕ.

The system of forces acting on one sliding block from a system of interacting rock columns is shown in Fig. 3-15.

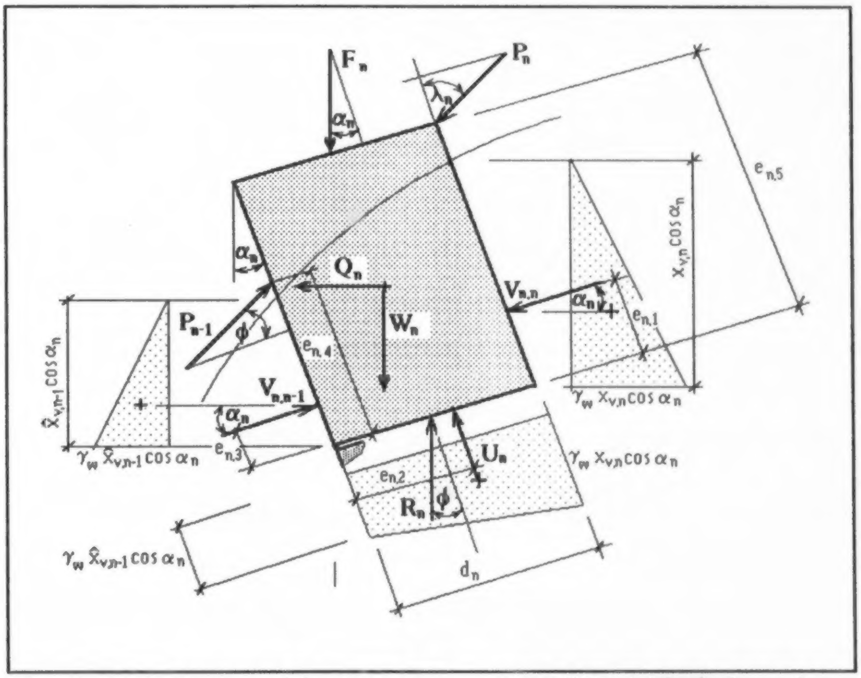
F_n
P_n
α_n
λ_n
e_n,5
x_v,n cos α_n
α_n
Q_n
V_n,n
α_n
e_n,1
P_n-1
φ
W_n
e_n,4
x̂_v,n-1 cos α_n
V_n,n-1
α_n
γ_w x_v,n cos α_n
γ_w x̂_v,n-1 cos α_n
e_n,3
U_n
γ_w x_v,n cos α_n
e_n,2
R_n
φ
γ_w x̂_v,n-1 cos α_n
d_n

Figure 3-15 System of forces acting on one (sliding) block from the system of interacting rock columns.

The nomenclature in the figure is the same as in Fig. 3-13. There are 4 unknowns present in Fig. 3-15 (P_{n-1},R_n and the position of both reactions), but for equilibrium equations in the directions perpendicular and parallel with bedding planes no information about the position of reactions in question is needed.

There are two kind of contacts, (shown in Fig. 3-16 next page), which may occur with a sliding block within the frame of the formulated assumptions. Face to face contact with another sliding block, or the contact with the face of an upper toppling block. Equations 3-21 and 3-22 describing the sliding of blocks are derived in Appendix F as equations F-12 and F-13.

$$P_{n-1} = \frac{P_n(\sin_{\lambda_n} - \cos\lambda_n \tan(\Gamma)) - [A]\tan\Gamma + [B]}{\cos\phi - \sin\phi\tan(\Gamma)} \tag{3-27}$$

and

$$P_{n-1} = P_n - \frac{[A]\tan\Gamma + [B]}{\cos\phi - \sin\phi\tan(\Gamma)} \tag{3-28}$$

There is theoretically another kind of contact possible between the last toppling, and the first sliding blocks, in addition to those shown in Fig. 3-16. When the deformation or movement is sufficient, the last toppling block can be allowed to topple so much that it would rest its' corner on the face of the first toppling block (Fig. 3-17, next page).

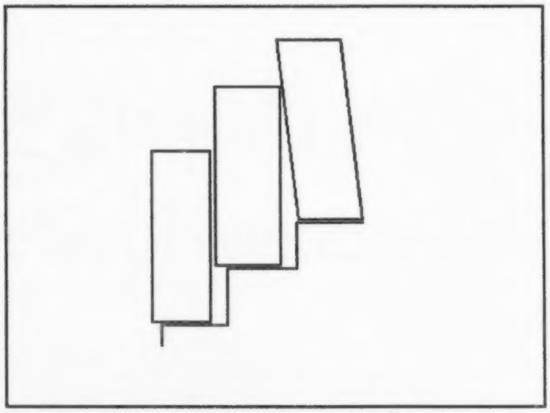

Figure 3-16 Possible contacts for the sliding blocks.

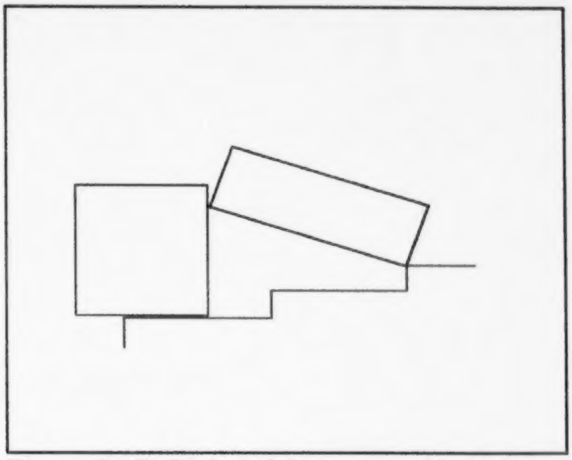

Figure 3-17 Excluded face-corner kind of contact for the sliding and toppling blocks.

Unfortunately, at that moment the assumptions 1 and 2 are no longer valid, all blocks are free to slide and rotate around the corners of the stepped base, and the whole situation becomes highly unpredictable, and it cannot be dealt with in terms of a limit equilibrium approach. It is too soon to talk about the computer model at this stage, but it should be at least noted, that if this situation happens to occur, the computation will be terminated, and the last available result will be the one before the critical one. This problem was actually one of the reasons why the assumption 2 was formulated. Fortunately, it is quite likely that for most of real the situations before the contact shown in Fig. 3-17 is established, the failure will regain the face to face contact again, and so this highly important state of deformation could be evaluated. The situation after establishing the critical contact can be reasonably described by the movement of a rock mass sliding on a stepped base, because the chance that the toppling movement would stabilize after reaching the problematic stage is likely close to zero, and it can be assumed that the toppling block will continue to revolve till it establishes contact between its' face and the stepped base. The new situation can be easily evaluated by using any of the widely available shear stress based limit equilibrium methods.

4. SOLUTION OF THE SYSTEM OF EQUATIONS FOR FLEXURAL TOPPLING.

In Chapter 3 the basic equations describing behaviour of a system of cantilevers loaded by a bending moment were defined in terms of linear equations in two different forms. Equations 3-3, 3-4, 3-19 and 3-20 were defined with continuous and constant reaction while equations 3-11, 3-12, 3-21 and 3-22 were defined with point reaction.

The continuous reaction would probably be closer to reality for most of the cantilevers in the system and, in the case of an inline arrangement of crossjoints (flat base), the solution would be easier. The derivation of the mathematical solution is presented in Appendix H.2. The system of reactions derived from the solution is a set of average reactions ensuring a constant angle of the tangents to the deflection curves along a defined radius across the system of cantilevers (Figure 3-6). For a different x coordinate along the cantilever (different radius), a different average reaction would result from the system, and it would have to be decided which position gives the deformation closest to the real one. Unfortunately, the solution is restricted to the radii common to all the cantilevers, and is thus restricted by the length of the shortest cantilever in the system. (Obviously, choosing a radius farther from the origin, which does not intersect some of the shorter cantilevers, neglects the support provided by those shorter cantilevers, and gives a result for a different system than the one desired). Furthermore, in the case of an offset arrangement of crossjoints (stepped base) it is impossible to find a radius intersecting all the cantilevers. It would be theoretically possible to calculate the deformation at the origin and at the end of each cantilever thus expanding the system of equations to 2 n, and thus following the shape of the base. This would be an optimal solution provided that the shape of the reaction is known. That is not the case (the shape is assumed to be continuous and constant), and an additional n-1 unknown reactions is introduced into the system, making the system indeterminate.

The system of point reactions acting at the ends of cantilevers might not be as close to the real distribution of the reaction force in the block of interacting cantilevers as would be the system of continuous constant reactions, but it can be determined for all possible geometrical arrangements; that is the fundamental advantage of this system, and the reason why it was selected to be used in the model. The derivation of the mathematical solution of the system is presented in Appendix H.3.

To solve problems in more than two dimensions, which is the case for the system of equations describing bending columns of rock, it is necessary to find points mutually common to N unrelated zero-contour hyperplanes each of dimension N-1. Analytical solution of such a problem is impossible However, once the approximate location of a root, or of a place where there might be a root, is identified then the problem can be solved by using the Newton - Raphson method generalized to multiple dimensions (Press, Flannery, Teukolsky and Vetterling, 1990). Solution of a system of nonlinear equations defined in Chapter 3. can be found in the form

$$[\partial x_n] = \left[\frac{\partial f_n}{\partial x_n}\right]^{-1} [-f_n] \tag{4-1}$$

where the matrix of partial derivatives is defined on the next page (Equation 4-2). Solution of such a system is obviously rather complicated, and time consuming. Allowing for 30 iterations at each step, the computer has to solve thirty times a system of 2 n linear equations for n cantilevers. In reality a rock slope usually consists of several hundred cantilevers and, assuming that the slope is unstable, the computer would have to solve subsequently the system of thirty times 2n, 2n-1, 2n-2 .... 2 equations. For example, for the system of 900 cantilevers the computation time would be over 80 hours on the SUN work station.

When the assumptions for the equations were formulated in Chapter 3, it was assumed that the origin of all cantilevers is fixed or, in other words, that the origin of the cantilevers will not move during loading. This assumption introduces great difficulties into the solution. Because the position of the cantilevers after loading is unknown prior to calculation, so is the distance from the origin of points with equal deflections, and thus the position of the common radius cannot be determined. An assumption which makes the solution possible (Equation 3-8) makes the system nonlinear. It was shown on a system of as many as 50 cantilevers, and over a range of Young's modulae from 10 to 80 GPa, by comparing the linear and nonlinear routines that the calculated deformations are so small that the differences in reactions are of no practical relevance, and that the linear system can be used with negligible error being introduced.

$$\begin{bmatrix}
\frac{\partial f_1}{\partial R_1} & \frac{\partial f_1}{\partial \theta_1} & 0 & 0 & 0 & 0 & \cdots & 0 & 0 & 0 & 0 \\
\frac{\partial f_2}{\partial R_1} & \frac{\partial f_2}{\partial \theta_1} & \frac{\partial f_2}{\partial R_2} & 0 & 0 & 0 & \cdots & 0 & 0 & 0 & 0 \\
\frac{\partial f_3}{\partial R_1} & 0 & \frac{\partial f_3}{\partial R_2} & \frac{\partial f_3}{\partial \theta_2} & 0 & 0 & \cdots & 0 & 0 & 0 & 0 \\
0 & 0 & \frac{\partial f_4}{\partial R_2} & \frac{\partial f_4}{\partial \theta_2} & \frac{\partial f_4}{\partial R_3} & 0 & \cdots & 0 & 0 & 0 & 0 \\
0 & 0 & \frac{\partial f_5}{\partial R_2} & 0 & \frac{\partial f_5}{\partial R_3} & \frac{\partial f_5}{\partial \theta_3} & \cdots & 0 & 0 & 0 & 0 \\
\vdots & \vdots & \vdots & \vdots & \vdots & \vdots & & \vdots & \vdots & \vdots & \vdots \\
0 & 0 & 0 & 0 & 0 & 0 & \cdots & \frac{\partial f_{n-2}}{\partial R_{\frac{n}{2}-1}} & \frac{\partial f_{n-2}}{\partial \theta_{\frac{n}{2}-1}} & \frac{\partial f_{n-2}}{\partial R_{\frac{n}{2}}} & 0 \\
0 & 0 & 0 & 0 & 0 & 0 & \cdots & \frac{\partial f_{n-1}}{\partial R_{\frac{n}{2}-1}} & 0 & \frac{\partial f_{n-1}}{\partial R_{\frac{n}{2}}} & \frac{\partial f_{n-1}}{\partial \theta_{\frac{n}{2}}} \\
0 & 0 & 0 & 0 & 0 & 0 & \cdots & 0 & 0 & \frac{\partial f_n}{\partial R_{\frac{n}{2}}} & \frac{\partial f_n}{\partial \theta_{\frac{n}{2}}}
\end{bmatrix} \tag{4-2}$$

The solution of the linear system can be then found in the form

$$[F_n]=[k_n][X_n] \tag{4-3}$$

where the matrix of coefficients $[k_n]$ (equation 4-4) is defined as

$$\begin{bmatrix}
R_1 & y_1 & 0 & 0 & 0 & 0 & \cdots & 0 & 0 & 0 & 0 \\
R_1 & y_1 & R_2 & 0 & 0 & 0 & \cdots & 0 & 0 & 0 & 0 \\
R_1 & 0 & R_2 & y_2 & 0 & 0 & \cdots & 0 & 0 & 0 & 0 \\
0 & 0 & R_2 & y_2 & R_3 & 0 & \cdots & 0 & 0 & 0 & 0 \\
0 & 0 & R_2 & 0 & R_3 & y_3 & \cdots & 0 & 0 & 0 & 0 \\
\vdots & \vdots & \vdots & \vdots & \vdots & \vdots & & \vdots & \vdots & \vdots & \vdots \\
0 & 0 & 0 & 0 & 0 & 0 & \cdots & R_{\frac{n}{2}-1} & y_{\frac{n}{2}-1} & R_{\frac{n}{2}} & 0 \\
0 & 0 & 0 & 0 & 0 & 0 & \cdots & R_{\frac{n}{2}-1} & 0 & R_{\frac{n}{2}} & y_{\frac{n}{2}} \\
0 & 0 & 0 & 0 & 0 & 0 & \cdots & 0 & 0 & R_{\frac{n}{2}} & y_{\frac{n}{2}}
\end{bmatrix} \tag{4-4}$$

To illustrate better how was this matrix formed, rather than constants ($k_{1,1}$, $k_{1,2}$...$k_{n,n}$) the unknowns belonging to the constants were used.

Numerical solution of the system 4-3 is straightforward. The only problem is the size of the matrix with respect to the size of the RAM of common PCs. Fortunately, matrix 4-4 is a sparse matrix, and there are programming techniques available allowing the reduction of the size of the matrix to (n,4).

5. TOPPLING MODEL

5.1. Description of the model.

As mentioned in previous chapters, a slope susceptible to toppling is a slope consisting of distinct layers of rock divided by bedding planes, dipping at an unfavourable angle into the slope, such as the one in Figure 5-1.

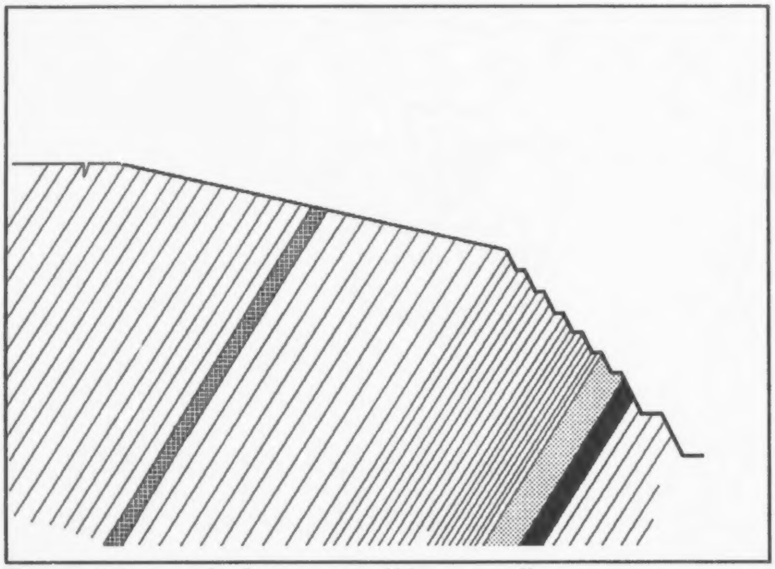

Figure 5-1 A rock slope susceptible to toppling.

Before the layers of the rock can start to bend, subsequently break, and then possibly topple in the block flexural or block toppling modes, the shear strength on at least some of the bedding planes must be overcome. Obviously, this cannot happen on all bedding planes simultaneously. Somewhere in the slope there exists a point where the shear strength/shear stress ratio is a minimum. Even if this ratio is less then unity it is not a sufficient condition for the shear failure to occur along this critical bedding plane. The shear strength/shear stress ratio is not constant along the bedding plane, and so the deformation has the character of progressive failure with, the deformation spreading from the point of origin causing a simultaneous redistribution of stresses. This rather complicated process is replaced in the model by the assumption that failure first takes place along the bedding plane next to the cantilever with the lowest average shear strength/average shear stress ratio (denoted as the shearing safety factor, SSF, in the rest of the text). Derivations of these average stresses are presented in Appendix G.

The process of calculation of stresses in the system of interacting cantilevers was explained in Chapters 3 and 4, and the flow chart of the computation is shown in Appendix H (page 205). To briefly characterize this process it is important to realize that, once all loads are known, to calculate the deformation of cantilevers is a simple mathematical problem. What makes this problem complicated is the fact that a significant portion of these loads, namely the interaction forces (called reactions in the text), are unknown. But these reactions are the main component of the normal forces responsible for the available shear strength of the rock. Hence, the solution is really about the determination of reactions. Once the reactions are known, all stresses, SSFs and deformations of cantilevers in the system can be calculated, and a decision about the slope behaviour can be made.

The result of plotting SSFs along a rock slope would be a curve with , for

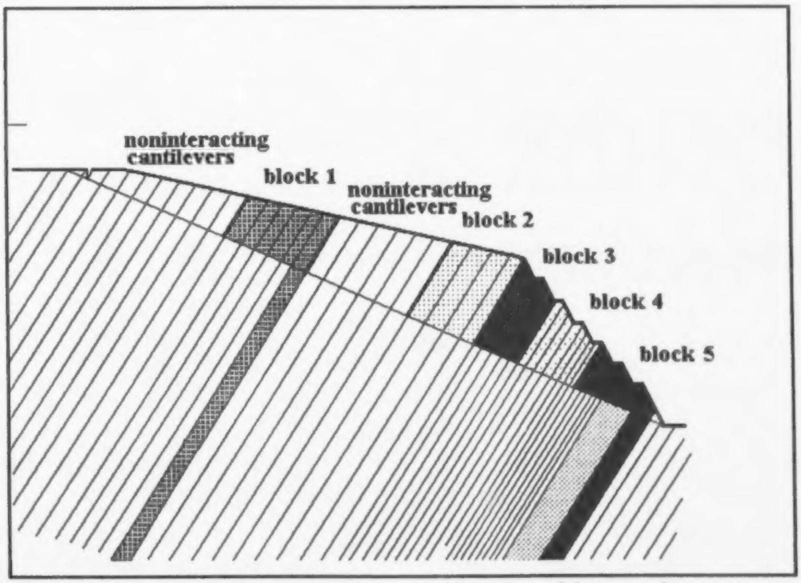

Figure 5-2 Rock slope consisting of blocks of interacting cantilevers and blocks of non-interacting cantilevers.

example, minima above strong cantilevers (high Youngs Modulus) holding the load from softer rock leaning from above, or short cantilevers imbedded among longer ones (area of benches in the highwall) etc. In a slope like the one in Figure 5-1 there would be several local and, of course, one absolute minimum with SSF less then one.

It was assumed in the model that the shear resistance on these critical contacts is zero, and the only forces transmitted through the contacts are reactions which act normal to the contact surfaces. This assumption is not unreasonable because, if the calculation reveals that the average SSF on the contact is less than one, then shearing on the contact will take place, and it is unimportant how big is the resistance against the movement.

At this stage the cantilevers in the slope are divided by the frictionless surfaces into blocks of interacting cantilevers, and into the zones where cantilevers do not interact (do not lean on the lower ones). An example of such a slope is shown in Figure 5-2 (previous page).

The program starts with the slope as shown in Figure 5-1. But as explained earlier, the slope cannot behave as a system of cantilevers defined by bedding planes before the shear takes place on at least a few surfaces. To find these surfaces, the program calculates SSFs for all cantilevers in the slope 5-1, and divides the cantilevers into blocks of interacting cantilevers, and zones of non-interacting cantilevers (the upper cantilever does not lean on the lower one) such as those illustrated in Figure 5-2. The blocks of interacting cantilevers can be considered initially to behave as very thick homogeneous cantilevers. Now a new, stiffer slope has been defined but the forces in this new slope are again unknown. The routine then iterates around again, determining new SSFs, and creating an increasingly stiffer slope. It was shown by numerous tests on fictional slopes that, after the third run, the changes in the geometry of the slope (size of the blocks of interacting cantilevers and the zones of non-interacting cantilevers) become insignificant, and at the same time the resultant geometry does not depart too far from the basic assumptions formulated in Chapter 3.

After the model of the slope has been created, the program starts to test the slope against shear failure along bedding planes within the newly composed blocks. The strength of a block depends on the normal stress and the shear strength parameters of the weakest bedding plane within that block. If the lowest SSF determined is less than one, the block containing this lowest SSF splits into two thinner interacting blocks, now divided by a frictionless surface. Thus a new slope is defined, and the stresses are recalculated. The splitting continues as long as there is a composite block in the slope, and the SSF in that block is less than one. When the splitting is completed, the resulting system of cantilevers is tested for the tensile strength. When the maximum tensile stress exceeds the tensile strength of a block or single cantilever, it is assumed that this block or cantilever breaks, and the surcharge load is assigned to the cantilever below. This, again, defines a new slope, and the procedure returns to the splitting routine (beginning of the paragraph). When all splitting and breaking is finished, either the rest of the slope is stable or the whole slope has failed.

The broken blocks and cantilevers are free to topple or slide along the established failure surface; however the program does not determine whether such sliding or toppling occurs. In case of sliding, the stability problem is of a very different nature, and a classical method of slices could be used to suit the specific geometry of the slope. In case of toppling, the mechanism defining behaviour of the slope above the failure plane is very complex. It is a combination of toppling, sliding, and further breaking of the rock columns, in some cases buried below already broken layers. A routine capable of handling such a problem would have to be of very different nature than the one used for establishing the failure plane.

5.2. The computing routine.

The body of the program is divided into four independent routines. The first one (Input) generates the data describing the geometry of the highwall as defined by the user. The second one (Fredy) incorporates, into the input, the results calculated from the previous runs, the third one (Inshav) tests the slope for the minimum shear strength/shear stress ratios and builds up the new slope from the blocks defined by those extreme ratios smaller than one. Finally, the last routine (Flex) calculates the shear and tensile stresses acting within the interacting blocks and does the splitting and breaking of the rock columns in the slope.

The first and the second routines do not involve in any calculations directly related to the bending of the rock columns.

The third routine (Inshav) which builds the model of the slope to be tested, resembles closely the main, fourth routine Flex. It shares with Flex subroutines which calculate the reactions between the cantilevers, and also the structure of the routine is similar to Flex.

Flex is the main part of the model. It is based on the theory described in Chapters 3 and 4, and its logic structure, as well as the Fortran source codes of all routines, is presented in Appendix I.

6. BACKANALYSIS OF THE FAILURE OF THE HIGHWALL AT THE 50-A-5 OPEN PIT COAL MINE AT THE LUSCAR MINE, CARDINAL RIVER COALS LTD.

6.1. Introduction.

The Luscar Mine of Cardinal River Coals Ltd. is situated in the foothills of the Rocky Mountains at Luscar, Alberta, approximately 50 km southwest of the town of Hinton and 340 km west of Edmonton. The exact location of the pit, and its plan is shown in Appendix J.

Mining began at Luscar in 1921. Complex geology and rugged terrain at Cardinal have resulted in a series of open pits which are mined by the truck and shovel method. Expansion over the years have established the capacity at the current 2.6 million tonnes per year.

In recent years, the mine has experienced several stability problems, which were thought to have been originated by a toppling mechanism. Unfortunately, at that time, there were no methods for assessing the hazard of failure by toppling, except for the simple analysis by Goodman and Bray (1976) (Chapter 2), and that was meant to be more of an illustration of the problem, rather than an analysis.

The proposed method allows calculation of deformations and stresses caused by interacting columns of rock defined by bedding planes and cross joints, if present, and utilises the Mohr-Coulomb strength criterion to test the rock for failure. Furthermore the computer program based on the method enables modelling of the subsequent mining steps, thus following the real development of the mine, and tracing the failure potentially progressing with excavation of each bench. It was proved, as expected, that shear stresses on the bedding planes govern the stability of a slope susceptible to toppling.

6.2. Engineering geology of the 50-A-5 pit (Hebil, 1993)

The 50-A-5 pit was one of several geologically similar pits located along the side of a northwest trending ridge which slopes to the north at 23 degrees and is cut into a series of hills by several alpine valleys. A two phased development of the 50-A-5 south wall produced a 600 m long excavation into one of these hills. The top of this hill was at the 1940 m elevation and was located approximately 78 m above and 214 m behind the crest of the south wall.

The excavated highwall ranged between 90 and 120 m in height. However, the location of the hillside behind the wall resulted in an overall slope height of about 213 m in the central part of the pit.

A simplified cross-section (Figure 6-1) through the highest part of the south wall was used for the analysis. The highwall was excavated in the southern limb of an overturned syncline/anticline fold pair which plunges to the northeast at 23 degrees. The axial plane of the syncline dips to the southwest at about 40 degrees, intersecting the wall at approximately the 1758 m elevation. The mine plan is shown in Appendix J, (Figure J-2).

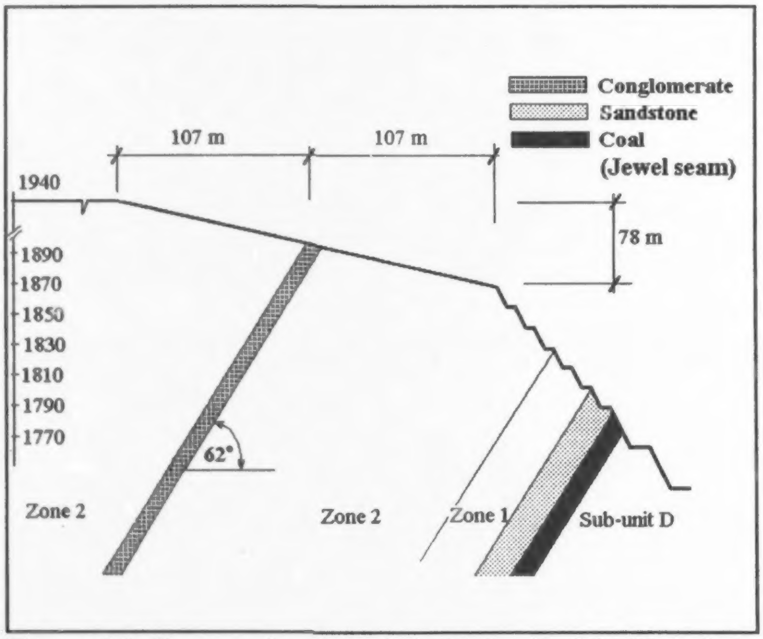

Figure 6-1 Cross-section through the highwall of the 50-A-5 pit

The hillside and highwall above the axial plane are susceptible to toppling because of overturned bedding which dips south at 60 to 70 degrees into the slope. Bedding below the axial plane is right way up and dips 20 to 30 degrees south.
Several joint sets occur in the rock above the axial plane but two dominant ones affect slope stability. One near vertical set strikes northeast, approximately perpendicular to the trend of the highwall. A second set is cross jointed approximately 90 degrees to bedding. This set dips between 25 and 40 degrees north out of the south wall.

The south wall was excavated entirely within Members of the Luscar Formation. Member "D" is the uppermost sub-unit and occurs in the syncline at the bottom of the south wall. It consists of massive siltstones and sandstones with minor shale and coal beds. This sub-unit at the top of the syncline did not cause any stability problems, and because of that it was not included in the analysis, and it is not shown in the figure 6-1.

The Jewel Coal Seam intersects the highwall at about elevation 1783 and defines the base of this sub-unit.

The Torrens Member is located in the central third of the south wall and consists mostly of interbedded siltstones and sandstones. This sub-unit is called Zone 1. It is characterised by an 18 m thick, massive sandstone which underlies (bedding is overturned) the Jewel Seam.

Marine shales of the Moosebar member are found in the upper third of the highwall. The lowermost Gladstone Member, consisting of thinly interbedded siltstones and shales (Zone 2), is located in the lower half of the hillside above the pit crest.

The 11 m thick Cadomin conglomerate occurs halfway up the hillside. It separates the Luscar Formation from the thin-bedded shales and siltstones of the Nikanassin Formation which form the top part of the hill.

Rocks in the Luscar Formation range in unconfined compressive strength from 150 MPa for the Torrens Sandstone to 25 to 50 MPa for the Moosebar Shales. Interbedded sequences of sandstone, shale and siltstone have strengths that are intermediate between these values and average between 25 and 70 MPa.

Friction angles for discontinuities vary from 16 degrees for bedding planes in carbonaceous shales to 35 degrees for joint surfaces in sandstone. The friction angle along sheared coal surfaces averages 20 degrees. Cohesion between these surfaces is less than 20 kPa.

Ground water levels in the south wall of the 50-A-5 Pit were obtained from development drilling logs. These placed the water table 60 m below ground surface. This depth was determined to be below the base of the failure.

6.3. **Highwall design and development** (Hebil 1993)

The 50-A-5 south wall was designed at an overall slope angle of 45 degrees with 12 m high benches having 65 degree bench face angles and 6.5 m wide safety berms.

Mining of the 50-A-5 Phase 2 wall started in February, 1989 and was completed by the summer of 1991. Slope movement was first observed in mid-September, 1989 when the upper two benches were excavated to the 1840 m elevation. This produced a 25 to 30 m high cut in the hillside which extended the 280 m long Phase 1 south wall 250 m further west. This extension initiated toppling almost immediately. Back facing obsequent scarps developed on the crest and benches of the highwall. Over the next several months small obsequent scarps developed progressively upslope to the top of the hill where eventually a 9 m wide tension crack defined the southern limit of the failure. By February 1990, when excavation of the 1780 bench was under way, nearly all the benches above this elevation had failed.

It is necessary to realize that Electronic Distance Measurement survey techniques used for monitoring the 50-A-5 pit are only capable of measuring surface displacements, and no borehole measurements were included in the monitoring program. Consequently, the position of the failure plane(s) was not recorded, and also the amount of deformation caused by toppling and shearing movements respectively could not be identified. On the other hand, it is unlikely that the final deformation of the surface, which at the crest area was as large as 20 m, can be explained in terms of toppling only. Unfortunately, the presented method, as well as all methods known to the author of this thesis used in stability calculations in geotechnics, cannot give any information about behaviour of a rock slope after the failure. Hence, not being able to distinguish between deformations before failure and after failure, and between deformations caused by toppling and deformations caused by sliding, the comparison of field measurements and the analysis results could not be done in terms of displacements.

There is, however, still a strong support for the correctness of the analysis results.

First, the safety factor against the shear failure calculated by the Luscar personnel (Hebil,1994) using the Janbu method is close to 2, even when using the combination of weakest strength parameters for each rock subunit. Hence, the shear failure was not likely to be the triggering mechanism of the deformation of the slope.

Second, the stepped character of the deformation of the surface (Figures 6-2, 6-3, 6-4 and 6-5 on the following pages), which developed during the excavation, supports the theory that toppling was present during slope movements. That is also what was agreed on by the geological and geotechnical personnel of Cardinal River Ltd.

Third, the calculated sequence of the consecutive failures following the excavation of the slope and the calculated volume of the rock involved in the failure zones correspond very well with the real sequence of deformation and volume of involved rock measured by the monitoring system on the surface (Hebil 1994).

Fourth, provided that the movements monitored on the surface (20 m at the crest area) were based on some deeply seated failure plane, which was the only explanation offered when using any conventional stability analysis, the amount of rock debris which would have failed into the pit must have been in order of millions of tons of rock (K. Hebil, 1993). In reality, the amount of rock debris removed from the pit after failure was in order of tens of thousands of tons. There was no other explanation of this phenomenon offered other than the result of this analysis (deep seated toppling failure with shallow based shear failure; section 6.4., Figure 6-12), and this explanation was accepted as satisfactory by the Luscar geotechnicians.

The presence of the solid block in the centre of the slope, as predicted by the model (Figure 6-12) is very interesting. Unfortunately, there were no deep seated measurements which would allow the direct conformation of its existence.

Figure 6-2 At the pit crest looking E from the section line (Figure J-1)

Figure 6-3 At the pit crest on the section line looking N (Figure J-1)

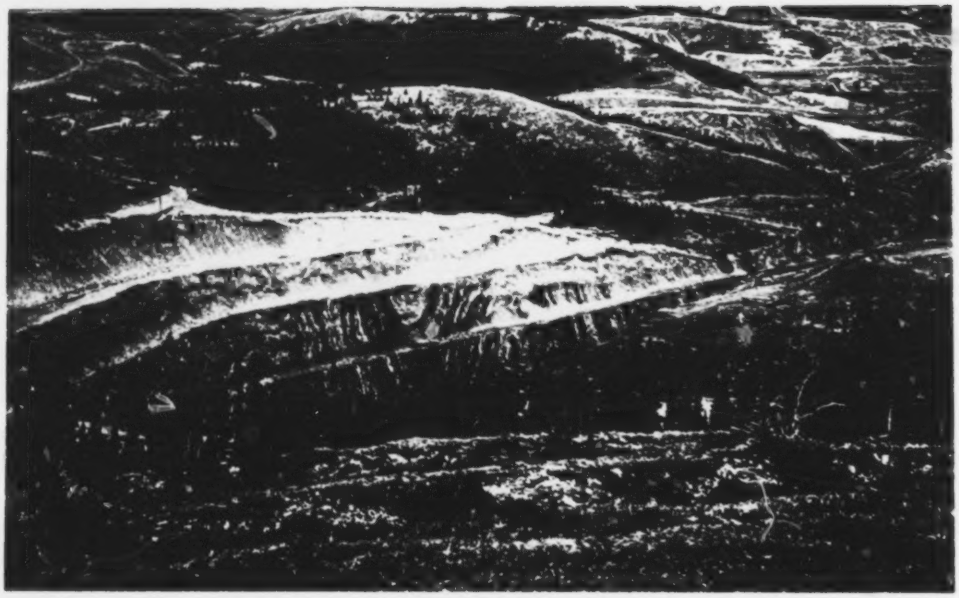

Figure 6-4 On the section line (elevation 1890 m) looking N (Figure J-1).

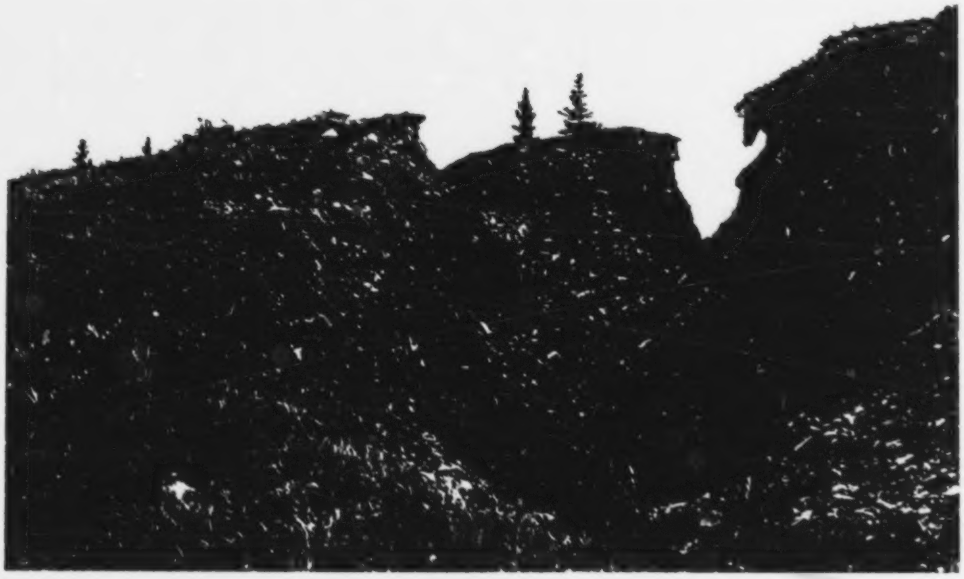

Figure 6-5 A crack at the top of the hill.

6.4. Analysis of the failure

The analysis was made on the Sun work station which allowed modelling of the full extent of the slope by the program described in section 2.

The following strength parameters, selected from the lower end of the range offered by geological survey and engineering testing, were used in the analysis.

	Internal angle of friction	cohesion [kPa]	tensile strength [kPa]	t* [m]
coal	25	4	2	12
Torr. sandstone	35	250	150	18
zone 1	25	10	5	1
zone 2	16	8	4	0.5
conglomerate	38	500	300	11

t* ....cantilever thickness within bed

The results of the analysis of the slope shown in the figure 6-1 are graphically presented in Figures 6-6 to 6-12 where each figure corresponds to one mining step. All deformations shown are due to bending, and the mechanism of the deformation was defined in the thesis as flexural toppling. The failed rock is shown as the spreading solid black area above the lowest basal failure plane. The slope geology and geometry was identified in Figure 6-1.

Following the results of the analysis, the failure started with mining of the first bench (elevation 1852 m) by breaking of a few cantilevers above the crest which were too short to interact with the lower and longer ones (Figure 6-6). The failure above the crest region spread even more with mining of the second bench (elevation 1840 m), and also the cantilevers in the second bench were lost (Figure 6-7). Mining of the third bench (elevation 1828 m) triggered the failure along the whole base plane by which the underlying cantilevers were trimmed to equal lengths, creating below the failed rock a very stable zone with very smooth distribution of shear stresses (Figure 6-8). Thus mining bench number four (elevation 1816 m) caused only some minor damage right below the conglomerate which holds the upper portion of the slope (Figure 6-9). Extracting the rock in the fifth bench (elevation 1804 m) completed the failure of the highwall, all the benches were lost (Figure 6-10). Mining bench six (elevation 1792 m) further reduced the support of the conglomerate and extended the damage on the face (Figure 6-11). Finally, mining the seventh bench (elevation 1768 m) caused the collapse of the conglomerate, and all the rest of the slope up to and beyond the crest of the hill (Figure 6-12) creating at the same time a crack at the top of the hill.

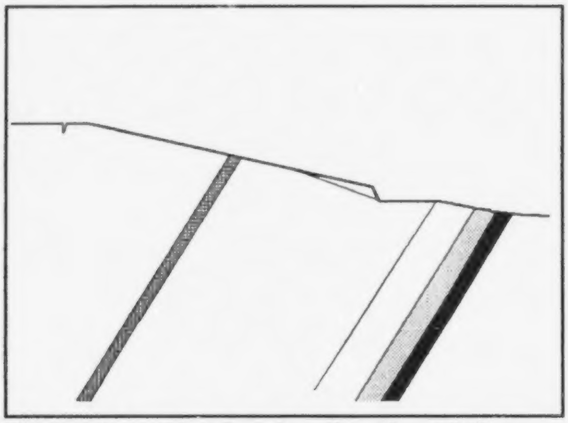

Figure 6-6 First bench - elevation 1852 m

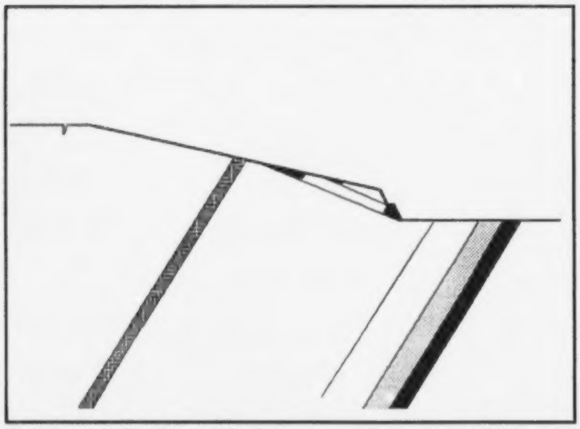

Figure 6-7 Second bench - elevation 1840 m

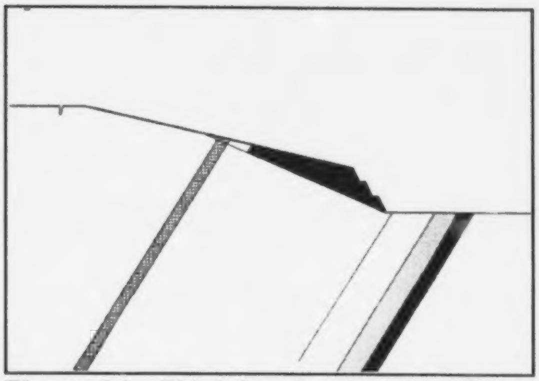

Figure 6-9 Third bench - elevation 1828 m

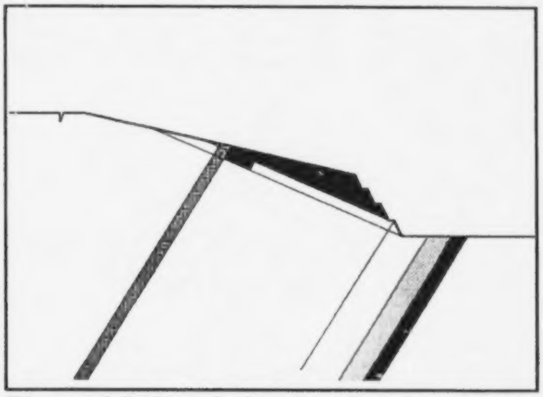

Figure 6-8 Fourth bench - elevation 1816 m

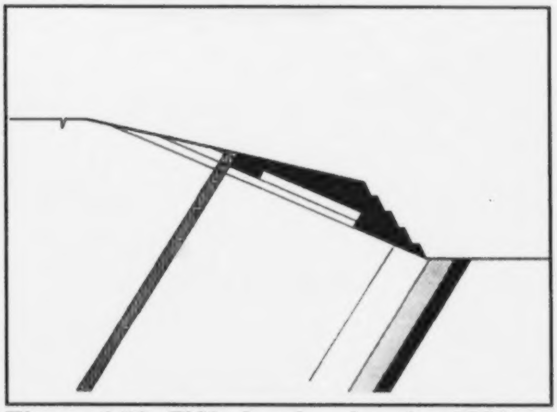

Figure 6-10 Fifth bench - elevation 1804 m

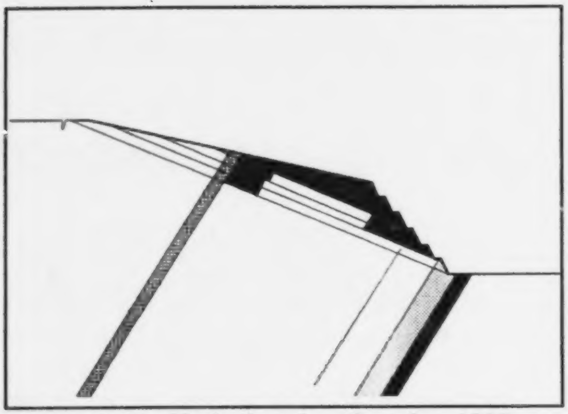

Figure 6-11 Sixth bench - elevation 1792 m

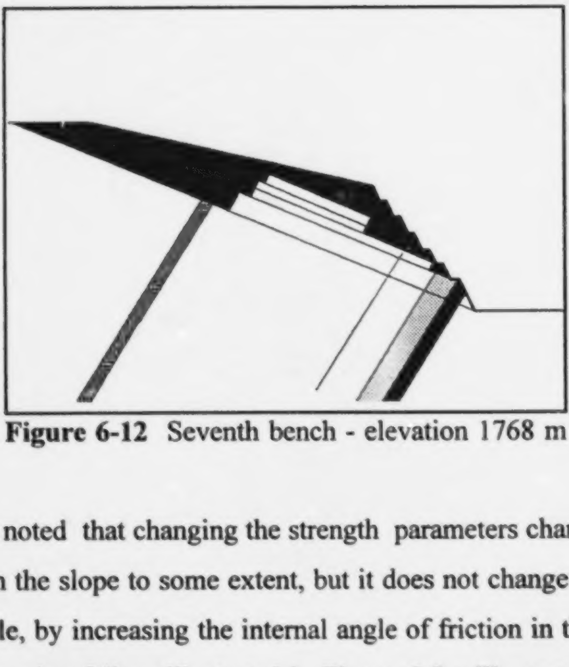

Figure 6-12 Seventh bench - elevation 1768 m

It should be noted that changing the strength parameters changes the distribution of the failure within the slope to some extent, but it does not change the character of the failure. For example, by increasing the internal angle of friction in the critical zone 2 to 25 degrees, the extensive failure illustrated in Figure 6-8 will move to the next mining step, and will be more violent with some minor breaking in the upper portion of the slope. This could possibly lead to a disastrous failure instead of the controlled one because the potential energy stored in the resisting system at the time of the failure (the weight of resisting cantilevers) would be much higher. But basically within the range of the given strength parameters, the program predicts very closely the sequence of deformations as monitored on the surface, and described in section 6.3.

It is apparent from Figure 6-8 that very large shear forces must act on the base of the stable block of rock columns in the middle of the slope, and that this block may possibly fail by simple plane shear. Some other routine should be used for that analysis. When treating the slope as a system of two interacting blocks, one within and the second above the stable area, simple shear plane failure analysis can be done, and results are presented in the following table .

	ϕ [deg.]	c [kPa]	SF
block 1	16	0	
block 2	30	130	1.1
block 1	22	0	
block 2	35	350	2.2

It is important to realize that the slope above the bottom of the pit is broken along multiple failure planes at multiple elevations. The blocks released by flexural toppling will in most cases start to topple in block or block flexural toppling modes, depending on the shape of the toppling blocks. This toppling movement will cause even more breaking within the slope, creating additional local failure planes. Prediction of further behaviour of such a slope is extremely difficult, and would also depend on the dynamics of the deformation process.

6.5. Influence of bedding dip.

For comparison, the stability of two other slopes differing in dip with otherwise identical geological strata were tested. Results of these analyses are presented graphically in Figures 6-13 to 6-28 (following pages).

Dip 50 degrees:

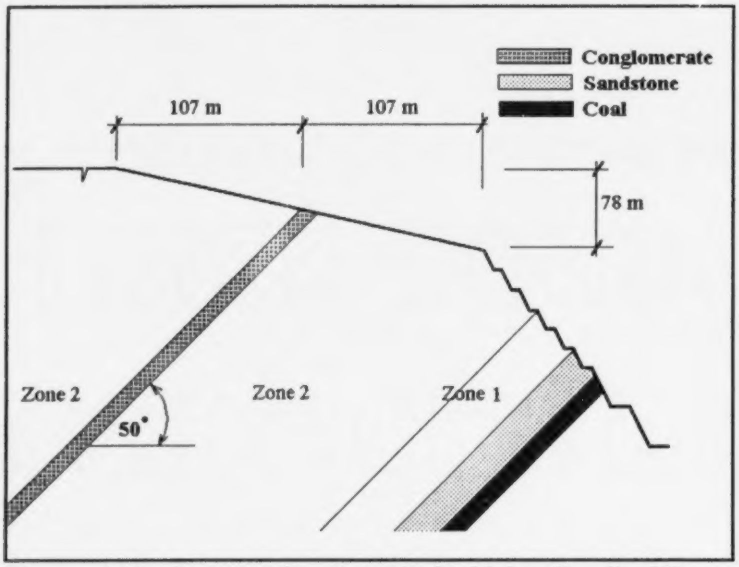
Conglomerate
Sandstone
Coal
107 m
107 m
78 m
Zone 2
Zone 2
Zone 1
50°

Figure 6-13 Cross-section through the highwall - dip 50°

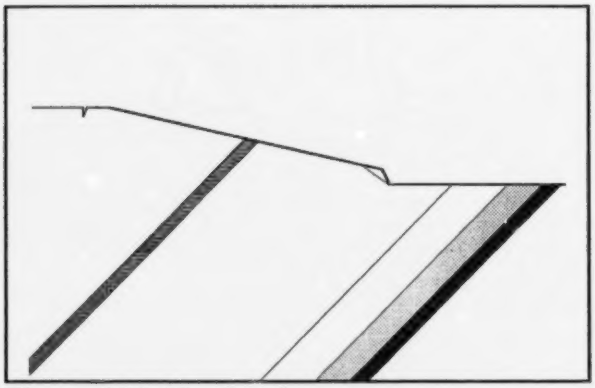

Figure 6-14 First bench

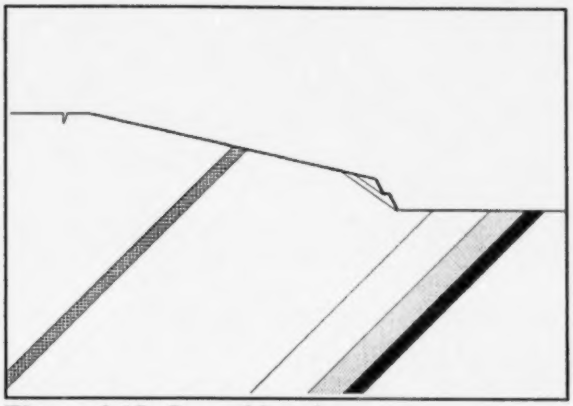

Figure 6-15 Second bench

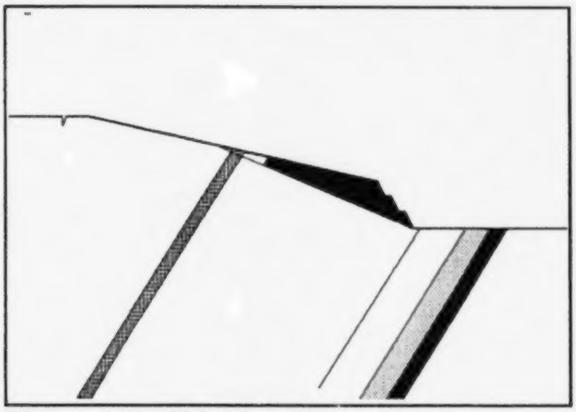

Figure 6-16 Third bench

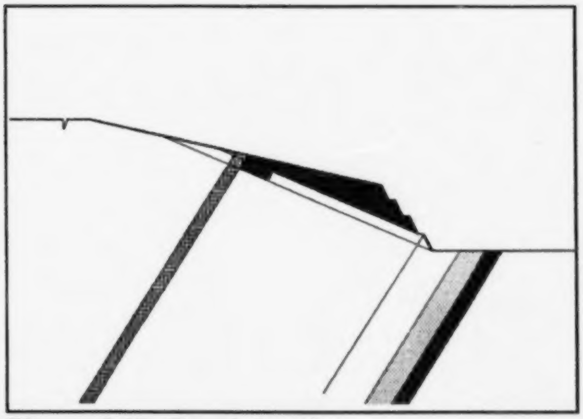

Figure 6-17 Fourth bench

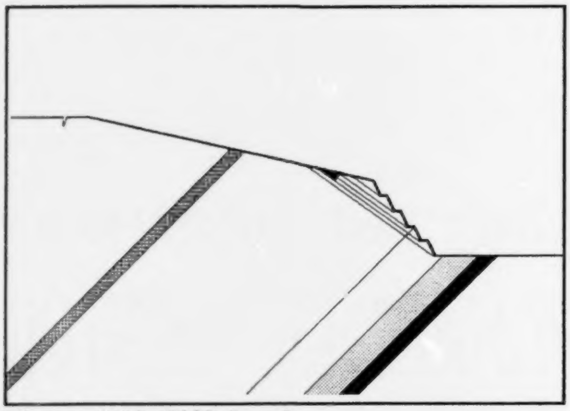

Figure 6-18 Fifth bench

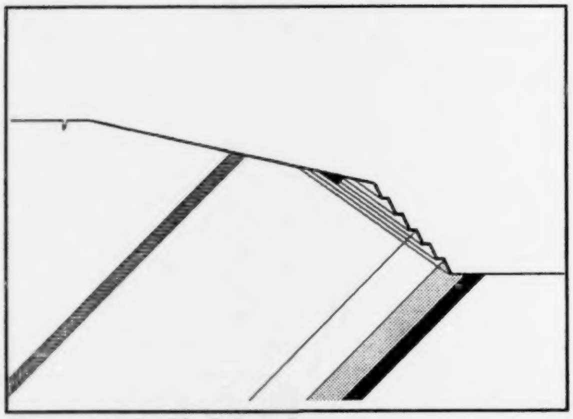

Figure 6-19 Sixth bench

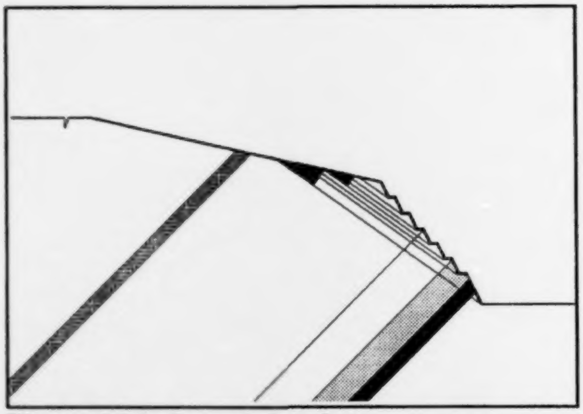

Figure 6-20 Seventh bench

Dip 70 degrees :

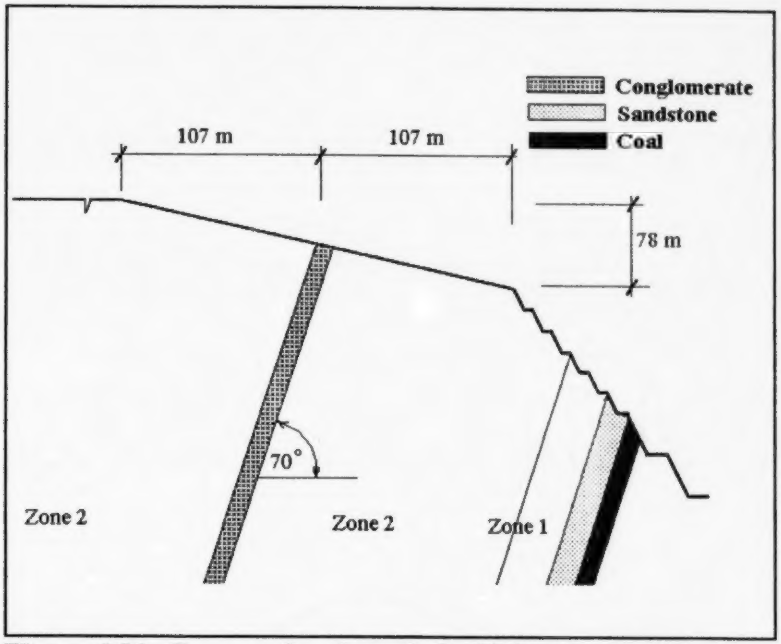
Conglomerate
Sandstone
Coal
107 m
107 m
78 m
70°
Zone 2
Zone 2
Zone 1

Figure 6-21 Cross-section through the highwall - dip 70°

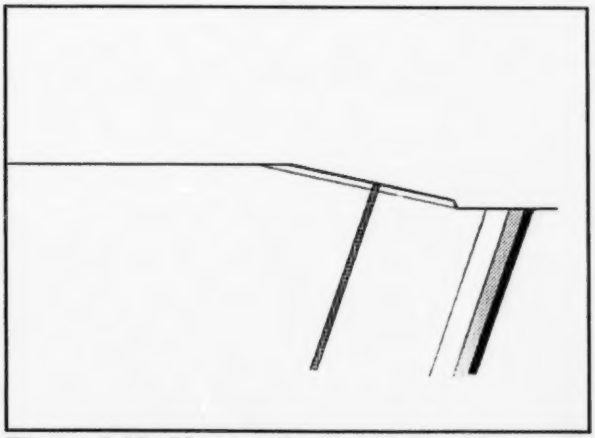

Figure 6-22 First bench

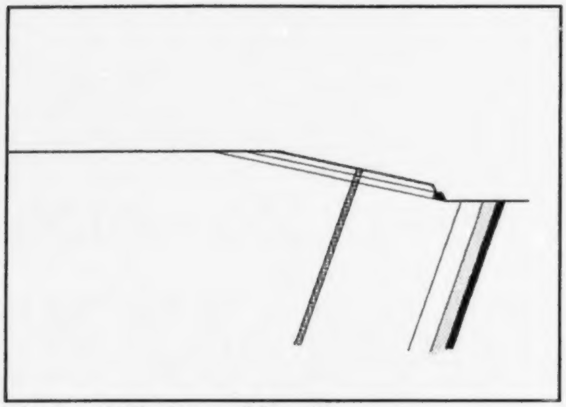

Figure 6-23 Second bench

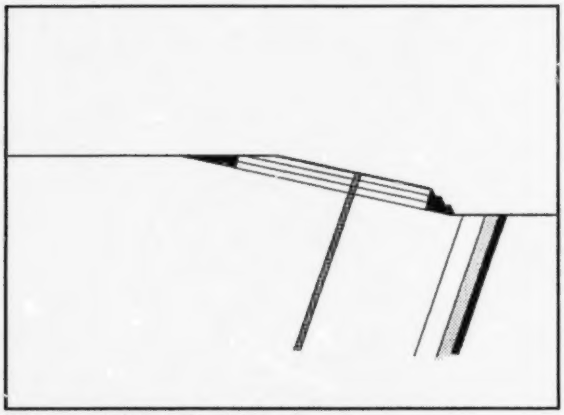

Figure 6-24 Third bench

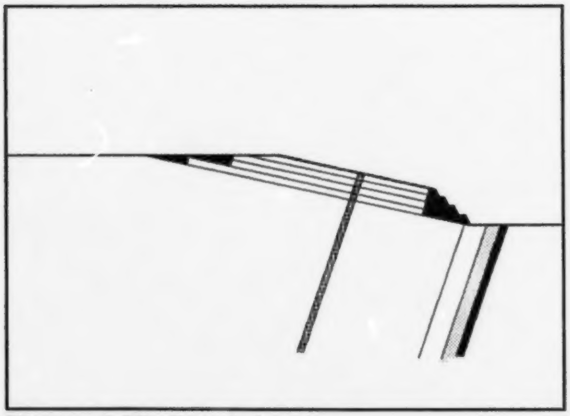

Figure 6-25 Fourth bench

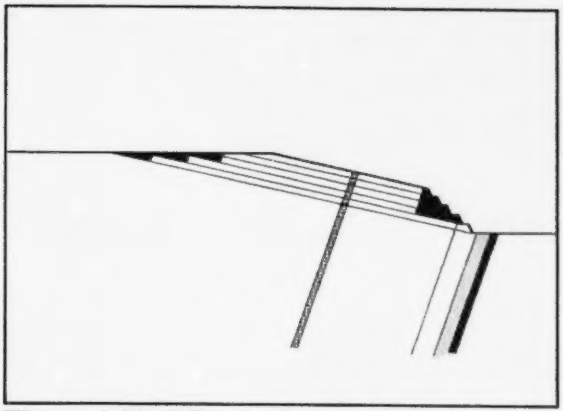

Figure 6-26 Fifth bench

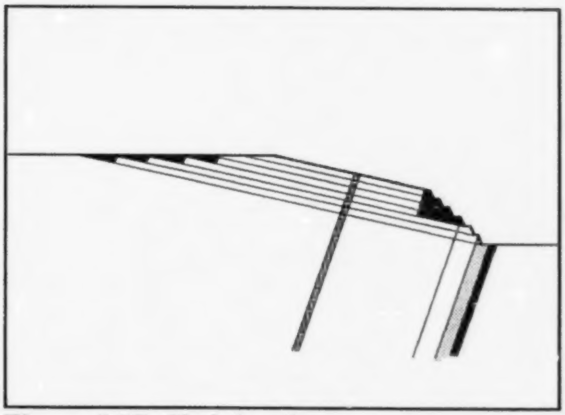

Figure 6-27 Sixth bench

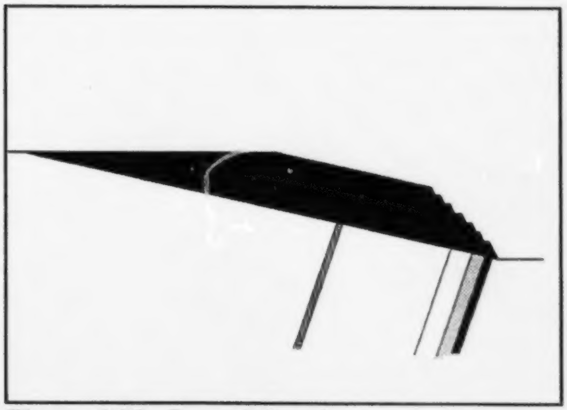

Figure 6-28 Seventh bench

The reason why, from all the program input parameters, the dip was chosen to be altered was not accidental. The purpose of this thesis was to develop a method capable of predicting of behaviour of slopes susceptible to toppling. The only way to prove that this method has a validity in practice was to test it on a real case history, and subsequently a computer program had to be created. To do a real parameter study using this program could be a topic for another thesis, and is obviously far beyond the scope of this thesis. For this reason, after the consultation with Luscar personnel, the parameter which is believed to be critical for toppling by both authors of the thesis and Luscar geotechnicians (the dip of strata), was chosen to be tested in two additional runs presented on previous pages. There was, in fact, another reason for this decision. A new pit is under excavation at Cardinal River in almost identical geological conditions as the pit 50-A-5, except the dip which is close to 50°. Preliminary results from the monitoring program showed so far zero deformations, and so did the computer model. In Figures 6-14, 6-15 and 6-16 the slope remains intact, and only after mining the fourth and the seventh benches (Figures 6-17 and 6-18) does some damage to the slope occur at the top region. The deformations are negligible, because the bottom part of the slope remains intact.

On the other hand increasing the dip to 70° causes the overall collapse of the slope after mining the seventh bench. An important aspect of comparison of the 50-A-5 slope (dip 62°) with the slope with the dip of bedding 70° is the relatively (with respect to the total volume) smaller damage of the slope with the steeper dip before the overall collapse. It is understood that by failing partially during the excavation, the 62° slope "released" some of the potential energy stored in the system, and consequently it was able to resist the enormous load (energy) released by the failure of the conglomerate in the middle of the slope after excavation of the seventh bench (Figure 6-8).

7. SUMMARY AND CONCLUSIONS

1) A new theory defining the toppling mechanism in terms of equations is formulated in this thesis, and a computer model based on this theory shows the validity of the theory in practice.

2) The comparison of the computer simulation with a case history shows that behaviour of a rock slope composed of bedded layers dipping at an angle which favours toppling deformation can be modeled with satisfactory precision as a set of interacting rock cantilevers.

There are two major reasons for the previous assertion based on the results of the backanalysis of the failure of the highwall at the Luscar Mine of Cardinal River Coals Ltd.

First, the calculated sequence of the consecutive failures following the excavation of the slope, and the calculated volume of the rock involved in the failure zones, correspond very well with the real sequence and area of deformation as measured by the monitoring system on the surface.

Second, if the movements monitored on the surface (20 m at the crest area) were based on some deeply-seated failure plane, which was the only explanation offered when using any conventional stability analysis, the amount of rock debris which would have failed into the pit would have been in order of millions of tons of rock (K. Hebil, 1993). In reality, the amount of rock debris removed from the pit after failure was in order of tens of thousands of tons. No other explanation of this phenomenon has been offered, other than the result of this analysis (deep-seated toppling failure with shallow based shear failure; section 6.4., Figure 6-12), and this explanation was accepted as satisfactory by the Luscar geotechnicians.

3) It was conceived that flexural toppling, block toppling and block flexural toppling could be three distinct stages of one deformation process rather than three different toppling mechanisms. Any deformation in a toppling slope starts with a bending, however small this movement may be, and in case of separation of the rock

block from the base could continue as a block toppling, and then possibly as a block flexural toppling (This is not to say that block and block flexural toppling could not exist in their own right).

4) It is possible to generalize at this stage, and to say that the failure in the flexural toppling mode will result in many cases in subsequent block or block flexural toppling. This further deformation may finally stabilize without causing an overall collapse of the slope. That does not mean that the slope will not collapse in some different failure mode like, for example, plain shear.

5) It is obvious, from the analysis results, and also from the developed theory, that the stepped base, such as used by Goodman and Bray in 1976 for derivation of their equations, can rarely exist in reality. The original Goodmans and Bray approach was developed much further in section 3.4.2. At that stage, it became obvious that the basic toppling or rather the overturning case is the one where rock blocks are overturning on a planar rather than stepped surface. Unfortunately, this deformation mechanism cannot be solved in terms of simple, safety factor based analysis, and probably some distinct element based routine would be necessary for the solution of the problem. Therefore the overturning on the stepped base, being a rather exceptional case, was not included in the computer model.

6) Failure of slopes by flexural toppling is governed by the shear forces generated by interacting blocks of bending rock columns. After the rock blocks start to split into smaller and smaller columns, and ultimately into the set of primary columns defined by individual bedding planes, the resultant failure surface can be found as the plane of highest tensile stresses.

7) Higher strength parameters define a stronger slope which would sustain more loading without a failure, but could finally fail in more violent way than the slopes defined with lower strength parameters which tend to break partially at an earlier stage.

8) The progressive block flexural and block toppling above the basal surface created by flexural toppling will create additional zones of fractured rock defined by lower strength parameters which may connect to form a new failure plane with an unfavourable inclination, and lead to triggering of an unexpected shear failure.

8. RECOMMENDATIONS.

The program in its present form can be used successfully to analyze bedded slopes such as those defined in section 3.4.1 for potential toppling without any restrictions. The result of the analysis is the position and the extent of the failure plane (the program deals with the progressive character of the failure). The program is also designed to be able to follow the sequential excavation or creation of the slope, for example that during open pit mining.

1) It would be useful at this stage to run a parametric study with the present model. It would add to the understanding of the toppling mechanism, and it would also help to clarify the priorities in the further development of the model.

The very first thing which could be improved rather easily is the routine for entering data defining a water table (subroutine input). At the present stage it is rather too complex, and it lacks necessary flexibility.

2) Secondly, at the present stage the model iterates around the splitting routine until any SSF (page 71) is smaller than unity, and then calls the breaking routines (see the flowchart in Figure I-1). The program would run faster if the sequence of the calculation was changed in such a way that, after each successful splitting, the breaking routines were called before another test for splitting was run. In this way, for some cases, larger blocks would fail at once without first being split into smaller units thus speeding the calculation up without changing results.

3) Third, it would be useful, if the position of the failure plane determined by the program were compared to the position of the real failure plane determined either from the core drilling or from geophysical testing.

4) The last recommendation which is made with respect to this model concerns the offset arrangement of crossjoints (Figure 3-9, page 50). The program now simulates the slope with an inline arrangement of joints which is rather rare in reality. Mostly, crossjoints are persistent only over several layers of rock, and so the offset arrangement of joints is more realistic. The resultant failure plane should not change very much

except that it would be curved at its top portion with a smaller vertical crack at the end, instead of being divided by only a vertical crack from the rest of the slope. The difference between the two routines would lie in the state of the rock above the separation plane. The inline arrangement of joints leads directly to the block toppling mechanism which would then be solely responsible for block flexural toppling. The offset arrangement of joints would leave the failed rock column already broken in several pieces.

A new routine resembling subroutine Newton would have to be written for this case. The matrix of coefficients would be identical to the matrix 4-4, page 69 except for several new coefficients at the places of some of the zeroes. The mathematical solution of the problem is straightforward. Unfortunately, the programming part would be difficult. In the present solution, advantage was taken of the sparsity of the matrix 4-4. The new matrix would still be a sparse matrix, but the position of the new coefficients would only be determined after the failure of some cantilever, thus complicating the solution, because the shape of the matrix will change with each calculation step. This could actually exclude the possibility of taking advantage of sparsity of the matrix, and basically destroy any possibility of a reasonable solution of the problem for a real slope with several hundred cantilevers using commonly available computers (time and RAM size concerns).

There is also a possibility of ignoring these new coefficients, accepting the error in the solution, and then only the geometry of the slope tracing routines (Chan, Change) would change. This way seems to be the more promising at present.

REFERENCES

1. **Aydan, O. and Ichikawa, I., 1991.** An integrated system for the stability of rock slopes. *Proc., the 7th Int. Conf. on Computer Methods and Advances in Geomechanics, Cairus,vol. I, pp 469-474.*

2. **Barton, N., 1974.** Rock slope performance as revealed by a physical joint model. *Proc., the 3rd Congress of the Int. Soc. for the Rock Mech. (ISRM), Denver, vol. II, part B, pp 765-773.*

3. **Brady, B.H.G. and Brown., E.T., 1985.** Rock mechanics for underground mining. *George Allen & Unwin (publishers) Ltd, London, pp 167-183.*

4. **Broadbent, C.D. and Zavodni, M.Z.,** 1981. *Proc., the 3rd Int. Conference on Stability in Surface Mining AIME, Vancouver, pp 1-19.*

5. **Bukovansky, M., Rodriguez, M. A. and Cedrun, G., 1974.** Three slides in stratified and jointed rocks. *Proc., the 3rd Congress ISRM,Denver, vol. II, Part B, pp 854-859.*

6. **Callaway, C., 1879.** On plagioclinal mountains. *Geological Magazine, vol. 15, pp 216-221.*

7. **Canizal, J. and Sagaseta, C., 1988.** Numerical analysis of discontinuous block systems. *Proc., the 6th Int. Conf. on numerical methods in geomechanics, Insbruck,vol. II, pp 895-900.*

8. **Chen, H.S. and Xiong, W.L., 1991.** An elastic-viscoplastic block theory for rock masses. *Proc., the 7th Int. Conf. on Computer Methods and Advances in Geomechanics, Cairus,vol. I, pp 311-314.*

9. **Cheung, K., 1977.** Beams, slabs, and pavements. *Numerical methods in Geotechnical engineering. Edited by Desai C. S. and Christian J.T., pp 176-210.*

10. **Choquet, P. and Tanon, D.D.B., 1985.** Monograms for the assessment of toppling failure in rock slopes. *Proc., the 26th Symposium on Rock Mechanics, Rapid City, vol. I, pp 19-30.*

11. **Cruden, D.M. and Hu X.Q., 1990.** Some recent developments in the analysis of rock slope movements in the Rockies. *Symposium on Landslide Hazards in the Canadian Cordillera, GAC/MAC Annual Meeting , Vancouver.*

12. **Cruden, D.M., 1989.** The limits to common toppling. *Canadian Geotechnical Journal, vol. 26, pp737-742.*

13. **Cundall, P.A., Voegele, M. and Fairhurst, Ch., 1975.** Computerized design of rock slopes using interactive graphics for the input and output of geometrical data. *Proc., the 16th Symposium on Rock Mechanics, Mineapolis, pp 5-14.*

14. **Cundall, P.A., 1987.** Distinct element models of rock and soil structure. *Analytical and computational methods in engineering rock mechanics. Edited by E.T. Brown, London, Allen & Unwin Ltd, pp 129-162.*

15. **Freitas de, M.H. and Watters, R.J., 1973.** Some field examples of toppling failure. *Geotechnique 23, no 4, pp 495-514.*

16. **Gillett, S.G. and De Natale, J.S., 1988.** A comparison of four slip surface search routines. *Proc., the 6th Int. Conf. on Numerical Methods in Geomechanics, Insbruck,vol. III, pp 2151-2156.*

17. **Goodman, R.E., 1976.** Methods of geological engineering in discontinuous rock. St. Paul: West.

18. **Goodman, R.E. and Bray, J.W., *1976.*** Toppling of rock slopes. *Proceedings, Specialty Conference on Rock engineering for Foundations and Slopes, ASCE, Boulder, Colorado, PP 201-234.*

19. **Greco, V.R., 1988.** Numerical methods for locating the critical slip surface in slope stability analysis. *Proc., the 6th Int. Conf. on Numerical Methods in Geomechanics, Insbruck,vol. II, pp 1219-1223.*

20. **Hebil, K.E., 1993.** Stability and Mining of Slopes Prone to Toppling Failure at the Cardinal River Mine, Luscar, Alberta. *95th Annual General Meeting, C.IM, Calgary.*

21. **Hebil, K.E., 1994.** Personal communication.

22. **Heslop, T.G., 1974.** Failure by overturning in ground adjacent to cave mining at Havelock mine. *Proc., the 3rd Congress ISRM, Denver, vol. II, part B, pp 1085-1089.*

23. **Hu, X.Q. and Cruden, D.M., 1992.** Topples on underdip slopes in the Highwood Pass, Alberta, Canada. *The paper prepared for submission to Quarterly Journal of Engineering Geology. University of Alberta, Civil Engineering dep.*

24. **Itasca Consulting Group, Inc. 1987.** FLAC, Fast Langrangian Analysis of Continua. *Manual, Minneapolis, US.*

25. **Kulatilake, P.H.S.W. and Wathugala D.N., 1991.** Probabilistic joint network modelling in three dimensions including a verification. *Proc., the 7th Int. Conf. on Computer Methods and Advances in Geomechanics, Cairus, vol. I, pp 359-364.*

26. **Manfredini, G. and Martinetti, S., 1975.** Inadequacy of limiting equilibrium methods for rock slopes design. *Proc., the 16th Symposium on Rock Mechanics, Minneapolis, pp35-42.*

27. **Miller, S.M., 1983.** Probabilistic analysis of bench stability for use in designing open pit mine slopes. *Proc., the 24th US Symposium on Rock Mech., Texas, pp 621-629.*

28. **Müller, L. and Hofmann, H., 1970.** Selection, compilation and assessment of geological data for the slope problem. *Proc., Symposium on Planning of Open Pit Mines, Johannesburg, pp 153-170.*

29. **Niyom, D. and Sakurai, S., 1985.** Study on rock slope protection of toppling failure by physical modelling. *Proc., the 26th Symposium on Rock Mechanics, Rapid City, vol. I, pp 11-18.*

30. **Orr, Ch.M. and Swindells, F., 1991.** Open pit toppling failures: Experience versus analysis. *Proc., the 7th Int. Conf. on Computer Methods and Advances in Geomechanics, Cairus, vol. I, pp 505-510.*

31. **Piteau, D.R. and Martin, D. C., 1981.** Mechanics of rock slope failure. *Proc., the 3rd Ing. Conference On Stability in surface mining AIME. Vancouver, pp 113-114.*

32. **Piteau, D.R., Stewart, A. F. and Martin, D. C., 1981.** Design examples of open pit slopes susceptible to toppling. *Proc., the 3rd Ing. Conference On Stability in surface mining AIME. Vancouver, pp 679-712.*

33. **Powell, J.W., 1875.** Exploration of the Colorado River of the West and its tributaries. *Government Printing Office, Washington, U.S.A, pp 291.*

34. **Press, W.H., Flannery, B.P., Teukolsky, S.A. and Vetterling, W.T., 1989.** Numerical recipes (Fortran version). *Cambridge university press, pp 271-273.*

35. **Richings, M., 1981.** The role of slope stability in the economics, design and operation of open pit mines - An update. *Proc., the 3rd Int. Conference on Stability in Surface Mining AIME, Vancouver, pp 1-19.*

36. **Scavia, C., Barla, G. and Bernaudo, V., 1990.** Probabilistic stability analysis of block toppling failure in rock slopes. *Int. J. Rock Mech. Min. Sci. & Geomech. Abstr., vol. 27, no. 6, pp 465-478.*

37. **Shi, G. and Goodman, E., 1988.** Discontinuous deformation analysis. A new method for computing stress, strain and sliding of block systems. *Proc., the 29th US Symposium on Rock Mechanics, Mineapolis, pp 5-14.*

38. **Shi, G. Goodman, R.E. and Tinucci, J.P., 1985.** The kinematics of block interpenetrations. *Proc., the 26th US Symposium on Rock Mechanics, Rapid City, vol. I, pp 121-130.*

39. **Teme, S.C. and West, T. R., 1983.** Some secondary toppling failure mechanisms in discontinuous rock slopes. *Proc. the 24th US Symposium on Rock Mechanics., Texas, pp 193-204.*

40. **Warburton, P. M., 1990.** Laboratory test of a computer model for blocky rock. *Int. J. Rock Mech, Min. Sci. & Geomech. Abstr., vol. 27, no. 5, pp 445-452.*

41. **Whyatt, J.K. and Julien, M., 1988.** A fundamental question: The role of numerical methods in rock mechanics design. *Proc. the 29th US Symposium on Rock Mechanics, Minneapolis, pp 311-315.*

42. **Wyllie, D. C., 1980.** Toppling rock slope failures examples of analysis and stabilization. *Rock Mechanics, vol. 13, pp 89-98.*

43. **Xing, Z., 1988.** Mathematical model of probabilistic analyses for a jointed rock slope. *Proc., the 6th Int. Conf. on Numerical Methods in Geomechanics, Insbruck,vol. II, pp 877-882.*

44. **Young, D.S. and Hoerger,D.F., 1988.** Geostatistics applications to rock mechanics. *Proc., the 29th US Symposium on Rock Mechanics, Minneapolis, pp 271-282.*

45. **Zanbak, C., 1983.** Design charts for rock slopes susceptible to toppling. *J. of Geotechnical engineering, vol. 109, pp 1039-1062.*

46. **Zischinsky, U., 1966.** On the deformation of high slopes. *Proc., the 1st Congress ISRM, Lisbon, vol. II, pp 179-185.*

Appendix A.

Derivation of equations of the system of interacting cantilevers for block flexural toppling.

There are generally two ways to deal with this problem. First, to find a form of the Airy's function for the given boundary conditions, and then either to try to find a closed form solution or to solve the equations by numerical methods. Second, to use beam theory. In this thesis beam theory was used. (The reasons for this choice were covered in the theoretical part of the thesis, chapter 3.).

This derivation is divided into several sections. Each section deals with a single load, and the final equations for combination of all loads for n cantilevers are simply the sum of all loading states. In the following derivations $y(x)_n$ is a deflection of the nth cantilever at a point x, $\Theta(x)_n$ is an angle of the tangent to the deflection curve of the nth cantilever at a point x with horizontal, $M(x)_n$ is a bending moment in the nth cantilever at a point x, $V(x)_n$ is a shear force in the nth cantilever at a point x, and $w(x)_n$ is a loading function of the nth beam at a point x.. For a single cantilever n=0.

Choosing the shape of the loading function then the basic equations of beam theory are given as:

$$\frac{dV}{dx} = w(x) \qquad \textbf{(A-1)}$$

$$\frac{dM}{dx} = V(x) \qquad \textbf{(A-2)}$$

$$\frac{d\theta}{dx} = M(x) \qquad \textbf{(A-3)}$$

$$\frac{dy}{dx} = \theta(x) \qquad \textbf{(A-4)}$$

Fortunately, for this particular problem the character of a loading of a system of cantilevers is such that all the bending moments, shear forces, and resultant deflections always occur on only one side of a cantilever, and so a little unusual but advantageous system of the axes as well as of the convention of the directions of the bending moments, shear forces, and deflections can be introduced. The chosen coordinate system is obvious from the following figures, and the inner forces as well as the deflections are assumed to be positive for the loading acting in the positive direction of the y axis, and negative for the loading acting in the negative direction of the y axis.

A.1. The own weight of a single rock cantilever.

A sketch of a loading of a cantilever by the gravity forces of the cantilever itself is shown in Fig. A-1 .

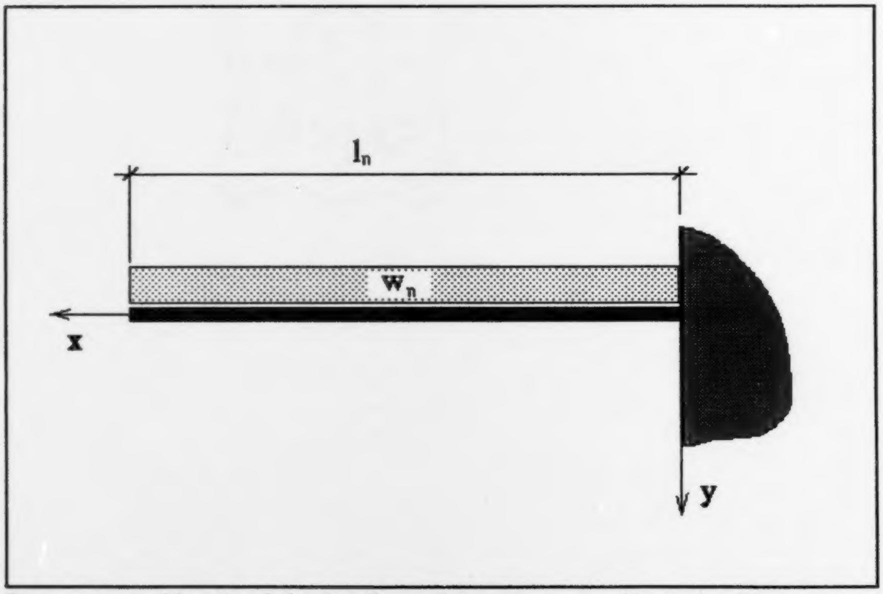

Figure A-1 Sketch of the loading of the single cantilever by it's own weight.

For the constant crossection of the cantilever, the loading is constant with respect to x. Then for the nth cantilever :

$$w(x)_n = w_n \tag{A-5}$$

Following equation A-1:

$$\begin{aligned} V(x)_n &= \int_x^{l_n} w_n\,dx = w_n[x]_x^{l_n} \\ V(x)_n &= w_n(l_n - x) \end{aligned} \tag{A-6}$$

From equation A-2:

$$\begin{aligned} M(x)_n &= w_n \int_x^{l_n} (l_n - x) = w_n[l_n x - \frac{x^2}{2}]_x^{l_n} \\ M(x)_n &= w_n \frac{(l_n - x)^2}{2} \end{aligned} \tag{A-7}$$

From equation A-3:

$$\begin{aligned} EI\theta(x)_n &= \frac{w_n}{2}\int (l_n - x)^2 dx = \frac{w_n}{6}(l_n - x)^3 + c_1 \\ &at\ x=0\ ;\quad \theta(x)_n = 0 \Rightarrow c_1 = -\frac{w_n l_n^3}{6} \\ EI\theta(x)_n &= \frac{w_n}{6}[(l_n - x)^3 - l_n^3] \end{aligned} \tag{A-8}$$

And finally from equation A-4:

$$EIy(x)_n = \frac{w_n}{6}\int[(l_n - x)^3 - l_n^3]\,dx = \frac{w_n}{6}[\frac{(l_n - x)^4}{4} - l_n^3(l - x)] + c_3$$

$$at\ \ x = 0 \quad ; \quad y(x)_n = 0 \ \ \Rightarrow c_4 = \frac{1}{8}w_n l_n^4 \qquad \textbf{(A-9)}$$

$$EIy(x)_n = \frac{w_n}{24}[(l_n - x)^4 - l_n^3(l - 4x)]$$

A.2. Loading by the underlying cantilever.

A sketch of the loading of the cantilever by the reaction caused by interaction with the underlying cantilever is shown in the Fig. A-2:

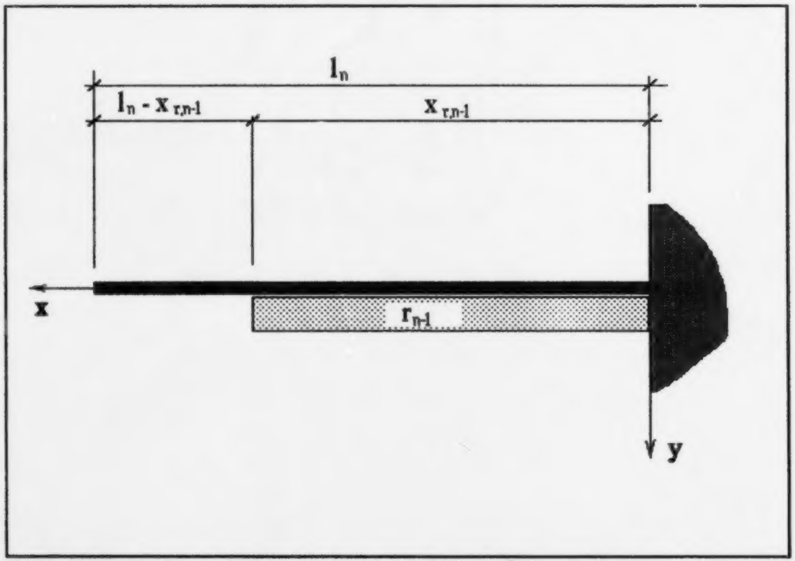

Figure A-2 Sketch of the loading of an nth cantilever by the reaction with the underlying cantilever.

The loading is assumed to be constant with respect to x :

$$r(x)_{n-1} = r_{n-1}\, u{<}x_{r,n-1} - x{>} \qquad \begin{array}{l} u{<}x_{r,n-1} - x{>} = 0 \;\; for \;\; x_{r,n-1} < x \\ u{<}x_{r,n-1} - x{>} = 1 \;\; for \;\; x_{r,n-1} \geq x \end{array} \tag{A-10}$$

Because of character of the loading the Singularity Step function "u" must be introduced.

Then from equation A-1:

$$\begin{aligned} &V(x)_{n-1} = \int r_{n-1}\, u{<}x_{r,n-1} - x{>} dx = r_{n-1} (x_{r,n-1} - x)\, u{<}x_{r,n-1} - x{>} + c_1 \\ &\qquad at \;\; x = x_{r,n-1} \;\; ; \;\; V(x)_{n-1} = 0 \;\Rightarrow\; c_1 = 0 \\ &V(x)_{n-1} = r_{n-1} (x_{r,n-1} - x)\, u{<}x_{r,n-1} - x{>} \end{aligned} \tag{A-11}$$

From equation A-2:

$$\begin{aligned} &M(x)_{n-1} = \int r_{n-1} (x_{r,n-1} - x)\, u{<}x_{r,n-1} - x{>} dx = \frac{r_{n-1}}{2} (x_{r,n-1} - x)^2\, u{<}x_{r,n-1} - x{>} + c_2 \\ &\qquad at \;\; x = x_{r,n-1} \;\; ; \;\; M(x)_{n-1} = 0 \;\Rightarrow\; c_2 = 0 \\ &M(x)_{n-1} = \frac{r_{n-1}}{2} (x_{r,n-1} - x)^2\, u{<}x_{r,n-1} - x{>} \end{aligned} \tag{A-12}$$

From equation A-3:

$$EI\theta(x)_{n-1} = \frac{r_{n-1}}{2}\int (x_{r,n-1}-x)^2\, u\langle x_{r,n-1}-x\rangle dx = \frac{r_{n-1}}{6}(x_{r,n-1}-x)^3\, u\langle x_{r,n-1}-x\rangle + c_3$$

$$at \quad x=0 \quad ; \quad \theta(x)_{n-1}=0 \;\Rightarrow\; c_3 = -\frac{r_{n-1}}{6}x^3_{r,n-1} \tag{A-13}$$

$$EI\theta(x)_{n-1} = \frac{r_{n-1}}{6}\left[(x_{r,n-1}-x)^3\, u\langle x_{r,n-1}-x\rangle - x^3_{r,n-1}\right]$$

And finally from equation A-4:

$$EIy(x)_{n-1} = \int\frac{r_{n-1}}{6}\left[(x_{r,n-1}-x)^3\, u\langle x_{r,n-1}-x\rangle - x^3_{r,n-1}\right]dx$$

$$= \frac{r_{n-1}}{6}\left[\frac{(x_{r,n-1}-x)^4}{4}\, u\langle x_{r,n-1}-x\rangle - x^3_{r,n-1}(x_{r,n-1}-x)\right] + c_4 \tag{A-14}$$

$$at \quad x=0 \quad ; \quad y(x)_{n-1}=0 \;\Rightarrow\; c_4 = \frac{1}{8}r_{n-1}x^4_{r,n-1}$$

$$EIy(x)_{n-1} = \frac{r_{n-1}}{24}\left[(x_{r,n-1}-x)^4\, u\langle x_{r,n-1}-x\rangle - x^3_{r,n-1}(x_{r,n-1}-4x)\right]$$

A.3. Loading by the overlying cantilever.

A sketch of the loading of the cantilever by the reaction caused by interaction with the overlying cantilever is shown in the Fig. A-3:

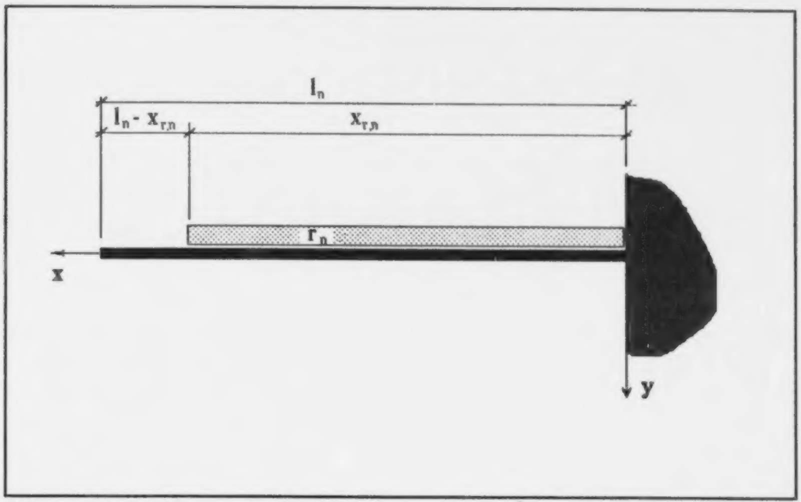

Figure A-3 Sketch of the loading of an nth cantilever by the reaction with the overlying cantilever.

The loading is assumed to be constant with respect to x :

$$-r(x)_n = r_n\, u<x_{r,n}-x> \qquad \begin{matrix} u<x_{r,n}-x>=0 \;\; for \;\; x_{r,n}<x \\ u<x_{r,n}-x>=1 \;\; for \;\; x_{r,n}\geq x \end{matrix} \tag{A-15}$$

The Singularity step function "u" was again introduced and from equation A.1.follows:

$$\begin{gathered} -V(x)_n = \int r_n\, u<x_{r,n}-x>dx = r_n(x_{r,n}-x)\, u<x_{r,n}-x>+c_1 \\ at\;\; x = x_{r,n} \quad ; \quad V(x)_n = 0 \;\Rightarrow\; c_1 = 0 \\ -V(x)_n = r_n\,(x_{r,n}-x)\, u<x_{r,n}-x> \end{gathered} \tag{A-16}$$

From equation A-2:

$$-M(x)_n = \int r_n (x_{r,n}-x)\, u{<}x_{r,n}-x{>}\, dx = \frac{r_n}{2}\,(x_{r,n}-x)^2\, u{<}x_{r,n}-x{>} + c_2$$

$$at \quad x = x_{r,n} \quad ; \quad M(x)_n = 0 \;\Rightarrow\; c_2 = 0 \qquad \textbf{(A-17)}$$

$$-M(x)_n = \frac{r_n}{2}\,(x_{r,n}-x)^2\, u{<}x_{r,n}-x{>}$$

From equation A-3:

$$-EI\theta(x)_n = \frac{r_n}{2}\int x_{r,n}-x)^2\, u{<}x_{r,n}-x{>}dx = \frac{r_n}{6}\,(x_{r,n}-x)^3\, u{<}x_{r,n}-x{>} + c_3$$

$$at \quad x = 0 \quad ; \quad \theta(x)_n = 0 \;\Rightarrow\; c_3 = -\frac{r_n}{6}\,x_{r,n} \qquad \textbf{(A-18)}$$

$$-EI\theta(x)_n = \frac{r_n}{6}\,[(x_{r,n}-x)^3\, u{<}x_{r,n}-x{>} - x^3_{r,n}]$$

And finally from equation A-4:

$$-EIy(x)_n = \int \frac{r_n}{6}\,[(x_{r,n}-x)^3\, u{<}x_{r,n}-x{>} - x^3_{r,n}]$$

$$= \frac{r_n}{6}\,[\frac{(x_{r,n}-x)^4}{4}\, u{<}x_{r,n}-x{>} - x^3_{r,n}(x_{r,n}-x)] + c_4 \qquad \textbf{(A-19)}$$

$$at \quad x = 0 \quad ; \quad y(x)_n = 0 \;\Rightarrow\; c_4 = \frac{1}{8}\,r_n x^4_{r,n}$$

$$-EIy(x)_n = \frac{r_n}{24}\,[(x_{r,n}-x)^4\, u{<}x_{r,n}-x{>} - x^3_{r,n}(x_{r,n}-4x)]$$

A.4. Loading by the underlying water.

A sketch of the loading of a cantilever by the hydrostatic forces generated by the water on the lower surface of the cantilever is shown in the Fig. A-4:

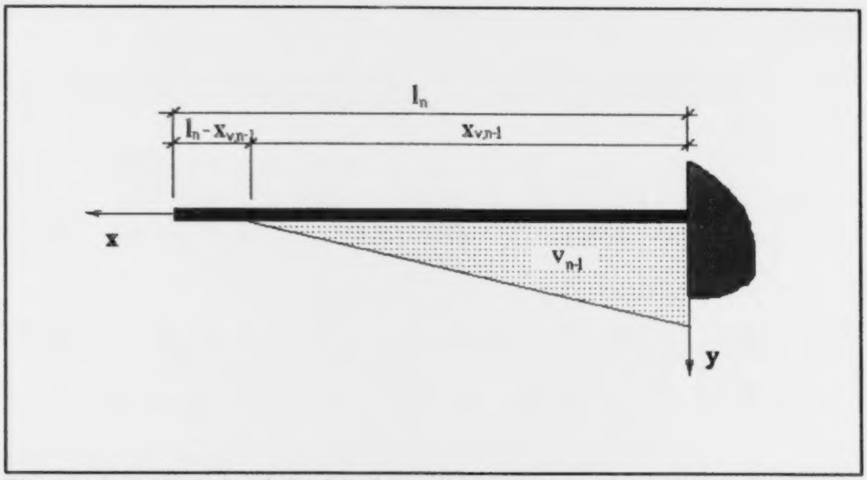

Figure A-4 Sketch of the loading of the lower surface of a cantilever by hydrostatic forces.

Loading is a linear function of a distance x :

$$v(x)_{n-1} = \gamma_w (x_{v,n-1} - x)\, u\langle x_{v,n-1} - x \rangle \qquad \begin{array}{l} u\langle x_{v,n-1} - x \rangle = 0 \;\; \textit{for} \;\; x_{v,n-1} < x \\ u\langle x_{v,n-1} - x \rangle = 1 \;\; \textit{for} \;\; x_{v,n-1} \geq x \end{array} \qquad \textbf{(A-20)}$$

From equation A-1:

$$V(x)_{n-1} = \int \gamma_w (x_{v,n-1} - x)\, u\langle x_{v,n-1} - x \rangle dx = \frac{\gamma_w}{2} (x_{v,n-1} - x)^2\, u\langle x_{v,n-1} - x \rangle + c_1$$

$$at \;\; x = x_{v,n-1} \;\; ; \quad V(x)_{n-1} = 0 \;\; \Rightarrow \;\; c_1 = 0 \qquad \textbf{(A-21)}$$

$$V(x)_{n-1} = \frac{\gamma_w}{2} (x_{v,n-1} - x)^2\, u\langle x_{v,n-1} - x \rangle$$

From equation A-2:

$$\begin{aligned}
M(x)_{n-1} &= \int \frac{\gamma_w}{2}(x_{v,n-1}-x)^2\, u<x_{v,n-1}-x>dx = \frac{\gamma_w}{6}(x_{v,n-1}-x)^3\, u<x_{v,n-1}-x> + c_2 \\
&\qquad at\ \ x = x_{v,n-1} \ \ ; \ \ M(x)_{n-1} = 0 \ \Rightarrow \ c_2 = 0 \\
M(x)_{n-1} &= \frac{\gamma_w}{6}(x_{v,n-1}-x)^3\, u<x_{v,n-1}-x>
\end{aligned} \tag{A-22}$$

From equation A-3:

$$\begin{aligned}
EI\theta(x)_{n-1} &= \int \frac{\gamma_w}{6}(x_{v,n-1}-x)^3\, u<x_{v,n-1}-x>dx = \frac{\gamma_w}{24}(x_{v,n-1}-x)^4\, u<x_{v,n-1}-x> + c_3 \\
&\qquad at\ \ x = 0 \ \ ; \ \ \theta(x)_{n-1} = 0 \ \Rightarrow \ c_3 = -\frac{\gamma_w}{24}x_{v,n-1}^4 \\
EI\theta(x)_{n-1} &= \frac{\gamma_w}{24}[(x_{v,n-1}-x)^4\, u<x_{v,n-1}-x> - x_{v,n-1}^4]
\end{aligned} \tag{A-23}$$

And finally from equation A-4:

$$\begin{aligned}
EIy(x)_{n-1} &= \int \frac{\gamma_w}{24}[(x_{v,n-1}-x)^4\, u<x_{v,n-1}-x> - x_{v,n-1}^4]dx \\
&= \frac{\gamma_w}{24}[\frac{(x_{v,n-1}-x)^5}{5}\, u<x_{v,n-1}-x> - x_{v,n-1}^4(x_{v,n-1}-x)] + c_4 \\
&\qquad at\ \ x = 0 \ \ ; \ \ y(x)_{n-1} = 0 \ \Rightarrow \ c_4 = \frac{1}{120}\gamma_w x_{v,n-1}^5(5 - u<x_{v,n-1}-x>) \\
EIy(x)_{n-1} &= \frac{\gamma_w}{120}[(x_{v,n-1}-x)^5\, u<x_{v,n-1}-x> - 5x_{v,n-1}^4(x_{v,n-1}-x) + x_{v,n-1}^5(5 - u<x_{v,n-1}-x>)]
\end{aligned} \tag{A-24}$$

A.5. Loading by the overlying water.

A sketch of the loading of a cantilever by the hydrostatic forces generated by the water on the upper surface of the cantilever is shown in the Fig. A-5 :

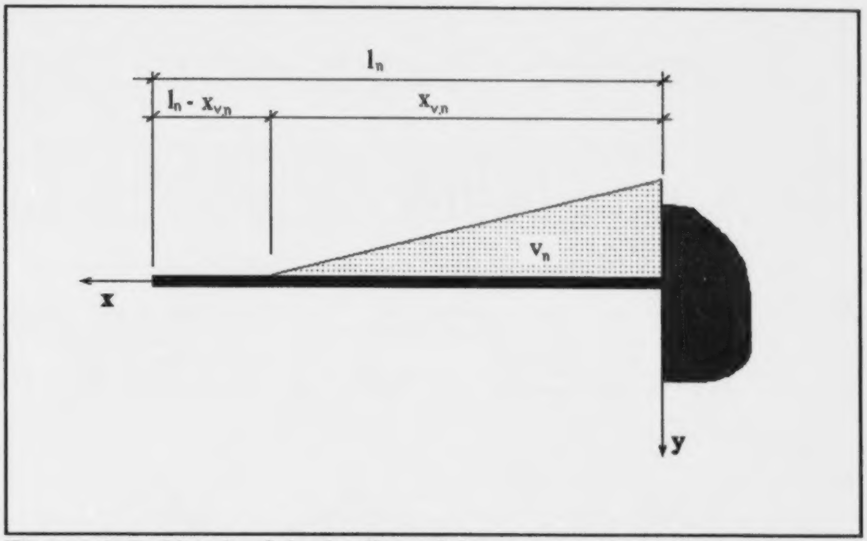

Figure A-5 Sketch of the loading of the upper surface of a cantilever by hydrostatic forces.

Loading is a linear function of a distance x :

$$-v(x)_n = \gamma_w (x_{v,n} - x)\, u<x_{v,n} - x> \qquad \begin{array}{l} u<x_{v,n}-x>=0 \;\; for \;\; x_{v,n}<x \\ u<x_{v,n}-x>=1 \;\; for \;\; x_{v,n} \geq x \end{array} \tag{A-25}$$

From equation A-1:

$$-V(x)_n = \int \gamma_w (x_{v,n} - x)\, u<x_{v,n} - x> dx = \frac{\gamma_w}{2} (x_{v,n} - x)^2\, u<x_{v,n} - x> + c_1$$

$$at \;\; x = x_{v,n} \;\; ; \;\; V(x)_n = 0 \;\; \Rightarrow \;\; c_1 = 0 \tag{A-26}$$

$$-V(x)_n = \frac{\gamma_w}{2} (x_{v,n} - x)^2\, u<x_{v,n} - x>$$

From equation A-2:

$$-M(x)_n = \int \frac{\gamma_w}{2}(x_{v,n}-x)^2\, u<x_{v,n}-x>dx = \frac{\gamma_w}{6}(x_{v,n}-x)^3\, u<x_{v,n}-x> + c_2$$

$$at\ \ x = x_{v,n} \quad ; \quad M(x)_n = 0 \ \Rightarrow \ c_2 = 0 \qquad \textbf{(A-27)}$$

$$-M(x)_n = \frac{\gamma_w}{6}(x_{v,n}-x)^3\, u<x_{v,n}-x>$$

From equation A-3:

$$-EI\theta(x)_n = \int \frac{\gamma_w}{6}(x_{v,n}-x)^3\, u<x_{v,n}-x>dx = \frac{\gamma_w}{24}(x_{v,n}-x)^4\, u<x_{v,n}-x> + c_3$$

$$at\ \ x = 0 \quad ; \quad \theta(x)_n = 0 \ \Rightarrow \ c_3 = -\frac{\gamma_w}{24}x_{v,n}^4 \qquad \textbf{(A-28)}$$

$$-EI\theta(x)_n = \frac{\gamma_w}{24}[(x_{v,n}-x)^4\, u<x_{v,n}-x> - x_{v,n}^4]$$

And finally from equation A-4:

$$-EIy(x)_n = \int \frac{\gamma_w}{24}[(x_{v,n}-x)^4\, u<x_{v,n}-x> - x_{v,n}^4]dx$$

$$= \frac{\gamma_w}{24}[\frac{(x_{v,n}-x)^5}{5}\, u<x_{v,n}-x> - x_{v,n}^4(x_{v,n}-x)] + c_4 \qquad \textbf{(A-29)}$$

$$at\ \ x = 0 \quad ; \quad y(x)_n = 0 \ \Rightarrow \ c_4 = \frac{1}{120}\gamma_w x_{v,n}^5(5 - u<x_{v,n}-x>)$$

$$-EIy(x)_n = \frac{\gamma_w}{120}[(x_{v,n}-x)^5 u<x_{v,n}-x> - 5x_{v,n}^4(x_{v,n}-x) + x_{v,n}^5(5 - u<x_{v,n}-x>)]$$

A.6. Loading by seismic forces.

A sketch of a cantilever loaded by seismic forces is shown in the Fig. A-5.

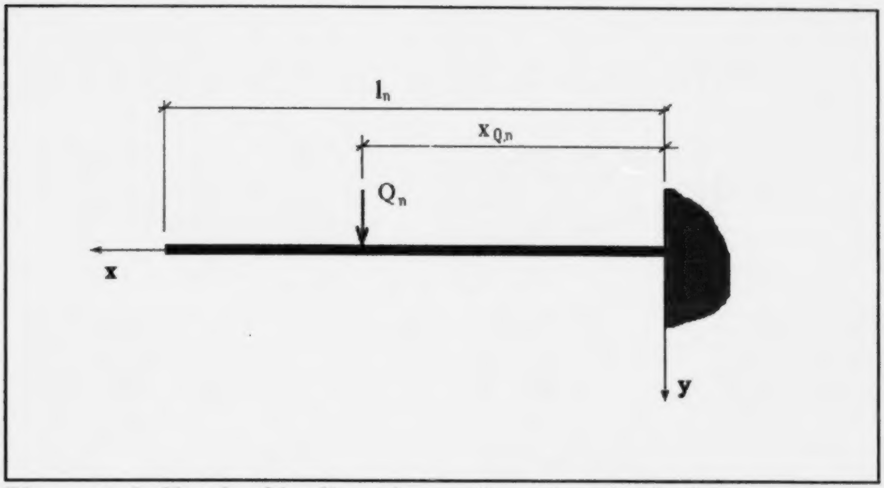

Figure A-6 Sketch of loading of a cantilever by seismic forces.

Force Q_n is expressed as a function of the weight of a cantilever W [kN], and of a dimensionless coefficient k_s as:

$$Q = k_s W \tag{A-30}$$

The loading of a cantilever n by the force Q_n with respect to the x is:

$$Q(x)_n = Q_n \delta < x_{Q,n} - x > \tag{A-31}$$

Where $\delta<>$ (Dirac function) is another Singularity function expressed as:

$$\frac{du<x_{Q,n}-x>}{dx} = \delta<x_{Q,n}-x> \quad \wedge \quad \begin{matrix} u<x_{Q,n}-x> = 0 & for\ x > x_{Q,n} \\ u<x_{Q,n}-x> = 1 & for\ x \le x_{Q,n} \end{matrix} \qquad \textbf{(A-32)}$$

Then from equations A-1 and A-32:

$$\begin{aligned} V(x)_n &= \int Q_n \delta<x_{Q,n}-x> dx \\ V(x)_n &= Q_n u<x_{Q,n}-x> \end{aligned} \qquad \textbf{(A-33)}$$

From equation A-2:

$$\begin{aligned} M(x)_n &= \int Q_n u<x_{Q,n}-x> dx = Q_n (x_{Q,n}-x) u<x_{Q,n}-x> + c_1 \\ &at\ \ x = x_{Q,n} \ \ ; \ \ M(x)_n = 0 \ \rightarrow \ c_1 = 0 \\ M(x)_n &= Q_n (x_{Q,n}-x) u<x_{Q,n}-x> \end{aligned} \qquad \textbf{(A-34)}$$

From equation A-3:

$$\begin{aligned} EI\theta(x)_n &= \int Q_n (x_{Q,n}-x)\, u<x_{Q,n}-x> dx = \frac{Q_n}{2}(x_{Q,n}-x)^2 u<x_{Q,n}-x> + c_2 \\ &at\ \ x = 0 \ \ ; \ \ \theta(x)_n = 0 \ \rightarrow \ c_2 = -\frac{Q_n}{2}(x_{Q,n})^2 \\ EI\theta(x)_n &= \frac{Q_n}{2}[(x_{Q,n}-x)^2 u<x_{Q,n}-x> - (x_{Q,n})^2] \end{aligned} \qquad \textbf{(A-35)}$$

And finally fom equation A-4:

$$EIy(x)_n = \int \frac{Q_n}{2}[(x_{Q,n}-x)^2 u{<}x_{Q,n}-x{>} - x_{Q,n}^2]dx$$

$$= \frac{Q_n}{2}[\frac{(x_{Q,n}-x)^3}{3} u{<}x_{Q,n}-x{>} - x_{Q,n}^2(x_{Q,n}-x)] + c_3 \qquad \textbf{(A-36)}$$

$$at \quad x=0 \quad ; \quad y(x)_n = 0 \Rightarrow c_3 = \frac{1}{3}Q_n x_{Q,n}^3$$

$$EIy(x)_n = \frac{Q_n}{6}[(x_{Q,n}-x)^3 u{<}x_{Q,n}-x{>} - 3x_{Q,n}^2(x_{Q,n}-x) + 2x_{Q,n}^3]$$

A.7. Derivation of equations for combination of loads for n cantilevers.

The geometry, and the system of numbering, used for the derivation is shown in the Fig. A-7:

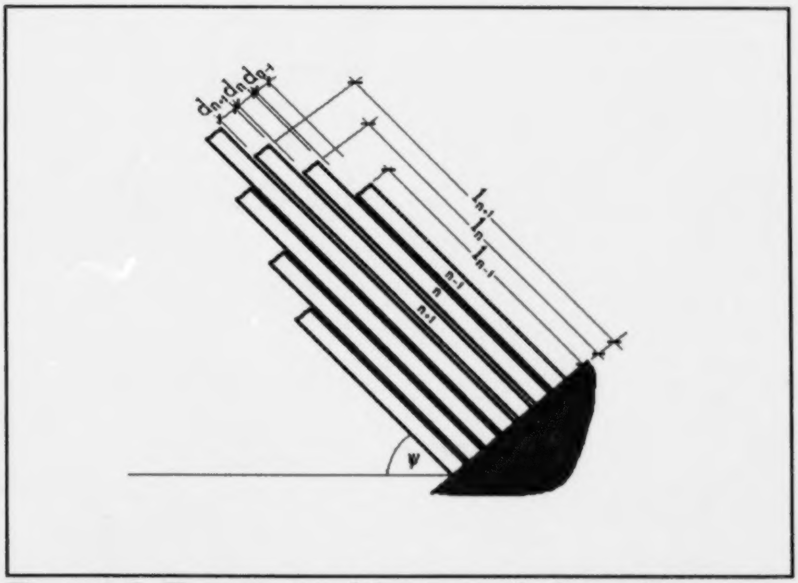

Figure A-7 The geometry of the system of n interacting cantilevers.

A sketch of a combination of loads acting on one of the system of interacting cantilevers is shown in Fig. A-8.

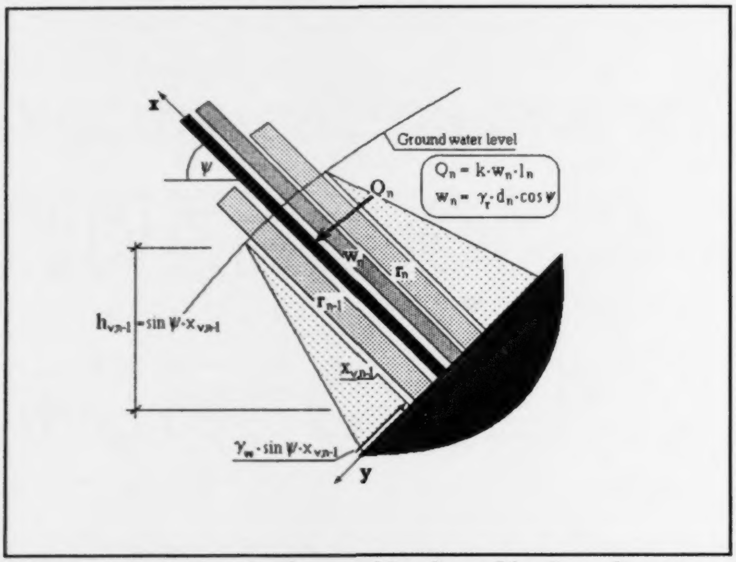
x
ψ
Ground water level
Q_n = k·w_n·l_n
w_n = γ_r·d_n·cos ψ
Q_n
w_n
r_n
r_n-1
h_v,n-1 = sin ψ·x_v,n-1
x_v,n-1
γ_w·sin ψ·x_v,n-1
y

Figure A-8 A sketch of a combination of loads acting on one of the system of interacting cantilevers.

Final equations for the system of interacting cantilevers loaded by a combination of forces are simply derived by adding separated loading states together, using the law of superposition.

So the resultant load w_x acting on the cantilever is equal to:

$$q(x)_n = w(x)_n - r(x)_{n-1} + r(x)_n - v(x)_{n-1} + v(x)_n + Q(x)_n \tag{A-37}$$

Using equations A-5, A-10, A15, A-20, A-26,A-31 and A-37

$$\begin{aligned} q(x)_n = {} & w_n - r_{n-1}\, u{<}x_{r,n-1} - x{>} + r_n\, u{<}x_{r,n} - x{>} - \\ & - \gamma_w \sin\psi\, (x_{v,n-1} - x)\, u{<}x_{v,n-1} - x{>} + \\ & + \gamma_w \sin\psi\, (x_{v,n} - x)\, u{<}x_{v,n} - x{>} + Q\,\delta{<}x_{Q,n} - x{>} \end{aligned} \tag{A-38}$$

Similarly using equations A-6, A-11, A-16, A21, A-27 and A32 the resultant shear force $V_{x,n}$ is equal to

$$
\begin{aligned}
V(x)_n = {} & w_n(l_n - x) - r_{n-1}\,(x_{r,n-1} - x)\, u<x_{r,n-1} - x> + r_n\,(x_{r,n} - x)\, u<x_{r,n} - x> - \\
& - \frac{\gamma_w \sin\psi}{2}(x_{v,n-1} - x)^2\, u<x_{v,n-1} - x> + \frac{\gamma_w \sin\psi}{2}(x_{v,n} - x)^2\, u<x_{v,n} - x> + \\
& + Q u<x_{Q,n} - x>
\end{aligned}
\qquad \textbf{(A-39)}
$$

Using equations A-7, A-12, A-17, A-22, A-28 and A-33

$$
\begin{aligned}
M(x)_n = {} & \frac{w_n}{2}(l_n - x)^2 - \frac{r_{n-1}}{2}(x_{r,n-1} - x)^2\, u<x_{r,n-1} - x> + \frac{r_n}{2}(x_{r,n} - x)^2\, u<x_{r,n} - x> - \\
& - \frac{\gamma_w \sin\psi}{6}(x_{v,n-1} - x)^3\, u<x_{v,n-1} - x> + \frac{\gamma_w \sin\psi}{6}(x_{v,n} - x)^3\, u<x_{v,n} - x> + \\
& + Q_n(x_{Q,n} - x)\, u<x_{Q,n} - x>
\end{aligned}
\qquad \textbf{(A-40)}
$$

From equations A-8, A-13, A-18, A-23, A-29 and A-34

$$
\begin{aligned}
EI\theta(x)_n = {} & \frac{w_n}{6}[(l_n - x)^3 - l_n^3] - \frac{r_{n-1}}{6}[(x_{r,n-1} - x)^3\, u<x_{r,n-1} - x> - x_{r,n-1}^3] + \\
& + \frac{r_n}{6}[(x_{r,n} - x)^3\, u<x_{r,n} - x> - x_{r,n}^3] - \\
& - \frac{\gamma_w \sin\psi}{24}[(x_{v,n-1} - x)^4\, u<x_{v,n-1} - x> - x_{v,n-1}^4] + \\
& + \frac{\gamma_w \sin\psi}{24}[(x_{v,n} - x)^4\, u<x_{v,n} - x> - x_{v,n}^4] + \\
& + \frac{Q_n}{2}[(x_{Q,n} - x)^2\, u<x_{Q,n} - x> - (x_{Q,n})^2]
\end{aligned}
\qquad \textbf{(A-41)}
$$

And finally from equations A-9, A-14, A-19, A-24, A-30 and A-35

$$
\begin{aligned}
EIy(x)_n = {} & \frac{w_n}{24}[(l_n - x)^4 - l_n^3(l - 4x)] - \\
& - \frac{r_{n-1}}{24}[(x_{r,n-1} - x)^4\, u{<}x_{r,n-1} - x{>} - x_{r,n-1}^3(x_{r,n-1} - 4x)] + \\
& + \frac{r_n}{24}[(x_{r,n} - x)^4\, u{<}x_{r,n} - x{>} - x_{r,n}^3(x_{r,n} - 4x)] + \\
& + \frac{Q_n}{6}[(x_{Q,n} - x)^3 u{<}x_{Q,n} - x{>} - x_{Q,n}^2(x_{Q,n} - 3x)] - \qquad \textbf{(A-42)} \\
& + \frac{\gamma_w \sin\psi}{120}[(x_{v,n} - x)^5 u{<}x_{v,n} - x{>} - 5x_{v,n}^4(x_{v,n} - x) + x_{v,n}^5(5 - u{<}x_{v,n} - x{>})] - \\
& - \frac{\gamma_w \sin\psi}{120}[(x_{v,n-1} - x)^5\, u{<}x_{v,n-1} - x{>} - 5x_{v,n-1}^4(x_{v,n-1} - x) + \\
& + x_{v,n-1}^5(5 - u{<}x_{v,n-1} - x{>})]
\end{aligned}
$$

Unfortunately, for reasons explained in appendix H, the approximation of the contact force by the uniformly distributed load would not always work during solving the system of nonlinear equations. For such a case another system of equations is presented as equations A-43, A-44, and A-45 (next page). The new system is identical to the previous one with the exception of the reaction between cantilevers which is approximated by a force acting at the end of the shorter cantilever. The derivation is analogous to the derivation of the force F (appendix B), and so only the resultant equations are presented in this text.

Analogous to equation A-40

$$M(x)_n = \frac{w_n}{2}(l_n - x)^2 - R_{n-1}(x_{r,n-1} - x)\, u{<}x_{r,n-1} - x{>} + R_n(x_{r,n} - x)\, u{<}x_{r,n} - x{>} -$$

$$- \frac{\gamma_w \sin\psi}{6}(x_{v,n-1} - x)^3\, u{<}x_{v,n-1} - x{>} + \frac{\gamma_w \sin\psi}{6}(x_{v,n} - x)^3\, u{<}x_{v,n} - x{>} + \qquad \textbf{(A-43)}$$

$$+ Q_n(x_{Q,n} - x)\, u{<}x_{Q,n} - x{>}$$

to equation A-41

$$EI\theta(x)_n = \frac{w_n}{6}[(l_n - x)^3 - l_n^3] - \frac{R_{n-1}}{2}[(x_{r,n-1} - x)^2\, u{<}x_{r,n-1} - x{>} - x_{r,n-1}^2] +$$

$$+ \frac{R_n}{2}[(x_{r,n} - x)^2\, u{<}x_{r,n} - x{>} - x_{r,n}^2] -$$

$$- \frac{\gamma_w \sin\psi}{24}[(x_{v,n-1} - x)^4\, u{<}x_{v,n-1} - x{>} - x_{v,n-1}^4] + \qquad \textbf{(A-44)}$$

$$+ \frac{\gamma_w \sin\psi}{24}[(x_{v,n} - x)^4\, u{<}x_{v,n} - x{>} - x_{v,n}^4] +$$

$$+ \frac{Q_n}{2}[(x_{Q,n} - x)^2\, u{<}x_{Q,n} - x{>} - x_{Q,n}^2]$$

and finally from equation A-42

$$
\begin{aligned}
EIy(x)_n = {} & \frac{w_n}{24}[(l_n - x)^4 - l_n^3(l - 4x)] - \\
& - \frac{R_{n-1}}{6}[(x_{r,n-1} - x)^3\, u{<}x_{r,n-1} - x{>} - x_{r,n-1}^2(x_{r,n-1} - 3x)] + \\
& + \frac{R_n}{6}[(x_{r,n} - x)^3\, u{<}x_{r,n} - x{>} - x_{r,n}^2(x_{r,n} - 3x)] + \\
& + \frac{Q_n}{6}[(x_{Q,n} - x)^3\, u{<}x_{Q,n} - x{>} - x_{Q,n}^2(x_{Q,n} - 3x)] - \\
& + \frac{\gamma_w \sin\psi}{120}[(x_{v,n} - x)^5\, u{<}x_{v,n} - x{>} - 5x_{v,n}^4(x_{v,n} - x) + x_{v,n}^5(5 - u{<}x_{v,n} - x{>})] - \\
& - \frac{\gamma_w \sin\psi}{120}[(x_{v,n-1} - x)^5\, u{<}x_{v,n-1} - x{>} - 5x_{v,n-1}^4(x_{v,n-1} - x) + \\
& + x_{v,n-1}^5(5 - u{<}x_{v,n-1} - x{>})]
\end{aligned}
\tag{A-45}
$$

Appendix B.

Derivation of equations of the system of interacting cantilevers for the block toppling.

For the following derivation beam theory is being used, and the derivation is again divided into several sections. The nomenclature, the shape of the functions and the basic equations B-1, B-2, B-3 and B-4 introduced in Appendix A as A-1, A-2, A-3 and A-4 are the same.

$$\frac{dV}{dx} = w(x) \tag{B-1}$$

$$\frac{dM}{dx} = V(x) \tag{B-2}$$

$$\frac{d\theta}{dx} = M(x) \tag{B-3}$$

$$\frac{dy}{dx} = \theta(x) \tag{B-4}$$

Also the same are the equations for all loads, except the reaction with overlying cantilever.

It is however necessary to define the new load acting at the end of each cantilever. In open pit mining, the pit is created in a series of steps, bench after bench, and during each step a new failure plane could develop, loading the under-lying rock columns by the weight of the failed mass. The magnitude of this force is a function of the state of the deformation of the failing rock which determines the shape of the rock mass block above the failure plane. This force will be introduced as some function of the height of the failed blocks, and it will be called F.

B.1. Loading by the failed rock .

The sketch of a cantilever loaded by the weight of already failed rock is shown in Fig. B-1.

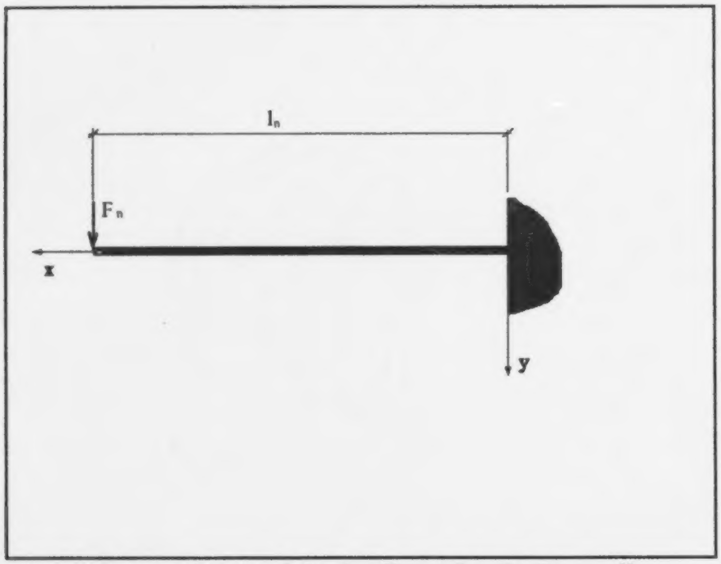

Figure B-1 Sketch of the loading of a single cantilever by the weight of already failed rock.

It is obvious from Fig. B-1 that the force F_n is not a function of x. As a result the inner shear force is constant over the cantilever, and has the magnitude of the load F_n.

From equation A-1

$$V(x)_n = F_n \tag{B-5}$$

From equation A-2:

$$\begin{aligned} M(x)_n &= \int_x^{l_n} F_n dx = F_n(l_n - x) \\ M(x)_n &= F_n(l_n - x) \end{aligned} \tag{B-6}$$

From equation A-3:

$$\begin{aligned} EI\theta(x)_n &= \int E_n(l_n - x)\,dx = \frac{F_n}{2}(l_n - x)^2 + c_2 \\ &\quad at\ \ x = 0 \quad ; \quad \theta(x)_n = 0 \quad \Rightarrow \quad c_2 = -\frac{F_n}{2}(l_n)^2 \\ EI\theta(x)_n &= \frac{F_n}{2}[(l_n - x)^2 - (l_n)^2] \end{aligned} \tag{B-7}$$

And finally from equation A-4:

$$EIy(x)_n = \int \frac{F_n}{2}[(l_n - x)^2 - l_n^2]\,dx$$

$$= \frac{F_n}{2}[\frac{(l_n - x)^3}{3} - l_n^2(l_n - x)] + c_3$$

$$at \quad x = 0 \quad ; \quad y(x)_n = 0 \quad \Rightarrow \quad c_3 = \frac{1}{3}F_n l_n^3 \qquad \textbf{(B-8)}$$

$$EIy(x)_n = \frac{F_n}{6}[(l_n - x)^3 - 3l_n^2(l_n - x) + 2l_n^3] =$$

$$= \frac{F_n}{6}[(l_n - x)^3 - l_n^2(l_n - 3x)]$$

There are several ways to define the force F_n. It seems to be reasonable to determine the force F_n as a weight of the broken part of a cantilever in question. This assumption will be accepted for both block, and block flexural toppling modes of failure. Equations describing the toppling, and sliding forces are derived in appendices E and F; equations describing the geometry of toppling blocks are derived in the appendix D.

Another problem is the determination of the character of the failed rock mass. There are basically two ways to deal with this problem. First, the failed rock could be assumed to behave as a debris, but determination of strength properties may proved to be difficult in some cases. Second, the deformation of the failed blocks can be followed by geometrical equations, comparing them at the same time with the changing safety factor. Again, there is the problem of determining the residual strength parameters on the failure plane, and at some stage the problem of interlocking of the failed rock blocks might prove to be extremely difficult to model. In the computer model the failed rock will be dealt with as a rock debris.

B.2. Loading by the overlying cantilever.

A sketch of loading of a cantilever by the reaction caused by interaction with an overlying cantilever is shown in Fig. B-2.

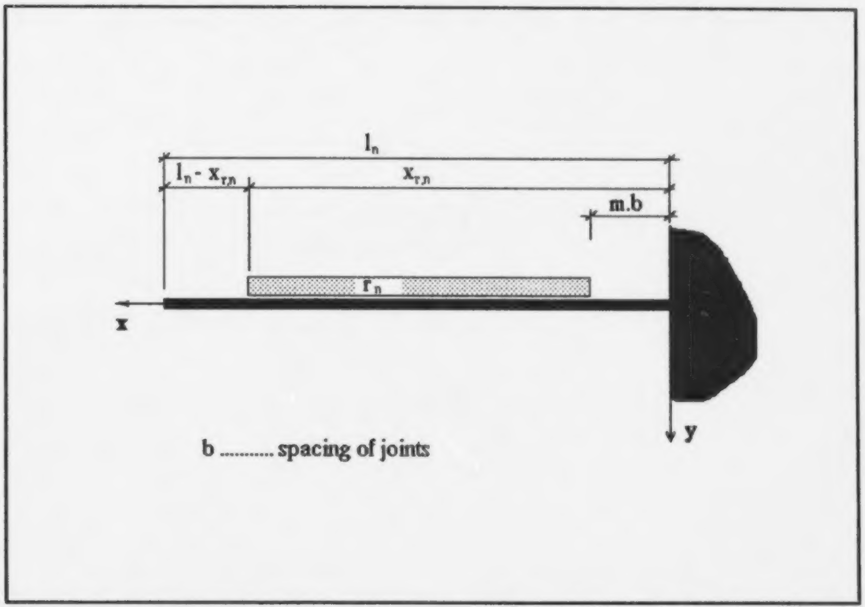

Figure B-2 Sketch of the loading of an n^{th} cantilever by the reaction with the overlying cantilever (block toppling).

Loading is assumed to be constant with respect to x:

$$\begin{aligned} & r(x)_n = r_n\, u\langle x_{r,n} - x\rangle - r_n\, u\langle mb - x\rangle \\ & \quad \textit{where} \\ & \quad u\langle x_{r,n} - x\rangle = 0 \;\; \textit{for} \;\; x_{r,n} < x \\ & \quad u\langle x_{r,n} - x\rangle = 1 \;\; \textit{for} \;\; x_{r,n} \geq x \\ & \quad u\langle mb - x\rangle = 0 \quad \textit{for} \;\; mb \leq x \\ & \quad u\langle mb - x\rangle = 1 \quad \textit{for} \;\; mb > x \end{aligned} \qquad \textbf{(B-9)}$$

Then from Fig. 2

$$V(x)_n = V'(x)_n - V''(x)_n \qquad \textbf{(B-10)}$$

Where V'(x) is the shear force caused by continuous load from the point $x_{r,n-1}$ to the origin, and V"(x) is the shear force caused by continuous load from the distance mb to the origin. From superposition, the difference of these shear forces is the shear force caused by the loading in the Fig. 2. It should be mentioned at this time that the sign for prime (') does not mean derivative of x in this thesis. The derivative is always written in the full form (for example, df/dx). The following primed characters are simply the names of components of the resultant, unprimed inner force or deformation characteristics.

From equation B-1:

$$\begin{aligned}
&V'(x)_n = \int r_n\, u{<}x_{r,n}-x{>}dx = r_n (x_{r,n}-x)\, u{<}x_{r,n}-x{>} + c_1 \\
&\qquad at\ x = x_{r,n} \quad ; \quad V'(x)_n = 0 \Rightarrow c_1 = 0 \\
&V'(x)_n = r_n\,(x_{r,n}-x)\, u{<}x_{r,n}-x{>}
\end{aligned} \tag{B-11}$$

and

$$\begin{aligned}
&V''(x)_n = \int r_n\, u{<}mb-x{>}dx = r_n (mb-x)\, u{<}mb-x{>} + c_1 \\
&\qquad at\ x = mb \quad ; \quad V'(x)_n = 0 \Rightarrow c_1 = 0 \\
&V''(x)_n = r_n\,(mb-x)\, u{<}mb-x{>}
\end{aligned} \tag{B-12}$$

And finally from equations B-10, B-11 and B-12

$$V(x)_n = r_n\,(x_{r,n}-x)\, u{<}x_{r,n}-x{>} - r_n\,(mb-x)\, u{<}mb-x{>} \tag{B-13}$$

It is obvious from equation B-13 that between the point at the distance mb, and between the origin, the shear force remains constant, as it should be according to Fig. B-2.

Similarly to the shear force equation, the moment equation holds:

$$M(x)_n = M'(x)_n - M''(x)_n \tag{B-14}$$

From equation B-2:

$$M'(x)_n = \int r_n (x_{r,n}-x)\, u{<}x_{r,n}-x{>}\, dx = \frac{r_n}{2}(x_{r,n}-x)^2 {<}x_{r,n}-x{>} + c_2$$

$$at \quad x = x_{r,n} \quad ; \quad M(x)_n = 0 \;\Rightarrow\; c_2 = 0 \qquad \textbf{(B-15)}$$

$$M'(x)_n = \frac{r_n}{2}(x_{r,n}-x)^2\, u{<}x_{r,n}-x{>}$$

and

$$M''(x)_n = \int r_n (mb-x)\, u{<}mb-x{>}\, dx = \frac{r_n}{2}(mb-x)^2\, u{<}mb-x{>} + c_2$$

$$at \quad x = mb \quad ; \quad M''(x)_n = 0 \;\Rightarrow\; c_2 = 0 \qquad \textbf{(B-16)}$$

$$M''(x)_n = \frac{r_n}{2}(mb-x)^2\, u{<}mb-x{>}$$

Finally from equations B-14, B-15 and B-16

$$M(x)_n = \frac{r_n}{2}(x_{r,n}-x)^2\, u{<}x_{r,n}-x{>} - \frac{r_n}{2}(mb-x)^2\, u{<}mb-x{>} \qquad \textbf{(B-17)}$$

It is obvious from equation B-17 again that between the point at the distance mb, and between the origin, the moment remains constant as it should be according to Fig B-2.

Following the same procedure as for the shear force and for the moment equations:

$$EI\theta(x)_n = EI\theta'(x)_n - EI\theta''(x)_n \qquad \textbf{(B-18)}$$

From equation B-3

$$EI\theta'(x)_n = \frac{r_n}{2}\int (x_{r,n}-x)^2\, u<x_{r,n}-x>dx = \frac{r_n}{6}\,(x_{r,n}-x)^3\, u<x_{r,n}-x> + c_3$$

$$at\ \ x=0\ \ ;\ \ \theta'(x)_n = 0 \Rightarrow c_3 = -\frac{r_n}{6}\,x_{r,n}^3 \qquad \textbf{(B-19)}$$

$$EI\theta'(x)_n = \frac{r_n}{6}\,[(x_{r,n}-x)^3\, u<x_{r,n}-x> - x_{r,n}^3]$$

and

$$EI\theta''(x)_n = \frac{r_n}{2}\int (mb-x)^2\, u<mb-x>dx = \frac{r_n}{6}\,(mb-x)^3\, u<mb-x> + c_3$$

$$at\ \ x=0\ \ ;\ \ \theta''(x)_n = 0 \Rightarrow c_3 = -\frac{r_n}{6}\,(mb)^3 \qquad \textbf{(B-20)}$$

$$EI\theta''(x)_n = \frac{r_n}{6}\,[(mb-x)^3\, u<mb-x> - (mb)^3]$$

Finally from equations B-18, B-19 and B-20:

$$\begin{aligned} EI\theta(x)_n &= \frac{r_n}{6}\,[(x_{r,n}-x)^3\, u<x_{r,n}-x> - x_{r,n}^3] - \\ &-\frac{r_n}{6}\,[(mb-x)^3\, u<mb-x> - (mb)^3] \end{aligned} \tag{B-21}$$

The last step is derivation of the equation for deflection.

$$EIy(x)_n = EIy'(x)_n - EIy''(x)_n \tag{B-22}$$

From equation B-4:

$$\begin{aligned} EIy'(x)_n &= \int \frac{r_n}{6}\,[(x_{r,n}-x)^3\, u<x_{r,n}-x> - x_{r,n}^3]\,dx \\ &= \frac{r_n}{6}\,[\frac{(x_{r,n}-x)^4}{4}\, u<x_{r,n}-x> - x_{r,n}^3(x_{r,n}-x)] + c_4 \\ &at\ \ x=0 \ \ ; \ \ y'(x)_n = 0 \ \Rightarrow \ c_4 = \frac{1}{8}\,r_n\,x_{r,n}^4 \\ EIy'(x)_n &= \frac{r_n}{24}[(x_{r,n}-x)^4\, u<x_{r,n}-x> - x_{r,n}^3(x_{r,n}-4x)] \end{aligned} \tag{B-23}$$

and

$$\begin{aligned} EIy''(x)_n &= \int \frac{r_n}{6}\,[(mb-x)^3\,u\langle mb-x\rangle - (mb)^3]\,dx \\ &= \frac{r_n}{6}\,[\frac{(mb-x)^4}{4}\,u\langle mb-x\rangle - (mb)^3(mb-x)] + c_4 \\ at\ \ x=0\ \ &;\ \ y''(x)_n = 0 \ \Rightarrow\ c_4 = \frac{1}{8}r_n\,(mb)^4 \\ EIy''(x)_n &= \frac{r_n}{24}[(mb-x)^4\,u\langle mb-x\rangle - (mb)^3(mb-4x)] \end{aligned} \qquad \textbf{(B-24)}$$

And finally from equations B-22, B-23 and B-24

$$\begin{aligned} EIy(x)_n &= \frac{r_n}{24}[(x_{r,n}-x)^4\,u\langle x_{r,n}-x\rangle - x_{r,n}^3(x_{r,n}-4x)] - \\ &- \frac{r_n}{24}[(mb-x)^4\,u\langle mb-x\rangle - (mb)^3(mb-4x)] \end{aligned} \qquad \textbf{(B-25)}$$

B.3. Derivation of equations for combination of loads for n cantilevers.

The geometry, and the system of numbering, used for the derivation is shown in Fig. B-3 (next page).

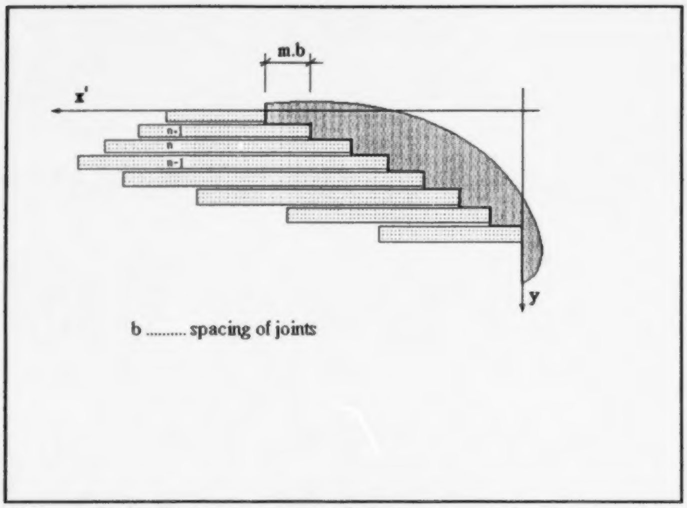
m.b
x'
n+
n
n-1
y
b .... spacing of joints

Figure B-3 The geometry of the system of n interacting cantilevers. (Block toppling).

A sketch of a combination of loads acting on one of the system of interacting cantilevers is shown in Fig. B-4 .

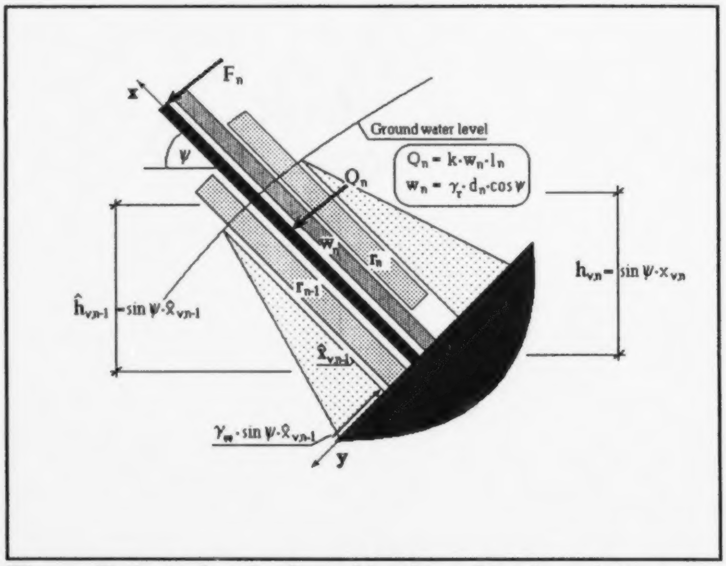
F$_n$
x
Ground water level
ψ
$Q_n = k \cdot w_n \cdot l_n$
$w_n = \gamma_r \cdot d_n \cdot \cos\psi$
Q$_n$
w$_n$
r$_n$
r$_{n-1}$
$h_{v,n} = \sin\psi \cdot x_{v,n}$
$\hat{h}_{v,n-1} = \sin\psi \cdot \hat{\ell}_{v,n-1}$
$\hat{\ell}_{v,n-1}$
$\gamma_w \cdot \sin\psi \cdot \hat{\ell}_{v,n-1}$
y

Figure B-4 A sketch of combination of loads acting on one of the system of interacting cantilevers (block toppling).

Final equations for the system of interacting cantilevers on the stepped base (Fig. B-3) loaded by a combination of forces (Fig. B-4) are again derived by adding each of the loading states, using the law of superposition. Notice that the length of the submerged, lower surface of each cantilever is marked by a hat because, in the case of the stepped base, obviously $\hat{x}_{v,n} \neq x_{v,n}$.

So the resultant load w_x acting on the cantilever is given by:

$$q(x)_n = w(x)_n - r(x)_{n-1} + r(x)_n - v(x)_{n-1} + v(x)_n + Q(x)_n + F(x)_n \qquad \textbf{(B-26)}$$

Similarly using equations A-6, A-16, A-21, A-27, A-32, B-5 and B-13 the resultant shear force $V_{x,n}$ is equal to:

$$\begin{aligned} V(x)_n = {} & w_n(l_n - x) + r_n\,(x_{r,n} - x)\,u\!<\!x_{r,n} - x\!> - r_n\,(mb - x)\,u\!<\!mb - x\!> - \\ & - r_{n-1}\,(x_{r,n-1} - x)\,u\!<\!x_{r,n-1} - x\!> + \\ & + Q_n u\!<\!x_{Q,n} - x\!> + F_n - \\ & - \frac{\gamma_w \sin\psi}{2}(\hat{x}_{v,n-1} - x)^2\,u\!<\!\hat{x}_{v,n-1} - x\!> + \frac{\gamma_w \sin\psi}{2}(x_{v,n} - x)^2\,u\!<\!x_{v,n} - x\!> \end{aligned} \qquad \textbf{(B-27)}$$

Using equations A-7, A-17, A-22, A-28, A-33, B-6 and B-17

$$\begin{aligned} M(x)_n = {} & w_n \frac{(l_n - x)^2}{2} + \\ & + \frac{r_n}{2} (x_{r,n} - x)^2 \, u\langle x_{r,n} - x \rangle - \frac{r_n}{2} (mb - x)^2 \, u\langle mb - x \rangle - \\ & - \frac{r_{n-1}}{2} (x_{r,n-1} - x)^2 \, u\langle x_{r,n-1} - x \rangle - \\ & - \frac{\gamma_w \sin\psi}{6} (\hat{x}_{v,n-1} - x)^3 \, u\langle \hat{x}_{v,n-1} - x \rangle + \frac{\gamma_w \sin\psi}{6} (x_{v,n} - x)^3 \, u\langle x_{v,n} - x \rangle + \\ & + Q (x_{Q,n} - x) \, u\langle x_{Q,n} - x \rangle + F_n (l_n - x) \end{aligned} \tag{B-28}$$

From equations A-8, A-18, A-23, A-29, A-34, B-7 and B-21

$$\begin{aligned} EI\theta(x)_n = {} & \frac{w_n}{6} [(l_n - x)^3 - l_n^3] + \\ & + \frac{r_n}{6} [(x_{r,n} - x)^3 \, u\langle x_{r,n} - x \rangle - x_{r,n}^3] - \frac{r_n}{6} [(mb - x)^3 \, u\langle mb - x \rangle - (mb)^3] - \\ & - \frac{r_{n-1}}{6} [(x_{r,n-1} - x)^3 \, u\langle x_{r,n-1} - x \rangle - x_{r,n-1}^3] - \\ & - \frac{\gamma_w \sin\psi}{24} [(\hat{x}_{v,n-1} - x)^4 \, u\langle \hat{x}_{v,n-1} - x \rangle - \hat{x}_{v,n-1}^4] + \\ & + \frac{\gamma_w \sin\psi}{24} [(x_{v,n} - x)^4 \, u\langle x_{v,n} - x \rangle - x_{v,n}^4] + \\ & + \frac{Q_n}{2} [(x_{Q,n} - x)^2 \, u\langle x_{Q,n} - x \rangle - (x_{Q,n})^2] + \frac{F_n}{2} [(l_n - x)^2 - (l_n)^2] \end{aligned} \tag{B-29}$$

And finally from equations A-9, A-19, A-24, A-30, A-35, B-8 and B-25

$$
\begin{aligned}
EIy(x)_n = {} & \frac{w_n}{24}[(l_n-x)^4-l_n^3(l-4x)] + \\
& + \frac{r_n}{24}[(x_{r,n}-x)^4\, u<x_{r,n}-x> - x_{r,n}^3(x_{r,n}-4x)] - \\
& - \frac{r_n}{24}[(mb-x)^4\, u<mb-x> - (mb)^3(mb-4x)] - \\
& - \frac{r_{n-1}}{24}[(x_{r,n-1}-x)^4\, u<x_{r,n-1}-x> - x_{r,n-1}^3(x_{r,n-1}-4x)] + \\
& + \frac{Q_n}{6}[(x_{Q,n}-x)^3 u<x_{Q,n}-x> - 3x_{Q,n}^2(x_{Q,n}-x) + 2x_{Q,n}^3] + \\
& + \frac{F_n}{6}[(l_n-x)^3 - 3l_n^2(l_n-x) + 2l_n^3] + \\
& + \frac{\gamma_w \sin\psi}{120}[(x_{v,n}-x)^5 u<x_{v,n}-x> - 5x_{v,n}^4(x_{v,n}-x) + x_{v,n}^5(5-u<x_{v,n}-x>)] - \\
& - \frac{\gamma_w \sin\psi}{120}[(\hat{x}_{v,n-1}-x)^5\, u<\hat{x}_{v,n-1}-x> - 5\hat{x}_{v,n-1}^4(\hat{x}_{v,n-1}-x) + \\
& + \hat{x}_{v,n-1}^5(5-u<\hat{x}_{v,n-1}-x>)]
\end{aligned}
\qquad \textbf{(B-30)}
$$

Unfortunately, from reasons explained in appendix H, the approximation of the contact force by the uniformly distributed load would not always work during solving the system of nonlinear equations. For such a case another system of equations is presented as equations B-31, B-32, and B-33 (next page). The new system is identical to the previous one with the exception of the reaction between cantilevers which is approximated by a force acting at the end of the shorter cantilever. The derivation is analogous to the derivation of the force F, and so only the resultant equations are presented in this text.

Following equation B-28

$$
\begin{aligned}
M(x)_n = {} & \frac{w_n}{2}(l_n - x)^2 + \\
& + R_n\,(x_{r,n} - x)\,u\langle x_{r,n} - x\rangle - R_{n-1}\,(x_{r,n-1} - x)\,u\langle x_{r,n-1} - x\rangle - \\
& - \frac{\gamma_w \sin\psi}{6}(\hat{x}_{v,n-1} - x)^3\,u\langle \hat{x}_{v,n-1} - x\rangle + \frac{\gamma_w \sin\psi}{6}(x_{v,n} - x)^3\,u\langle x_{v,n} - x\rangle + \\
& + Q_n(x_{Q,n} - x)\,u\langle x_{Q,n} - x\rangle + F_n(l_n - x)
\end{aligned}
\qquad \textbf{(B-31)}
$$

equation B-29

$$
\begin{aligned}
EI\theta(x)_n = {} & \frac{w_n}{6}[(l_n - x)^3 - l_n^3] + \\
& + \frac{R_n}{2}[(x_{r,n} - x)^2\,u\langle x_{r,n} - x\rangle - x_{r,n}^2] - \\
& - \frac{R_{n-1}}{2}[(x_{r,n-1} - x)^2\,u\langle x_{r,n-1} - x\rangle - x_{r,n-1}^2] - \\
& - \frac{\gamma_w \sin\psi}{24}[(\hat{x}_{v,n-1} - x)^4\,u\langle \hat{x}_{v,n-1} - x\rangle - \hat{x}_{v,n-1}^4] + \\
& + \frac{\gamma_w \sin\psi}{24}[(x_{v,n} - x)^4\,u\langle x_{v,n} - x\rangle - x_{v,n}^4] + \\
& + \frac{Q_n}{2}[(x_{Q,n} - x)^2\,u\langle x_{Q,n} - x\rangle - (x_{Q,n})^2] + \frac{F_n}{2}[(l_n - x)^2 - (l_n)^2]
\end{aligned}
\qquad \textbf{(B-32)}
$$

and finally following equation B-30

$$\begin{aligned}
EIy(x)_n = {} & \frac{w_n}{24}[(l_n-x)^4-l_n^3(l-4x)] + \\
& + \frac{R_n}{6}[(x_{r,n}-x)^3\, u<x_{r,n}-x> -x_{r,n}^2(x_{r,n}-3x)] - \\
& - \frac{R_{n-1}}{6}[(x_{r,n-1}-x)^3\, u<x_{r,n-1}-x> -x_{r,n-1}^2(x_{r,n-1}-3x)] + \\
& + \frac{Q_n}{6}[(x_{Q,n}-x)^3 u<x_{Q,n}-x> -x_{Q,n}^2(x_{Q,n}-3x)] + \\
& + \frac{F_n}{6}[(l_n-x)^3-l_n^2(l_n-3x)] + \\
& + \frac{\gamma_w \sin\psi}{120}[(x_{v,n}-x)^5 u<x_{v,n}-x> - 5x_{v,n}^4(x_{v,n}-x) + x_{v,n}^5(5-u<x_{v,n}-x>)] - \\
& - \frac{\gamma_w \sin\psi}{120}[(\hat{x}_{v,n-1}-x)^5\, u<\hat{x}_{v,n-1}-x> - 5\hat{x}_{v,n-1}^4(\hat{x}_{v,n-1}-x) + \\
& + \hat{x}_{v,n-1}^5(5-u<\hat{x}_{v,n-1}-x>)]
\end{aligned} \qquad \textbf{(B-33)}$$

Appendix C

Geometrical equations of circle.

The equation of the circle with the center on the y axes (Fig. C-1) is:

$$x^2 + (y - y_o)^2 = y_o^2 \tag{C-1}$$

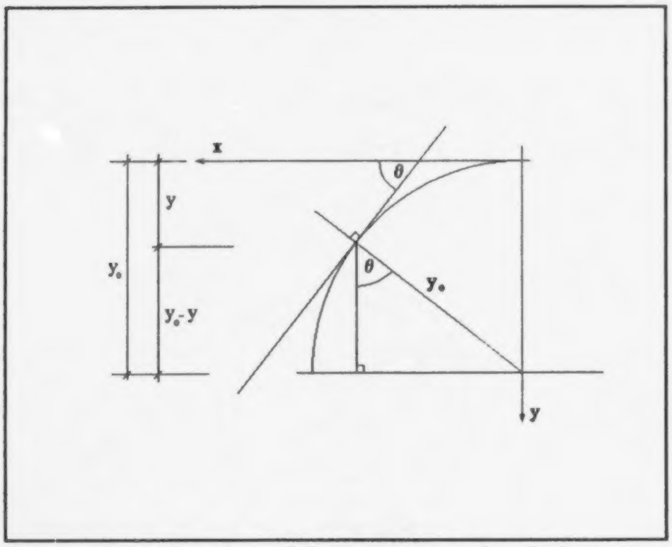

Figure C-1 Notation of the geometry of a circle.

Then from equation C-1 it follows

$$x^2 + y^2 - 2yy_o = 0 \tag{C-2}$$

and, from the fig. C-1

$$\frac{(y_o - y)}{y_o} = \cos\theta \tag{C-3}$$

and consequently

$$y_o = \frac{y}{(1 - \cos\theta)} \tag{C-4}$$

then from equations C-2 and C-4

$$0 = x^2 + y^2 - \frac{2y^2}{(1 - \cos\theta)} \tag{C-5}$$

multiplying equation C-4 by (1-cosθ) yields

$$\begin{aligned} 0 &= (1 - \cos\theta)(x^2 + y^2) - 2y^2 \\ 0 &= x^2 + y^2 - \cos\theta\, x^2 - \cos\theta\, y^2 - 2y^2 \end{aligned} \tag{C-6}$$

and finally

$$y = x\,(\frac{1 - \cos\theta}{1 + \cos\theta})^{\frac{1}{2}} \tag{C-7}$$

Equation C-6 has two roots, but the negative one is not of interest.

Appendix D.

Geometrical description of the toppling movement of interacting blocks on a stepped base.

To model the motion of a system of toppling rock blocks, it is necessary to find a relation between the motion of any two adjacent blocks of the system. This can be done in terms of geometrical relationships which express the angle of rotation of one block as a function of rotation of the adjacent block. There are actually four different geometrical cases to describe.

D.1. Two toppling blocks - case A.

The geometry of the case A is shown in Fig. D-1.

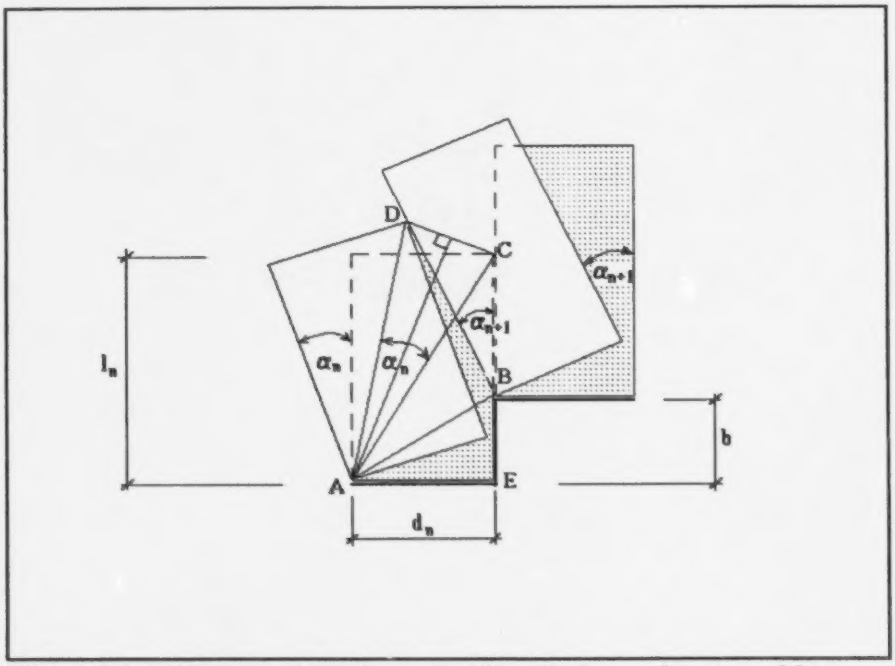

Figure D-1 The geometry of two toppling blocks on the stepped base - case A.

In Fig. D-1 the height l_n of the block n, the width d_n and the height b (spacing of joints) of the step AEB, and the angle of rotation of the block n are known. The unknown is the angle of rotation of the block n+1. From the Fig. D-1 a basic geometrical equation can be formed:

$$\frac{BD}{\sin BCD} = \frac{DC}{\sin \alpha_{n+1}} \tag{D-1}$$

In the equation D-1 :

$$\begin{aligned}
BD &= \sqrt{AB^2 + AD^2 - 2\,AB\,AD\cos BAD} \\
AB &= \sqrt{d_n^2 + b^2} = \frac{d_n}{\cos BAE} \\
AD &= \sqrt{l_n^2 + d_n^2} = \frac{d_n}{\cos CAE} = AC \\
BAD &= CAB + \alpha_n \\
CAB &= CAE - BAE \\
CAE &= \arctan\frac{l_n}{d_n} \\
BAE &= \arctan\frac{b}{d_n}
\end{aligned} \tag{D-2}$$

From the triangle ACD:

$$\frac{\frac{1}{2}DC}{AD} = \sin\frac{\alpha_n}{2} \quad \Rightarrow \quad DC = 2\,AD\sin\frac{\alpha_n}{2} \tag{D-3}$$

and

$$\begin{aligned} BCD &= ACD + ACE \\ ACD &= 90 - \frac{\alpha_n}{2} = \frac{1}{2}(180 - \alpha_n) \\ ACE &= 90 - CAE \\ CAE &= \arctan\frac{l_n}{d_n} \end{aligned} \tag{D-4}$$

So all components of the equation D-1 are known, and the angle α_{n+1} can be expressed as :

$$\alpha_{n+1} = \arcsin[\frac{DC}{BD}\sin BCD] \tag{D-5}$$

Where BD, DC and BCD are given by equations D-2, D-3 and D-4.

D.2. Two toppling blocks - Case B.

The geometry of the case B is shown in the Fig. D-2:

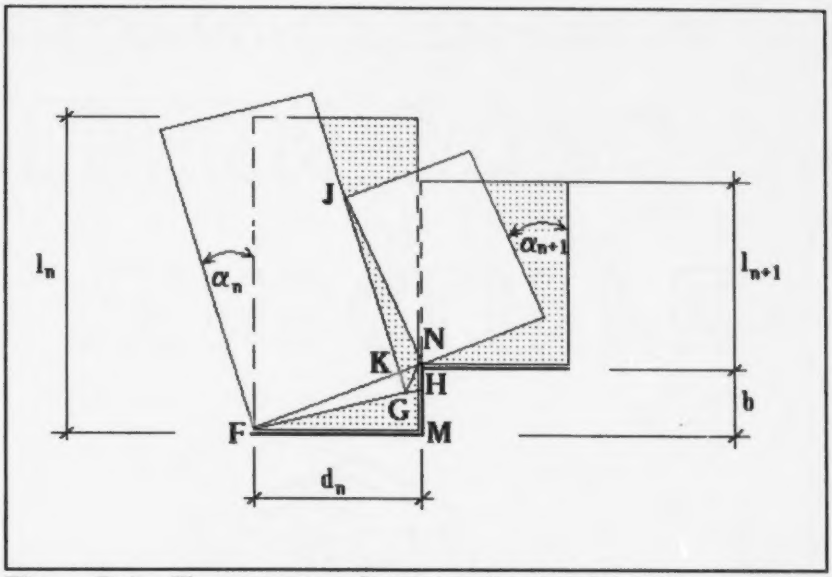

Figure D-2 The geometry of two toppling blocks on the stepped base - case B.

In the Fig. D-1 the heights l_n and l_{n+1} of blocks n and n+1, the width d_n and the height b (spacing of joints) of the step FMH, and the angle of rotation of the block n, α_n, are known. The unknown is again the angle of rotation of the block n+1. From the Fig. D-2 the basic geometric equation for the case B can be formed as:

$$\alpha_{n+1} = \alpha_n + NJG \qquad \textbf{(D-6)}$$

The angle NJG can be expressed as:

$$NJG = \arcsin[\frac{GN}{JN} \sin NGK] \qquad \textbf{(D-7)}$$

in equation D-8

$$
\begin{aligned}
GN &= \sqrt{FN^2 + FG^2 - 2\,FN\,FG\cos NFG} \\
FN &= \sqrt{D_n^2 + N^2} \\
NFG &= NFM - GFM \\
NFM &= \arctan\frac{b}{d_n} \\
GFM &= \alpha_n - 90 + \psi
\end{aligned}
\qquad \textbf{(D-8)}
$$

Where ψ is the angle of bedding planes with horizontal (see Fig. D-3).

$$JN = l_{n+1} \qquad \textbf{(D-9)}$$

and finally

$$
\begin{aligned}
NGK &= 90 - NGH \\
NGH &= \arcsin[\frac{HN}{GN}\sin GHN] \\
HN &= b - HM \\
HM &= d_n \tan HFM \\
HFM &= \alpha_n - 90 + \psi \\
GHN &= FHN = NFM - HFM \\
NFM &= \arctan\frac{b_n}{\alpha_n}
\end{aligned}
\qquad \textbf{(D-10)}
$$

D.3. The lower block is sliding, the upper block is toppling - case C.

The geometry of this situation is shown in Fig. D-3.

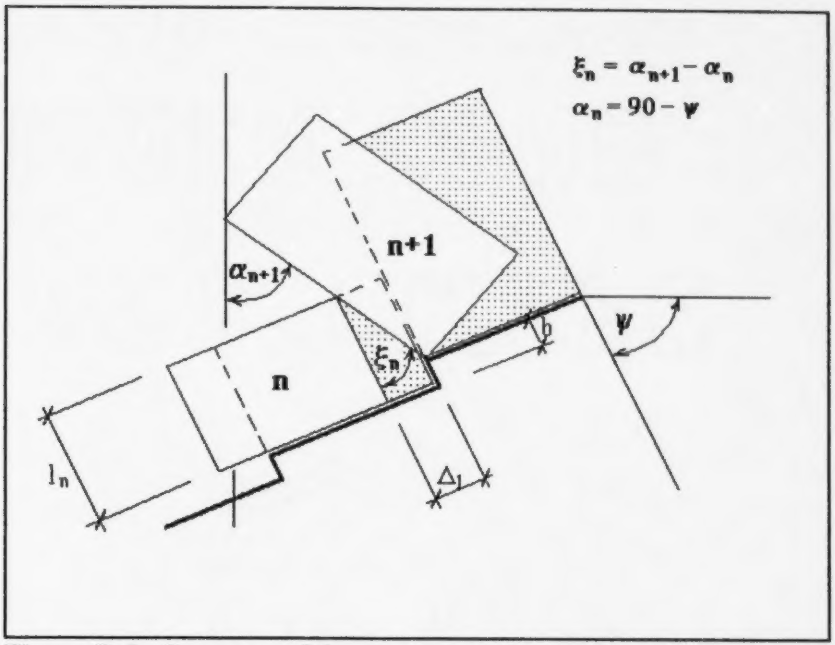
$\xi_n = \alpha_{n+1} - \alpha_n$
$\alpha_n = 90 - \psi$
n+1
α_{n+1}
ξ_n
n
l_n
Δ_1
b
ψ

Figure D-3 Geometry of the movement of one sliding and one toppling block on the stepped base.

The angle α_{n+1} is an unknown in this case, and is a function of the distance Δ_1 that the lower block has slid.

Derivation of this functional relation is straightforward:

From Fig. D-3 it follows:

$$\frac{\Delta_1}{(l_n - b)} = \tan \xi_n \qquad \textbf{(D-11)}$$

$$\xi_n = \alpha_{n+1} - 90 + \psi$$

and from equation D-12

$$\alpha_{n+1} = \arctan \frac{\Delta_1}{(l_n - b)} + 90 - \psi$$

As mentioned at the beginning of this appendix, there is a fourth basic case geometrically possible. This case is shown in the fig. D-4. Unfortunately, when the upper block tends to topple, and the lower block slides so far that the contact corner to corner is finally established, any further movement has so many geometrical variants that its' mathematical description in terms of geometrical equations is unsatisfactory. If this situation occurs during computation, the last safety factor of the present state of deformation will be the one just before the corner-corner contact occurs.

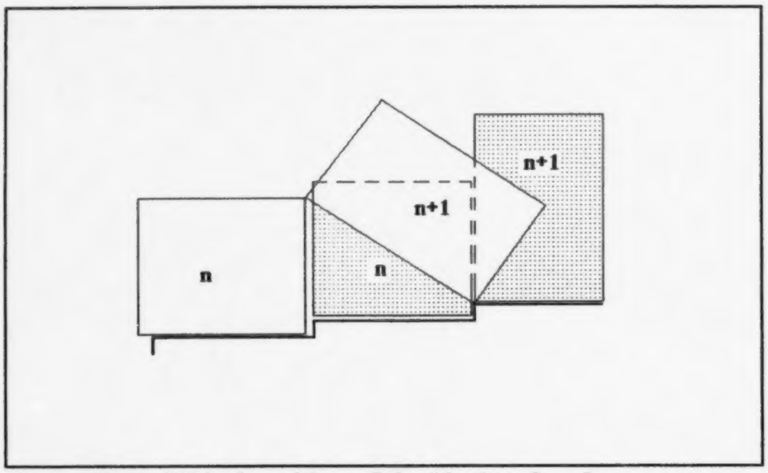

Figure D-4 Critical position of the blocks after the contact corner-corner was established.

Appendix E.

Derivation of equations for the system of toppling blocks.

The system of forces acting on one block from the system of interacting, toppling blocks is shown in the Fig. E-1.

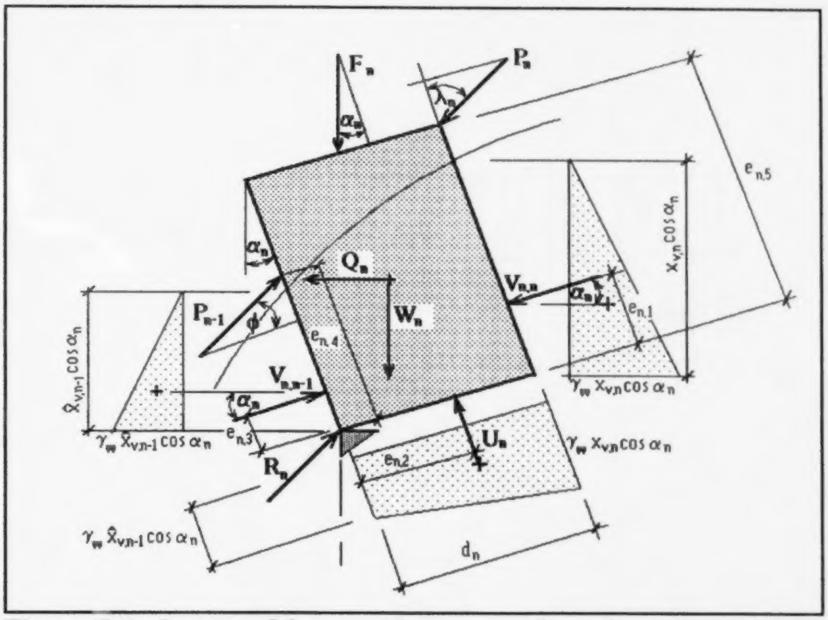
F_n
P_n
λ_n
α_n
e_n5
x_v,n cos α_n
V_n,n
α_n
e_n1
γ_w x_v,n cos α_n
Q_n
W_n
α_n
P_n-1
φ
e_n4
x̂_v,n-1 cos α_n
V_n,n-1
α_n
γ_w x̂_v,n-1 cos α_n
e_n3
R_n
e_n2
U_n
γ_w x_v,n cos α_n
γ_w x̂_v,n-1 cos α_n
d_n

Figure E-1 System of forces acting on one from the system of interacting blocks.

There are actually several possible arrangements of how three blocks can be in contact when toppling. It is obvious from Fig. E-1 that whatever the combination, the only forces changing their direction are the contact forces P_n and P_{n-1}. The rest of the forces are not affected by the adjacent blocks. The nomenclature of the acting forces remain the same as for the cantilever equations (Appendices A,B), the only new element is the uplift force U_n

The contacts that can occur within a system of toppling blocks are shown in the Fig. E-2 (next page). Case a) shows blocks below the crest, case b) is a crest block and case c) depicts blocks behind the crest. When the deformation is in progress, case a) may change to case b). In all cases the contact is always between a corner and a plane. The contact force P is assumed to act in the direction inclined from the normal to the contact plane by the angle of internal friction ϕ.

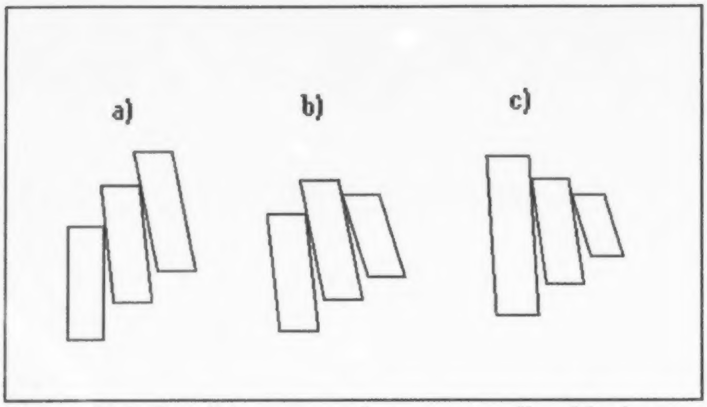

Figure E-2 Possible contacts between toppling blocks.

Geometry of possible arrangements is shown in figures E-3 and E-4.

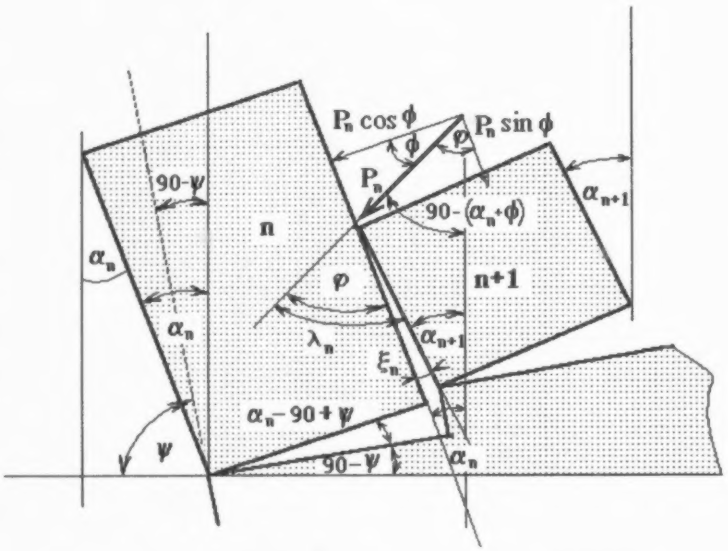
$P_n \cos\phi$
ϕ
φ
$P_n \sin\phi$
P_n
α_{n+1}
$90-(\alpha_n+\phi)$
n
$90-\psi$
α_n
φ
n+1
λ_n
α_{n+1}
ξ_n
α_n
$\alpha_n-90+\psi$
ψ
$90-\psi$
ξ
α_n

The angle of the force P_n with vertical .... $90-(\alpha_n-\phi) = \varphi-\alpha_n$

The angle of the force P_n with the block n+1 ..... $\varphi+(\alpha_{n+1}-\alpha_n)=\varphi+\xi_n=\lambda_n$

Figure E-3 Geometry of toppling blocks - block n being the higher one.

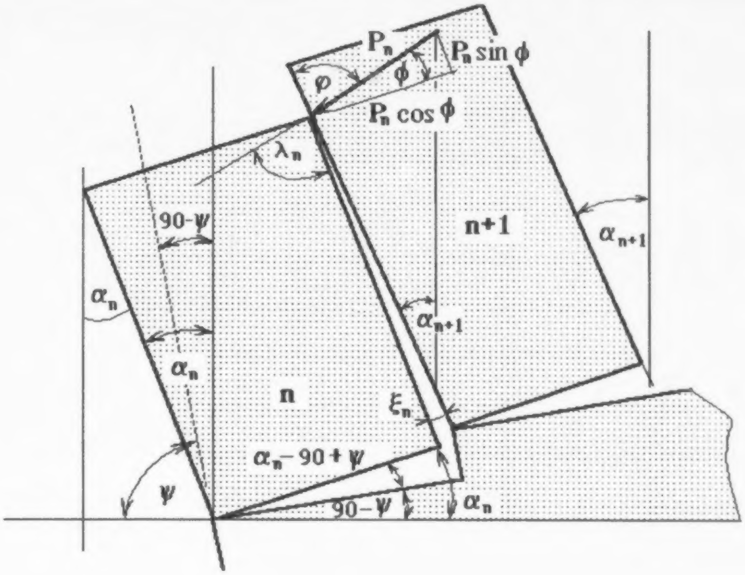

P_n
$P_n \sin\phi$
φ
ϕ
$P_n \cos\phi$
λ_n
90-ψ
n+1
α_{n+1}
α_n
α_{n+1}
α_n
n
ξ_n
$\alpha_n - 90 + \psi$
ψ
90-ψ
α_n

The angle of the force P_n with vertical .... $90-(\alpha_{n+1}+\phi)=\varphi-\alpha_{n+1}$

The angle of the force P_n with the block **n** .... $\varphi-(\alpha_{n+1}-\alpha_n)=\varphi-\xi_n=\lambda_n$

Figure E-4 Geometry of the toppling blocks - Block n being the lower one.

From the Fig. E-1 the moment equilibrium of the forces can be defined for the three different cases in the Fig. E-2 as:

Case a)

$$\begin{aligned} 0 = {} & P_n \sin\lambda_n l_n - P_n \cos\lambda_n d_n + V_{n,n} e_{n,1} - V_{n,n-1} e_{n,3} - \\ & - W_n \cos\alpha_n \frac{d_n}{2} + W_n \sin\alpha_n \frac{l_n}{2} + Q_n \cos\alpha_n \frac{l_n}{2} - Q_n \sin\alpha_n \frac{d_n}{2} - \qquad \text{(E-1)} \\ & - F_n \cos\alpha_n \frac{d_n}{2} + F_n \sin\alpha_n \frac{l_n}{2} - P_{n-1} \cos\phi \, e_{n,4} + U_n e_{n,2} \end{aligned}$$

Case b)

$$\begin{aligned}0 &= P_n\cos\phi\, e_{n,5} - P_n\sin\phi\, d_n + V_{n,n}e_{n,1} - V_{n,n-1}e_{n,3} - \\ &- W_n\cos\alpha_n\frac{d_n}{2} + W_n\sin\alpha_n\frac{l_n}{2} + Q_n\cos\alpha_n\frac{l_n}{2} - Q_n\sin\alpha_n\frac{d_n}{2} - \\ &- F_n\cos\alpha_n\frac{d_n}{2} + F_n\sin\alpha_n\frac{l_n}{2} - P_{n-1}\cos\phi\, e_{n,4} + U_n e_{n,2}\end{aligned} \tag{E-2}$$

Case c)

$$\begin{aligned}0 &= P_n\cos\phi\, e_{n,5} - P_n\sin\phi\, d_n + V_{n,n}e_{n,1} - V_{n,n-1}e_{n,3} - \\ &- W_n\cos\alpha_n\frac{d_n}{2} + W_n\sin\alpha_n\frac{l_n}{2} + Q_n\cos\alpha_n\frac{l_n}{2} - Q_n\sin\alpha_n\frac{d_n}{2} - \\ &- F_n\cos\alpha_n\frac{d_n}{2} + F_n\sin\alpha_n\frac{l_n}{2} - P_{n-1}\sin\lambda_n l_n + U_n e_{n,2}\end{aligned} \tag{E-3}$$

Then from equation E-1

$$\begin{aligned}P_{n-1} &= \frac{P_n(\sin\lambda_n l_n - \cos\lambda_n d_n)}{\cos\phi\, e_{n,4}} + \\ &+ \frac{1}{\cos\phi\, e_{n,4}}[V_{n,n}e_{n,1} - V_{n,n-1}e_{n,3} - W_n\cos\alpha_n\frac{d_n}{2} + W_n\sin\alpha_n\frac{l_n}{2} + \\ &+ Q_n\cos\alpha_n\frac{l_n}{2} - Q_n\sin\alpha_n\frac{d_n}{2} - F_n\cos\alpha_n\frac{d_n}{2} + F_n\sin\alpha_n\frac{l_n}{2} + U_n e_{n,2}]\end{aligned} \tag{E-4}$$

From equation E-2

$$\begin{aligned} P_{n-1} &= \frac{P_n(\cos\phi\, e_{n,5} - \sin\phi\, d_n)}{\cos\phi\, e_{n,4}} + \\ &+ \frac{1}{\cos\phi\, e_{n,4}}[V_{n,n}e_{n,1} - V_{n,n-1}e_{n,3} - W_n\cos\alpha_n\frac{d_n}{2} + W_n\sin\alpha_n\frac{l_n}{2} + \\ &+ Q_n\cos\alpha_n\frac{l_n}{2} - Q_n\sin\alpha_n\frac{d_n}{2} - F_n\cos\alpha_n\frac{d_n}{2} + F_n\sin\alpha_n\frac{l_n}{2} + U_n e_{n,2}] \end{aligned} \tag{E-5}$$

At the very beginning, before any movement takes place, all sides of all blocks are parallel because they are in face to face contact position. For this situation equation E-5 will be used for all geometrical arrangements for calculating the safety factor of the slope ($\xi_n = 0$; $\lambda_n = \phi$, see figures E-3 and E-4) .

And finally from equation E-3

$$\begin{aligned} P_{n-1} &= \frac{P_n(\cos\phi\, e_{n,5} - \sin\phi\, d_n)}{\sin\lambda_n l_n} + \\ &+ \frac{1}{\sin\lambda_n l_n}[V_{n,n}e_{n,1} - V_{n,n-1}e_{n,3} - W_n\cos\alpha_n\frac{d_n}{2} + W_n\sin\alpha_n\frac{l_n}{2} + \\ &+ Q_n\cos\alpha_n\frac{l_n}{2} - Q_n\sin\alpha_n\frac{d_n}{2} - F_n\cos\alpha_n\frac{d_n}{2} + F_n\sin\alpha_n\frac{l_n}{2} + U_n e_{n,2}] \end{aligned} \tag{E-6}$$

It is possible to define

$$[C] = [\,V_{n,n}e_{n,1} - V_{n,n-1}e_{n,3} - W_n\cos\alpha_n\frac{d_n}{2} + W_n\sin\alpha_n\frac{l_n}{2} + \\ + Q_n\cos\alpha_n\frac{l_n}{2} - Q_n\sin\alpha_n\frac{d_n}{2} - F_n\cos\alpha_n\frac{d_n}{2} + F_n\sin\alpha_n\frac{l_n}{2} + U_ne_{n,2}] \tag{E-7}$$

Equations E-4, E-5 and E-6 then appear as equations E-8, E-9 and E-10.

$$P_{n-1} = \frac{P_n(\sin\lambda_n l_n - \cos\lambda_n d_n)}{\cos\phi\, e_{n,4}} + \frac{1}{\cos\phi\, e_{n,4}}[C] \tag{E-8}$$

$$P_{n-1} = \frac{P_n(\cos\phi\, e_{n,5} - \sin\phi\, d_n)}{\cos\phi\, e_{n,4}} + \frac{1}{\cos\phi\, e_{n,4}}[C] \tag{E-9}$$

and

$$P_{n-1} = \frac{P_n(\cos\phi\, e_{n,5} - \sin\phi\, d_n)}{\sin\lambda_n l_n} + \frac{1}{\sin\lambda_n l_n}[C] \tag{E-10}$$

Appendix F.

Derivation of equations for the system of sliding blocks.

The system of forces acting on one block from the system of interacting blocks is shown in the Fig. F-1.

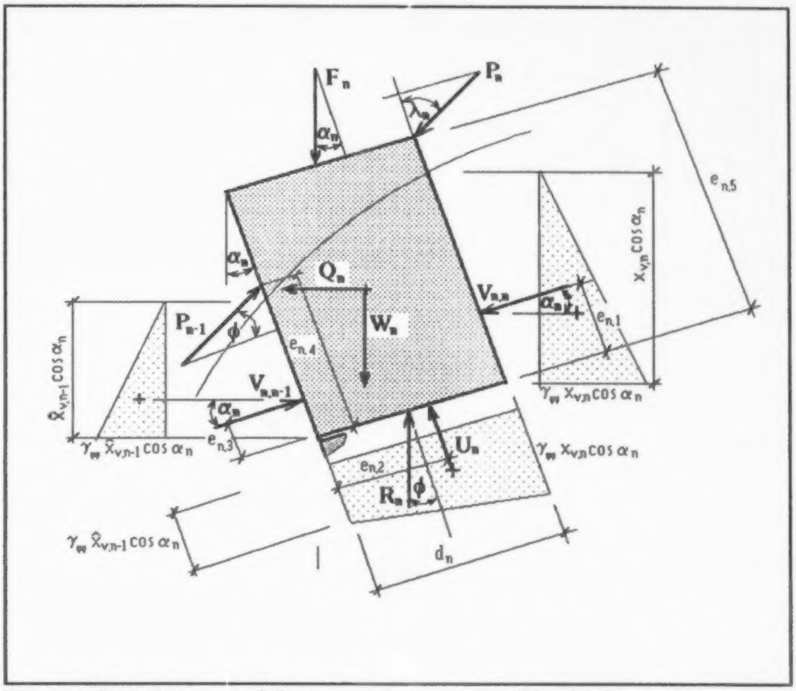
Fn
Pn
αn
λn
en,5
xv,n cos αn
αn
Qn
Wn
Vn,n
αn
en,1
Pn-1
φ
en,4
Vn,n-1
αn
x̂v,n-1 cos αn
γw x̂v,n-1 cos αn
en,3
γw xv,n cos αn
en,2
Un
γw xv,n cos αn
Rn
φ
dn
γw x̂v,n-1 cos αn

Figure F-1 System of forces acting on one block, from the system of interacting blocks.

The figure is identical to the Fig. E-1 with one exception. The reaction R_n does not act at the corner of the block and its' position is unknown. This is the reason why an assumption about the direction of the force is made, and the reaction force R is assumed to act in the direction inclined from the normal to the contact plane by the angle of internal friction ϕ. The rest of the forces are defined the same way as for the toppling movement, and their directions are shown in Fig. F-1. The nomenclature of the forces in the figure remains the same as in appendix E Fig. E-1, and in the appendices A,B.

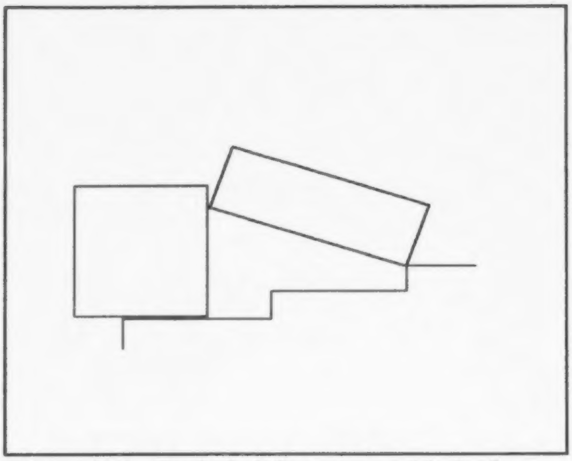

Figure F-2 Excluded face-corner kind of contact for the sliding and toppling blocks.

The contacts that can occur within a system of sliding blocks are shown in the Fig. F-2. It is obvious from the figure that all sliding blocks are assumed to be in face to face contact, except the first one, which is in corner- face contact with the last toppling block. This restricted number of possible contacts is caused by the assumption, that the blocks in question either slide or topple, but never change the mode of movement. Another assumption accommodated is the one which bans the contact between the corner of the toppling block, and the side of the sliding block as shown in Fig. F-3. This kind of contact would make the previous assumption unreasonable, and it would allow highly unpredictable movements of both sliding, and toppling blocks. A more detailed explanation is given in the main body of the thesis.

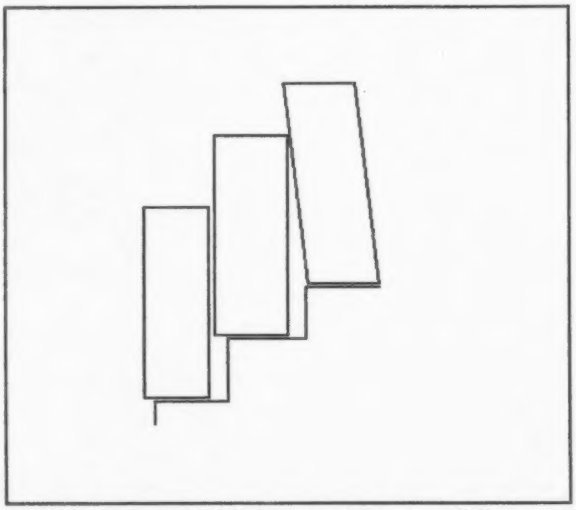

Figure F-3 Possible contact for the sliding blocks.

The geometry, including contact forces, their direction and the position of the blocks from the Fig. F-2, is shown in the Fig. F-4 (next page).

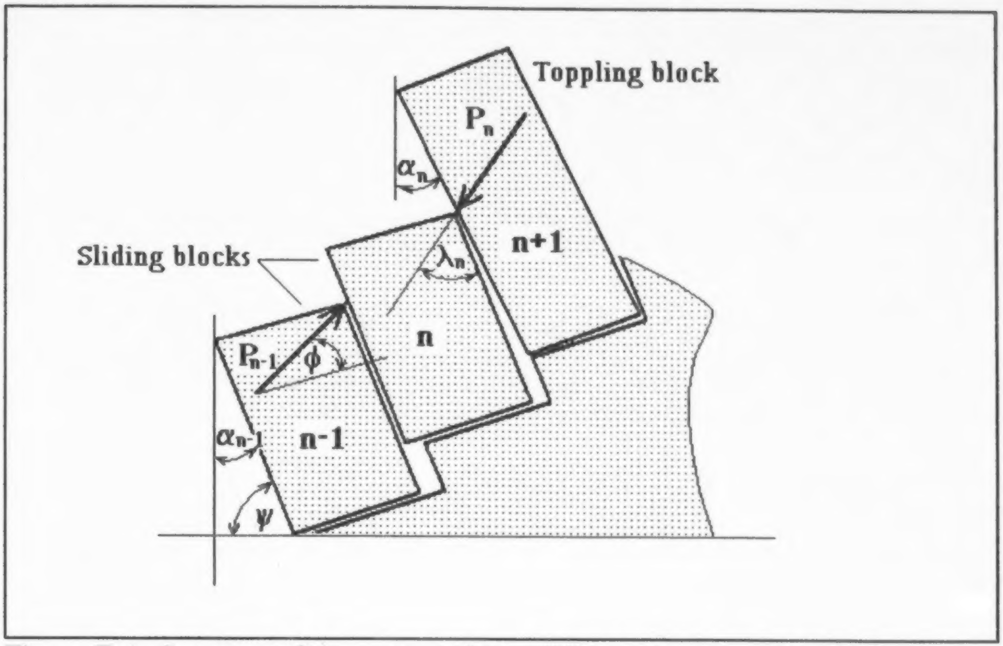
Toppling block
P_n
α_n
Sliding blocks
λ_n
n+1
n
P_{n-1}
ϕ
α_{n-1}
n-1
ψ

Figure F-4 Geometry of the system of two sliding and one toppling blocks.

From Fig. F-1, equilibrium of forces parallel to the sliding blocks can be defined for the two kinds of contact in Fig. F-2 as:

$$\begin{aligned} \|: \quad 0 &= P_n \cos\lambda_n - P_{n-1}\sin\phi - R_n\cos(\alpha_n + \psi + \phi - 90) + \\ &+ F_n\cos\alpha_n - Q_n\sin\alpha_n - U_n + W_n\cos\alpha_n \end{aligned} \tag{F-1}$$

and

$$\begin{aligned} \|: \quad 0 &= P_n \sin\phi - P_{n-1}\sin\phi - R_n\cos(\alpha_n + \psi + \phi - 90) + \\ &+ F_n\cos\alpha_n - Q_n\sin\alpha_n - U_n + W_n\cos\alpha_n \end{aligned} \tag{F-2}$$

And again from Fig. F-1, equilibrium of forces perpendicular to the sliding blocks can be defined for the two kinds of contact in Fig. F-2 as:

$$\perp: \quad 0 = P_n \sin_{\lambda_n} - P_{n-1}\cos\phi - R_n \sin(\alpha_n + \psi + \phi - 90) + \\ + V_{n,n} - V_{n,n-1} + F_n \sin\alpha_n + W_n \sin\alpha_n + Q_n \cos\alpha_n \qquad \textbf{(F-3)}$$

and

$$\perp: \quad 0 = P_n \cos\phi - P_{n-1}\cos\phi - R_n \sin(\alpha_n + \psi + \phi - 90) + \\ + V_{n,n} - V_{n,n-1} + F_n \sin\alpha_n + W_n \sin\alpha_n + Q_n \cos\alpha_n \qquad \textbf{(F-4)}$$

Then, from equation F-1

$$R_n = \frac{1}{\cos(\alpha_n + \psi + \phi - 90)} [P_n \cos\lambda_n - P_{n-1}\sin\phi + \\ + F_n \cos\alpha_n - Q_n \sin\alpha_n - U_n + W_n \cos\alpha_n] \qquad \textbf{(F-5)}$$

From equation F-2

$$R_n = \frac{1}{\cos(\alpha_n + \psi + \phi - 90)} [P_n \sin\phi - P_{n-1}\sin\phi + \\ + F_n \cos\alpha_n - Q_n \sin\alpha_n - U_n + W_n \cos\alpha_n] \qquad \textbf{(F-6)}$$

From equations F-3 and F-5

$$\begin{aligned}0 = P_n \sin_{\lambda_n} - P_{n-1}\cos\phi - \frac{\sin(\alpha_n + \psi + \phi - 90)}{\cos(\alpha_n + \psi + \phi - 90)}[P_n \cos\lambda_n - \\ - P_{n-1}\sin\phi + F_n \cos\alpha_n - Q_n \sin\alpha_n - U_n + W_n \cos\alpha_n] + \\ + V_{n,n} - V_{n,n-1} + F_n \sin\alpha_n + W_n \sin\alpha_n + Q_n \cos\alpha_n\end{aligned} \qquad \textbf{(F-7)}$$

From equations F-4 and F-6

$$\begin{aligned}0 = P_n \cos\phi - P_{n-1}\cos\phi - \frac{\sin(\alpha_n + \psi + \phi - 90)}{\cos(\alpha_n + \psi + \phi - 90)}[P_n \sin\phi - \\ - P_{n-1}\sin\phi + F_n \cos\alpha_n - Q_n \sin\alpha_n - U_n + W_n \cos\alpha_n] + \\ + V_{n,n} - V_{n,n-1} + F_n \sin\alpha_n + W_n \sin\alpha_n + Q_n \cos\alpha_n\end{aligned} \qquad \textbf{(F-8)}$$

Finally, from equation F-7

$$\begin{aligned}P_{n-1} = \frac{P_n \sin_{\lambda_n} - \cos\lambda_n \tan(\alpha_n + \psi + \phi - 90)}{\cos\phi - \sin\phi \tan(\alpha_n + \psi + \phi - 90)} - \\ - \frac{[F_n \cos\alpha_n - Q_n \sin\alpha_n - U_n + W_n \cos\alpha_n]\tan(\alpha_n + \psi + \phi - 90)}{\cos\phi - \sin\phi \tan(\alpha_n + \psi + \phi - 90)} + \\ + \frac{V_{n,n} - V_{n,n-1} + F_n \sin\alpha_n + W_n \sin\alpha_n + Q_n \cos\alpha_n}{\cos\phi - \sin\phi \tan(\alpha_n + \psi + \phi - 90)}\end{aligned} \qquad \textbf{(F-9)}$$

and from equation F-8

$$P_{n-1} = P_n - \frac{[F_n \cos\alpha_n - Q_n \sin\alpha_n - U_n + W_n \cos\alpha_n] \tan(\alpha_n + \psi + \phi - 90)}{\cos\phi - \sin\phi \tan(\alpha_n + \psi + \phi - 90)} - $$
$$- \frac{V_{n,n} - V_{n,n-1} + F_n \sin\alpha_n + W_n \sin\alpha_n + Q_n \cos\alpha_n}{\cos\phi - \sin\phi \tan(\alpha_n + \psi + \phi - 90)} \qquad \textbf{(F-10)}$$

It is possible to introduce

$$\begin{aligned}
[A] &= [F_n \cos\alpha_n - Q_n \sin\alpha_n - U_n + W_n \cos\alpha_n] \\
[B] &= [V_{n,n} - V_{n,n-1} + F_n \sin\alpha_n + W_n \sin\alpha_n + Q_n \cos\alpha_n] \\
\Gamma &= \alpha_n + \psi + \phi - 90
\end{aligned} \qquad \textbf{(F-11)}$$

Then equation F-9 now appears as

$$P_{n-1} = \frac{P_n(\sin_{\lambda_n} - \cos\lambda_n \tan(\Gamma)) - [A]\tan\Gamma + [B]}{\cos\phi - \sin\phi \tan(\Gamma)} \qquad \textbf{(F-12)}$$

and equation F-10 appears as

$$P_{n-1} = P_n - \frac{[A]\tan\Gamma + [B]}{\cos\phi - \sin\phi \tan(\Gamma)} \qquad \textbf{(F-13)}$$

Appendix G.

Shear strength on the bedding planes.

The problem of calculating the stability of a set of cantilevers against shearing lies in incapability of the program to express the progressive mode of failure which very likely takes place between two bending cantilevers. The failure initiates at the place of the lowest strength/stress ratio, and then gradually spreads along the bedding plane. However, the overall shear stability on the bedding planes can be expressed in terms of average stresses.

Shear force within the composite beam can be calculated as:

$$\begin{aligned} V(x)_n &= w_n(l_n - x) + R_n u{<}x_{r,n} - x{>} - R_{n-1} u{<}x_{r,n-1} - x{>} + F_n \\ &\quad + Q_n u{<}x_{Q,n} - x{>} - \frac{\gamma_w \sin\psi}{2}(x_{v,n-1} - x)^2 u{<}x_{v,n-1} - x{>} \\ &\quad + \frac{\gamma_w \sin\psi}{2}(x_{v,n} - x)^2 u{<}x_{v,n} - x{>} \end{aligned} \tag{G-1}$$

Maximum shear stress can be then calculated as

$$\tau(x)_{n,\max} = \frac{3}{2}\frac{V(x)_n}{\bar{b}h_n} \tag{G-2}$$

The summation of the shear force over the length of the cantilever equals

$$\sum \tau(x)_{n,\max} = \frac{3}{2\bar{b}h_n}\int_0^{l_{nV}} (x)_n \tag{G-3}$$

or

$$\sum \tau(x)_{n,\max} = \frac{3}{2\tilde{b}h_n}\{\int_0^{l_n} w_n(l_n - x) + \int_0^{x_{r,n}} R_n - \int_0^{x_{r,n-1}} R_{n-1} + \int_0^{l} F_n + \frac{\gamma_w \sin\psi}{2}[\int_0^{x_{v,n}} (xv_n - x)^2 - \int_0^{x_{v,n-1}} (xv_{n-1} - x)^2]\} \quad \textbf{(G-4)}$$

and after simplification

$$\sum \tau(x)_{n,\max} = \frac{3}{2\tilde{b}h_n}[w_n \frac{l_n^2}{2} + R_n x_{r,n} - R_{n-1} x_{r,n-1} + F l_n + + \frac{\gamma_w si\psi}{2}(x_{v,n} - x_{v,n-1})] \quad \textbf{(G-5)}$$

The average shear stress over a cantilever equals

$$\tau_{aver} = \frac{\sum \tau(x)_{n,\max}}{l_n} \quad \textbf{(G-6)}$$

Normal stress acting across the cantilever can be expressed as

$$\sigma_{n,aver} = \frac{\frac{w_n l_n}{2} + R_n + F_n + \gamma_w \frac{x_{v,n}^2}{2}}{l_n} \tag{G-7}$$

and consequently shear strength can be expressed as

$$\tau_{strength} = c + \tan\phi \, \sigma_{n,aver} \tag{G-8}$$

Appendix H

Solution of the system of nonlinear equations for toppling.

H.1. Newton - Raphson method.

To solve problems in more than two dimensions, which is the case of the system of equations describing bending columns of rock, it is necessary to find points mutually common to N unrelated zero-contour hyperplanes each of dimension N-1. Analytical solution of such a problem is impossible, however, once the approximate location of a root, or of a place where there might be a root is identified, the problem can be solved by using the Newton - Raphson method generalized to multiple dimensions (Press, Flannery, Teukolsky and Vetterling, 1990).

A typical problem gives N functional relations to be zeroed, involving variables x_i , i = 1,2,3,........,N:

$$f_i(x_1,x_2,........,x_n) = 0 \qquad i = 1,2,.......,n \tag{H-1}$$

Then if the entire vector of values x_i is denoted as X, each of the functions f_i can be, in the neighbourhood of X, expanded in Taylor series

$$f_i(X + \delta X) = f_i(X) + \sum_{j=1}^{n} \frac{\partial f_i}{\partial x_j} \delta x_j + O(\delta X^2) \tag{H-2}$$

By neglecting terms of order δX^2 and higher, the set of linear equations can be created for the corrections δX that move each function closer to zero simultaneously. Equation H-1 can be rewritten as

$$f_i(X) + \sum_{j=1}^{n} \frac{\partial f_i}{\partial x_j} \delta x_j = 0 \tag{H-3}$$

or

$$\sum_{j=1}^{n} \frac{\partial f_i}{\partial x_j} \delta x_j = -f_i(X) \qquad \textbf{(H-4)}$$

Equation H-4 can be solved for δx_i knowing the magnitude of the function f_i and its' derivatives $\partial f_i / \partial x_j$ for the initial guess of x_j. The corrections are then added to the solution vector,

$$x_i^{new} = x_i^{old} + \delta x_i \qquad i = 1,2,........,n \qquad \textbf{(H-5)}$$

and the process is iterated to convergence.

H.2. Bending equations for the Newton - Raphson method.

Flat base-continuous reaction.

Equation H-4 can be written in the matrix form as:

$$\begin{bmatrix} \frac{\partial f_1}{\partial x_1} & \frac{\partial f_1}{\partial x_2} & \frac{\partial f_1}{\partial x_3} & \cdots & \frac{\partial f_n}{\partial x_1} \\ \frac{\partial f_2}{\partial x_1} & \frac{\partial f_2}{\partial x_2} & \frac{\partial f_2}{\partial x_3} & \cdots & \frac{\partial f_2}{\partial x_n} \\ \vdots & \vdots & \vdots & & \vdots \\ \frac{\partial f_n}{\partial x_1} & \frac{\partial f_n}{\partial x_2} & \frac{\partial f_n}{\partial x_3} & \cdots & \frac{\partial f_n}{\partial x_n} \end{bmatrix} \times \begin{bmatrix} \delta x_1 \\ \delta x_2 \\ \vdots \\ \delta x_n \end{bmatrix} = \begin{bmatrix} -f_1 \\ -f_2 \\ \vdots \\ -f_n \end{bmatrix} \qquad \textbf{(H-6)}$$

Function f_n (force F_n included) was derived for the flat base in appendix A as

$$\begin{aligned} f_n = {} & \frac{w_n}{6}[(l_n-x_n)^3-l_n^3] - \frac{r_{n-1}}{6}[(x_{r,n-1}-x_n)^3\, u<x_{r,n-1}-x_n> - x^3_{r,n-1}] + \\ & + \frac{r_n}{6}[(x_{r,n}-x_n)^3\, u<x_{r,n}-x_n> - x^3_{r,n}] - \\ & - \frac{\gamma_w \sin\psi}{24}[(x_{v,n-1}-x_n)^4\, u<x_{v,n-1}-x_n> - x^4_{v,n-1}] + \\ & + \frac{\gamma_w \sin\psi}{24}[(x_{v,n}-x_n)^4\, u<x_{v,n}-x_n> - x^4_{v,n}] + \frac{q_n}{6}[(l_n-x_n)^3-l_n^3] + \\ & + \frac{F_n}{2}[(l_n-x_n)^2-(l_n)^2] - EI\theta(x)_n \end{aligned} \tag{H-7}$$

For the first cantilever equation H-7 yields

$$\begin{aligned} f_1 = {} & \frac{w_n}{6}[(l_n-x_n)^3-l_n^3] + \\ & + \frac{r_n}{6}[(x_{r,n}-x_n)^3\, u<x_{r,n}-x_n> - x^3_{r,n}] - \\ & - \frac{\gamma_w \sin\psi}{24}[(x_{v,n-1}-x_n)^4\, u<x_{v,n-1}-x_n> - x^4_{v,n-1}] + \\ & + \frac{\gamma_w \sin\psi}{24}[(x_{v,n}-x_n)^4\, u<x_{v,n}-x_n> - x^4_{v,n}] + \frac{q_n}{6}[(l_n-x_n)^3-l_n^3] + \\ & + \frac{F_n}{2}[(l_n-x_n)^2-(l_n)^2] - EI\theta(x)_n \end{aligned} \tag{H-8}$$

and for the last cantilever i , n = 1,2,.....,i

$$\begin{aligned} f_i = {} & \frac{w_n}{6}[(l_n - x_n)^3 - l_n^3] - \\ & - \frac{r_{n-1}}{6}[(x_{r,n-1} - x_n)^3\, u\!<\!x_{r,n-1} - x_n\!> - x_{r,n-1}^3] - \\ & - \frac{\gamma_w \sin\psi}{24}[(\hat{x}_{v,n-1} - x_n)^4\, u\!<\!\hat{x}_{v,n-1} - x_n\!> - \hat{x}_{v,n-1}^4] + \\ & + \frac{\gamma_w \sin\psi}{24}[(x_{v,n} - x_n)^4\, u\!<\!x_{v,n} - x_n\!> - x_{v,n}^4] + \\ & + \frac{Q_n}{2}[(x_{Q,n} - x_n)^2 u\!<\!x_{Q,n} - x_n\!> - (x_{Q,n})^2] + \frac{F_n}{2}[(l_n - x_n)^2 - (l_n)^2] - \\ & - EI\theta(x)_n \end{aligned} \tag{H-9}$$

At this stage, in the equation H-10 (next page), singularity functions vanished from the brackets following unknowns r_n and r_{n-1} . The reason is simple; to calculate the unknowns, the coordinate x_n has to be chosen on the cantilever contact ($r_n \neq 0$), and in that case the singularity function is defined to be 1.

From equation H-7

$$\begin{aligned}
f_n = {} & \frac{w_n}{6}[-3l_n^2x_n + 3l_nx_n^2 - x_n^3] + \\
& + \frac{r_n}{6}[x_{r,n}^3 u<x_{r,n} - x_n> - 3x_{r,n}^2 x_n u<x_{r,n} - x_n> + 3x_{r,n} x_n^2 u<x_{r,n} - x_n> - \\
& \qquad - x_n^3 u<x_{r,n} - x_n> - x_{r,n}^3] - \\
& - \frac{r_{n-1}}{6}[x_{r,n-1}^3 u<x_{r,n-1} - x_n> - 3x_{r,n-1}^2 x_n u<x_{r,n-1} - x_n> + 3x_{r,n-1} x_n^2 u<x_{r,n-1} - x_n> - \\
& \qquad - x_n^3 u<x_{r,n-1} - x_n> - x_{r,n-1}^3] + \\
& + \frac{\gamma_w \sin\psi}{24}[x_{v,n}^4 u<x_{v,n} - x_n> - 4x_{v,n}^3 x_n u<x_{v,n} - x_n> + 6x_{v,n}^2 x_n^2 u<x_{v,n} - x_n> - \\
& \qquad - 4x_{v,n} x_n^3 u<x_{v,n} - x_n> + x_n^4 u<x_{v,n} - x_n> - x_{v,n}^4] + \\
& - \frac{\gamma_w \sin\psi}{24}[x_{v,n-1}^4 u<x_{v,n-1} - x> - 4x_{v,n-1}^3 x_n u<x_{v,n-1} - x_n> + 6x_{v,n-1}^2 x_n^2 u<x_{v,n-1} - x_n> - \\
& \qquad - 4x_{v,n-1} x_n^3 u<x_{v,n-1} - x_n> + x_n^4 u<x_{v,n-1} - x_n> - x_{v,n-1}^4] + \\
& + \frac{Q_n}{2}[x_{Q,n}^2 u<x_{Q,n} - x_n> - 2x_{Q,n} x_n u<x_{Q,n} - x_n> + x_n^2 u<x_{Q,n} - x_n> - x_{Q,n}^2] + \\
& + \frac{F_n}{2}[-2l_nx_n + x_n^2] - EI\theta(x)_n
\end{aligned} \qquad \textbf{(H-10)}$$

Than equation H-10 can be rearranged to

$$\begin{aligned}
f_n = x_n\,[& -\frac{w_n}{2}l_n^2 - \frac{r_n}{2}x_{r,n}^2 + \frac{r_{n-1}}{2}x_{r,n-1}^2 + \frac{\gamma_w \sin\psi}{6}x_{v,n-1}^3 u<x_{v,n-1}-x_n> - \\
& -\frac{\gamma_w \sin\psi}{6}x_{v,n}^3 u<x_{v,n}-x_n> - \frac{q_n}{2}l_n^2 - F_n l_n] + \\
+x_n^2\,[& +\frac{w_n}{2}l_n + \frac{r_n}{2}x_{r,n} - \frac{r_{n-1}}{2}x_{r,n-1} - \frac{\gamma_w \sin\psi}{4}x_{v,n-1}^2 u<x_{v,n-1}-x_n> + \\
& +\frac{\gamma_w \sin\psi}{4}x_{v,n}^2 u<x_{v,n}-x_n> + \frac{q_n}{2}l_n + \frac{F_n}{2}] + \\
+x_n^3\,[& -\frac{w_n}{6} - \frac{r_n}{6} + \frac{r_{n-1}}{6} + \frac{\gamma_w \sin\psi}{6}x_{v,n-1} u<x_{v,n-1}-x_n> - \\
& -\frac{\gamma_w \sin\psi}{6}x_{v,n} u<x_{v,n}-x_n> - \frac{q_n}{6}] + \\
+x_n^4\,[& -\frac{\gamma_w \sin\psi}{24}u<x_{v,n-1}-x_n> - \frac{\gamma_w \sin\psi}{24}u<x_{v,n}-x_n>] - \\
-EI\theta(x)_n & - \frac{\gamma_w \sin\psi}{24}[x_{v,n-1}^4 u<x_{v,n-1}-x_n> - \hat{x}_{v,n-1}^4] + \frac{\gamma_w \sin\psi}{24}[x_{v,n}^4 u<x_{v,n}-x_n> - x_{v,n}^4]
\end{aligned} \tag{H-11}$$

Now in all the brackets there are only constants with respect to θ, and so the equation H-11 can be rewritten as

$$\begin{aligned}
f_n = {} & x_n[D_n] + x_n^2[E_n] + x_n^3[F_n] + x_n^4[G_n] - EI\theta - \\
& - \frac{\gamma_w \sin\psi}{24}[x_{v,n-1}^4 u<x_{v,n-1}-x_n> - x_{v,n-1}^4] + \frac{\gamma_w \sin\psi}{24}[x_{v,n}^4 u<x_{v,n}-x_n> - x_{v,n}^4]
\end{aligned} \tag{H-12}$$

In these equations

$$\begin{aligned}[\bar{D}_n] = [-\frac{w_n}{2}l_n^2 - \frac{r_n}{2}x_{r,n}^2 + \frac{r_{n-1}}{2}x_{r,n-1}^2 + \frac{\gamma_w \sin\psi}{6}x_{v,n-1}^3 u<x_{v,n-1}-x_n> - \\ - \frac{\gamma_w \sin\psi}{6}x_{v,n}^3 u<x_{v,n}-x_n> - \frac{q_n}{2}l_n^2 - F_n l_n]\end{aligned} \tag{H-13}$$

$$\begin{aligned}[\bar{E}_n] = [\frac{w_n}{2}l_n + \frac{r_n}{2}x_{r,n} - \frac{r_{n-1}}{2}x_{r,n-1} - \frac{\gamma_w \sin\psi}{4}x_{v,n-1}^2 u<x_{v,n-1}-x_n> + \\ + \frac{\gamma_w \sin\psi}{4}x_{v,n}^2 u<x_{v,n}-x_n> + \frac{q_n}{2}l_n + \frac{F_n}{2}]\end{aligned} \tag{H-14}$$

$$\begin{aligned}[\bar{F}_n] = -\frac{w_n}{6} - \frac{r_n}{6} + \frac{r_{n-1}}{6} + \frac{\gamma_w \sin\psi}{6}x_{v,n-1} u<x_{v,n-1}-x_n> - \\ - \frac{\gamma_w \sin\psi}{6}x_{v,n} u<x_{v,n}-x_n> - \frac{q_n}{6}]\end{aligned} \tag{H-15}$$

$$[\bar{G}_n] = [-\frac{\gamma_w \sin\psi}{24}u<x_{v,n-1}-x_n> - \frac{\gamma_w \sin\psi}{24}u<x_{v,n}-x_n>] \tag{H-16}$$

X_n was defined in chapter 3 by equation (3-7). For the flat base equation (3-7) is unchanged

$$x_n = x_1 + \sin\theta \sum_{j=1}^{n-1} d_j \tag{H-17}$$

Now the final step can be easily done, and for the flat base:

$$\frac{\partial f_n}{\partial \theta} = [\bar{D}_n]\frac{\partial x_n}{\partial \theta} + [\bar{E}_n]2x_n\frac{\partial x_n}{\partial \theta} + [\bar{F}_n]3x_n^2\frac{\partial x_n}{\partial \theta} + [\bar{G}_n]4x_n^3\frac{\partial x_n}{\partial \theta} - EI \tag{H-18}$$

In equation H-18

$$\frac{\partial x_n}{\partial \theta} = \cos\theta \sum_{j=1}^{n-1} d_j \tag{H-19}$$

Finally for the flat base from equation H-18

$$\frac{\partial f_n}{\partial \theta} = \cos\theta \sum_{j=1}^{n-1} d_j \left[[\bar{D}_n] + [\bar{E}_n]2x_n + [\bar{F}_n]3x_n^2 + [\bar{G}_n]4x_n^3 \right] - EI \tag{H-20}$$

From equation H-7 (dropping the singularity functions)

$$\frac{\partial f_n}{\partial r_n} = \frac{1}{6}\left[(x_{r,n} - x_n)^3 - x_{r,n}^3 \right] \tag{H-21}$$

and

$$\frac{\partial f_n}{\partial r_{n-1}} = -\frac{1}{6}\left[(x_{r,n-1}-x_n)^3 - x_{r,n-1}^3\right] \tag{H-22}$$

Now the matrix of partial derivatives from equation H-6 can be specified closer in terms of equations H-20, H-21, and H-22.

$$\begin{bmatrix}
\frac{\partial f_1}{\partial r_1} & 0 & 0 & 0 & \dots & 0 & 0 & \frac{\partial f_1}{\partial \theta} \\
\frac{\partial f_2}{\partial r_1} & \frac{\partial f_2}{\partial r_2} & 0 & 0 & \dots & 0 & 0 & \frac{\partial f_2}{\partial \theta} \\
0 & \frac{\partial f_3}{\partial r_2} & \frac{\partial f_3}{\partial r_3} & 0 & \dots & 0 & 0 & \frac{\partial f_3}{\partial \theta} \\
0 & 0 & \frac{\partial f_4}{\partial r_3} & \frac{\partial f_4}{\partial r_4} & \dots & 0 & 0 & \frac{\partial f_4}{\partial \theta} \\
\vdots & \vdots & \vdots & \vdots & & \vdots & \vdots & \vdots \\
0 & 0 & 0 & 0 & \dots & \frac{\partial f_{n-1}}{\partial r_{n-2}} & \frac{\partial f_{n-1}}{\partial r_{n-1}} & \frac{\partial f_{n-1}}{\partial \theta} \\
0 & 0 & 0 & 0 & \dots & 0 & \frac{\partial f_n}{\partial r_{n-1}} & \frac{\partial f_n}{\partial \theta}
\end{bmatrix} \tag{H-23}$$

Matrix H-23 is a sparse matrix, and so some special routine for its inversion can be used, as well as any general routine such as LU decomposition, Gauss elimination or Gauss-Jordan elimination. Solution of the system of equations H-6 can be then found in the form

$$[\partial x_n] = \left[\frac{\partial f_n}{\partial x_n}\right]^{-1} [-f_n] \tag{H-24}$$

Where all the expressions in brackets are matrices.

H.3. Bending equations for the Newton -Raphson method.

Stepped base-point reaction.

Function $f_{(x)}$ (equation H-4) was derived for the stepped base in Appendix B (equation B-32) as

$$
\begin{aligned}
f_n = \frac{w_n}{6}[(l_n - x_n)^3 - l_n^3] + \frac{F_n}{2}[(l_n - x_n)^2 - (l_n)^2] - \\
- \frac{R_{n-1}}{2}[(x_{r,n-1} - x_n)^2\, u{<}x_{r,n-1} - x_n{>} - x_{r,n-1}^2] + \\
+ \frac{R_n}{2}[(x_{r,n} - x_n)^2\, u{<}x_{r,n} - x_n{>} - x_{r,n}^2] - \\
- \frac{\gamma_w \sin\psi}{24}[(\hat{x}_{v,n-1} - x_n)^4\, u{<}\hat{x}_{v,n-1} - x_n{>} - \hat{x}_{v,n-1}^4] + \\
+ \frac{\gamma_w \sin\psi}{24}[(x_{v,n} - x_n)^4\, u{<}x_{v,n} - x_n{>} - x_{v,n}^4] + \\
+ \frac{Q_n}{2}[(x_{Q,n} - x_n)^2\, u{<}x_{Q,n} - x_n{>} - x_{Q,n}^2] - EI\theta(x)_n
\end{aligned}
\tag{H-25}
$$

For the first cantilever (n=1) equation H-25 yields

$$
\begin{aligned}
f_n = \frac{w_n}{6}[(l_n - x_n)^3 - l_n^3] + \frac{F_n}{2}[(l_n - x_n)^2 - (l_n)^2] + \\
+ \frac{R_n}{2}[(x_{r,n} - x_n)^2\, u{<}x_{r,n} - x_n{>} - x_{r,n}^2] - \\
- \frac{\gamma_w \sin\psi}{24}[(\hat{x}_{v,n-1} - x_n)^4\, u{<}\hat{x}_{v,n-1} - x_n{>} - \hat{x}_{v,n-1}^4] + \\
+ \frac{\gamma_w \sin\psi}{24}[(x_{v,n} - x_n)^4\, u{<}x_{v,n} - x_n{>} - x_{v,n}^4] + \\
+ \frac{Q_n}{2}[(x_{Q,n} - x_n)^2\, u{<}x_{Q,n} - x_n{>} - x_{Q,n}^2] - EI\theta(x)_n
\end{aligned}
\tag{H-26}
$$

and for the last cantilever i (n=1,2,3,......,i)

$$\begin{aligned} f_i = {} & \frac{w_n}{6}[(l_n - x_n)^3 - l_n^3] + \frac{F_n}{2}[(l_n - x_n)^2 - (l_n)^2] - \\ & - \frac{R_{n-1}}{2}[(x_{r,n-1} - x_n)^2\, u{<}x_{r,n-1} - x_n{>} - x_{r,n-1}^2] - \\ & - \frac{\gamma_w \sin\psi}{24}[(\hat{x}_{v,n-1} - x_n)^4\, u{<}\hat{x}_{v,n-1} - x_n{>} - \hat{x}_{v,n-1}^4] + \\ & + \frac{\gamma_w \sin\psi}{24}[(x_{v,n} - x_n)^4\, u{<}x_{v,n} - x_n{>} - x_{v,n}^4] + \\ & + \frac{Q_n}{2}[(x_{Q,n} - x_n)^2\, u{<}x_{Q,n} - x_n{>} - x_{Q,n}^2] - EI\theta(x)_n \end{aligned} \tag{H-27}$$

Then from equation H-25

$$\begin{aligned} \frac{\partial f_n}{\partial \theta_n} = {} & [\frac{w_n}{6} 3(l_n - x_n)^2 \frac{\partial x_n}{\partial \theta_n}(-1) - \\ & - \frac{R_{n-1}}{2} u{<}x_{r,n-1} - x_n{>} 2(x_{r,n-1} - x_n)\frac{\partial x_n}{\partial \theta_n}(-1) + \\ & + \frac{R_n}{2} u{<}x_{r,n} - x_n{>} 2(x_{r,n} - x_n)\frac{\partial x_n}{\partial \theta_n}(-1) - \\ & - \frac{\gamma_w}{24} u{<}x_{r,n-1} - x_n{>} 4(\hat{x}_{v,n-1} - x_n)^3\frac{\partial x_n}{\partial \theta_n}(-1) + \\ & + \frac{\gamma_w}{24} u{<}x_{r,n} - x_n{>} 4(\hat{x}_{v,n} - x_n)^3\frac{\partial x_n}{\partial \theta_n}(-1) + \\ & + \frac{Q_n}{2} u{<}x_{Q,n} - x_n{>} 2(x_{Q,n} - x_n)\frac{\partial x_n}{\partial \theta_n}(-1) + \\ & + \frac{F_n}{2} 2(l_n - x_n)\frac{\partial x_n}{\partial \theta_n}(-1)] - EI \end{aligned} \tag{H-28}$$

but

$$x_n = x_1 - (n-1)(mb) + \sin\theta \sum_{j=1}^{n-1} d_j \tag{H-29}$$

and

$$\frac{\partial x_n}{\partial \theta_n} = \cos\theta_n \sum_{j=1}^{j=n} d_j \tag{H-30}$$

then from equations H-28 and H-30

$$\begin{aligned} \frac{\partial f_n}{\partial \theta_n} = \cos\theta_n \sum_{j=1}^{j=n} d_j [\, & x_n \, (w_{nl_n} - R_{n-1} u<x_{r,n-1} - x_n> + R_n u<x_{r,n} - x_n> - \frac{\gamma_w \sin\Psi}{2} u<\hat{x}_{v,n-1} - x_n> \hat{x}_{v,}^2 \\ & + \frac{\gamma_w \sin\psi}{2} u<x_{v,n} - x_n> x_{v,n}^2 + Q_n u<x_{Q,n} - x_n> + F_n) + \\ & + x_n^2 \, (-\frac{w_n}{2} + \frac{\gamma_w \sin\psi}{2} u<\hat{x}_{v,n-1} - x_n> x_{v,n-1} - \frac{\gamma_w \sin\psi}{2} u<x_{v,n} - x_n> x_{v,n}) + \\ & + x_n^3 \, (-\frac{\gamma_w \sin\psi}{2} u<\hat{x}_{v,n-1} - x_n> + \frac{\gamma_w \sin\psi}{2} u<x_{v,n} - x_n>) + \\ & + (-\frac{w_n}{2} l_n^2 + R_{n-1} u<x_{r,n-1} - x_n> x_{r,n-1} - R_n u<x_{r,n} - x_n> x_{r,n} + \\ & + \frac{\gamma_w \sin\Psi}{2} u<\hat{x}_{v,n-1} - x_n> \hat{x}_{v,n-1}^3 - \frac{\gamma_w \sin\psi}{2} u<x_{v,n} - x> x_{v,n}^3 - \\ & - Q_n u<x_{Q,n} - x_n> x_{Q,n} - F_n l_n)] - EI \end{aligned} \tag{H-31}$$

Now in all round brackets there are only constants with respect to θ, and so equation H-31 can be rewritten as

$$\frac{\partial f_n}{\partial \theta_n} = x_n [\bar{H}_n] + x_n^2 [\bar{I}_n] + x_n^3 [\bar{J}_n] + [\bar{K}_n] \tag{H-32}$$

In equation H-32

$$\begin{aligned}[\bar{H}_n] = (&w_{nl_n} - R_{n-1} u{<}x_{r,n-1} - x_n{>} + R_n u{<}x_{r,n} - x_n{>} - \\ &- \frac{\gamma_w \sin\Psi}{2} u{<}\hat{x}_{v,n-1} - x_n{>} \hat{x}_{v,n-1}^2 + \frac{\gamma_w \sin\psi}{2} u{<}x_{v,n} - x_n{>} x_{v,n}^2 + \\ &+ Q_n u{<}x_{Q,n} - x_n{>} + F_n)\end{aligned} \tag{H-33}$$

$$[\bar{I}_n] = (-\frac{w_n}{2} + \frac{\gamma_w \sin\psi}{2} u{<}\hat{x}_{v,n-1} - x_n{>}\, x_{v,n-1} - \frac{\gamma_w \sin\psi}{2} u{<}x_{v,n} - x_n{>}\, x_{v,n}) \tag{H-34}$$

$$[\bar{J}_n] = (-\frac{\gamma_w \sin\psi}{2} u{<}\hat{x}_{v,n-1} - x_n{>} + \frac{\gamma_w \sin\psi}{2} u{<}x_{v,n} - x_n{>}) \tag{H-35}$$

$$
\begin{aligned}
[\bar{K}_n] = [(-\frac{w_n}{2} l_n^2 + R_{n-1} u{<}x_{r,n-1} - x_n{>} x_{r,n-1} - R_n u{<}x_{r,n} - x_n{>} x_{r,n} + \\
+ \frac{\gamma_w \sin\Psi}{2} u{<}\hat{x}_{v,n-1} - x_n{>} \hat{x}_{v,n-1}^3 - \frac{\gamma_w \sin\psi}{2} u{<}x_{v,n} - x{>} x_{v,n}^3 - \\
- Q_n u{<}x_{Q,n} - x_n{>} x_{Q,n} - F_n l_n) - EI]
\end{aligned}
\qquad \textbf{(H-36)}
$$

From equation H-25

$$
\frac{\partial f_n}{\partial R_n} = \frac{1}{2} [(x_{r,n} - x_n)^2 u{<}x_{r,n} - x_n{>} - x_{r,n}^2] \qquad \textbf{(H-37)}
$$

and

$$
\frac{\partial f_n}{\partial R_{n-1}} = -\frac{1}{2} [(x_{r,n-1} - x_n)^2 u{<}x_{r,n-1} - x_n{>} - x_{r,n-1}^2] \qquad \textbf{(H-38)}
$$

Now the new matrix of partial derivations (equation H-6) can be specified closer (see next page).

$$\begin{bmatrix}
\frac{\partial f_1}{\partial R_1} & \frac{\partial f_1}{\partial \theta_1} & 0 & 0 & 0 & 0 & \dots & 0 & 0 & 0 & 0 \\
\frac{\partial f_2}{\partial R_1} & \frac{\partial f_2}{\partial \theta_1} & \frac{\partial f_2}{\partial R_2} & 0 & 0 & 0 & \dots & 0 & 0 & 0 & 0 \\
\frac{\partial f_3}{\partial R_1} & 0 & \frac{\partial f_3}{\partial R_2} & \frac{\partial f_3}{\partial \theta_2} & 0 & 0 & \dots & 0 & 0 & 0 & 0 \\
0 & 0 & \frac{\partial f_4}{\partial R_2} & \frac{\partial f_4}{\partial \theta_2} & \frac{\partial f_4}{\partial R_3} & 0 & \dots & 0 & 0 & 0 & 0 \\
0 & 0 & \frac{\partial f_5}{\partial R_2} & 0 & \frac{\partial f_5}{\partial R_3} & \frac{\partial f_5}{\partial \theta_3} & \dots & 0 & 0 & 0 & 0 \\
\vdots & \vdots & \vdots & \vdots & \vdots & \vdots & & \vdots & \vdots & \vdots & \vdots \\
0 & 0 & 0 & 0 & 0 & 0 & \dots & \frac{\partial f_{n-2}}{\partial R_{\frac{n}{2}-1}} & \frac{\partial f_{n-2}}{\partial \theta_{\frac{n}{2}-1}} & \frac{\partial f_{n-2}}{\partial R_{\frac{n}{2}}} & 0 \\
0 & 0 & 0 & 0 & 0 & 0 & \dots & \frac{\partial f_{n-1}}{\partial R_{\frac{n}{2}-1}} & 0 & \frac{\partial f_{n-1}}{\partial R_{\frac{n}{2}}} & \frac{\partial f_{n-1}}{\partial \theta_{\frac{n}{2}}} \\
0 & 0 & 0 & 0 & 0 & 0 & \dots & 0 & 0 & \frac{\partial f_n}{\partial R_{\frac{n}{2}}} & \frac{\partial f_n}{\partial \theta_{\frac{n}{2}}}
\end{bmatrix} \tag{H-39}$$

The system of coefficients in the matrix H-39 is obviously more complicated than the one described in matrix H-23. The reason is that in the system H-39 for each cantilever are defined two equations; one for the point of contact with an overlying cantilever,and one for the point of contact with an underlying cantilever. Thus this matrix has twice as many members than the matrix H-23. However matrix H-39 is again a sparse matrix and so a special routine based on Gausse-Jordan elimination can be used to avoid handling n times n operations when solving the system of equations H-6 . The general solution of the system H-6 can be again found in the form H-24.

Appendix I

Fortran source codes.

I.1. Program Input

Program Input asks the user for input parameters, and creates data files containing geometrical and physical information to be used by the other routines, or to be altered manually by the user, and then used by the other routines.

Resulting data files:

Geom.dat - geometrical description of the slope in horizontal -vertical (X,Y) coordinate system

Fyzic.dat - physical parameters of the slope

Input.dat - length, depth and Young's Modulus of every cantilever in the slope, and the length of the water column between cantilevers.

Distan.dat - strength parameters, and their distance from the origin.

FF.dat - creates the preliminary version of FF.dat from zeros

Geom.dat - geometrical description of the slope in horizontal -vertical (X,Y) coordinate system

Fyzic.dat - physical parameters of the slope

Input.dat - length, depth and Young's Modulus of every cantilever in the slope, and the length of the water column between cantilevers.

Distan.dat - strength parameters, and their distance from the beginning.

```
      PROGRAM INPUT
C     asks the user's data, and stores them in the data file
C     to be used later by program Flex
      INTEGER NH,I,NP
      PARAMETER (NP=2000)
      REAL DETA,DZETA,DPSI,ETA,ZETA,PSI,DSBETA,SBETA
      REAL HEIGHT(10),HC,BENCH,RATIO,BHAT
      REAL HWATER,VX(NP),KOEF,GAMA,DGAMA
      LOGICAL SWITCH
      SWITCH=.FALSE.
      PRINT*, 'input h1 [m]-press enter '
      READ*,HEIGHT(1)
      PRINT*, 'input h2 [m]-press enter '
      PRINT*,'if there is no h2 input 0'
      READ*,HEIGHT(2)
      IF (HEIGHT(2).LT.1.)GO TO 1
      PRINT*, 'input h3 [m]-press enter '
      PRINT*,'if there is no h3 input 0'
      READ*,HEIGHT(3)
      IF (HEIGHT(3).LT.1.)GO TO 1
      PRINT*, 'input h4 [m]-press enter '
      PRINT*,'if there is no h4 input 0'
      READ*,HEIGHT(4)
      IF (HEIGHT(4).LT.1.)GO TO 1
      PRINT*, 'input h5 [m]-press enter '
      PRINT*,'if there is no h5 input 0'
      READ*,HEIGHT(5)
      IF (HEIGHT(5).LT.1.)GO TO 1
      PRINT*, 'input h6 [m]-press enter '
      PRINT*,'if there is no h6 input 0'
      READ*,HEIGHT(6)
      IF (HEIGHT(6).LT.1.)GO TO 1
      PRINT*, 'input h7 [m]-press enter '
      PRINT*,'if there is no h7 input 0'
      READ*,HEIGHT(7)
      IF (HEIGHT(7).LT.1.)GO TO 1
      PRINT*, 'input h8 [m]-press enter '
      PRINT*,'if there is no h8 input 0'
      READ*,HEIGHT(8)
      IF (HEIGHT(8).LT.1.)GO TO 1
      PRINT*, 'input h9 [m]-press enter '
      PRINT*,'if there is no h9 input 0'
      READ*,HEIGHT(9)
      IF (HEIGHT(9).LT.1.)GO TO 1
      PRINT*, 'input h10 [m]-press enter '
      PRINT*,'if there is no h10 input 0'
      READ*,HEIGHT(10)
      IF (HEIGHT(8).LT.1.)GO TO 1
1       PRINT*, 'input h water [m]-press enter '
      PRINT*,'if there is no water input 0'
      READ*,HWATER
      IF (HWATER.LT.1.)THEN
      SWITCH=.TRUE.
      ENDIF
      I=1
2       IF(HEIGHT(I).NE.0.)THEN
          I=I+1
          GO TO 2
      ELSE
          NH=I-1
      ENDIF
      PRINT*,'HC=?'
      READ*,HC
      PRINT*,'enter the angle of the highwall ZETA and bedding pl. PSI'
      READ*,DZETA,DPSI
      PRINT*,'enter the slope angle ETA, and the slope behind the top'
      PRINT*,'if the slope behind the top goes downhill enter -(angle)'
      PRINT*,'the slope behind the top must be less than',90-DPSI
      READ*,DETA,DSBETA
      RADIAN=3.141592654/180
      ZETA=DZETA*RADIAN
      PSI=DPSI*RADIAN
      ETA=DETA*RADIAN
      SBETA=DSBETA*RADIAN
      PRINT*,'WIDTH OF THE BENCH=?'
      READ*,BENCH
 3     PRINT*,
   &  'enter the density of the rock [kN/M^3] and the width BHAT'
      READ*,DGAMA,BHAT
         GAMA=DGAMA*1000.
      PRINT*,'enter the height/width cantilever ratio'
      READ*,RATIO
      PRINT*,'enter the blasting koef.(>1)'
      READ*,KOEF
C    This is the end of the input dialog
      CALL GEOMETRY(NH,HEIGHT,HC,BENCH,ZETA,PSI,ETA,SBETA,
   &    SWITCH,HWATER,GAMA,VX,KOEF,BHAT,
   &    RATIO)
      END
CCCCCCCCCCCCCCCCCCCCCCCCCCCCCCCCCCCCCCCCCCCCCCCC


      SUBROUTINE GEOMETRY(NH,HEIGHT,HC,BENCH,ZETA,PSI,ETA,
   &       SBETA,SWITCH,HWATER,GAMA,VX,KOEF,BHAT,
   &       RATIO)
      INTEGER NP
      PARAMETER (NP=2000)
      REAL HEIGHT(8),HC,BENCH,ZETA,PSI,ETA,CONV,GAMA,SBETA,TBETA
      REAL HWAT,HWATER,VX(NP),RATIO,KOEF,BHAT
      REAL BASE(20),XG(20),YG(20),XC(20),YC(20)
      REAL XV(20),YV(20),XVC,YVC,XVT,YVT,XVE,YVE
      REAL XCC,YCC,XCT,YCT,XCE,YCE
      REAL XGNEW(20),YGNEW(20),XCNEW(20),YCNEW(20)
      REAL XCCNEW,YCCNEW,XCTNEW,YCTNEW,XCENEW,YCENEW,YVENEW
      REAL XVNEW(20),YVNEW(20),XVCNEW,YVCNEW,XVTNEW,YVTNEW,XVENEW
      LOGICAL SWITCH
      INTEGER NH
      OPEN (UNIT=10,FILE='GEOM.DAT')
      BETA=3.141592654/2-PSI
      TBETA=BETA-SBETA
      PRINT*,'BETA=',BETA
      DO 1 I=1,NH
         BASE(I)=HEIGHT(I)/TAN(ZETA)
```

```
1     CONTINUE
    XG(1)=0.
    YG(1)=0.
    IF (.NOT.SWITCH)THEN
    XV(1)=0.
    YV(1)=0.
    ENDIF
    XC(1)=-BENCH
    YC(1)=0.
    DO 2 I=2,NH
        XG(I)=XG(I-1)+BASE(I-1)+BENCH
        YG(I)=YG(I-1)+HEIGHT(I-1)
            IF (.NOT.SWITCH)THEN
              XV(I)=XG(I)
              YV(I)=YG(I)
            ENDIF
        XC(I)=XG(I-1)+BASE(I-1)
        YC(I)=YG(I)
2     CONTINUE
    XCC=XG(NH)+BASE(NH)
    YCC=YG(NH)+HEIGHT(NH)
    XCT=XCC+HC/TAN(ETA)
    YCT=YCC+HC
    IF (.NOT.SWITCH)THEN
      HWAT=YCT-HWATER
      PRINT*,'XCC=',XCC
      PRINT*,'YCC=',YCC
      PRINT*,'enter XVC and YVC'
      PRINT*,'YVC must be within',YG(NH),'and',HWAT,'limits.'
      READ*,XVC,YVC
    ENDIF
    IF (.NOT.SWITCH)THEN
      YVT=HWAT
      XVT=(YVT-YVC)/TAN(ETA)+XVC
    ENDIF
C rotation of axes
    DO 3 I=1,NH
        XGNEW(I)=XG(I)*COS(BETA)+YG(I)*SIN(BETA)
        YGNEW(I)=-XG(I)*SIN(BETA)+YG(I)*COS(BETA)
C
        XCNEW(I)=XC(I)*COS(BETA)+YC(I)*SIN(BETA)
        YCNEW(I)=-XC(I)*SIN(BETA)+YC(I)*COS(BETA)
 3    CONTINUE
C
        XCCNEW=XCC*COS(BETA)+YCC*SIN(BETA)
        YCCNEW=-XCC*SIN(BETA)+YCC*COS(BETA)
C
        XCTNEW=XCT*COS(BETA)+YCT*SIN(BETA)
        YCTNEW=-XCT*SIN(BETA)+YCT*COS(BETA)
C
```

```
           XCENEW=XCTNEW+YCTNEW/TAN(BETA-SBETA)
           YCENEW=0.0
           XCE=XCENEW*COS(BETA)-YCENEW*SIN(BETA)
           YCE=XCENEW*SIN(BETA)+YCENEW*COS(BETA)
      IF (.NOT.SWITCH)THEN
         IF (HWAT.LT.YCE)THEN
            YVE=HWAT
            XVE=YVT/TAN(BETA)
         ELSE
            YVE=YCE
            XVE=XCE
         ENDIF
      ENDIF
      PRINT*,'YCE=',YCE
      PRINT*,'YCT=',YCT
      PRINT*,'XCE=',XCE
      IF (.NOT.SWITCH)THEN
         DO 4 I=1,NH
             XVNEW(I)=XV(I)*COS(BETA)+YV(I)*SIN(BETA)
             YVNEW(I)=-XV(I)*SIN(BETA)+YV(I)*COS(BETA)
4        CONTINUE
C
             XVCNEW=XVC*COS(BETA)+YVC*SIN(BETA)
             YVCNEW=-XVC*SIN(BETA)+YVC*COS(BETA)
C
             XVTNEW=XVT*COS(BETA)+YVT*SIN(BETA)
             YVTNEW=-XVT*SIN(BETA)+YVT*COS(BETA)
C
             XVENEW=XVE*COS(BETA)+YVE*SIN(BETA)
             YVENEW=-XVE*SIN(BETA)+YVE*COS(BETA)
      ENDIF
      CONV=180/3.1415927
      WRITE(10,5)
5     FORMAT (T6,'ZETA',T22,'ETA',T40,'PSI',T55,'BETA')
      WRITE(10,6)ZETA*CONV,ETA*CONV,PSI*CONV,BETA*CONV
6     FORMAT (T3,F8.5,T21,F8.5,T38,F8.5,T53,F8.5)
      WRITE(10,7)
7     FORMAT(T20,'No',T40,'HEIGHT')
      DO 20 I=1,NH
           WRITE(10,8)I,HEIGHT(I)
8          FORMAT(T19,I3,T39,F4.1)
20     CONTINUE
      WRITE(10,10)HC
10     FORMAT(T20,'HC',T39,F3.1)
      WRITE(10,11)
11     FORMAT(T25,'X COORDINATE',T45,'Y COORDINATE')
      DO 21 I=1,NH
           WRITE(10,12)I,XG(I),YG(I)
12          FORMAT(T5,'G',I2,T28,F8.4,T47,F8.4)
           WRITE(10,13)I,XC(I),YC(I)
13          FORMAT(T5,'C',I2,T28,F8.4,T47,F8.4)
```

```
21      CONTINUE
        WRITE(10,14)XCC,YCC
14      FORMAT(T5,'CC',T28,F8.4,T47,F8.4)
        WRITE(10,15)XCT,YCT
15      FORMAT(T5,'CT',T28,F8.4,T47,F8.4)
        WRITE(10,16)XCE,YCE
16      FORMAT(T5,'CE',T28,F8.4,T47,F8.4)
        IF (.NOT.SWITCH)THEN
             WRITE(10,17)
17           FORMAT(T25,'X COORDINATE',T45,'Y COORDINATE')
             DO 22 I=1,NH
                  WRITE(10,18)I,XV(I),YV(I)
18                FORMAT(T5,'V',I2,T28,F8.4,T47,F8.4)
22           CONTINUE
             WRITE(10,19)XVC,YVC
19           FORMAT(T5,'VC',T28,F8.4,T47,F8.4)
             WRITE(10,24)XVT,YVT
24           FORMAT(T5,'VT',T28,F8.4,T47,F8.4)
             WRITE(10,23)XVE,YVE
23           FORMAT(T5,'VE',T28,F8.4,T47,F8.4)
        ENDIF
        CALL CANTILEVER (XGNEW,YGNEW,XCNEW,YCNEW,
      & PSI,ZETA,ETA,BETA,NH,XCCNEW,YCCNEW,XCTNEW,XCENEW,
      & CONV,GAMA,SWITCH,VX,SBETA,KOEF,BHAT,XVNEW,YVNEW,
      & XVCNEW,YVCNEW,XVTNEW,YVTNEW,XVENEW,RATIO)
        END
CCCCCCCCCCCCCCCCCCCCCCCCCCCCCCCCCCCCCCCCCCCCCCCCCCCCCC


        SUBROUTINE CANTILEVER (XGNEW,YGNEW,XCNEW,YCNEW,
      & PSI,ZETA,ETA,BETA,NH,XCCNEW,YCCNEW,XCTNEW,XCENEW,
      & CONV,GAMA,SWITCH,VX,SBETA,KOEF,BHAT,XVNEW,YVNEW,
      & XVCNEW,YVCNEW,XVTNEW,YVTNEW,XVENEW,RATIO)
        INTEGER NH,I,K,SWIT
        INTEGER NP
        PARAMETER (NP=2000)
        REAL XGNEW(20),YGNEW(20),XCNEW(20),YCNEW(20),EMODUL(NP)
        REAL XCCNEW,YCCNEW,XCTNEW,XCENEW,DEPTH(NP)
        REAL XCANT,XAPEX(40),YAPEX(40),LENGTH(NP),BHAT,CONV,GAMA
        REAL XVNEW(20),YVNEW(20),XVCNEW,YVCNEW,XVTNEW,YVTNEW,XVENEW
        REAL VX(NP),TANG,SBETA,RATIO,XDEPTH(NP)
        REAL REACH,DIST(10),BMODUL(10),BDEPTH(10)
        REAL COHESION(10),FI(10),TENSILE(10),KOEF
        INTEGER DIS
        LOGICAL SWITCH

C       determines the number and the lengths of cantilevers
        OPEN(UNIT=19,FILE='FYZIC.DAT')
        OPEN(UNIT=20,FILE='INPUT.DAT')
        OPEN(UNIT=21,FILE='DISTAN.DAT')
        OPEN(UNIT=22,FILE='FF.DAT')
```

```
************************************************************************
      PRINT*,'enter the DISTANCE 1, DEPTH 1, AND E 1'
      PRINT*,'if there is only one distance-enter 0 for the DISTANCE'
      READ*, DIST(1),BDEPTH(1),BMODUL(1)
      PRINT*,'enter FI,COHES. and TENSILE STR. for the DISTANCE 1'
      READ*,FI(1),COHESION(1),TENSILE(1)
      IF(DIST(1).EQ.0)THEN
          DIS=1
          DIST(1)=XCENEW+50
              DO 148 I=1,NP
                  DEPTH(I)=BDEPTH(1)
                  EMODUL(I)=BMODUL(1)*1000000000.0
148           CONTINUE
          GO TO 149
      ENDIF
      PRINT*,'enter the DISTANCE 2, DEPTH 2, AND E 2'
      PRINT*,'if DISTANCE 2 = END, enter 0 for the DISTANCE '
      READ*,DIST(2),BDEPTH(2),BMODUL(2)
      PRINT*,'enter FI,COHES. and TENSILE STR. for the DISTANCE 2'
      READ*,FI(2),COHESION(2),TENSILE(2)
      IF(DIST(2).EQ.0)THEN
          DIST(2)=XCENEW+50
          DIS=2
          GO TO 146
      ENDIF
      PRINT*,'enter the DISTANCE 3, DEPTH 3, AND E 3'
      PRINT*,'if DISTANCE 3 = END, enter 0 for the DISTANCE '
      READ*,DIST(3),BDEPTH(3),BMODUL(3)
      PRINT*,'enter FI,COHES. and TENSILE STR. for the DISTANCE 3'
      READ*,FI(3),COHESION(3),TENSILE(3)
      IF(DIST(3).EQ.0)THEN
          DIST(3)=XCENEW+50
          DIS=3
          GO TO 146
      ENDIF
      PRINT*,'enter the DISTANCE 4, DEPTH 4, AND E 4'
      PRINT*,'if DISTANCE 4 = END, enter 0 for the DISTANCE '
      READ*,DIST(4),BDEPTH(4),BMODUL(4)
      PRINT*,'enter FI,COHES. and TENSILE STR. for the DISTANCE 4'
      READ*,FI(4),COHESION(4),TENSILE(4)
      IF(DIST(4).EQ.0)THEN
          DIST(4)=XCENEW+50
          DIS=4
          GO TO 146
      ENDIF
      PRINT*,'enter the DISTANCE 5, DEPTH 5, AND E 5'
      PRINT*,'if DISTANCE 5 = END, enter 0 for the DISTANCE '
      READ*,DIST(5),BDEPTH(5),BMODUL(5)
      PRINT*,'enter FI,COHES. and TENSILE STR. for the DISTANCE 5'
      READ*,FI(5),COHESION(5),TENSILE(5)
      IF(DIST(5).EQ.0)THEN
```

```
              DIST(5)=XCENEW+50
              DIS=5
              GO TO 146
         ENDIF
         PRINT*,'enter the DISTANCE 6, DEPTH 6, AND E 6'
         PRINT*,'if DISTANCE 6 = END, enter 0 for the DISTANCE '
         READ*,DIST(6),BDEPTH(6),BMODUL(6)
         PRINT*,'enter FI,COHES. and TENSILE STR. for the DISTANCE 6'
         READ*,FI(6),COHESION(6),TENSILE(6)
         IF(DIST(6).EQ.0)THEN
              DIST(6)=XCENEW+50
              DIS=6
              GO TO 146
         ENDIF
         PRINT*,'enter the DISTANCE 7, DEPTH 7, AND E 7'
         PRINT*,'if DISTANCE 7 = END, enter 0 for the DISTANCE '
         READ*,DIST(7),BDEPTH(7),BMODUL(7)
         PRINT*,'enter FI,COHES. and TENSILE STR. for the DISTANCE 7'
         READ*,FI(7),COHESION(7),TENSILE(7)
         IF(DIST(7).EQ.0)THEN
              DIST(7)=XCENEW+50
              DIS=7
              GO TO 146
         ENDIF
         PRINT*,'enter the DISTANCE 8, DEPTH 8, AND E 8'
         PRINT*,'if DISTANCE 8 = END, enter 0 for the DISTANCE '
         READ*,DIST(8),BDEPTH(8),BMODUL(8)
         PRINT*,'enter FI,COHES. and TENSILE STR. for the DISTANCE 8'
         READ*,FI(8),COHESION(8),TENSILE(8)
         IF(DIST(8).EQ.0)THEN
              DIST(8)=XCENEW+50
              DIS=8
              GO TO 146
         ENDIF
         PRINT*,'enter the DISTANCE 9, DEPTH 9, AND E 9'
         PRINT*,'if DISTANCE 9 = END, enter 0 for the DISTANCE '
         READ*,DIST(9),BDEPTH(9),BMODUL(9)
         PRINT*,'enter FI,COHES. and TENSILE STR. for the DISTANCE 9'
         READ*,FI(9),COHESION(9),TENSILE(9)
         IF(DIST(9).EQ.0)THEN
              DIST(9)=XCENEW+50
              DIS=9
              GO TO 146
         ENDIF
         PRINT*,'enter  DEPTH 10, AND E 10'
         READ*,BDEPTH(10),BMODUL(10)
         PRINT*,'enter FI,COHES. and TENSILE STR. for the DISTANCE 10'
         READ*,FI(10),COHESION(10),TENSILE(10)
              DIST(10)=XCENEW+50
              DIS=10
146       REACH=0.0
```

```
      REACH=0.0
      I=1
151    IF(REACH.LT.DIST(1))THEN
           DEPTH(I)=BDEPTH(1)
               print*,'depth',i,'=',depth(i)
                 IF(I.GT.NP)THEN
                 PRINT*,'ALLOWABLE NUMBER OF BLOCKS EXCEEDED'
                 STOP
                 ENDIF
           EMODUL(I)=BMODUL(1)*1000000000.0
           I=I+1
           REACH=REACH+BDEPTH(1)
           GO TO 151
      ENDIF
      IF(DIS.GE.2)THEN
152          IF(REACH.GE.DIST(1).AND.REACH.LT.DIST(2))THEN
                 DEPTH(I)=BDEPTH(2)
                 IF(I.GT.NP)THEN
                 PRINT*,'ALLOWABLE NUMBER OF BLOCKS EXCEEDED'
                 STOP
                 ENDIF
                 EMODUL(I)=BMODUL(2)*1000000000.0
                 I=I+1
                 REACH=REACH+BDEPTH(2)
                 GO TO 152
           ENDIF
      ENDIF
      IF(DIS.GE.3)THEN
153          IF(REACH.GE.DIST(2).AND.REACH.LT.DIST(3))THEN
                DEPTH(I)=BDEPTH(3)
                 IF(I.GT.NP)THEN
                 PRINT*,'ALLOWABLE NUMBER OF BLOCKS EXCEEDED'
                 STOP
                 ENDIF
                 EMODUL(I)=BMODUL(3)*1000000000.0
                 I=I+1
                 REACH=REACH+BDEPTH(3)
                 GO TO 153
           ENDIF
      ENDIF
      IF(DIS.GE.4)THEN
154          IF(REACH.GE.DIST(3).AND.REACH.LT.DIST(4))THEN
                 DEPTH(I)=BDEPTH(4)
                  IF(I.GT.NP)THEN
                 PRINT*,'ALLOWABLE NUMBER OF BLOCKS EXCEEDED'
                 STOP
                 ENDIF
                EMODUL(I)=BMODUL(4)*1000000000.0
                 I=I+1
                 REACH=REACH+BDEPTH(4)
                 GO TO 154
```

```
              ENDIF
         ENDIF
         IF(DIS.GE.5)THEN
155            IF(REACH.GE.DIST(4).AND.REACH.LT.DIST(5))THEN
                   DEPTH(I)=BDEPTH(5)
                   IF(I.GT.NP)THEN
                   PRINT*,'ALLOWABLE NUMBER OF BLOCKS EXCEEDED'
                   STOP
                   ENDIF
                   EMODUL(I)=BMODUL(5)*1000000000.0
                   I=I+1
                   REACH=REACH+BDEPTH(5)
                   GO TO 155
              ENDIF
         ENDIF
         IF(DIS.GE.6)THEN
156            IF(REACH.GE.DIST(5).AND.REACH.LT.DIST(6))THEN
                   DEPTH(I)=BDEPTH(6)
                   EMODUL(I)=BMODUL(6)*1000000000.0
                   IF(I.GT.NP)THEN
                   PRINT*,'ALLOWABLE NUMBER OF BLOCKS EXCEEDED'
                   STOP
                   ENDIF
                   I=I+1
                   REACH=REACH+BDEPTH(6)
                   GO TO 156
              ENDIF
         ENDIF
         IF(DIS.GE.7)THEN
157            IF(REACH.GE.DIST(6).AND.REACH.LT.DIST(7))THEN
                   DEPTH(I)=BDEPTH(7)
                   EMODUL(I)=BMODUL(7)*1000000000.0
                   IF(I.GT.NP)THEN
                   PRINT*,'ALLOWABLE NUMBER OF BLOCKS EXCEEDED'
                   STOP
                   ENDIF
                   I=I+1
                   REACH=REACH+BDEPTH(7)
                   GO TO 157
              ENDIF
         ENDIF
         IF(DIS.GE.8)THEN
158            IF(REACH.GE.DIST(7).AND.REACH.LT.DIST(8))THEN
                   DEPTH(I)=BDEPTH(8)
                   EMODUL(I)=BMODUL(8)*1000000000.0
                   IF(I.GT.NP)THEN
                   PRINT*,'ALLOWABLE NUMBER OF BLOCKS EXCEEDED'
                   STOP
                   ENDIF
                   I=I+1
                   REACH=REACH+BDEPTH(8)
```

```
                  GO TO 158
            ENDIF
      ENDIF
      IF(DIS.GE.9)THEN
159          IF(REACH.GE.DIST(8).AND.REACH.LT.DIST(9))THEN
                  DEPTH(I)=BDEPTH(9)
                  EMODUL(I)=BMODUL(9)*1000000000.0
                  IF(I.GT.NP)THEN
                  PRINT*,'ALLOWABLE NUMBER OF BLOCKS EXCEEDED'
                  STOP
                  ENDIF
                  I=I+1
                  REACH=REACH+BDEPTH(9)
                  GO TO 159
            ENDIF
      ENDIF
      IF(DIS.EQ.10)THEN
161         IF(REACH.LE.DIST(10))THEN
                  DEPTH(I)=BDEPTH(10)
                  IF(I.GT.NP)THEN
                  PRINT*,'ALLOWABLE NUMBER OF BLOCKS EXCEEDED'
                  STOP
                  ENDIF
                  EMODUL(I)=BMODUL(10)*1000000000.0
                  I=I+1
                  REACH=REACH+BDEPTH(10)
                  GO TO 161
            ENDIF
      ENDIF
149    SWIT=1
      K=2
      XAPEX(1)=0
      YAPEX(1)=0
      DO 1 I=2,2*NH-1
            IF(SWIT.EQ.1)THEN
                  XAPEX(I)=XCNEW(K)
                  YAPEX(I)=YCNEW(K)
            ELSE
                  XAPEX(I)=XGNEW(K)
                  YAPEX(I)=YGNEW(K)
                  K=K+1
            ENDIF
            SWIT=SWIT*(-1)
 1     CONTINUE
      I=1
      K=1
      XCANT=DEPTH(1)/2.
10     IF (XCANT.LT.XAPEX(I+1))THEN
                  print*,'test11'
      PRINT*,'NP=',NP,'K=',K,'XCANT=',XCANT
            LENGTH(K)=YAPEX(I)+TAN(ZETA-BETA)*(XCANT-XAPEX(I))
            K=K+1
                  IF(K.GT.NP)THEN
                  print*,'test1'
                  PRINT*,'ALLOWABLE NUMBER OF BLOCKS EXCEEDED'
                  STOP
                  ENDIF
            XCANT=XCANT+(DEPTH(K-1)+DEPTH(K))/2
            GO TO 10
      ENDIF
      I=I+1
20     IF (XCANT.LT.XAPEX(I+1))THEN
                  print*,'test22'
      PRINT*,'NP=',NP,'K=',K,'XCANT=',XCANT
            LENGTH(K)=YAPEX(I)-TAN(BETA)*(XCANT-XAPEX(I))
            K=K+1
                  IF(K.GT.NP)THEN
                  print*,'test2'
                  PRINT*,'ALLOWABLE NUMBER OF BLOCKS EXCEEDED'
                  STOP
                  ENDIF
            XCANT=XCANT+(DEPTH(K-1)+DEPTH(K))/2
            GO TO 20
      ENDIF
      I=I+1
      IF (I.LT.2*NH-1)GO TO 10
C
30     IF (XCANT.LT.XCCNEW)THEN
                  print*,'test33'
      PRINT*,'NP=',NP,'K=',K,'XCANT=',XCANT
            LENGTH(K)=YAPEX(I)+TAN(ZETA-BETA)*(XCANT-XAPEX(I))
            K=K+1
                  IF(K.GT.NP)THEN
                  print*,'test3'
                  PRINT*,'ALLOWABLE NUMBER OF BLOCKS EXCEEDED'
                  STOP
                  ENDIF
            XCANT=XCANT+(DEPTH(K-1)+DEPTH(K))/2
            GO TO 30
      ENDIF
40     IF (XCANT.LT.XCTNEW)THEN
                  print*,'test44'
      PRINT*,'NP=',NP,'K=',K,'XCANT=',XCANT
            LENGTH(K)=YCCNEW+TAN(ETA-BETA)*(XCANT-XCCNEW)
            K=K+1
                  IF(K.GT.NP)THEN
                  print*,'test4'
                  PRINT*,'ALLOWABLE NUMBER OF BLOCKS EXCEEDED'
                  STOP
                  ENDIF
            XCANT=XCANT+(DEPTH(K-1)+DEPTH(K))/2
            GO TO 40
      ENDIF
50     IF (XCANT.LT.XCENEW)THEN
                 print*,'test55'
      PRINT*,'NP=',NP,'K=',K ,'XCANT=',XCANT
            LENGTH(K)=TAN(BETA-SBETA)*(XCENEW-XCANT)
            K=K+1
                 IF(K.GT.NP)THEN
                 print*,'test5'
                 PRINT*,'ALLOWABLE NUMBER OF BLOCKS EXCEEDED'
                 STOP
                 ENDIF
            XCANT=XCANT+(DEPTH(K-1)+DEPTH(K))/2
            GO TO 50
      ENDIF
***********************************************************************
C      calculates the heights XV of the water columns between cantilevers
C
      IF (.NOT.SWITCH)THEN
      XDEPTH(1)=DEPTH(1)
      IF (NH.GE.2)THEN
      J=1
        DO 60 I=2,NH
            TANG=(YVNEW(I)-YVNEW(I-1))/(XVNEW(I)-XVNEW(I-1))
 61          IF (XDEPTH(J).LT.XVNEW(I))THEN
               VX(J)=TANG*(XDEPTH(J)-XVNEW(I-1))+YVNEW(I-1)
               J=J+1
               XDEPTH(J)=XDEPTH(J-1)+DEPTH(J)
               GO TO 61
            ELSE
            ENDIF
 60       CONTINUE
      ENDIF
C
            TANG=(YVCNEW-YVNEW(NH))/(XVCNEW-XVNEW(NH))
62     IF (XDEPTH(J).LT.XVCNEW)THEN
            VX(J)=TANG*(XDEPTH(J)-XVNEW(NH))+YVNEW(NH)
            J=J+1
            XDEPTH(J)=XDEPTH(J-1)+DEPTH(J)
            GO TO 62
      ELSE
      ENDIF
C
            TANG=(YVTNEW-YVCNEW)/(XVTNEW-XVCNEW)
63     IF (XDEPTH(J).LT.XVTNEW)THEN
            VX(J)=TANG*(XDEPTH(J)-XVCNEW)+YVCNEW
            J=J+1
            XDEPTH(J)=XDEPTH(J-1)+DEPTH(J)
            GO TO 63
      ELSE
      ENDIF
C
```

```
64      IF (XDEPTH(J).LT.XVENEW)THEN
                VX(J)=TAN(BETA-SBETA)*(XVENEW-XDEPTH(J))
                J=J+1
                XDEPTH(J)=XDEPTH(J-1)+DEPTH(J)
                GO TO 64
        ELSE
        J=J-1
        ENDIF
 65     IF (J.LT.K)THEN
                J=J+1
                VX(J)=0.00
                GO TO 65
        ENDIF
        ELSE
                DO 66 I=1,K
                        VX(I)=0.00
 66              CONTINUE
        ENDIF
        DIST(DIS)=XCENEW
        WRITE (21,110)
110     FORMAT (T10,'NO. OF DIST.')
        WRITE (21,111)DIS
111     FORMAT(T15,I2)
        WRITE (21,2)
2       FORMAT(T15,'DIST',T30,'COH',T45,'FI',T60,'TENS.STR.')
        DO 222 I=1,DIS
              WRITE (21,3)DIST(I),COHESION(I),FI(I),TENSILE(I)
3             FORMAT(T14,F6.2,T29,F6.2,T45,F4.1,T62,F6.2)
222     CONTINUE
        WRITE(19,43)
43      FORMAT(T16,'BHAT',T28,'RATIO')
        WRITE(19,44)BHAT,RATIO
44      FORMAT(T15,F5.1,T30,F3.1)
        WRITE (19,4)
4       FORMAT(T15,'GAMA',T40,'PSI',T65,'KOEF')
        WRITE (19,5)GAMA,PSI*CONV,KOEF
5       FORMAT(T12,F8.1,T38,F9.6,T64,F6.2)
        WRITE(20,9)
9        FORMAT(T10,'N')
        WRITE(20,11)K
11      FORMAT(T8,I4)
        WRITE(20,6)
6       FORMAT(T3,'No',T15,'LENGTH',T30,'DEPTH',T50,'EMODUL',T70,'VX')
        DO 71 I=1,K
                WRITE(20,7)I,LENGTH(I),DEPTH(I),EMODUL(I),VX(I)
7                FORMAT(T2,I3,T15,F6.2,T30,F6.2,T48,E10.3,T69,F6.2)
                WRITE(22,72)I
72              FORMAT(T4,I4,T45,'0.00')
71       CONTINUE
         END
```

I.2. Program Fredy

Program Fredy reads the output files created by Flex during previous runs, and incorporates the results from the previous runs into the data files created by Input.

Affected data files:

Input.dat - the original length of cantilevers as calculated by Input is reduced by the length which was broken of during the previous runs of Flex..

FF.dat - weights of the broken cantilevers are assigned to the proper positions in the slope replacing the zeroes written by Input.

Brake.dat - the results written by Flex into the Result.dat are incorporated into the list of the broken cantilevers including their position in the slope

```
      PROGRAM FREDY
      INTEGER NP
      PARAMETER (NP=2000)
      INTEGER I,J,K,L,M,N,NUM,MERGE
      INTEGER FAIL(NP),BRAK(NP,10),BREAK(NP,10)
      REAL LENG(NP),FLEN(NP),LENGTH(NP),F(NP),DEPTH(NP),EMOD(NP)
      REAL DPSI,PSI,DZETA,ZETA,GAMA,HA,PI,WAT(NP),BHAT
      REAL HEIGHT(10),HEIT(10),BENCH,AR(10),BEN,RATIO
      CHARACTER*5 FAL
      OPEN(UNIT=90,FILE='RESULT.DAT',STATUS='OLD')
      OPEN(UNIT=91,FILE='INPUT.DAT',STATUS='OLD')
      OPEN(UNIT=93,FILE='FYZIC.DAT',STATUS='OLD')
      OPEN(UNIT=94,FILE='FF.DAT')
      OPEN(UNIT=95,FILE='GEOM.DAT',STATUS='OLD')
      PRINT*, 'Enter the number of the border cant. MERGE'
      READ*, MERGE
      PRINT*, 'Enter the number of benches NUM.'
      PRINT*,'NUM can not be less than 2'
      READ*, NUM
      PI=3.141592654/2.
      READ(93,147)BHAT,RATIO
147    FORMAT(/,T16,F6.1,T30,F4.1)
      READ(93,47)GAMA,DPSI
47    FORMAT(/,T12,F7.1,T37,F7.4)
      PRINT*,'GAMA=',GAMA,'      PSI=',DPSI
      PSI=DPSI*3.141592654/180.
      READ(95,196)DZETA
196    FORMAT(/,T3,F4.1)
      PRINT*,'ZETA=',DZETA
      ZETA=DZETA*3.141592654/180.
      READ(95,197)
197    FORMAT(2X)
      DO 194 I=1,NUM
           READ(95,195)HEIT(I)
```

```
195          FORMAT(T39,F5.1)
194     CONTINUE
       READ (95,198)BEN
198     FORMAT (////,T27,F6.1)
       BENCH=BEN*(-1)
       DO 298 I=1,NUM
            AR(I)=TAN(3.141592654/2.-PSI)*((HEIT(I)/TAN(ZETA))+BENCH)
            HEIGHT(I)=COS(3.141592654/2.-PSI)*(HEIT(I)-AR(I))
298     CONTINUE
       READ(90,44) M
44      FORMAT(T8,I5)
       IF (NUM.EQ.2)THEN
            OPEN(UNIT=92,FILE='BRAKE.DAT')
            DO 60 I=1,M
                  WRITE (92,50)
50                 FORMAT(T5,'1',T10,'1',T15,'1',T20,'1',T25,'1',
   &                    T30,'1',T35,'1',T40,'1',T45,'1')
60           CONTINUE
           REWIND(UNIT=92)
       ELSE
            OPEN(UNIT=92,FILE='BRAKE.DAT',STATUS='OLD')
       ENDIF
       READ(91,40) N
40      FORMAT(/,T8,I5)

       READ(91,45)
45      FORMAT(2X)
       DO 30 I=1,N
             READ(91,4)K,LENGTH(I),DEPTH(I),EMOD(I),WAT(I)
4            FORMAT(T2,I3,T15,F6.2,T30,F6.2,T48,E10.3,T69,F6.2)
               IF(I.GT.10) THEN
                    IF(LENGTH(I).LT.0.4)THEN
                        N=I-1
                        GO TO 555
                    ENDIF
               ENDIF
             PRINT*,'LENGTH',I,'=',LENGTH(I)
30      CONTINUE
555     CLOSE (UNIT=91)
       OPEN (UNIT=20,FILE='INPUT.DAT')
       READ(90,46)
46      FORMAT(2X)
       DO 31 I=1,M
             READ(90,42) FAL
42            FORMAT(T29,A6)
             IF (FAL.EQ.'G')THEN
                  FAIL(I)=1
             ELSE
                  FAIL(I)=0
             ENDIF
                READ(92,43)BRAK(I,1),BRAK(I,2),BRAK(I,3),BRAK(I,4),
    &     BRAK(I,5),BRAK(I,6),BRAK(I,7),BRAK(I,8),BRAK(I,9)
43                   FORMAT(T5,I2,T10,I2,T15,I2,T20,I2,T25,I2,
    &                         T30,I2,T35,I2,T40,I2,T45,I2)
31      CONTINUE
        CLOSE (UNIT=92)
        OPEN (UNIT=96,FILE='BRAKE.DAT')

        DO 131 I= 1,M
              PRINT*,'FAIL',I,'=',FAIL(I)
131     CONTINUE
        DO 11 I=1,M
              BRAK(I,1)=FAIL(I)
11      CONTINUE
ccccccccccccccccccccccccccccccccccccccccccccccccccccccccccc
cBLOCK-  creates BREAK from 1s                             c
ccccccccccccccccccccccccccccccccccccccccccccccccccccccccccc
        DO 12 I=1,N
              DO 122 J=1,10
                    BREAK(I,J)=1
122           CONTINUE
12      CONTINUE
        K=1
        L=1
        DO 13 I=MERGE,MERGE+M-1
              DO 133 J=2,10
                    BREAK(I,J)=BRAK(K,L)
                    L=L+1
133           CONTINUE
              L=1
              K=K+1
13      CONTINUE
        DO 531 I=1,N
          WRITE(96,533)BREAK(I,1),BREAK(I,2),BREAK(I,3),BREAK(I,4),
    &     BREAK(I,5),BREAK(I,6),BREAK(I,7),BREAK(I,8),BREAK(I,9)
533                  FORMAT(T5,I2,T10,I2,T15,I2,T20,I2,T25,I2,
    &                         T30,I2,T35,I2,T40,I2,T45,I2)
531     CONTINUE
        DO 14 I=1,N
              F(I)=0.0
              FLEN(I)=0.0
14      CONTINUE
        DO 15 I=1,N
              HA=0.0
              DO 155 J=2,NUM
                    HA=HA + HEIGHT(J-1)
                    IF (BREAK(I,J).EQ.0)THEN
                         LENG(I)=HA
                         FLEN(I)=LENGTH(I)-LENG(I)
                         F(I)=FLEN(I)*GAMA*COS(PSI)*BHAT*DEPTH(I)
                         LENGTH(I)=LENG(I)
                               GO TO 15
```

```
                ENDIF
155           CONTINUE
15      CONTINUE
       WRITE(20,912)
912     FORMAT(T10,'N')
       WRITE(20,112)N
112     FORMAT(T8,I4)
       WRITE(20,612)
612     FORMAT(T3,'No',T15,'LENGTH',T30,'DEPTH',T50,'EMODUL',T70,'VX')
       DO 16 I=1,N
             WRITE(20,7)I,LENGTH(I),DEPTH(I),EMOD(I),WAT(I)
7             FORMAT(T2,I3,T15,F6.2,T30,F6.2,T48,E10.3,T69,F6.2)
             WRITE(94,29)I,LENGTH(I),FLEN(I),F(I)
29           FORMAT(T5,I3,T15,F6.2,T25,F6.2,T40,E12.7)
16      CONTINUE
       CALL INP2(N,LENGTH,DEPTH,WAT,EMOD,RATIO)
       END
**********************************************************


  SUBROUTINE INP2(N,LENGTH,DEPTH,VX,EMODUL,RATIO)
       INTEGER N,NP,K,I
       PARAMETER (NP=400)
       REAL LENGTH(NP),DEPTH(NP),VX(NP),EMODUL(NP)
       REAL TOP,BOTTOM,SIDE,DOWN,LEN(NP),DEP(NP),WAT(NP)
       REAL EMOD(NP),MOD,MODUL,RATIO
       OPEN (UNIT=80,FILE='INPUT1.DAT')
       I=1
       K=1
9       TOP=0.
       BOTTOM=0.
       DOWN=0.
       SIDE=0.
       MOD=0.
10      IF (I.LE.N)THEN
              TOP=TOP+LENGTH(I)
              BOTTOM=BOTTOM+DEPTH(I)
              DOWN=DOWN+1
              MOD=MOD+DEPTH(I)*EMODUL(I)
              SIDE=TOP/DOWN
              MODUL=MOD/BOTTOM
              IF (SIDE/BOTTOM.GT.RATIO)THEN
                   I=I+1
                   GO TO 10
              ELSE
                   DEP(K)=BOTTOM
                   LEN(K)=SIDE
                   IF (LEN(K).GT.VX(I))THEN
                         WAT(K)=VX(I)
                   ELSE
                         WAT(K)=LEN(K)*0.98
                ENDIF
                EMOD(K)=MODUL
                K=K+1
                I=I+1
                GO TO 9
            ENDIF
        ENDIF

        WRITE (80,2)
2       FORMAT(T10,'N')
        WRITE (80,3)K
3       FORMAT(T8,I4)
        WRITE(80,6)
6       FORMAT(T3,'No',T15,'LENGTH',T30,'DEPTH',T50,'EMODUL',T70,'VX')
        DO 71 I=1,K
             WRITE(80,7)I,LEN(I),DEP(I),EMOD(I),WAT(I)
7            FORMAT(T2,I3,T15,F6.2,T30,F5.2,T48,E10.3,T69,F5.2)
71      CONTINUE
        END
```

I.3. Program Inshav

Program Inshav builds the model of the slope to be tested by Flex, from the blocks of cantilevers,and the zones of non-interacting cantilevers.

Resulting data file:

Input3.dat - information about the length,width and the Young's modulus of all blocks and non-interacting cantilevers in the slope (geometry of the new slope), and about the length of the columns of water in the slope.

```
        PROGRAM INSHAV
        INTEGER N,NP,K,DIS
        INTEGER RUNCNT,RUN
        PARAMETER (NP=2000)
        REAL LENGTH(NP),WEIGHM(NP),WEIGHT(NP)
        REAL DEPTH(NP),GAMA,EMODUL(NP),PSID,PSI,BHAT
        REAL  X(NP),XV(NP),COHESION(10),FID(10),FI(10),TENSILE(10),KOEF
        REAL DEP(NP),DIST(10),F(NP)
        COMMON /ABBA/RUNCNT,RUN
        COMMON /BBBA/ DEP
        OPEN (UNIT=20,FILE='FYZIC.DAT',STATUS='old')
        OPEN (UNIT=21,FILE='INPUT.DAT',STATUS='old')
        OPEN (UNIT=22,FILE='DISTAN.DAT',STATUS='old')
        OPEN (UNIT=23,FILE='FF.DAT',STATUS='old')
        OPEN (UNIT=24,FILE='F.DAT')
        OPEN (UNIT=91,FILE='INPUT3.DAT')
        PRINT*,'Enter the number of runs'
```

```
      READ*,RUN
      RUNCNT=1
      READ (22,1)DIS
1     FORMAT (/,T15,I2)
      READ (22,11)
11    FORMAT(2X)
      DO 2 I=1,DIS
         READ (22,3)DIST(I),COHESION(I),FID(I),TENSILE(I)
3         FORMAT(T13,F6.2,T29,F6.2,T45,F4.1,T62,F6.2)
         PRINT 4, DIST(I),COHESION(I),FID(I),TENSILE(I)
4         FORMAT(T16,F6.2,T29,F6.2,T44,F5.1,T62,F6.2)
2     CONTINUE
      READ (20,55)BHAT
55    FORMAT (/,T15,F5.1)
      READ (20,5)GAMA,PSID,KOEF
5     FORMAT(/,T13,F7.1,T38,F9.6,T64,F6.2)
      PRINT*,'GAMA=',GAMA,'PSI=',PSID,'KOEF=',KOEF
      READ(21,66)N
66     FORMAT(/,T9,I4)
      PRINT*,'N=',N
      READ (21,6)
6     FORMAT(1X)
      DO 60 I=1,N
                READ(23,233)F(I)
233             FORMAT(T39,E13.7)
           READ(21,7)K,LENGTH(I),DEPTH(I),EMODUL(I),XV(I)
7           FORMAT(T2,I3,T15,F6.2,T30,F6.2,T48,E10.3,T69,F6.2)
           IF(I.GT.10) THEN
                IF(LENGTH(I).LT.0.4)THEN
                     N=I-1
                     GO TO 71
                ENDIF
           ENDIF
60     CONTINUE
71     PSI= PSID *(3.141593D00)/180.D00
       DO 72 I=1,DIS
          FI(I)= FID(I) *(3.141593D00)/180.D00
          print 44, FI(I),FID(I),DIST(I)
44          FORMAT(T16,F6.4,T29,F6.2,T40,F6.2)
72     CONTINUE
       DO 61 I=1,N
            print 8, I,LENGTH(I),DEPTH(I),EMODUL(I),XV(I)
8            FORMAT(T2,I3,T15,F5.2,T30,F5.2,T48,E10.3,T69,F5.2)
61     CONTINUE
       DO 10 I=1,N
            WEIGHM(I)=0.0D0
            WEIGHT(I)=0.0D0
            WEIGHM(I) =GAMA*DEPTH(I)*BHAT*COS(PSI)*KOEF
            WEIGHT(I) =GAMA*DEPTH(I)*BHAT*SIN(PSI)
 10    CONTINUE
        CALL ISAAC(N,EMODUL,X,LENGTH,WEIGHM,PSI,
     &            DEPTH,BHAT,XV,DIS,DIST,
     &            COHESION,FI,F)
      END
CCCCCCCCCCCCCCCCCCCCCCCCCCCCCCCCCCCCCCCCCCCCCCCCCCCC


      SUBROUTINE ISAAC(N,EMODUL,X,LENGTH,WEIGHM,PSI,
     &            DEPTH,BHAT,XV,DIS,DIST,
     &            COHESION,FI,F)
C     program solves the system of nonlinear equations for n cantil.
C
C                ...........            EMODUL....Young's modulus[Pa]
C              /         /:             INERTIA...Moment of inertia
C            /         /  :depth        GAMA......Density of rock [N/m^3]
C          /         /    :
C        /........./     /
C        : bhat :     /length
C        :        :  /
C        :.........:/
C
       INTEGER NTRIAL,N,NP,AN,AB,I,DAB,DIS
       PARAMETER(NP=2000,NTRIAL=25)
       DOUBLE PRECISION ALPHA(NP,4),BETA(NP)
       REAL XV(NP),REAC(NP),X(NP)
       REAL INERTIA(NP),LENGTH(NP),WEIGHM(NP),EMODUL(NP)
       REAL PSI,XLEN(NP),DEPTH(NP),BHAT
       REAL COHESION(10),FI(10)
       REAL DIST(10),F(NP)
       REAL LENG
       REAL DEP(NP)
       INTEGER COUNT
       COMMON /BBBA/ DEP
       LOGICAL DONE
       DONE=.FALSE.
       COUNT=0
****************************************************************
*BLOCK 1- calculates reactions between blocks in question*
****************************************************************
C  INLINE calculates distances where reactions are acting
400     CALL INLINE(LENGTH,XLEN,N)
       DO 401 I=1,N
            REAC(I)=0.0
401     CONTINUE
       CALL INERT(N,NP,BHAT,DEPTH,INERTIA)
C DO LOOP 1 locates the crest block  DAB
       LENG=0.
       DAB=0
       AN=1
       print*,'n=',n
       DO 1 I=1,N
            IF (LENGTH(I).GT.LENG)THEN
```

```
                LENG=LENGTH(I)
                DAB=I
           ENDIF
 1    CONTINUE
**************************
C next block calculates reactions from AN to the crest
C DAB...........number of the crest block
C AN.........1
C AB.........DAB
*************************
      PRINT*, 'DAB=',DAB
      IF(DAB.EQ.1)THEN
           AN=1
           AB=2
           GO TO 202
      ENDIF
10     IF (AN.LT.DAB)THEN
           AB=DAB
      ELSE
           AB=DAB+1
      ENDIF
      NB=AB-AN+1
      CALL USRFUN(AN,AB,NB,WEIGHM,LENGTH,INERTIA,EMODUL,PSI,
     &      XV,ALPHA,BETA,XLEN,F)
      print*,'NB=',NB,'AN=',AN,'AB=',AB
      PRINT*,'reactions to the crest'
      CALL NEWTON(NB,ALPHA,BETA,X)
      DO 402 I=AN,AB
           REAC(I)=0.0
402   CONTINUE
C DO LOOP 2 renumberes reactions from AN to AB
      J=AN
      DO 2 I=1,2*NB-3,2
           REAC(J)=X(I)
           J=J+1
 2    CONTINUE
*******************************
C DO LOOP 3 locates the first 0. reaction before crest if any,
C and sets AB to the number of the located cant. I
C AB...........I
******************************
      K=AN
      DO 3 I=K,J-1
           IF(REAC(I).LE.0.0)THEN
                IF(I.EQ.AN.AND.AN.LT.DAB-1)THEN
                     AB=AN+1
                     GO TO 201
                ELSEIF(I.EQ.AN.AND.AN.EQ.DAB-1)THEN
                     GO TO 202
                ELSEIF(I.EQ.AN.AND.AN.EQ.DAB)THEN
                     AB=DAB+1
```

```
                    GO TO 202
               ELSEIF(I.EQ.DAB-1)THEN
                    AN=DAB
                    AB=DAB+1
                    GO TO 202
               ELSE
                    AB=I
                    GO TO 201
               ENDIF
          ENDIF
 3     CONTINUE
       IF (AN.LT.DAB)THEN
            AB=DAB
       ELSE
            AB=DAB+1
       ENDIF
       GO TO 202
201     CALL ITER(N,AN,AB,WEIGHM,LENGTH,INERTIA,EMODUL,PSI,
    &        XV,XLEN,REAC,ALPHA,BETA,X,DAB,F)
       IF (AB.NE.N)THEN
            IF(AN.EQ.1.AND.AB.EQ.DAB)THEN
                 AN=DAB
                 AB=DAB+1
                 GO TO 202
            ELSEIF(AN.EQ.DAB-2.AND.AB.EQ.DAB)THEN
                 AN=DAB-1
                 AB=DAB
                 GO TO 10
               ELSEIF(AN.LT.DAB-2.AND.AB.EQ.DAB)THEN
                    AN=DAB
                    AB=DAB+1
                    GO TO 202
            ELSE
                 GO TO 10
            ENDIF
       ELSE
            GO TO 501
       ENDIF
C
202     CALL ITERUN(N,AN,AB,WEIGHM,LENGTH,INERTIA,EMODUL,PSI,
    &        XV,XLEN,REAC,ALPHA,BETA,X,F)
       DO 20 J=1,N-1
       PRINT*,'REACTION',J,'=',REAC(J)
 20    CONTINUE

501     CALL SHEARS (N,WEIGHM,LENGTH,INERTIA,PSI,EMODUL,DIS,DIST,
    &        XLEN,XV,REAC,F,DEPTH,BHAT,COHESION,FI)
       GO TO 400
       END
CCCCCCCCCCCCCCCCCCCCCCCCCCCCCCCCCCCCCCCCCCCCCCCCCCCCCCCCCC
```

```
      SUBROUTINE SHEARS (N,WEIGHM,LENGTH,INERTIA,PSI,EMODUL,DIS,DIST,
     &       XLEN,XV,REAC,F,DEPTH,BHAT,COHESION,FI)
      INTEGER NP,N,DIS
      INTEGER I,K,J,DOWN
      INTEGER RUNCNT,RUN
      PARAMETER (NP=2000)
      REAL REAC(NP),BHAT,XLEN(NP),STRE,FF(NP)
      REAL PSI,GAMAW,GAMW,DEPTH(NP),STREN(NP),SF(NP)
      REAL WEIGHM(NP),LENGTH(NP),INERTIA(NP),EMODUL(NP)
      REAL F(NP),XV(NP),SHEAR(NP),SHEAV(NP),FORCE
      REAL LEN(NP),DEP(NP),EMOD(NP),WAT(NP),BOTTOM,MOD,SIDE
      REAL COHES,COHESION(10),FIK,FI(10),DIST(10)
      COMMON /ABBA/RUNCNT,RUN
      PARAMETER (GAMAW=9.81D03)
      GAMW=GAMAW*SIN(PSI)/6.D0
C       for the first cantilever the reaction from below and the loading
C       caused by the water below are zero.
C
*******************************************************
*block 1
      print*,'Test 1'
      DO 300 I=1,2*(N-1)
            SHEAR(I)=0.0
            SHEAV(I)=0.0
 300  CONTINUE
          SHEAV(1)=((WEIGHM(1)*LENGTH(1)**2)/2+REAC(1)*XLEN(1)
     &          +F(1)*LENGTH(1)+GAMW*(XV(1)**3))/LENGTH(1)
      DO 10 I=2,N-1
          J=2*I-2
          K=2*I-1
          SHEAV(I)=((WEIGHM(I)*LENGTH(I)**2)/2+REAC(I)*XLEN(I)
     &          -REAC(I-1)*XLEN(I-1)+F(1)*LENGTH(1)
     &          +GAMW*(XV(I)**3-XV(I-1)**3))/LENGTH(I)
 10   CONTINUE

C       For the last cantilever the reaction from above is zero.
          J=2*N-2
          K=2*N-1
          SHEAV(I)=((WEIGHM(N)*LENGTH(N)**2)/2
     &          -REAC(N-1)*XLEN(N-1)+F(N)*LENGTH(N)
     &          +GAMW*(XV(N)**3-XV(N-1)**3))/LENGTH(N)

C The next block calculates  shear stresses, and shear forces
C and tests if the resulting SF is greater than 1.
       XCANT=0.0
       DO 11 I=1,N
          XCANT=XCANT+DEPTH(I)
          DO 600 J=1,DIS
              IF((XCANT-DEPTH(I)/2.).EQ.DIST(J))THEN
                 IF(FI(J).LE.FI(J+1))THEN
                       COHES=COHESION(J)
```

```
                        FIK=FI(J)
                        GO TO 601
                  ELSE
                        IF(J.LT.DIS)THEN
                            COHES=COHESION(J+1)
                            FIK=FI(J+1)
                            GO TO 601
                        ELSE
                            COHES=COHESION(J)
                            FIK=FI(J)
                            GO TO 601
                        ENDIF
                  ENDIF
              ELSEIF((XCANT-DEPTH(I)/2.).LT.DIST(J))THEN
                        COHES=COHESION(J)
                        FIK=FI(J)
                        GO TO 601
              ENDIF
600       CONTINUE
601         QMAX=0.0
           STRE=0.0
           QMAX=(BHAT/2.)*(DEPTH(I)**2/4)
           SHEAR(I)=((SHEAV(I)*QMAX)/(INERTIA(I)*BHAT))/1000.
C          WRITE (97,*) 'SHEAR',I,'=',SHEAR(I),'kPa'
C           WRITE (97,*) '****************************'
              STRE=(REAC(I)+F(I)+(GAMAW*XV(I)**2)/2
    &                 +(WEIGHM(I)*LENGTH(I))/2)/(LENGTH(I)*BHAT)
              STREN(I)=COHES+STRE*TAN(FIK)/1000.
           SF(I)=STREN(I)/SHEAR(I)
c            WRITE(91,8)I,SHEAR(I),STREN(I),SF(I)
C             print*,'SF=',SF(I)
c8           FORMAT(T6,I3,T20,F7.2,T30,F7.2,T40,F7.2)
 11     CONTINUE
*********************************************************
*FIRST ROUND-creating the first set of blocks acc. to SF *
*********************************************************
C
**************************************************************
*BLOCK 1 - finds the number of the longest cantil.-crest block *
**************************************************************
      TYPIC=DEPTH(1)
      LONGEST=0.
      DO 1 I=1,N
            IF (LONGEST.LT.LENGTH(I))THEN
                  LONGEST=LENGTH(I)
                  NTOP=I
            ENDIF
1      CONTINUE
*****************************************************************
*BLOCK 2- finds the distance of the crest block from the beginning*
*****************************************************************
```

```
      XTOP=0.
      DO 2 I=1,NTOP
            XTOP=XTOP+DEPTH(I)
2     CONTINUE
******************************************************************
*BLOCK 3- makes the first round set of blocks*
**********************************************
      PRINT*,'RUN no.',RUNCNT
      K=1
      SIDE=0.
      BOTTOM=0.
      FORCE=0.
      DOWN=0.
      MOD=0.
      DO 12 I=1,N
            SIDE=SIDE+LENGTH(I)
            BOTTOM=BOTTOM+DEPTH(I)
                FORCE=FORCE+F(I)
            DOWN=DOWN+1
            MOD=MOD+DEPTH(I)*EMODUL(I)
         IF ((ABS(SF(I)).GT.ABS(SF(I+1)).AND.
    &        ABS(SF(I+1)).LT.ABS(SF(I+2)).AND.
    &        ABS(SF(I+1)).LT.1).OR.
    &        REAC(I).EQ.0.)THEN
                  DEP(K)=BOTTOM
                        FF(K)=FORCE
                  LEN(K)=SIDE/DOWN
                  EMOD(K)=MOD/BOTTOM
                  IF (LEN(K).GT.XV(I))THEN
                        WAT(K)=XV(I)
                  ELSE
                        WAT(K)=LEN(K)*0.98
                  ENDIF
C
                  SIDE=0.
                  BOTTOM=0.
                        FORCE=0.
                  DOWN=0.
                  MOD=0.
                  K=K+1
         ENDIF
12     CONTINUE
       K=K-1
       DO 13 I=1,N
             LENGTH(I)=0.
             DEPTH(I)=0.
                F(I)   =0.
             EMODUL(I)=0.
             XV(I)=0.0
13     CONTINUE
       N=K
```

```
        DO 14 I=1,N
              LENGTH(I)=LEN(I)
              DEPTH(I)=DEP(I)
                  F(I)    =FF(I)
              EMODUL(I)=EMOD(I)
              XV(I)=WAT(I)
14      CONTINUE
************************************
******************************
        IF (RUNCNT.EQ.RUN)THEN
           REWIND(UNIT=91)
           WRITE (91,3)
3          FORMAT(T10,'N')
           WRITE (91,4)K
4          FORMAT(T8,I4)
           WRITE(91,6)
6       FORMAT(T3,'No',T15,'LENGTH',T30,'DEPTH',T50,'EMODUL',T70,'VX')
          DO 71 I=1,K
                   WRITE(24,244)I,FF(I)
244                FORMAT(T20,I3,T40,E12.7)
               WRITE(91,7)I,LEN(I),DEP(I),EMOD(I),WAT(I)
7              FORMAT(T2,I3,T15,F6.2,T30,F6.2,T48,E10.3,T69,F6.2)
               PRINT 72,I,LEN(I),DEP(I),EMOD(I),WAT(I)
72               FORMAT(T2,I3,T15,F6.2,T30,F6.2,T48,E10.3,T69,F6.2)
71          CONTINUE
           PRINT*,'DATA READY'
           STOP
        ENDIF
        RUNCNT=RUNCNT+1
        END
```

Program Inshav shares subroutines Usrfun and Newton with Flex.

I.4. Program Flex.

Program flex is the main routine of the model. It calculates the stresses and deformations in the slope, and changes the geometry of the slope according to those changes.

Resulting data file:

Result.dat - gives the information about which cantilevers were broken and which remain intact .

The structural chart of the program is shown in the next page.

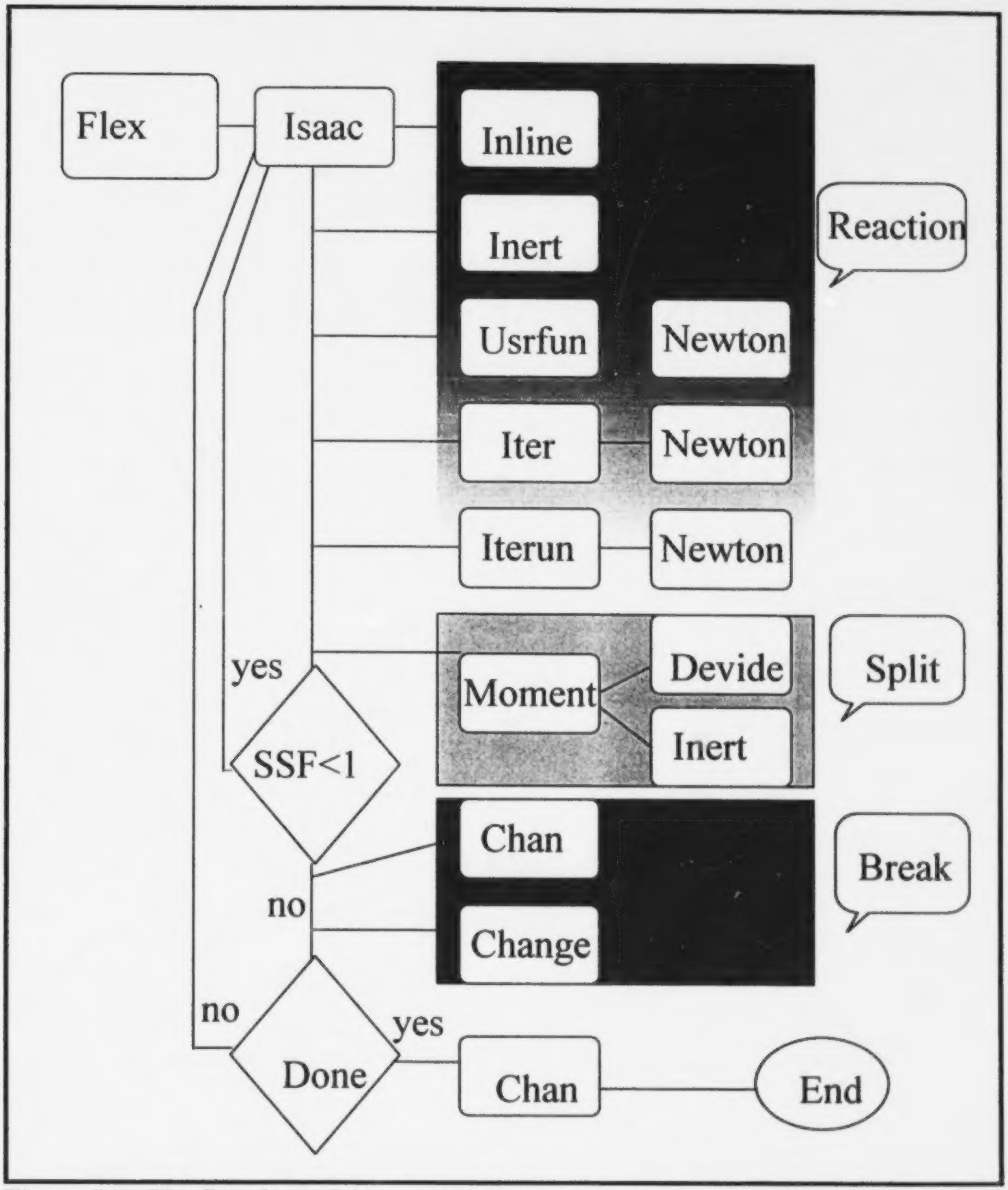
Flex
Isaac
Inline
Inert
Usrfun
Newton
Iter
Newton
Iterun
Newton
Reaction
yes
Moment
Devide
Inert
Split
SSF<1
Chan
Change
Break
no
no
Done
yes
Chan
End

Figure I-1 The flowchart of the routine Flex.

```
      PROGRAM FLEX
       INTEGER N,NP,K,DIS
       PARAMETER (NP=2000)
       REAL LENGTH(NP),WEIGHM(NP),WEIGHT(NP),F(NP)
       REAL DEPTH(NP),GAMA,EMODUL(NP),PSID,PSI,BHAT
       REAL X(NP),XV(NP),COHESION(10),FID(10),FI(10),TENSILE(10),KOEF
       REAL DEP(NP),DIST(10),DI
       LOGICAL RDATA
       COMMON /ABBA/RDATA,KOEF
       COMMON /BBBA/ DEP
       OPEN (UNIT=20,FILE='FYZIC.DAT',STATUS='old')
       OPEN (UNIT=21,FILE='INPUT3.DAT',STATUS='old')
       OPEN (UNIT=22,FILE='DISTAN.DAT',STATUS='old')
       OPEN (UNIT=23,FILE='F.DAT',STATUS='old')
       OPEN (UNIT=24,FILE='FF.DAT',STATUS='old')
       OPEN (UNIT=10,FILE='INPUT.DAT',STATUS='old')
       OPEN (UNIT=65,FILE='CHEC.DAT')
       RDATA=.TRUE.
       READ (22,1)DIS
1       FORMAT (/,T15,I2)
       READ (22,11)
11     FORMAT(2X)
       DO 2 I=1,DIS
              READ (22,3)DIST(I),COHESION(I),FID(I),TENSILE(I)
3              FORMAT(T13,F6.2,T29,F6.2,T45,F4.1,T62,F6.2)
2     CONTINUE
       READ (20,55)BHAT
55     FORMAT (/,T15,F5.1)
       READ (20,5)GAMA,PSID,KOEF
5       FORMAT(/,T13,F7.1,T38,F9.6,T64,F6.2)
       READ(21,66)N
66     FORMAT(/,T9,I4)
       READ (21,6)
6       FORMAT(1X)
       DO 60 I=1,N
             READ(23,9)F(I)
9             FORMAT(T39,E13.7)
             READ(21,7)K,LENGTH(I),DEPTH(I),EMODUL(I),XV(I)
7             FORMAT(T2,I3,T15,F6.2,T30,F6.2,T48,E10.3,T69,F6.2)
             IF(I.GT.10) THEN
                   IF(LENGTH(I).LT.0.4)THEN
                        N=I-1
                        GO TO 71
                   ENDIF
             ENDIF
60    CONTINUE
71    PSI= PSID *(3.141593D00)/180.D00
       DI=0.
       DO 711 I=1,N
             DI=DI+DEPTH(I)
```

```
711  CONTINUE
      DIST(DIS)=DI
      DO 72 I=1,DIS
           FI(I)= FID(I) *(3.141593D00)/180.D00
72    CONTINUE
      DO 10 I=1,N
              WEIGHM(I)=0.0D0
              WEIGHT(I)=0.0D0
              WEIGHM(I) =GAMA*DEPTH(I)*BHAT*COS(PSI)*KOEF
              WEIGHT(I) =GAMA*DEPTH(I)*BHAT*SIN(PSI)
 10   CONTINUE
      CALL ISAAC(N,EMODUL,X,LENGTH,WEIGHM,PSI,
     &        DEPTH,GAMA,BHAT,WEIGHT,XV,DIS,DIST,
     &        COHESION,FI,TENSILE,F)
      END

CCCCCCCCCCCCCCCCCCCCCCCCCCCCCCCCCCCCCCCCCCCCCCCCCCCCCCCCC



      SUBROUTINE ISAAC(N,EMODUL,X,LENGTH,WEIGHM,PSI,
     &             DEPTH,GAMA,BHAT,WEIGHT,XV,DIS,DIST,
     &             COHESION,FI,TENSILE,F)
C     program solves the system of nonlinear equations for n cantil.
C
C                 ...........       EMODUL....Young's modulus[Pa]
C               /        /:         INERTIA...Moment of inertia
C             /        /  :depth    GAMA......Density of rock [N/m^3]
C           /        /    :
C          /........./    /
C          : bhat :    /length
C          :        :  /
C          :.........:/
C
       integer NTRIAL,N,NP,AN,AB,I,NUM,DAB,ND,DIS
       parameter(NP=2000,NTRIAL=25)
       double precision ALPHA(NP,4),BETA(NP)
       real XV(NP),REAC(NP),X(NP),F(NP)
       real INERTIA(NP),LENGTH(NP),WEIGHM(NP),EMODUL(NP)
       real PSI,XLEN(NP),DEPTH(NP),GAMA,BHAT
       real TEST,WEIGHT(NP),LENG
       real DEP(NP),XCANT
       real COHESION(10),FI(10),TENS,TENSILE(10),DIST(10)
       integer NOR,COUNT
       COMMON /BBBA/ DEP
       logical DONE
       DONE=.FALSE.
       COUNT=0
C
C
```

```
********************************************************
*BLOCK 1- calculates reactions between blocks in question*
********************************************************
C  INLINE calculates distances where reactions are acting
400     CALL INLINE(LENGTH,XLEN,N)
      DO 401 I=1,N
            REAC(I)=0.0
401     CONTINUE
      CALL INERT(N,NP,BHAT,DEPTH,INERTIA)
C DO LOOP 1 locates the crest block  DAB
      LENG=0.
      DAB=0
      AN=1
      DO 1 I=1,N
            IF (LENGTH(I).GT.LENG)THEN
                  LENG=LENGTH(I)
                  DAB=I
            ENDIF
 1      CONTINUE
*************************
C next block calculates reactions from AN to the crest
C DAB...........number of the crest block
C AN.........1
C AB.........DAB
*************************
      IF(DAB.EQ.1)THEN
            AN=1
            AB=2
            GO TO 202
      ENDIF
10     IF (AN.LT.DAB)THEN
            AB=DAB
      ELSE
           AB=DAB+1
      ENDIF
      NB=AB-AN+1
      CALL USRFUN(AN,AB,NB,WEIGHM,LENGTH,INERTIA,EMODUL,PSI,
   &        XV,ALPHA,BETA,XLEN,F)
C    PRINT*,'REACTIONS TO THE CREST'
C    PRINT*,'AB=',AB,'   AN=',AN
      CALL NEWTON(NB,ALPHA,BETA,X)
      DO 402 I=AN,AB
            REAC(I)=0.0
402    CONTINUE
C DO LOOP 2 renumberes reactions from AN to AB
      J=AN
      DO 2 I=1,2*NB-3,2
            REAC(J)=X(I)
            J=J+1
 2      CONTINUE
*****************************
```

```
C DO LOOP 3 locates the first 0. reaction before crest if any,
C and sets AB to the number of the located cant. I
C AB...........I
****************************
        K=AN
        DO 3 I=K,J-1
              IF(REAC(I).LE.0.0)THEN
                    IF(I.EQ.AN.AND.AN.LT.DAB-1)THEN
                          AB=AN+1
                          GO TO 201
                    ELSEIF(I.EQ.AN.AND.AN.EQ.DAB-1)THEN
                          GO TO 202
                    ELSEIF(I.EQ.AN.AND.AN.EQ.DAB)THEN
                          AB=DAB+1
                          GO TO 202
C
                    ELSEIF(I.EQ.DAB-1)THEN
                          AB=AN+1
                          GO TO 202
C
                    ELSE
                          AB=I
                          GO TO 201
                    ENDIF
              ENDIF
 3      CONTINUE
        IF (AN.LT.DAB)THEN
              AB=DAB
        ELSE
              AB=DAB+1
        ENDIF
        GO TO 202
201     CALL ITER(N,AN,AB,WEIGHM,LENGTH,INERTIA,EMODUL,PSI,
    &        XV,XLEN,REAC,ALPHA,BETA,X,DAB,F)
        IF (AB.NE.N)THEN
              IF(AN.EQ.1.AND.AB.EQ.DAB)THEN
                    AN=DAB
                    AB=DAB+1
                    GO TO 202
              ELSEIF(AN.EQ.DAB-2.AND.AB.EQ.DAB)THEN
                    AN=DAB-1
                    AB=DAB
                    GO TO 10
          ELSEIF(AN.LT.DAB-2.AND.AB.EQ.DAB)THEN
              AN=DAB
              AB=DAB+1
              GO TO 202
               ELSE
                    GO TO 10
               ENDIF
        ELSE
```

```
            GO TO 501
      ENDIF
202    CALL ITERUN(N,AN,AB,WEIGHM,LENGTH,INERTIA,EMODUL,PSI,
    &       XV,XLEN,REAC,ALPHA,BETA,X,F)
      DO 20 J=1,N-1
 20    CONTINUE
       CALL DEFLEX(N,WEIGHM,LENGTH,INERTIA,EMODUL,PSI,
    &                  XV,REAC,XLEN)

*******************************************************
*BLOCK 2-does the splitting and the breaking of cantilevers*
*******************************************************
    PRINT*,'NOR=',NOR,'   ND=',ND,'   N=',N

501    CALL MOMENT (N,WEIGHM,LENGTH,INERTIA,PSI,EMODUL,
    &           NOR,XV,REAC,XLEN,F,DEPTH,GAMA,BHAT,
    &             DIS,DIST,COHESION,FI,WEIGHT,TEST,NUM,ND,TIP)
      IF(N.LT.ND.AND.TIP.LT.1.0)THEN
            GO TO 400
      ELSE
            PRINT*,'DEVIDING FINISHED'
      ENDIF
      XCANT=0.0
      DO 502 I=1,NUM
                 XCANT=XCANT+DEPTH(I)
502    CONTINUE
      DO 503 I=1,DIS
            IF((XCANT-DEPTH(NUM)/2.).LE.DIST(I))THEN
                 TENS=TENSILE(I)
                 GO TO 505
            ENDIF
503    CONTINUE

505    IF (TEST.GE.TENS)THEN
          DO 504 I=1,DIS
             IF(XCANT.LE.DIST(I))THEN
                  IF(I.EQ.1)THEN
                         DIST(1)=DIST(1)-DEPTH(NUM)
                         IF(DIS.GT.1)THEN
                                DO 604 J=2,DIS
                                     DIST(J)=DIST(J)-DEPTH(NUM)
604                               CONTINUE
                         ENDIF
                  ELSE
                         IF(XCANT-DEPTH(NUM).LT.DIST(I-1))THEN
                                DIST(I-1)=XCANT-DEPTH(NUM)
                                DO 704 J=I,DIS
                                     DIST(J)=DIST(J)-DEPTH(NUM)
704                               CONTINUE
                         ELSE
                                DO 804 J=I,DIS
```

```
                           DIST(J)=DIST(J)-DEPTH(NUM)
804                      CONTINUE
                   ENDIF
               ENDIF
               GO TO 605
            ENDIF
504       CONTINUE
      ENDIF
605    DO 507 I=1,DIS
507    CONTINUE
      IF (TEST.GE.TENS)THEN
          CALL CHAN  (DEPTH,ND,NUM,COUNT,DONE,NOR)
          CALL CHANGE(N,NUM,LENGTH,WEIGHM,DEPTH,EMODUL,INERTIA,
   &              WEIGHT,XV,F,DONE,PSI)
      ELSE
           DONE=.TRUE.
          CALL CHAN  (DEPTH,ND,NUM,COUNT,DONE,NOR)
       PRINT*,'THE REST OF THE SLOPE STABILE'
           STOP
      ENDIF

      IF (N.EQ.1)THEN
           DONE=.TRUE.
           CALL CHAN  (DEPTH,ND,NUM,COUNT,DONE,NOR)
           PRINT*, 'FAILURE COMPLETED'
           STOP
      ENDIF
      GO TO 400
      END
CCCCCCCCCCCCCCCCCCCCCCCCCCCCCCCCCCCCCCCCCCCCCCCCCCCCCC


  SUBROUTINE USRFUN(AN,AB,NB,WEIGHM,LENGTH,INERTIA,
   &                          EMODUL,PSI, XV,ALPHA,BETA,XLEN,F)
      INTEGER NP,NB,AN,AB
      INTEGER R,I,J,K,M,P
      PARAMETER (NP=2000)
      DOUBLE PRECISION ALPHA(NP,4),BETA(NP)
      REAL EMODUL(NP),PSI,GAMAW,GAMW
      REAL WEIGHM(NP),LENGTH(NP),XLEN(NP),INERTIA(NP)
      REAL UR(NP),F(NP),XV(NP)
C
      PARAMETER (GAMAW=9.81D03)
      GAMW=GAMAW*SIN(PSI)/120.D0
C       for the first cantilever the reaction from below and the loading
C       caused by the water below are zero.
C       AB first cantilever in the block
C       AN last cantilever in the block
C       NB....number of cantilevers currently in question
C       Each cantilever is evaluated in two crossections for reaction and
C       deflection;for adjacent cantilevers reaction and defl. are equal.
```

```
C      Therefore there are 2*NB-2 BETAS and (2*NB-2)*3 ALPHAS
C      Linear eq. with coefficients ALPHA and BETA
C         ALPHA(i,1)*R(m)+ALPHA(i,2)*R(n)+ALPHA(i,3)*Y(m)+BETA(i)=0

****************************************
      DO 303 I=1,2*(NB-1)
            BETA(I)=0.0D0
            DO 304 J=1,4
                 ALPHA(I,J)=0.0D0
 304             CONTINUE
 303  CONTINUE
*****************************************
      IF (LENGTH(AN).LE.LENGTH(AN+1))THEN
C
     BETA(1)=(WEIGHM(AN)/24.)*(-LENGTH(AN)**3*(LENGTH(AN)-4.*XLEN(AN)))
    &  +(F(AN)/6.)*(-LENGTH(AN)**2)*(LENGTH(AN)-3.*XLEN(AN))
    &  -GAMW*(-XV(AN)**4)*(XV(AN)-5.*XLEN(AN))
C
      ALPHA(1,3)=(1.D0/6)*2.D0*(XLEN(AN)**3)
      ALPHA(1,4)=-(EMODUL(AN)*INERTIA(AN))
      ELSE

     BETA(1)=(WEIGHM(AN)/24.)*((LENGTH(AN)-XLEN(AN))**4
    &               -LENGTH(AN)**3*(LENGTH(AN)-4.*XLEN(AN)))
    &  +(F(AN)/6.)*((LENGTH(AN)-XLEN(AN))**3
    &               -LENGTH(AN)**2*(LENGTH(AN)-3.*XLEN(AN)))
    &  -GAMW*(-XV(AN)**4)*(XV(AN)-5.*XLEN(AN))
C
      ALPHA(1,3)=+(1.D0/6.)*2.*(XLEN(AN)**3)
      ALPHA(1,4)=-(EMODUL(AN)*INERTIA(AN))
      ENDIF

C
C      for the last cantilever the reaction from above is zero
      I=2*AB-2
      K=2*AB-1
      R=AB-1
C      BETA and ALPHA are for newton, and are calculated from 1...J
      J=2*NB-2
C
      IF(LENGTH(AB).GT.LENGTH(AB-1))THEN

     BETA(J)=(WEIGHM(AB)/24.D0)*((LENGTH(AB)-XLEN(R))**4
    &               -LENGTH(AB)**3*(LENGTH(AB)-4*XLEN(R)))
    &  +(F(AB)/6)*((LENGTH(AB)-XLEN(R))**3
    &               -LENGTH(AB)**2*(LENGTH(AB)-3*XLEN(R)))
    &  +GAMW*(-XV(K)**4)*(XV(K)-5*XLEN(R))
    &  -GAMW*(-XV(I)**4)*(XV(I)-5*XLEN(R))
C
      ALPHA(J,3)=-(1.D0/6)*2*(XLEN(R)**3)
      ALPHA(J,4)=-(EMODUL(AB)*INERTIA(AB))
      ELSEIF(LENGTH(AB).LE.LENGTH(AB-1))THEN

     BETA(J)=(WEIGHM(AB)/24.)*(-LENGTH(AB)**3*(LENGTH(AB)-4*XLEN(R)))
     &  +(F(AB)/6)*(-LENGTH(AB)**2*(LENGTH(AB)-3*XLEN(R)))
     &  +GAMW*(-XV(K)**4)*(XV(K)-5*XLEN(R))
     &  -GAMW*(-XV(I)**4)*(XV(I)-5*XLEN(R))
C
      ALPHA(J,3)=-(1.D0/6.)*2.*(XLEN(R)**3)
      ALPHA(J,4)=-(EMODUL(AB)*INERTIA(AB))

      ELSE
      ENDIF


C       (M)........number of the cant. in the block
C       (R)........cant. below (M)
C       (I)........water below cantilever (M)
C       (K)........water above cantilever (M)
C       between adjacent cant. there are two values for water hight
C       for flat base they are equal, for stepped base they differ
C       (J),(P)....are coef. (M),(R) shifted to 1,nb
C
      IF(NB.GT.2)THEN
      DO 10 M=AN+1,AB-1
            R=M-1
            I=2*M-2
            K=2*M-1
C       BETA and ALPHA calculated from 2 to
            J=2*(M-AN)
            P=J+1
        IF(LENGTH(M).GT.LENGTH(M-1).AND.LENGTH(M).LE.LENGTH(M+1))THEN


C       ___________________________________
C  m+1[___________________________________XLEN(k)=l(m)=XLEN(M)
C  m              [___________________________
C  m-1=R                    [____________________   XLEN(i)=l(m-1)=XLEN(R)
C
C       crossection 1, closer to the beginning of the cantilever


     BETA(J)=(WEIGHM(M)/24)*((LENGTH(M)-XLEN(R))**4
     &               -LENGTH(M)**3*(LENGTH(M)-4*XLEN(R)))
     &  +(F(M)/6)*((LENGTH(M)-XLEN(R))**3
     &               -LENGTH(M)**2*(LENGTH(M)-3*XLEN(R)))
     &  +GAMW*(-XV(K)**4)*(XV(K)-5*XLEN(R))
     &  -GAMW*(-XV(I)**4)*(XV(I)-5*XLEN(R))
C
      ALPHA(J,1)=-(1.D0/6)*2*(XLEN(R)**3)
      ALPHA(J,2)=-(EMODUL(M)*INERTIA(M))
      ALPHA(J,3)=
     &  (1.D0/6)*((XLEN(M)-XLEN(R))**3-XLEN(M)**2*(XLEN(M)-3*XLEN(R)))
        ALPHA(J,4)=0.0D0
C       crossection 2, closer to the end of the cantilever


       BETA(P)=(WEIGHM(M)/24)*(-LENGTH(M)**3*(LENGTH(M)-4*XLEN(M)))
     &  +(F(M)/6)*(-LENGTH(M)**2*(LENGTH(M)-3*XLEN(M)))
     &  +GAMW*(-XV(K)**4)*(XV(K)-5*XLEN(M))
     &  -GAMW*(-XV(I)**4)*(XV(I)-5*XLEN(M))
C
        ALPHA(P,1)=-(1.D0/6)*(-XLEN(R)**2*(XLEN(R)-3*XLEN(M)))
        ALPHA(P,2)=0.0D0
        ALPHA(P,3)=(1.D0/6)*(-XLEN(M)**2*(XLEN(M)-3*XLEN(M)))
        ALPHA(P,4)=-(EMODUL(M)*INERTIA(M))



ELSEIF(LENGTH(M).GT.LENGTH(M-1).AND.LENGTH(M).GT.LENGTH(M+1))THEN

C                  _________________________
C  m+1      ____[_________________________ 1 XLEN(k)=l(m)=XLEN(M)
C  m      [_________________________
C  m-1            [_______________________   XLEN(i)=l(m-1)=XLEN(R)


C       crossection 1, closer to the beginning of the cantilever

             IF(XLEN(M).GT.XLEN(R))THEN
                   UR(M)=1.0D0
                   ELSE
                   UR(M)=0.0D0
             ENDIF

       BETA(J)=(WEIGHM(M)/24)*((LENGTH(M)-XLEN(R))**4
     &                 -LENGTH(M)**3*(LENGTH(M)-4*XLEN(R)))
     &  +(F(M)/6)*((LENGTH(M)-XLEN(R))**3
     &                 -LENGTH(M)**2*(LENGTH(M)-3*XLEN(R)))
     &  +GAMW*(-XV(K)**4)*(XV(K)-5*XLEN(R))
     &  -GAMW*(-XV(I)**4)*(XV(I)-5*XLEN(R))
C
        ALPHA(J,1)=-(1.D0/6)*2*(XLEN(R)**3)
        ALPHA(J,2)=-(EMODUL(M)*INERTIA(M))
        ALPHA(J,3)=(1.D0/6)*((XLEN(M)-XLEN(R))**3*UR(M)
     &                 -XLEN(M)**2*(XLEN(M)-3*XLEN(R)))
        ALPHA(J,4)=0.0D0
C       crossection 2, closer to the end of the cantilever

             IF(XLEN(M).GT.XLEN(R))THEN
                   UR(R)=0.0D0
                   ELSE
                   UR(R)=1.0D0
```

```
              ENDIF

       BETA(P)=(WEIGHM(M)/24)*((LENGTH(M)-XLEN(M))**4
      &              -LENGTH(M)**3*(LENGTH(M)-4*XLEN(M)))
      &   +(F(M)/6)*((LENGTH(M)-XLEN(M))**3
      &              -LENGTH(M)**2*(LENGTH(M)-3*XLEN(M)))
      &   +GAMW*(-XV(K)**4)*(XV(K)-5*XLEN(M))
      &   -GAMW*(-XV(I)**4)*(XV(I)-5*XLEN(M))
C
        ALPHA(P,1)=-(1.D0/6)*((XLEN(R)-XLEN(M))**3*UR(R)
      &             -XLEN(R)**2*(XLEN(R)-3*XLEN(M)))
        ALPHA(P,2)=0.0D0
        ALPHA(P,3)=(1.D0/6)*(-XLEN(M)**2*(XLEN(M)-3*XLEN(M)))
        ALPHA(P,4)=-(EMODUL(M)*INERTIA(M)
ELSEIF(LENGTH(M).LE.LENGTH(M-1).AND.LENGTH(M).GT.LENGTH(M+1))THEN


C                          ______________________
C  m+1             _______[______________________l XLEN(k)=l(m+1)=XLEN(M)
C  m       ________[_____________________________l
C  m-1[__________________________________________l XLEN(i)=l(m)=XLEN(R)
C
C
C       crossection 1, closer to the beginning of the cantilever


       BETA(J)=(WEIGHM(M)/24)*(-LENGTH(M)**3*(LENGTH(M)-4*XLEN(R)))
      &   +(F(M)/6)*(-LENGTH(M)**2*(LENGTH(M)-3*XLEN(R)))
      &   +GAMW*(-XV(K)**4)*(XV(K)-5*XLEN(R))
      &   -GAMW*(-XV(I)**4)*(XV(I)-5*XLEN(R))
C
        ALPHA(J,1)=-(1.D0/6)*(-XLEN(R)**2*(XLEN(R)-3*XLEN(R)))
        ALPHA(J,2)=-(EMODUL(M)*INERTIA(M))
        ALPHA(J,3)=(1.D0/6)*(-XLEN(M)**2*(XLEN(M)-3*XLEN(R)))
        ALPHA(J,4)=0.0D0
C       crossection 2, closer to the end of the cantilever

       BETA(P)=(WEIGHM(M)/24)*((LENGTH(M)-XLEN(M))**4
      &              -LENGTH(M)**3*(LENGTH(M)-4*XLEN(M)))
      &   +(F(M)/6)*((LENGTH(M)-XLEN(M))**3
      &              -LENGTH(M)**2*(LENGTH(M)-3*XLEN(M)))
      &   +GAMW*(-XV(K)**4)*(XV(K)-5*XLEN(M))
      &   -GAMW*(-XV(I)**4)*(XV(I)-5*XLEN(M))
C
        ALPHA(P,1)=-(1.D0/6)*((XLEN(R)-XLEN(M))**3
      &             -XLEN(R)**2*(XLEN(R)-3*XLEN(M)))
        ALPHA(P,2)=0.0D0
        ALPHA(P,3)=(1.D0/6)*(-XLEN(M)**2*(XLEN(M)-3*XLEN(M)))
        ALPHA(P,4)=-(EMODUL(M)*INERTIA(M))

ELSEIF(LENGTH(M).LE.LENGTH(M-1).AND.LENGTH(M).LE.LENGTH(M+1))THEN
```

```
C                              l
C        ________________________________l
C m+1  [________________________________l XLEN(k)=l(m)=XLEN(M)
C m     _______[_________________________l
C m-1[__________________________________l XLEN(i)=l(m)=XLEN(R)
C                              l
C
     BETA(J)=(WEIGHM(M)/24)*(-LENGTH(M)**3*(LENGTH(M)-4*XLEN(R)))
    &   +(F(M)/6)*(-LENGTH(M)**2*(LENGTH(M)-3*XLEN(R)))
    &   +GAMW*(-XV(K)**4)*(XV(K)-5*XLEN(R))
    &   -GAMW*(-XV(I)**4)*(XV(I)-5*XLEN(R))
C
      ALPHA(J,1)=-(1.D0/6)*(-XLEN(R)**2*(XLEN(R)-3*XLEN(R)))
      ALPHA(J,2)=-(EMODUL(M)*INERTIA(M))
      ALPHA(J,3)=(1.D0/6)*(-XLEN(M)**2*(XLEN(M)-3*XLEN(R)))
      ALPHA(J,4)=0.0D0
C      crossection 2, closer to the end of the cantilever


     BETA(P)=(WEIGHM(M)/24)*(-LENGTH(M)**3*(LENGTH(M)-4*XLEN(M)))
    &   +(F(M)/6)*(-LENGTH(M)**2*(LENGTH(M)-3*XLEN(M)))
    &   +GAMW*(-XV(K)**4)*(XV(K)-5*XLEN(M))
    &   -GAMW*(-XV(I)**4)*(XV(I)-5*XLEN(M))
C
      ALPHA(P,1)=-(1.D0/6)*(-XLEN(R)**2*(XLEN(R)-3*XLEN(M)))
      ALPHA(P,2)=0.0D0
      ALPHA(P,3)=(1.D0/6)*(-XLEN(M)**2*(XLEN(M)-3*XLEN(M)))
      ALPHA(P,4)=-(EMODUL(M)*INERTIA(M))
         ELSE
         ENDIF
 10    CONTINUE
      ENDIF
      DO 11 I=1,2*(NB-1)
           BETA(I)=(-1)*BETA(I)
c          write(93,*) 'beta',i,'=',beta(i)
           do 12 j=1,4
c                 write(93,*)'alpha',i,j,'=',alpha(i,j)
 12          continue
 11    CONTINUE
      END
****************************************

     SUBROUTINE NEWTON (NB,ALPHA,BETA,X)
      INTEGER I,J,K,NP,NB
      PARAMETER (NP=2000)
      DOUBLE PRECISION  ALPHA(NP,4),BETA(NP)
      REAL X(NP)
      M=(NB-1)*2
      DO 1 I=1,M
           X(I)=0.0D0
 1     CONTINUE
```

```
      ALPHA(1,4)=ALPHA(1,4)/ALPHA(1,3)
      BETA(1)=BETA(1)/ALPHA(1,3)
      DO 10 I=2,M,2
      J=I+1
      K=I-1
C      loop 10 nulifies all values to the left from diagonal and
C      changes all values in the diagonal to 1.
           IF(J.LT.M)THEN
                ALPHA(I,2)=(-ALPHA(I,1))*ALPHA(K,4)+ALPHA(I,2)
                ALPHA(I,3)=ALPHA(I,3)/ALPHA(I,2)
           BETA(I)=((-ALPHA(I,1))*BETA(K)+BETA(I))/ALPHA(I,2)
                ALPHA(J,2)=(-ALPHA(J,1))*ALPHA(K,4)+ALPHA(J,2)
                ALPHA(J,3)=(-ALPHA(J,2))*ALPHA(I,3)+ALPHA(J,3)
                ALPHA(J,4)=ALPHA(J,4)/ALPHA(J,3)
           BETA(J)=(((-ALPHA(J,1))*BETA(K)+BETA(J))-ALPHA(J,2)
     *                   *BETA(I))/ALPHA(J,3)
           ELSE
           K=I-1
                ALPHA(I,4)=(-ALPHA(I,3))*ALPHA(K,4)+ALPHA(I,4)
           BETA(I)=((-ALPHA(I,3))*BETA(K)+BETA(I))/ALPHA(I,4)
           ALPHA(I,4)=1.00D0
           ENDIF
 10   CONTINUE
      DO 11 I=M-1,1,(-2)
C      loop 11 nulifies all values to the right from diagonal
      J=I+1
      K=I-1
           IF(I.NE.1)THEN
                BETA(I)=(-ALPHA(I,4))*BETA(J)+BETA(I)
                BETA(K)=(-ALPHA(K,3))*BETA(I)+BETA(K)
           ELSE
                BETA(I)=(-ALPHA(I,4))*BETA(J)+BETA(I)
           ENDIF
 11   CONTINUE
C
C      Loop 12 is changing matrix X(i), for finding the new
C      values of ALPHA and BETA. Matrix X(i) is sent to
C      subroutine USERFUN for new iteration.
      DO 300 I=1,M
c            WRITE(92,*) 'X',I,'=',BETA(I)
 300  CONTINUE
      DO 12 I=1,M
           X(I)=BETA(I)
 12   CONTINUE
      END
******************************************
```

```
      SUBROUTINE INLINE (LENGTH,XLEN,N)
      INTEGER NP
      PARAMETER (NP=2000)
      REAL LENGTH(NP),XLEN(NP)
        DO 02 M=1,N-1
                 P=M+1
            IF(LENGTH(M).LE.LENGTH(P))THEN
                 XLEN(M)=LENGTH(M)
            ELSE
                 XLEN(M)=LENGTH(P)
            ENDIF
 02     CONTINUE
C
      END
CCCCCCCCCCCCCCCCCCCCCCCCCCCCCCCCCCCCCCCCCCCCCCCCCCCCCCCCCCCCCCCCCC


      SUBROUTINE CHANGE(N,NUM,LENGTH,WEIGHM,DEPTH,
    &           EMODUL,INERTIA, WEIGHT,XV,F,DONE,PSI)
      INTEGER N,NP,NUM
      PARAMETER (NP=2000)
      REAL LENGTH(NP),WEIGHM(NP),DEPTH(NP),EMODUL(NP),INERTIA(NP)
      REAL XV(NP),F(NP),WEIGHT(NP)
      REAL CRACK,PSI
      LOGICAL DONE
***************************************************************
C    DONE  logical which skips or enters block 1 set in ISSAC
C    NUM   number of the cantilever with highest tensile stress
C    CRACK weight of the NUM cant. scaled to the length of NUM-1 cant.
********************************************
*block 1-
*********************************************
    IF(.NOT.DONE)THEN
**********************************************************************************
*BLOCK 1.1-increases the weight of the NUM-1 cant. by the weight of  *
*          the failed cant. N scaled to the length of the NUM-1 cant.*
**********************************************************************************
          IF (NUM.NE.1)THEN
       IF(LENGTH(I)/TAN(PSI).GT.DEPTH(I))THEN
               CRACK=(WEIGHM(NUM)*LENGTH(NUM))/LENGTH(NUM-1)
               WEIGHM(NUM-1)=WEIGHM(NUM-1)+CRACK
       ENDIF
             F(NUM-1)=F(NUM-1)+F(NUM)
          ENDIF
**************************************************************
*BLOCK 1.2-renumbers all cants. above the broken one*
**************************************************************
            IF (NUM.LT.N)THEN
                 DO 1 I=NUM,N-1
                       LENGTH(I) =LENGTH(I+1)
                       WEIGHM(I) =WEIGHM(I+1)
```

```
                      WEIGHT(I) =WEIGHT(I+1)
                      DEPTH(I)  =DEPTH(I+1)
                      EMODUL(I) =EMODUL(I+1)
                      INERTIA(I)=INERTIA(I+1)
                      XV(I)     =XV(I+1)
                      F(I)      =F(I+1)
 1                  CONTINUE
               ENDIF
     ENDIF
500     N=N-1
101     END
CCCCCCCCCCCCCCCCCCCCCCCCCCCCCCCCCCCCCCCCCCCCCCCCCCCCCCCCCCCCCC



      SUBROUTINE ITER(N,AN,AB,WEIGHM,LENGTH,INERTIA,EMODUL,PSI,
     &        XV,XLEN,REAC,ALPHA,BETA,X,DAB,F)
       INTEGER N,NP,NB,AN,AB,DAB
       INTEGER I,J
       PARAMETER (NP=2000)
       REAL EMODUL(NP),PSI
       REAL WEIGHM(NP),LENGTH(NP),XLEN(NP),INERTIA(NP)
       REAL F(NP),XV(NP)
       DOUBLE PRECISION ALPHA(NP,4),BETA(NP)
       REAL X(NP),RHOLD(NP),REAC(NP)
200      NB=AB-AN+1
       CALL USRFUN(AN,AB,NB,WEIGHM,LENGTH,INERTIA,EMODUL,PSI,
     &        XV,ALPHA,BETA,XLEN,F)
C    IF (N.GT.745)THEN
C    PRINT*,' REACTIONS RETURN'
C    PRINT*,'AN=',AN,'     AB=',AB
C    ENDIF
       CALL NEWTON(NB,ALPHA,BETA,X)
c      write (92,*)'******************************'
       DO 404 I=AN,AB
            REAC(I)=0.0
404     CONTINUE
       J=AN
       DO 14 I=1,2*NB-3,2
            REAC(J)=X(I)
            J=J+1
14      CONTINUE
C    IF (N.GT.745)THEN
C    PRINT*,'REAC AB-1 =',REAC(AB-1)
C    ENDIF
     IF(AB+1.LE.N.AND.REAC(AB-1).GT.0.D0)THEN
            DO 15 I=AN,AB-1
                 RHOLD(I)=REAC(I)
 15            CONTINUE
                      AB=AB+1
                      IF(AB.EQ.DAB)GO TO 300
```

```
              GO TO 200
C
      ELSEIF(AB+1.LE.N.AND.REAC(AB-1).LE.0.D0)THEN
             REAC(AB-1)=0.0D0
          IF (AB-AN.GT.1)THEN
             DO 16 I=AN,AB-2
                 REAC(I)=RHOLD(I)
 16           CONTINUE
          ENDIF
             AN=AB
        AB=DAB+1
             GO TO 300
      ELSEIF(AB.EQ.N.AND.REAC(AB-1).GT.0.D0)THEN
             GO TO 300
      ELSEIF(AB.EQ.N.AND.REAC(AB-1).LE.0.D0)THEN
             REAC(AB-1)=0.00D0
          IF (AB-AN.GT.1)THEN
             DO 18 I=AN,AB-2
                 REAC(I)=RHOLD(I)
 18           CONTINUE
          ENDIF
      ELSE
 300  ENDIF
      END
******************************************************************


       SUBROUTINE ITERUN(N,AN,AB,WEIGHM,LENGTH,INERTIA,
     &     EMODUL,PSI,XV,XLEN,REAC,ALPHA,BETA,X,F)
       INTEGER N,NP,NB,AN,AB
       INTEGER I,J
       PARAMETER (NP=2000)
       REAL EMODUL(NP),PSI
       REAL WEIGHM(NP),LENGTH(NP),XLEN(NP),INERTIA(NP)
       REAL F(NP),XV(NP)
       DOUBLE PRECISION ALPHA(NP,4),BETA(NP)
       REAL X(NP),RHOLD(NP),REAC(NP)
200      NB=AB-AN+1
       CALL USRFUN(AN,AB,NB,WEIGHM,LENGTH,INERTIA,EMODUL,PSI,
     &     XV,ALPHA,BETA,XLEN,F)
C     IF (N.GT.745)THEN
C     PRINT*, ' TO THE END'
C     PRINT*,'AN=',AN,'     AB=,',AB,'NB=',NB,'N=',N
C     ENDIF
       CALL NEWTON(NB,ALPHA,BETA,X)
c      write (92,*)'*******************************'
       DO 404 I=AN,AB
             REAC(I)=0.0
404     CONTINUE
       J=AN
       DO 14 I=1,2*NB-3,2
```

```
                REAC(J)=X(I)
                J=J+1
14        CONTINUE
C     IF (N.GT.745)THEN
C     PRINT*,'REAC (AB-1)=',REAC(AB-1)
C     ENDIF
      IF(AB+1.LE.N.AND.REAC(AB-1).GT.0.D0)THEN
                DO 15 I=AN,AB-1
                    RHOLD(I)=REAC(I)
 15              CONTINUE
                           AB=AB+1
                 GO TO 200
C
      ELSEIF(AB+1.LE.N.AND.REAC(AB-1).LE.0.D0)THEN
                REAC(AB-1)=0.0D0
            IF (AB-AN.GT.1)THEN
                DO 16 I=AN,AB-2
                    REAC(I)=RHOLD(I)
 16              CONTINUE
            ENDIF
                AN=AB
                AB=AN+1
                GO TO 200
C
      ELSEIF(AB.EQ.N.AND.REAC(AB-1).GT.0.D0)THEN
                GO TO 350
C
      ELSEIF(AB.EQ.N.AND.REAC(AB-1).LE.0.D0)THEN
                REAC(AB-1)=0.00D0
            IF (AB-AN.GT.1)THEN
                DO 18 I=AN,AB-2
                    REAC(I)=RHOLD(I)
 18              CONTINUE
            ENDIF
      ELSE
 350  ENDIF
        END
CCCCCCCCCCCCCCCCCCCCCCCCCCCCCCCCCCCCCCCCCCCCCCCCCCCC


        SUBROUTINE CHAN  (DEPTH,ND,NUM,COUNT,DONE,NOR)
        INTEGER NP
        PARAMETER (NP=2000)
        INTEGER I,J,K,L,NOR
        INTEGER ND,NUM,COUNT
        INTEGER CANT(NP,3)
        REAL DEPTH(NP),DEP(NP),LEN(NP)
        REAL XBEGIN,XEND,XF
        COMMON /BBBA/ DEP
        LOGICAL DONE
        CHARACTER*4 FAILED(NP)
      OPEN(UNIT=96,FILE='RESULT.DAT')
*****************************************************
C    DONE  logical which skips or enters block 1 set in ISSAC
C    NUM   number of the cantilever with highest tensile stress
C    NOR   the original number of cants. before any cant. is
C          broken of; (N original)
C    CANT  real with 3 columns:
C                    column 1....original cantilever number
C                    column 2....failed (0) or not failed (cant. no.)
C                    column 3....order in which the cant. failed
C    FAILED character marking the failed cant.
C    COUNT logical real originally set in ISSAC which skips
C          or enters block 1.1 and then counts the failed cantilevers
C          and sets the column 3 of CANT in the block 3
************************************************************************
*BLOCK 1.1-sets the starting valules to CANT and then it is switched of*
************************************************************************
          IF(COUNT.EQ.0)THEN
               DO 2 I=1,NOR
                    K=I
                    CANT(I,1)=K
                    CANT(I,2)=K
                    CANT(I,3)=0
 2             CONTINUE
          ENDIF
******************************************************************
*BLOCK 1.2-finds the distance of the broken block from the beginning*
******************************************************************
    IF (.NOT.DONE) THEN
5        XEND=0.0
        XBEGIN=0.0
        DO 6 I=1,NUM
             XEND=XEND+DEPTH(I)
6        CONTINUE
        XBEGIN=XEND-DEPTH(NUM)
C
*************************************************************
*BLOCK 1.3- renumbers elementary blocks behind the broken block*
*        and changes the number ND of elementary blocks      *
*************************************************************
        XF=0.0
770      DO 77 L=1,ND
          XF=XF+DEP(L)
          IF (XF.GT.XBEGIN.AND.XF.LE.XEND)THEN
**********************************
*BLOCK 1.3.4-sets the values of CANT*
**********************************
          COUNT=COUNT+1
          DO 3 I=1,NOR
               IF(CANT(I,2).EQ.L)THEN
                    CANT(I,3)=COUNT
```

```
                       CANT(I,2)=0
                       K=I+1
                       IF(K.LT.NOR)THEN
                             DO 4 J=K,NOR
                                 IF(CANT(J,2).NE.0)THEN
                                     CANT(J,2)=CANT(J,2)-1
                                  ENDIF
4                             CONTINUE
                             GO TO 100
                       ENDIF
                 ENDIF
3          CONTINUE
100             XEND=XEND-DEP(L)
                 DO 78 J=L,ND-1
                       DEP(J)=DEP(J+1)
78                CONTINUE
                 ND=ND-1
           ENDIF
           IF (XF.GT.XEND)THEN
                  GO TO 79
           ELSE
                 IF (XF.GT.XBEGIN) THEN
                       XF=0.0
                       GO TO 771
                 ENDIF
           ENDIF
77     CONTINUE
771    GO TO 770
    ENDIF
****************************************************************
*END OF THE BLOCK 1                                   *
*****************************************************************
C79     DO 200 I=1,NOR
C              PRINT*,CANT(I,1),CANT(I,2),CANT(I,3)
C200    CONTINUE
****************************************************************************************
*BLOCK 2-when the breaking is "DONE" block 2 writes the results of breaking*
****************************************************************************************
79   IF(DONE)THEN
            DO 55 I=1,NOR
                  FAILED(I)='G'
                  IF(CANT(I,2).EQ.0)THEN
                        FAILED(I)='FAIL'
                  ENDIF
55           CONTINUE
***********************************************************
      IF (NOR.EQ.0)THEN
    REWIND(UNIT=10)
            READ (10,331)ND
331           FORMAT (/,T8,I4)
            READ (10,332)
```

```
332            FORMAT(2X)
         DO 333 I=1,ND
            READ(10,334)LEN(I)
334            FORMAT(T15,F6.2)
              IF(I.GT.10) THEN
                   IF(LEN(I).LT.0.4)THEN
                        ND=I-1
                        NOR=ND
                        GO TO 434
                   ENDIF
              ENDIF
333        CONTINUE
          NOR=ND
434          DO 355 I=1,NOR
                  FAILED(I)='G'
355           CONTINUE
335            WRITE(96,91)NOR
91            FORMAT(T8,I5)
            WRITE(96,81)
81           FORMAT(T10,'CANT.NO.')
            DO 561 I=1,NOR
                 K=I
                   WRITE(96,71)K,FAILED(I)
 71                FORMAT(T15,I3,T30,A)
561           CONTINUE
      STOP
      ENDIF
**************************************************************
            WRITE(96,9)NOR
9           FORMAT(T8,I5)
            WRITE(96,8)
 8          FORMAT(T10,'CANT.NO.')
            DO 56 I=1,NOR
                  K=I
                  WRITE(96,7)K,FAILED(I)
 7                FORMAT(T15,I3,T30,A)
56          CONTINUE
    ENDIF
* *************************************************************
C   If the breaking was not finished block 2 was skipped and
C   the number of cantilevers is decreased by 1 to N-1, then
C   the program returns to ISSAC, to calculate new reactions
****************************************************************
      END
CCCCCCCCCCCCCCCCCCCCCCCCCCCCCCCCCCCCCCCCCCCCCCCC
```

```
 SUBROUTINE INERT(N,NP,BHAT,DEPTH,INERTIA)
       INTEGER N,NP
       REAL BHAT,DEPTH(NP),INERTIA(NP)
       DO 601 I=1,N
            INERTIA(I)=0.0D0
            INERTIA(I)=(BHAT*DEPTH(I)**3)/12.D00
601     CONTINUE
       END
**************************************************

    SUBROUTINE MOMENT (N,WEIGHM,LENGTH,INERTIA,PSI,EMODUL,
   &                  NOR,XV,REAC,XLEN,F,DEPTH,GAMA,BHAT,
   &                DIS,DIST,COHESION,FI,WEIGHT,TEST,NUM,ND,TIP)
       INTEGER NP,N,KN,ND,NOR,DIS,CHEC
       INTEGER I,K,J,NUM,KCRIT
       PARAMETER (NP=2000)
       INTEGER STORE(NP)
       REAL COHES,COHESION(10),FIK,FI(10)
       REAL DIST(10),STRE,KOEF
       REAL REAC(NP),MOMEN(NP),STRES(NP),GAMA,BHAT,SPLIT
       REAL PSI,GAMAW,GAMW,DEPTH(NP),WEIGHT(NP),STREN(NP),SF(NP)
       REAL WEIGHM(NP),LENGTH(NP),XLEN(NP),INERTIA(NP),EMODUL(NP)
       REAL F(NP),XV(NP),SHEAR(NP),SHEAV(NP),TEST,TIP
       REAL LEN(NP),DEP(NP),EMOD(NP),WAT(NP),FF(NP)
       LOGICAL RETURN,RDATA
       COMMON /ABBA/ RDATA,KOEF
       COMMON /BBBA/ DEP
       PARAMETER (GAMAW=9.81D03)
       GAMW=GAMAW*SIN(PSI)/6.D0
C       for the first cantilever the reaction from below and the loading
C       caused by the water below are zero.
C
*****************************
* block 1 reads data        *
*****************************
       IF (RDATA) THEN
         RDATA=.FALSE.
            READ (10,1)ND
1           FORMAT (/,T8,I4)
            READ (10,2)
2           FORMAT(2X)
          DO 3 I=1,ND
         READ(24,244)FF(I)
244       FORMAT(T39,E13.7)
            READ(10,4)K,LEN(I),DEP(I),EMOD(I),WAT(I)
4           FORMAT(T2,I3,T15,F6.2,T30,F6.2,T48,E10.3,T69,F6.2)
              IF(I.GT.10) THEN
                  IF(LEN(I).LT.0.4)THEN
                      ND=I-1
                      NOR=ND
                      GO TO 55
```

```
                 ENDIF
              ENDIF
3            CONTINUE
             NOR=ND
          ENDIF
*****************************************************
*block 1
55       DO 300 I=1,2*(N-1)
              MOMEN(I)=0.0
              SHEAR(I)=0.0
              SHEAV(I)=0.0
 300     CONTINUE
             MOMEN(1)=(WEIGHM(1)/2)*LENGTH(1)**2
    &                 +(REAC(1)*XLEN(1))
    &                 +GAMW*XV(1)**3
    &                 +F(1)*LENGTH(1)
C
             SHEAV(1)=((WEIGHM(1)*LENGTH(1)**2)/2+REAC(1)*XLEN(1)
    &            +F(1)*LENGTH(1)+GAMW*(XV(1)**3))/LENGTH(1)

        DO 10 I=2,N-1
             J=2*I-2
             K=2*I-1
             MOMEN(I)=(WEIGHM(I)/2)*LENGTH(I)**2
    &                 +(REAC(I)*XLEN(I))-(REAC(I-1)*XLEN(I-1))
    &                 -GAMW*XV(J)**3+GAMW*XV(K)**3
    &                 +F(I)*LENGTH(I)
             SHEAV(I)=((WEIGHM(I)*LENGTH(I)**2)/2+REAC(I)*XLEN(I)
    &            -REAC(I-1)*XLEN(I-1)+F(1)*LENGTH(1)
    &            +GAMW*(XV(I)**3-XV(I-1)**3))/LENGTH(I)
 10      CONTINUE

C        For the last cantilever the reaction from above is zero.
             J=2*N-2
             K=2*N-1
             MOMEN(N)=(WEIGHM(N)/2)*LENGTH(N)**2
    &                  -(REAC(N-1)*XLEN(N-1))
    &                 -GAMW*XV(J)**3+GAMW*XV(K)**3
    &                 +F(N)*LENGTH(N)
             SHEAV(I)=((WEIGHM(N)*LENGTH(N)**2)/2
    &            -REAC(N-1)*XLEN(N-1)+F(N)*LENGTH(N)
    &            +GAMW*(XV(N)**3-XV(N-1)**3))/LENGTH(N)
C
*****************************************************
C  The next block calculates  shear stresses, and shear forces
C  and tests if the resulting SF is greater than 1.
*****************************************************
        XCANT=0.0
        DO 11 I=1,N
           XCANT=XCANT+DEPTH(I)
           DO 600 J=1,DIS
```

```
                   IF((XCANT-DEPTH(I)/2.).EQ.DIST(J))THEN
                        IF(FI(J).LE.FI(J+1))THEN
                                COHES=COHESION(J)
                                FIK=FI(J)
                                GO TO 601
                        ELSE
                                IF(J.LT.DIS)THEN
                                     COHES=COHESION(J+1)
                                     FIK=FI(J+1)
                                     GO TO 601
                                ELSE
                                     COHES=COHESION(J)
                                     FIK=FI(J)
                                     GO TO 601
                                ENDIF
                        ENDIF
                   ELSEIF((XCANT-DEPTH(I)/2.).LT.DIST(J))THEN
                                COHES=COHESION(J)
                                FIK=FI(J)
                                GO TO 601
                   ENDIF
600          CONTINUE
601              QMAX=0.0
               STRE=0.0
               QMAX=(BHAT/2.)*(DEPTH(I)**2/4)
               SHEAR(I)=((SHEAV(I)*QMAX)/(INERTIA(I)*BHAT))/1000.
               STRE=(REAC(I)+F(I)+(GAMAW*XV(I)**2)/2
     &                 +(WEIGHM(I)*LENGTH(I))/2)/(LENGTH(I)*BHAT)
                   STREN(I)=COHES+STRE*TAN(FIK)/1000.
               SF(I)=STREN(I)/SHEAR(I)
  11       CONTINUE
     IF(CHEC.EQ.0)THEN
                DO 147 I=1,N
                       WRITE(65,*)I,'SF=',SF(I)
147               CONTINUE
          CHEC=10
     ENDIF
C Loop 14 finds the smallest SF which is less then 1.1
400       RETURN=.FALSE.
         SPLIT=1.1
         TIP=1.1
         K=1
  14     IF(ABS(SF(K)).LT.SPLIT)THEN
                DO 144 J=1,KN
                        IF(STORE(J).EQ.K)GO TO 145
144               CONTINUE
                SPLIT=SF(K)
                TIP=SPLIT
                KCRIT=K
         ENDIF
 145      IF(K.LT.N)THEN
```

```
              K=K+1
              GO TO 14
          ENDIF
C   The next block calls DEVIDE if  SPLIT is less then 1.0.
         IF (SPLIT.LE.1.0) THEN
              CALL DEVIDE (KCRIT,N,LENGTH,DEPTH,XV,EMODUL,STORE,
     &           KN,ND ,NOR,GAMA,BHAT,PSI,WEIGHT,WEIGHM,RETURN
     &                ,LEN,EMOD,WAT,F,FF)
              IF(RETURN)THEN
                        GO TO 400
              ENDIF
              IF (N.NE.ND)THEN
                   GO TO 15
              ELSE
                   GO TO 148
              ENDIF
         ELSE
C              DO 146 I=1,KN
C                     WRITE(65,*)I,'STORE=',STORE(I)
C146              CONTINUE
148            PRINT*,'DEVIDING FINISHED-THE REST STABILE'
         ENDIF
         CALL INERT(N,NP,BHAT,DEPTH,INERTIA)
         DO 13 I=1,N
              STRES(I)=(MOMEN(I)*DEPTH(I))/(2*INERTIA(I))
     &           -(WEIGHT(I)*LENGTH(I))/(DEPTH(I)*BHAT)
     &           -F(I)*(sin(psi)/cos(psi))/(DEPTH(I)*BHAT)
              STRES(I)=STRES(I)/1000.
13       CONTINUE
         TEST=0.
         DO 12 I=1,N
              IF (STRES(I).GT.TEST)THEN
                   TEST=STRES(I)
                   NUM=I
              ENDIF
12       CONTINUE
15       END

****************************************************************


      SUBROUTINE DEVIDE(KCRIT,N,LENGTH,DEPTH,XV,EMODUL,STORE,
     &           KN,ND ,NOR,GAMA,BHAT,PSI,WEIGHT,WEIGHM,RETURN
     &                ,LEN,EMOD,WAT,F,FF)
         INTEGER KCRIT,DOWN,NP,I,NUM,NUME,KN
         INTEGER ND,NOR
         INTEGER N
         PARAMETER (NP=2000)
         INTEGER STORE(NP)
         REAL XEND,XCENT,XBEGIN,XFCENT,WEST,BOTTOM,LAN,EMO
         REAL LEN(NP),DEP(NP),WAT(NP),EMOD(NP),GAMA,BHAT,PSI
      REAL LENGTH(NP),DEPTH(NP),XV(NP),EMODUL(NP),F(NP),FF(NP)
      REAL WEIGHM(NP),WEIGHT(NP),KOEF,FORCE
      LOGICAL SKIP,RETURN,RDATA
      COMMON /ABBA/ RDATA,KOEF
      COMMON /BBBA/ DEP
      SKIP=.FALSE.
*********************************************************
*block 2 finds distances to the beginning,end and the centre *
*       of the critical block                       *
*********************************************************
      XEND=0.0
      XCENT=0.0
      XBEGIN=0.0
      DO 6 I=1,KCRIT
           XEND=XEND+DEPTH(I)
6       CONTINUE
      XCENT=XEND-DEPTH(KCRIT)/2
      XBEGIN=XEND-DEPTH(KCRIT)
********************************************************
*blocks 3,4  find the geometry ala bl. 2 for elementary blocks*
********************************************************
      XFEND=0.0
      DO 77 I=1,ND
            XFEND=XFEND+DEP(I)
            IF(XFEND.GE.XEND)THEN
                  NUME=I
                  GO TO 100
            ENDIF
77      CONTINUE
***********************************
*    block 4                                        *
***********************************
100     XFCENT=0.0
      DO 7 I=1,ND
            XFCENT=XFCENT+DEP(I)
             IF(XFCENT.GE.XCENT.AND.XEND-DEP(NUME).NE.XBEGIN)THEN
                  IF(XFCENT.EQ.XEND)THEN
                        XFCENT=XFCENT-DEP(I)
                        NUM=I-1
                        GO TO 101
                  ELSE
                       NUM=I
                       GO TO 101
                  ENDIF
            ENDIF
7       CONTINUE
********************************************************
*block 5 tests if the critical block is elementary or composed              *
********************************************************
101     IF(XEND-DEP(NUME).EQ.XBEGIN)THEN
            KN=KN+1
```

```
          STORE(KN)=KCRIT
          SKIP=.TRUE.
          RETURN=.TRUE.
     ENDIF
*******************************************************
*block 6 - if crit. cant. is composed, bl.6 calculates the sizes*
*        of new blocks, and renumberes blocks up the slope    *
*******************************************************
    IF (.NOT.SKIP)THEN
         N=N+1
         IF(KCRIT.LT.N-1)THEN
            DO 8 I=N,KCRIT+2,-1
                DEPTH(I) =DEPTH(I-1)
                LENGTH(I)=LENGTH(I-1)
           F(I)     =F(I-1)
                EMODUL(I)=EMODUL(I-1)
                XV(I)    =XV(I-1)
                WEIGHM(I)=WEIGHM(I-1)
                WEIGHT(I)=WEIGHT(I-1)
8           CONTINUE
            DO 88 I=1,KN
               IF(STORE(I).GT.KCRIT)THEN
                    STORE(I)=STORE(I)+1
               ENDIF
 88         CONTINUE
        ENDIF
         DEPTH(KCRIT)=XFCENT-XBEGIN
         DEPTH(KCRIT+1)=XEND-XFCENT
C
c   Loop 9 calculates parameters for the first split block
         WEST=0.0
         DOWN=0.0
         BOTTOM=0.0
       FORCE=0.0
         EMO=0.0
         LAN=0.0
         DO 9 I=1,ND
            WEST=WEST+DEP(I)
            IF (WEST.GT.XBEGIN.AND.WEST.LE.XFCENT)THEN
               LAN=LAN+LEN(I)
               EMO=EMO+EMOD(I)*DEP(I)
               DOWN=DOWN+1
               BOTTOM=BOTTOM+DEP(I)
          FORCE=FORCE+FF(I)
            ENDIF
            IF (WEST.GT.XFCENT)GO TO 110
9        CONTINUE
110       LENGTH(KCRIT)=LAN/DOWN
        EMODUL(KCRIT)=EMO/BOTTOM
      F(KCRIT)     =FORCE
        IF (WAT(NUM).LT.LENGTH(KCRIT))THEN
```

```
                    XV(KCRIT)=WAT(NUM)
                ELSE
                    XV(KCRIT)=LENGTH(KCRIT)*0.98
                ENDIF
                WEIGHM(KCRIT) =GAMA*DEPTH(KCRIT)*BHAT*COS(PSI)*KOEF
                WEIGHT(KCRIT) =GAMA*DEPTH(KCRIT)*BHAT*SIN(PSI)
c loop 10 calculates the parameters for the second split block
                WEST=0.0
                DOWN=0.0
                BOTTOM=0.0
              FORCE=0.0
                EMO=0.0
                LAN=0.0
                DO 10 I=1,ND
                    WEST=WEST+DEP(I)
                    IF (WEST.GT.XFCENT.AND.WEST.LE.XEND)THEN
                        LAN=LAN+LEN(I)
                        EMO=EMO+EMOD(I)*DEP(I)
                        DOWN=DOWN+1
                        BOTTOM=BOTTOM+DEP(I)
                  FORCE=FORCE+FF(I)
                    ENDIF
                    IF (WEST.GT.XEND)GO TO 111
10              CONTINUE
111              LENGTH(KCRIT+1)=LAN/DOWN
                EMODUL(KCRIT+1)=EMO/BOTTOM
              F(KCRIT+1)          =FORCE
                IF (WAT(NUME).LT.LENGTH(KCRIT+1))THEN
                    XV(KCRIT+1)=WAT(NUME)
                ELSE
                    XV(KCRIT+1)=LENGTH(KCRIT+1)*0.98
                ENDIF
                WEIGHM(KCRIT+1)=GAMA*DEPTH(KCRIT+1)*BHAT*COS(PSI)*KOEF
                WEIGHT(KCRIT+1)=GAMA*DEPTH(KCRIT+1)*BHAT*SIN(PSI)
            ENDIF
            DO 11 I=1,N
            WRITE(11,*)I,'       DEPTH=',DEPTH(I)
11                CONTINUE
                IF (ND.EQ.N)THEN
                  PRINT*,'DEVIDING FINISHED'
                ENDIF
             END
```

I.5. Subroutine Deflex.

Subroutine deflex calculates deflections of the cantilevers in the slope.

```
      SUBROUTINE DEFLEX(N,WEIGHM,LENGTH,INERTIA,EMODUL,PSI,LAN,
     &                  XQ,X,XLEN)
      INTEGER NP,N
      INTEGER R,I,J,K,M
      PARAMETER (NP=200)
      DOUBLE PRECISION X(NP),Y(NP)
      DOUBLE PRECISION EMODUL(NP),PSI,GAMAW,GAMW
      DOUBLE PRECISION WEIGHM(NP),LENGTH(NP),XLEN(NP),INERTIA(NP)
      DOUBLE PRECISION UR(NP),F(NP),Q(NP),XQ(NP),UQ,LAN(NP)
      PARAMETER (GAMAW=9.81D03)
      GAMW=GAMAW*SIN(PSI)/120.D0
C      for the first cantilever the reaction from below and the loading
C      caused by the water below are zero.
C
      DO 300 I=1,2*(N-1)
            Y(I)=0.0
 300  CONTINUE
      IF (LAN(1).LT.LAN(2))THEN
     Y(1)=((WEIGHM(1)/24)*(-LENGTH(1)**3*(LENGTH(1)-4*XLEN(1)))
     &  +(X(1)/6)*2*(XLEN(1)**3)
     &  +(Q(1)/6)*(-(LENGTH(1)/2)**2*((LENGTH(1)/2)-3*XLEN(1))
     &  +(F(1)/6)*(-LENGTH(1)**2)*(LENGTH(1)-3*XLEN(1))
     &  -GAMW*(-XV(1)**4)*(XV(1)-5*XLEN(1))
     &  )/(EMODUL(1)*INERTIA(1))
      ELSE
            IF(LENGTH(1)/2.LT.XLEN(1))THEN
                  UQ=0.0D0
                  ELSE
                  UQ=1.0D0
            ENDIF

     Y(1)=((WEIGHM(1)/24)*((LENGTH(1)-XLEN(1))**4
     &               -LENGTH(1)**3*(LENGTH(1)-4*XLEN(1)))
     &  +(X(1)/6)*2*(XLEN(1)**3)
     &  +(Q(1)/6)*((LENGTH(1)/2-XLEN(1))**3*UQ
     &              -LENGTH(1)/2**2*((LENGTH(1)/2)-3*XLEN(1)))
     &  +(F(1)/6)*((LENGTH(1)-XLEN(1))**3
     &               -LENGTH(1)**2*(LENGTH(1)-3*XLEN(1)))
     &  -GAMW*(-XV(1)**4)*(XV(1)-5*XLEN(1))
     &   /(EMODUL(1)*INERTIA(1))
      ENDIF
C      J is smaller than I
C      X(J).............reaction with the lower cantilever
C      X(K).............reaction with the upper cantilever
C      X(I).............tangent at the contact with the lower cantilever
C      X(L).............tangent at the contact with the upper cantilever
```

```
C      ..(M)............related to the upper cantilever
C      ..(L)............related to the lower cantilever
C      unknowns X() are related to the indexis of function (J,I);the rest
C      of the expressions (constants) are related by their indexis (M,O) to
C      the number of the cantilever they are acting on.

       IF(N.GT.2)THEN

       DO 10 M=2,N-1
            R=M-1
            J=2*M-3
            I=2*M-2
            K=2*M-1

        IF(LAN(M).GT.LAN(M-1).AND.LAN(M).LT.LAN(M+1))THEN


C           ______________________________________________
C  m+1 [____________________________________________
C  m        [______________________________________
C  m-1            [___________________________
C

C       crossection 1, closer to the beginning of the cantilever

            IF(LENGTH(N)/2.LT.XLEN(R))THEN
                  UQ=0.0D0
                  ELSE
                  UQ=1.0D0
            ENDIF

      Y(I)=((WEIGHM(M)/24)*((LENGTH(M)-XLEN(R))**4
     &             -LENGTH(M)**3*(LENGTH(M)-4*XLEN(R)))
     &  -(X(J)/6)*2*(XLEN(R)**3)
     &  +(X(K)/6)*((XLEN(M)-XLEN(R))**3-XLEN(M)**2*(XLEN(M)-3*XLEN(R)))
     &  +(Q(M)/6)*((LENGTH(M)/2-XLEN(R))**3*UQ
     &             -(LENGTH(M)/2)**2*((LENGTH(M)/2)-3*XLEN(R)))
     &  +(F(M)/6)*((LENGTH(M)-XLEN(R))**3
     &             -LENGTH(M)**2*(LENGTH(M)-3*XLEN(R)))
     &  +GAMW*(-XV(K)**4)*(XV(K)-5*XLEN(R))
     &  -GAMW*(-XV(I)**4)*(XV(I)-5*XLEN(R))
     &  )/(EMODUL(M)*INERTIA(M))
C

C       crossection 2, closer to the end of the cantilever


      Y(K)=((WEIGHM(M)/24)*(-LENGTH(M)**3*(LENGTH(M)-4*XLEN(M)))
     &  -(X(J)/6)*(-XLEN(R)**2*(XLEN(R)-3*XLEN(M)))
     &  +(X(K)/6)*(-XLEN(M)**2*(XLEN(M)-3*XLEN(M)))
     &  +(Q(M)/6)*(-(LENGTH(M)/2)**2*((LENGTH(M)/2)-3*XLEN(M)))
     &   +(F(M)/6)*(-LENGTH(M)**2*(LENGTH(M)-3*XLEN(M)))
     &   +GAMW*(-XV(K)**4)*(XV(K)-5*XLEN(M))
     &   -GAMW*(-XV(I)**4)*(XV(I)-5*XLEN(M))
     &   )/(EMODUL(M)*INERTIA(M))


      ELSEIF(LAN(M).GT.LAN(M-1).AND.LAN(M).GT.LAN(M+1))THEN


C                  ____________________________
C  m+1      ____[____________________________
C  m    [________________________________
C  m-1              [______________________

C


C       crossection 1, closer to the beginning of the cantilever

            IF(XLEN(M).GT.XLEN(R))THEN
                  UR(M)=1.0D0
                  ELSE
                  UR(M)=0.0D0
            ENDIF
            IF(LENGTH(N)/2.LT.XLEN(R))THEN
                  UQ=0.0D0
                  ELSE
                  UQ=1.0D0
            ENDIF

      Y(I)=((WEIGHM(M)/24)*((LENGTH(M)-XLEN(R))**4
     &                  -LENGTH(M)**3*(LENGTH(M)-4*XLEN(R)))
     &   -(X(J)/6)*2*(XLEN(R)**3)
     &   +(X(K)/6)*((XLEN(M)-XLEN(R))**3*UR(M)
     &                  -XLEN(M)**2*(XLEN(M)-3*XLEN(R)))
     &   +(Q(M)/6)*((LENGTH(M)/2-XLEN(R))**3*UQ
     &                 -(LENGTH(M)/2)**2*((LENGTH(M)/2)-3*XLEN(R)))
     &   +(F(M)/6)*((LENGTH(M)-XLEN(R))**3
     &                  -LENGTH(M)**2*(LENGTH(M)-3*XLEN(R)))
     &   +GAMW*(-XV(K)**4)*(XV(K)-5*XLEN(R))
     &   -GAMW*(-XV(I)**4)*(XV(I)-5*XLEN(R))
     &   )/(EMODUL(M)*INERTIA(M))
C

C       crossection 2, closer to the end of the cantilever

            IF(XLEN(M).GT.XLEN(R))THEN
                  UR(R)=0.0D0
                  ELSE
                  UR(R)=1.0D0
            ENDIF
            IF(LENGTH(N)/2.LT.XLEN(M))THEN
                  UQ=0.0D0
                  ELSE
                  UQ=1.0D0
            ENDIF


      Y(K)=((WEIGHM(M)/24)*((LENGTH(M)-XLEN(M))**4
     &              -LENGTH(M)**3*(LENGTH(M)-4*XLEN(M)))
     &   -(X(J)/6)*((XLEN(R)-XLEN(M))**3*UR(R)
     &              -XLEN(R)**2*(XLEN(R)-3*XLEN(M)))
     &   +(X(K)/6)*(-XLEN(M)**2*(XLEN(M)-3*XLEN(M)))
     &   +(Q(M)/6)*((LENGTH(M)/2-XLEN(M))**3*UQ
     &              -(LENGTH(M)/2)**2*((LENGTH(M)/2)-3*XLEN(M)))
     &   +(F(M)/6)*((LENGTH(M)-XLEN(M))**3
     &              -LENGTH(M)**2*(LENGTH(M)-3*XLEN(M)))
     &   +GAMW*(-XV(K)**4)*(XV(K)-5*XLEN(M))
     &   -GAMW*(-XV(I)**4)*(XV(I)-5*XLEN(M))
     &  )/(EMODUL(M)*INERTIA(M))

      ELSEIF(LAN(M).LT.LAN(M-1).AND.LAN(M).GT.LAN(M+1))THEN


C                        _______________________
C  m-1           _______[_______________________
C  m    _________[__________________________________
C  m-1[_____________________________________________

C
C      crossection 1, closer to the beginning of the cantilever


      Y(I)=((WEIGHM(M)/24)*(-LENGTH(M)**3*(LENGTH(M)-4*XLEN(R)))
     &   -(X(J)/6)*(-XLEN(R)**2*(XLEN(R)-3*XLEN(R)))
     &   +(X(K)/6)*(-XLEN(M)**2*(XLEN(M)-3*XLEN(R)))
     &   +(Q(M)/6)*(-(LENGTH(M)/2)**2*((LENGTH(M)/2)-3*XLEN(R)))
     &   +(F(M)/6)*(-LENGTH(M)**2*(LENGTH(M)-3*XLEN(R)))
     &   +GAMW*(-XV(K)**4)*(XV(K)-5*XLEN(R))
     &   -GAMW*(-XV(I)**4)*(XV(I)-5*XLEN(R))
     &  )/(EMODUL(M)*INERTIA(M))
        WRITE (95,*)'LENGTH',M,'=',LENGTH(M)
        WRITE (95,*)'XLEN',R,'=',XLEN(R)
        WRITE (95,*)'XLEN',M,'=',XLEN(M)
        WRITE (95,*)'X',J,'=',X(J)
        WRITE (95,*)'X',K,'=',X(K)
        WRITE (95,*)'Y',I,'=',Y(I)
C      crossection 2, closer to the end of the cantilever

            IF(LENGTH(N)/2.LT.XLEN(M))THEN
                  UQ=0.0D0
                  ELSE
                  UQ=1.0D0
              ENDIF


        Y(K)=((WEIGHM(M)/24)*((LENGTH(M)-XLEN(M))**4
     &                  -LENGTH(M)**3*(LENGTH(M)-4*XLEN(M)))
     &  -(X(J)/6)*((XLEN(R)-XLEN(M))**3
     &                -XLEN(R)**2*(XLEN(R)-3*XLEN(M)))
     &  +(X(K)/6)*(-XLEN(M)**2*(XLEN(M)-3*XLEN(M)))
     &  +(Q(M)/6)*((LENGTH(M)/2-XLEN(M))**3*UQ
     &                 -(LENGTH(M)/2)**2*((LENGTH(M)/2)-3*XLEN(M)))
     &  +(F(M)/6)*((LENGTH(M)-XLEN(M))**3
     &                  -LENGTH(M)**2*(LENGTH(M)-3*XLEN(M)))
     &  +GAMW*(-XV(K)**4)*(XV(K)-5*XLEN(M))
     &  -GAMW*(-XV(I)**4)*(XV(I)-5*XLEN(M))
     &  )/(EMODUL(M)*INERTIA(M))

             ELSE
             ENDIF
 10       CONTINUE
          ENDIF
C         for the last cantilever the reaction from above is zero
          I=2*N-2
          J=2*N-3
          K=2*N-1
          R=N-1
          IF(LAN(N).GT.LAN(N-1))THEN
              IF(LENGTH(N)/2.LT.XLEN(N-1))THEN
                  UQ=0.0D0
                  ELSE
                  UQ=1.0D0
              ENDIF

        Y(I)=((WEIGHM(N)/24)*((LENGTH(N)-XLEN(R))**4
     &                  -LENGTH(N)**3*(LENGTH(N)-4*XLEN(R)))
     &  -(X(J)/6)*2*(XLEN(R)**3)
     &  +(Q(N)/6)*((LENGTH(N)/2-XLEN(R))**3*UQ
     &                 -(LENGTH(N)/2)**2*((LENGTH(N)/2)-3*XLEN(R)))
     &  +(F(N)/6)*((LENGTH(N)-XLEN(R))**3
     &                  -LENGTH(N)**2*(LENGTH(N)-3*XLEN(R)))
     &  +GAMW*(-XV(K)**4)*(XV(K)-5*XLEN(R))
     &  -GAMW*(-XV(I)**4)*(XV(I)-5*XLEN(R))
     &  )/(EMODUL(N)*INERTIA(N))

          ELSEIF(LAN(N).LT.LAN(N-1))THEN
        Y(I)=((WEIGHM(N)/24)*(-LENGTH(N)**3*(LENGTH(N)-4*XLEN(R)))
     &  -(X(J)/6)*2*(XLEN(R)**3)
     &  +(Q(N)/6)*((LENGTH(N)/2-XLEN(R))**3*UQ
     &                 -(LENGTH(N)/2)**2*((LENGTH(N)/2)-3*XLEN(R)))
     &  +(F(N)/6)*(-LENGTH(N)**2*(LENGTH(N)-3*XLEN(R)))
```

```
    &   +GAMW*(-XV(K)**4)*(XV(K)-5*XLEN(R))
    &   -GAMW*(-XV(I)**4)*(XV(I)-5*XLEN(R))
    &   )/(EMODUL(N)*INERTIA(N))

      ELSE
      ENDIF
      DO 11 I=1,2*(N-1)
             WRITE(95,*)'Y',I,'=',Y(I)
 11    CONTINUE
      END
```

I.6. Subroutines Newton and Usrfun (nonlinear version).

```
     SUBROUTINE NEWTON (nonlinear version)
C     program solves the system of nonlinear equations for n cantil.
C
      integer NTRIAL,N,NP,NB,M,I,J
      real TOLX
      parameter(TOLX=1.0E-8)
      parameter(N=3,NP=15,NTRIAL=25)
      double precision X(0:NP),ALPHA(NP,NP),BETA(NP),XLEN(NP)
      double precision XF(NP),DELTA(NP)
      double precision INERTIA(NP),LENGTH(NP),WEIGHM(NP),PSI
      double precision EMODUL,DEPTH,GAMA,PSID,BHAT,ERRF
      logical SWITCH,DONE
      parameter(BHAT=1.)
      data X(0),X(2)/0.0D00,0.017D00/
      SWITCH=.FALSE.
      DONE=.FALSE.
C
      OPEN (UNIT=91,FILE='B.dat',STATUS='old')
      READ (91,*) EMODUL,GAMA,PSID,DEPTH,XLEN(1)
      PRINT*, EMODUL,GAMA,PSID,DEPTH
      DO 01 I=1,N
      READ (91,*) LENGTH(I)
      PRINT*, LENGTH(I)
 01    CONTINUE
      close (UNIT=91)
C
      PSI= PSID *(3.141593D00)/180.D00
C
      DO 10 I=1,N
             WEIGHM(I) =GAMA*DEPTH*COS(PSI)
             INERTIA(I)=(BHAT*DEPTH**3)/12.D00
  10   CONTINUE
      X(1)=WEIGHM(1)/3.0D00
C
      NB=2
 200   DO 100 M=1,NTRIAL
C      DO 101 I=1,NB
```

```
C                   BETA(I)=0.0D0
C              DO 102 J=1,NB
C                   ALPHA(I,J)=0.0D0
C102            CONTINUE
C101     CONTINUE
      CALL USRFUN(NB,WEIGHM,LENGTH,INERTIA,EMODUL,PSI,DEPTH,
     *     XLEN,SWITCH,X,ALPHA,BETA)
      DO 40 I=1,NB
            DO 41 J=1,NB
            PRINT*, 'ALPHA',I,J,'=',ALPHA(I,J)
 41          CONTINUE
 40    CONTINUE
      BETA(1)=BETA(1)/ALPHA(1,1)
      ALPHA(1,NB)=ALPHA(1,NB)/ALPHA(1,1)
      DO 20 I=2,NB
            J=I-1
            IF (I.NE.NB)THEN
          ALPHA(I,NB)=(ALPHA(I,NB)-ALPHA(J,NB)*ALPHA(I,J))/ALPHA(I,I)
          BETA(I)=(BETA(I)-BETA(J)*ALPHA(I,J))/ALPHA(I,I)
            ELSE
           ALPHA(I,NB)=(ALPHA(I,NB)-ALPHA(J,NB)*ALPHA(I,J))
           BETA(I)=(BETA(I)-BETA(J)*ALPHA(I,J))/ALPHA(I,I)
           ALPHA(I,NB)=1.D00
            ENDIF
 20     CONTINUE
      DO 21 I=1,NB-1
            BETA(I)=BETA(NB)*(-ALPHA(I,NB))+BETA(I)
            X(I)=X(I)+BETA(I)
 21    CONTINUE
            X(NB)=X(NB)+BETA(NB)
      IF(X(NB-1).GT.0.0D00)THEN
      ERRF=0.0D00
      DO 22 I=1,NB
            ERRF=ABS(ERRF+BETA(I))
            XF(I)=X(I)
            DELTA(I)=BETA(I)
 22    CONTINUE
      ELSE
            GO TO 29
      ENDIF
           IF (ERRF.LT.TOLX)GO TO 23
           PRINT*,M
 100   CONTINUE
 23    IF(NB+1.LE.N)THEN
                      NB=NB+1
                      X(NB)=0.017
                      SWITCH=.FALSE.
      DO 24 I=1,NB-1
                X(I)=WEIGHM(I)/3.D00
 24    CONTINUE
                      GO TO 200
      ENDIF
 29    DO 30 I=1,N
      PRINT*,'BETA',I,'=',DELTA(I)
      PRINT*,'X',I,'=',XF(I)
 30    CONTINUE
      END
CCCCCCCCCCCCCCCCCCCCCCCCCCCCCCCCCCCCCCCCCCCCCCCCCCCCCC


      SUBROUTINE USRFUN(NB,WEIGHM,LENGTH,INERTIA,EMODUL,
     *          PSI,DEPTH, XLEN,SWITCH,X,ALPHA,BETA)
      INTEGER NP,NB
      LOGICAL SWITCH
      PARAMETER (NP=15)
      DOUBLE PRECISION ALPHA(NP,NP),BETA(NP),X(0:NP)
      DOUBLE PRECISION D(NP),E(NP),F(NP),G(NP),DEPSUM
      DOUBLE PRECISION EMODUL,PSI,DEPTH,GAMAW
      DOUBLE PRECISION WEIGHM(NP),LENGTH(NP),XLEN(NP),INERTIA(NP)
      DOUBLE PRECISION XR(0:NP),EF(NP),Q(NP)
      PARAMETER (GAMAW=9.81E03)
C
C     X(N).........R(1),R(2),...,R(N-1),THETA
C     XR...........length where the reaction acts
C     GAMAW........water density
C     PSI..........angle of the cantilevers with horisontal
C     UV...........singularity function for water
C     UR...........singularity function for reactions
C     Q............seismic force
C     EF...........force applied by the allready failed rock
C     XLEN(n)......x coordiante of the points with constant theta
C     THETA........angle between tangent at XLEN(N) to the bent
C                  cantilever and the streight cantilever
C
      PRINT*,'NB=',NB
      IF(.NOT.SWITCH)THEN
      PRINT*,'XLEN1',XLEN(1)
C           XLEN(1)=LENGTH(1)*0.6D00
          DO 01 I=2,NB
          DEPSUM=0.0D00
                DO 02 J=1,I-1
                      DEPSUM=DEPSUM+DEPTH
 02              CONTINUE
                XLEN(I)=1.0D00*XLEN(1)+SIN(X(NB))*DEPSUM
      PRINT*, 'XLEN',I,XLEN(I)
 01        CONTINUE
          DO 03 I=1,NB-1
                IF (LENGTH(I).LT.LENGTH(I+1))THEN
                      XR(I)=LENGTH(I)
                ELSE
                      XR(I)=LENGTH(I+1)
                ENDIF
 03          CONTINUE
       ENDIF
       SWITCH=.TRUE.
C
       XR(0)=0.0D00
       X(0)=0.0D00
 11     DO 20 I=1,NB-1
             D(I)=-(WEIGHM(I)/2)*LENGTH(I)**2-(X(I)/2)*XR(I)**2
   &          +(X(I-1)/2)*XR(I-1)**2
   &          +(GAMAW*SIN(PSI)/6)*XV(I-1)**3*
   &          UV(I-1)-(GAMAW*SIN(PSI)/6)*XV(I)**3*UV(I)-(Q(I)/2)*
   &          LENGTH(I)**2-EF(I)*LENGTH(I)
C
             E(I)=(WEIGHM(I)/2)*LENGTH(I)+(X(I)/2)*XR(I)
   &          -(X(I-1)/2)*XR(I-1)
   &          -(GAMAW*SIN(PSI)/4)*XV(I-1)**2*
   &          UV(I-1)+(GAMAW*SIN(PSI)/4)*XV(I)**2*UV(I)+(Q(I)/2)*
   &          LENGTH(I)+EF(I)/2
C
             F(I)=-WEIGHM(I)/6-X(I)/6+X(I-1)/6
   &          +(GAMAW*SIN(PSI)/6)*XV(I-1)*
   &          UV(I-1)-(GAMAW*SIN(PSI)/6)*XV(I)*UV(I)-Q(I)/6
C
            G(I)=(-GAMAW*SIN(PSI)/24)*UV(I-1)-(GAMAW*SIN(PSI)/24)*
   &           UV(I)
             G(I)=0.0D00
 20     CONTINUE
C
             D(NB)=-(WEIGHM(NB)/2)*LENGTH(NB)**2
   &          +(X(NB-1)/2)*XR(NB-1)**2
            +(GAMAW*SIN(PSI)/6)*XV(NB-1)**3*
   &         UV(NB-1)-(GAMAW*SIN(PSI)/6)*XV(NB)**3*UV(NB)-(Q(NB)/2)*
   &         LENGTH(NB)**2-EF(NB)*LENGTH(NB)

             E(NB)=(WEIGHM(NB)/2)*LENGTH(NB)
   &          -(X(NB-1)/2)*XR(NB-1)
            -(GAMAW*SIN(PSI)/4)*XV(NB-1)**2*
   &          UV(NB-1)+(GAMAW*SIN(PSI)/4)*XV(NB)**2*UV(NB)+(Q(NB)/2)*
   &          LENGTH(NB)+EF(NB)/2
C
             F(NB)=-(WEIGHM(NB)/6)+X(NB-1)/6
   &          +(GAMAW*SIN(PSI)/6)*XV(NB-1)*
   &          UV(NB-1)-(GAMAW*SIN(PSI)/6)*XV(NB)*UV(NB)-Q(NB)/6
C
            G(NB)=(-GAMAW*SIN(PSI)/24)*UV(NB-1)-(GAMAW*SIN(PSI)/24)*
   &          UV(NB)
             G(NB)=0.0
C
             ALPHA(1,NB)=-EMODUL*INERTIA(1)
       DO 30 I=2,NB
       DEPSUM=0.0D00
```

```
              DO 31 J=1,I-1
                   DEPSUM=DEPSUM+DEPTH
 31           CONTINUE
            ALPHA(I,NB)=COS(X(NB))*DEPSUM*(D(I)+E(I)*2*XLEN(I)+F(I)*3*
   &         XLEN(I)**2+G(I)*4*XLEN(I)**3)-EMODUL*INERTIA(I)
 30    CONTINUE
              ALPHA(1,1)=1./6.*((XR(1)-XLEN(1))**3-XR(1)**3)
       DO 32 I=2,NB-1
            ALPHA(I,I)=1.D00/6.*((XR(I)-XLEN(I))**3-XR(I)**3)
            ALPHA(I,I-1)=-1.D00/6.*((XR(I-1)-XLEN(I))**3-XR(I-1)**3)
 32    CONTINUE
            ALPHA(NB,NB-1)=-1./6.*((XR(NB-1)-XLEN(NB))**3-XR(NB-1)**3)
       X(0)=0.0D00
       DO 40 I=1,NB-1
         BETA(I)=-((WEIGHM(I)/6)*((LENGTH(I)-XLEN(I))**3-LENGTH(I)**3)
   &          -X(I-1)/6*((XR(I-1)-XLEN(I))**3-XR(I-1)**3)+
   &           X(I)/6*((XR(I)-XLEN(I))**3-XR(I)**3)-
   &           EMODUL*INERTIA(I)*X(NB))-
   &      (GAMAW*SIN(PSI)/24)*((XV(I-1)-XLEN(I))**4*UV(I-1)-XV(I-1)**4)
   &          +(GAMAW*SIN(PSI)/24)*((XV(I)-XLEN(I))**4*UV(I)-XV(I)**4)-
   &           (Q(I)/6)*((LENGTH(I)-XLEN(I))**3-LENGTH(I)**3)+
   &           (EF(I)/2)*((LENGTH(I)-XLEN(I))**2-LENGTH(I)**2)
 40    CONTINUE
C
        BETA(NB)=-((WEIGHM(NB)/6)*((LENGTH(NB)-XLEN(NB))**3-
   &           LENGTH(NB)**3)-X(NB-1)/6*((XR(NB-1)-XLEN(NB))**3
   &           -XR(NB-1)**3)-EMODUL*INERTIA(NB)*X(NB))
   &           (GAMAW*SIN(PSI)/24)*((XV(NB-1)-XLEN(NB))**4*UV(NB-1)
   &           -XV(NB-1)**4)+(GAMAW*SIN(PSI)/24)*
   &           ((XV(NB)-XLEN(NB))**4*UV(NB)-XV(NB)**4)+
   &           Q(NB)/6((LENGTH(NB)-XLEN(NB))**3-LENGTH(NB)**3)+
   &           EF(NB)/2((LENGTH(NB)-XLEN(NB))**2-LENGTH(NB)**2)-
       END
CCCCCCCCCCCCCCCCCCCCCCCCCCCCCCCCCCCCCCCCCCCCCCCCCC
```

I.7. List of subroutines

Program Input:

Subroutine Geometry - calculates the shape of the slope in X,Y coordinates X being parallel with horizontal.

Subroutine Cantilever - rotates X,Y axes into new position, where Y is parallel with the dip of bedding planes, and calculates the lengths of the rock and water columns in the new coordinate system.

Program Fredy:

Subroutine Inp2 - builds an alternative model of the slope from blocks of defined length/depth ratio (was not used for the back analysis).

Program Inshav:

Subroutine Isaac - slightly different version of the routine used in Flex. It is a driving part of the program calling and organising the rest of routines. Takes also care of calculation of the reactions between the cantilevers before crest.

Subroutine Shears - Calculates the shear stresses in the slope, and builds the new slope from the composed blocks according to SSF (shear strength / shear stress ratio - Shear Safety Factor).

Subroutine Usrfun - see Flex

Subroutine Iterun - see Flex

Subroutine Iter - see Flex

Subroutine Inline - see Flex

Subroutine Inert - see Flex

Subroutine Newton - see Flex

Program Flex:

Subroutine Isaac - driving part of the program calling and organising the rest of the routines. Takes also care of calculation of the reactions between the cantilevers before crest.

Subroutine Usrfun - calculates values of the coefficients from the matrix 4-4 and the values of the functions from the matrix 4-3.

Subroutine Newton - solves the system of linear (or non linear) equations defined in equation ? using the values provided by Usrfun.

Subroutine Iter - calculates reactions between cantilevers before the crest which could not be handled by Isaac.

Subroutine Iterun - calculates reactions between cantilevers behind the crest

Subroutine Inline - Calculates the distances of the point reactions from the beginning of each cantilever.

Subroutine Inert - calculates moments of inertia for tested cantilevers.

Subroutine Chan - registers all changes below the broken cantilever caused by breaking of the cantilever. Keeps track of proper indexing of the cantilevers.

Subroutine Change - takes care of indexes of cantilevers laying above the broken one.

Subroutine Moment - Calculates the shear and normal stresses in the cantilevers, and also calculates SSFs.

Subroutine Devide - makes the splitting of unstable cantilevers marked by Moment and also takes care of proper indexing.

Appendix J

Location of the Luscar Mine, Cardinal River Coals Ltd and the 50-A-5 open pit coal mine.

The exact location of the 50-A-5 open pit mine is shown in Figure J-2 (next page), and the plan of the pit, including the position of the analysed cross section, is shown in Figure J-1.

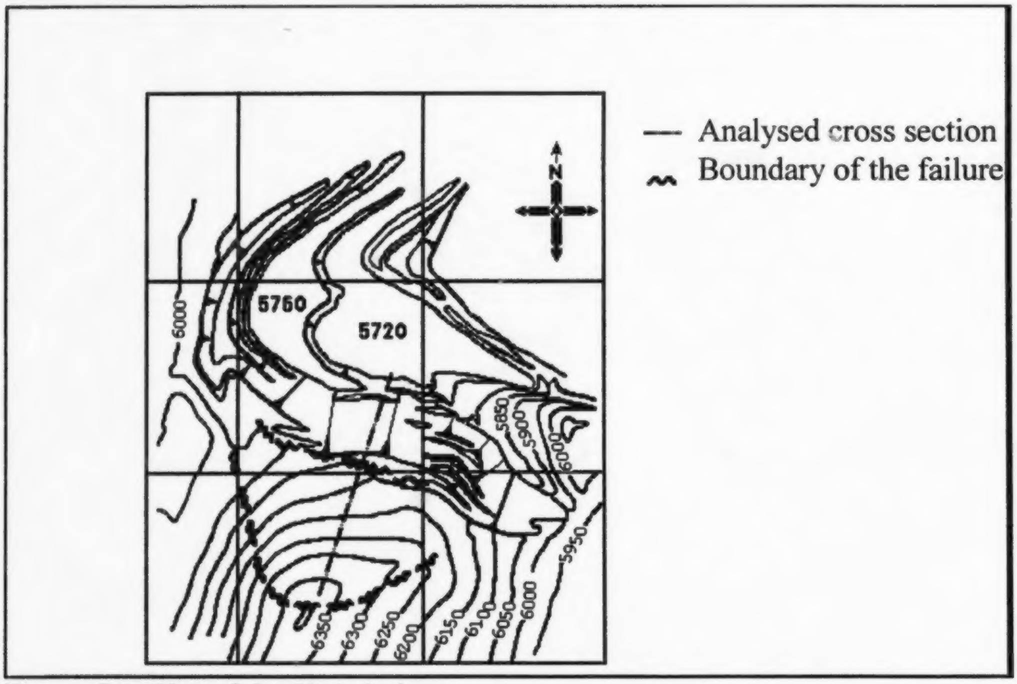
— Analysed cross section
Boundary of the failure
N
5760
5720
6000
5850
5900
5950
6000
6350
6300
6250
6200
6150
6100
6050
6000
5950

Figure J-1 Plan of the 50-A-5 pit

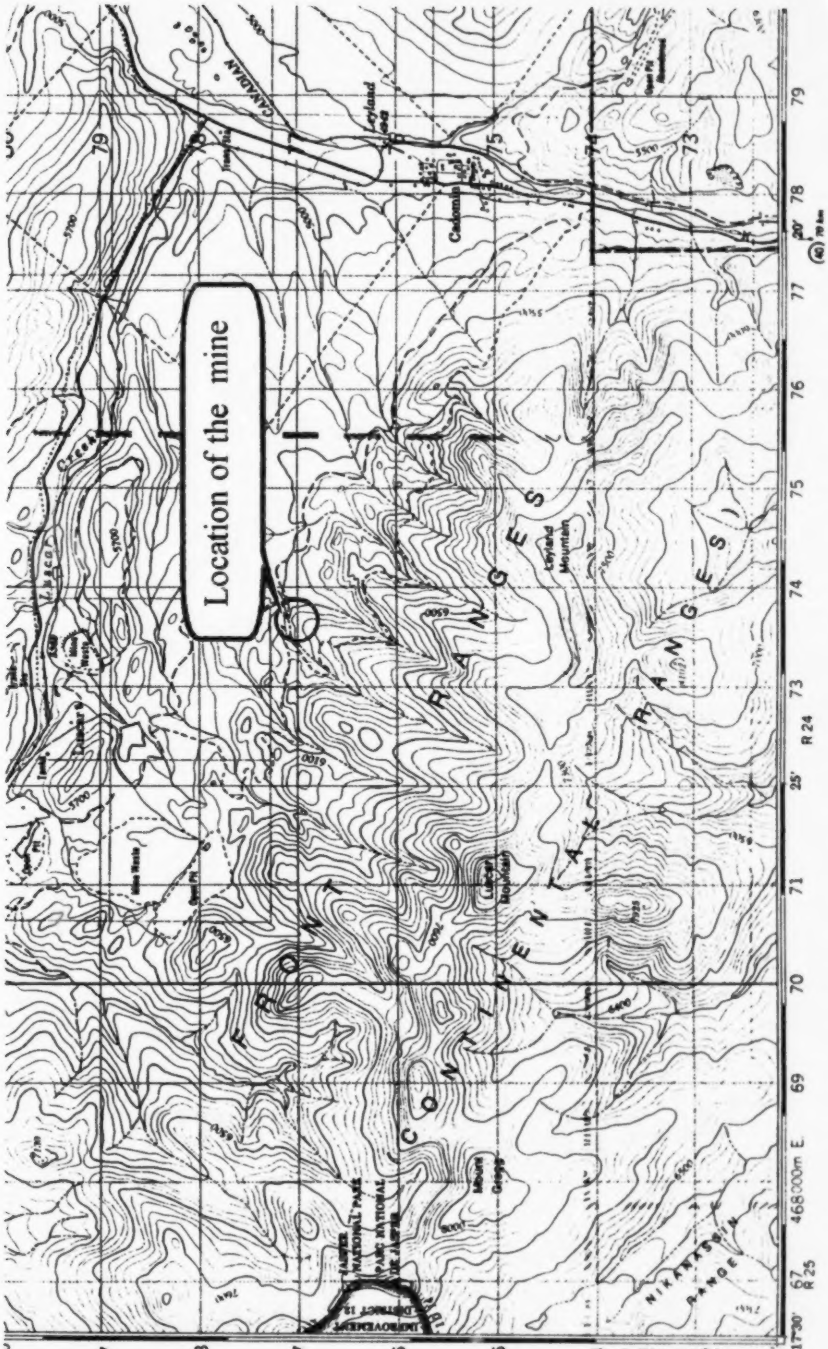
Location of the mine
FRONT RANGES
CONTINENTAL RANGES
NIKANASSIN RANGE
Leyland Mountain
Mount Gregg
Luscar Creek
Cadomin
Leyland
CANADIAN
JASPER NATIONAL PARK
PARC NATIONAL DE JASPER
Tp 47
Tp 46
R 24
R 25
468000m E
5873000m N
117°30'
53°00'
25'
20'
67
69
70
71
73
74
75
76
77
78
79

Figure J-2 Location of the 50-A-5 open pit mine